

Thèse



THESE INSA Rennes
sous le sceau de l'Université européenne de Bretagne
pour obtenir le titre de
DOCTEUR DE L'INSA DE RENNES
Spécialité : Électronique

présentée par

Fahad Syed Muhammad

ECOLE DOCTORALE : MATISSE

LABORATOIRE : IETR-INSA

Various resource
allocation and
optimization strategies
for high bit rate
communications on
power lines

Thèse soutenue le 17.03.2010

devant le jury composé de :

Jean-Claude Belfiore

Professeur à Telecom, ParisTech / président

Hikmet Sari

Professeur à SUPELEC, Gif-sur-Yvette / rapporteur

Daniel Roviras

Professeur au CNAM, Paris / rapporteur

Jean-Marie Gorce

Professeur à l'INSA de Lyon / examinateur

Rodolphe Le Gouable

Ingénieur de Recherche à Orange Labs / examinateur

Jean-Yves Baudais

Chargé de Recherche au CNRS-IETR / Co-encadrant de thèse

Jean-François Hélard

Professeur à l'INSA de Rennes / Directeur de thèse

2010

Fahad SYED MUHAMMAD

To my parents

Acknowledgements

A number of people have helped me and collaborated with me in various ways on technical, administrative and emotional aspects of my PhD studies. Here, I find myself in an extremely challenging situation to thank all those amazing people and this, I believe, is quasi impossible. I have no means to show all the gratitude I feel for their support and kindness. In the following paragraphs, however, I will try my best to present my sincere gratitude to all those to whom I am deeply indebted.

First of all, I would like to thank the director of my PhD, Prof. Jean-François H  lard for providing me such a wonderful opportunity and for his supervision of my research work. I owe my deepest gratitude to Dr. Jean-Yves Baudais, my co-supervisor, for his help and support during all these years. He has been a source of motivation and encouragement for me. In addition to his mathematical and technical expertise, I particularly appreciate his human qualities. A bundle of thanks for all the time that he spent working with me. All those discussions are like a treasure for me that I will never forget.

My sincere thanks to Prof. Jean-Claude Belfiore for presiding over my PhD defense. All my gratitude to Prof. Hikmet Sari and Prof. Daniel Roviras for the time they spent reading and commenting on my thesis, and for the report they wrote. Special thanks to Prof. Jean-Marie Gorce and Dr. Rodolphe Le Gouable for being the jury member.

I would also like to thank all the administrative staff in IETR for their help and guidance in all administrative matters, particularly Mrs. Ghislaine Denis, Ms. Yolande Sambin and Mr. Pascal Richard.

I am grateful to Orange Labs (France T  l  com R&D) and to the European ICT FP7 OMEGA project for supporting this work. I am thankful to Dr. Matthieu Crus  re for letting me benefit from his outstanding previous work. Special thanks to Dr. Antoine Stephan for his collaboration. I would like to thank Jihane Benlahbib and Julie Karaki for all the hardwork they did during their Undergraduate and Master internships, respectively. It has been an enriching experience to supervise them.

Many thanks to all my colleagues in IETR specially Ijaz-Haider Naqvi, Ali Maiga, Youssef Nasser, Pierre Pasquero, Hassan Salti, Erwan Fourn, Ayman Khalil, Dany Obeid, Ir  ne Mahafeno, Fr  d  ric Queudet, St  phane Meric and Abdallah Hamini.

Last but not least, I am extremely thankful to my loving family, my parents, my brother and my sisters for their unconditional and unlimited support and affection. Ammi, thanks for guiding me throughout my life and for teaching me to embrace life with all of its challenges, to love the humanity and to believe in myself.

Contents

Résumé étendu en Français	ix
List of Figures	xxxiii
List of Tables	xxxvii
List of Acronyms and Abbreviations	xxxix
Introduction	1
1 Data transmission through PLC	7
1.1 History of power line communication	8
1.2 Application of power line technology	10
1.2.1 The power line grid	12
1.2.2 The power line channel	14
1.3 PLC technology of today	18
1.3.1 Consortiums	18
1.3.1.1 HomePlug powerline alliance	19
1.3.1.2 UPA	19
1.3.1.3 CEPCA	19
1.3.1.4 Other alliances	20
1.3.1.5 Projects	20
1.3.2 The OMEGA project	21
1.3.2.1 Main objectives	21
1.3.2.2 Use of high bandwidth	21
1.3.2.3 Channel modeling	22
1.3.2.4 Use of innovative technologies	22
1.4 Future of PLC	23
1.5 Conclusion	24
2 System specifications and resource allocation	25
2.1 Introduction	26
2.2 System specifications	26
2.2.1 OFDM	27
2.2.1.1 OFDM principle	27

2.2.1.2	The interest of adding channel coding and interleaving	30
2.2.1.3	Signal characteristics	30
2.2.1.4	ISI and ICI minimization	32
2.2.1.5	Pros and Cons of OFDM	33
2.2.2	Spread spectrum OFDM	34
2.2.2.1	Spread spectrum principle	34
2.2.3	Multiple access schemes	36
2.2.3.1	Principle of the combination	37
2.2.3.2	Mono block systems	38
2.2.3.3	Multi block systems	40
2.2.4	System selection	42
2.2.4.1	Selection of LP-OFDM	42
2.2.4.2	Signal characteristics	45
2.3	Resource allocation for multicarrier systems	45
2.3.1	Theoretical capacity	47
2.3.2	Fundamentals of multicarrier resource allocation	50
2.3.3	Rate maximization	52
2.3.3.1	Infinite granularity solution	53
2.3.3.2	Finite granularity solution	53
2.3.4	Robustness Maximization	54
2.3.4.1	Infinite granularity solution	55
2.3.4.2	Finite granularity solution	56
2.4	Conclusion	60
3	Bit rate maximization	61
3.1	Introduction	62
3.2	RM under peak BER constraint	63
3.2.1	RM for uncoded LP-OFDM	64
3.2.1.1	Mutual information for LP-OFDM	64
3.2.1.2	Mono block systems	65
3.2.1.3	Multi block systems	66
3.2.2	Mono block resource allocation	66
3.2.3	Multi block resource allocation	69
3.2.4	RM for coded LP-OFDM	70
3.2.4.1	Selected channel coding scheme	71
3.2.4.2	Wei's 4D 16-states trellis code	71
3.2.4.3	RS Codes	78
3.2.4.4	Theoretical coding effects on system performance	80
3.2.5	Coded LP-OFDM resource allocation	81
3.2.5.1	Structure of coded LP-OFDM	81
3.2.5.2	Resource allocation	83
3.2.5.3	Results	85
3.3	RM under mean BER constraint	88
3.3.1	OFDM systems	88

3.3.2	LP-OFDM systems	90
3.3.3	Results	91
3.4	Conclusion	94
4	Mean BER minimization	97
4.1	Introduction	98
4.2	MBM for OFDM systems	99
4.2.1	Proposed Loading Algorithm	100
4.2.2	Results	101
4.3	MBM for LP-OFDM systems	103
4.3.1	Mono block LP-OFDM	104
4.3.2	Proposed loading algorithm for mono block LP-OFDM	106
4.3.3	Multi block LP-OFDM	107
4.3.4	Proposed loading algorithm for multi block LP-OFDM	108
4.3.5	Results	109
4.4	MBM for Coded LP-OFDM	111
4.4.1	A textbook case	111
4.4.2	Algorithm for the textbook case	112
4.4.3	Mono block LP-OFDM	114
4.4.4	Results	117
4.5	Conclusion	117
5	Bit rate maximization with imperfect CSI	121
5.1	Introduction	122
5.2	Considered error model	123
5.3	Impacts on allocations	124
5.4	Allocation based on generalized error rate expressions	125
5.4.1	OFDM allocations	125
5.4.2	LP-OFDM allocations	126
5.4.3	Results	128
5.5	Allocations based on individual error rate expressions	132
5.5.1	Modified SER expressions	132
5.6	Proposed LP-OFDM allocation	135
5.6.1	Results	136
5.7	Conclusion	139
	Appendix	147
A	Modified error rate expressions	149
A.1	4 internal points	152
A.2	4 corner points of internal square	152
A.3	8 middle points of internal square	152
A.4	8 corner points of circumference	154
A.5	8 middle points of circumference	154
	Bibliography	157

Résumé étendu en Français

Introduction

Ces dernières années, le développement des réseaux de communication *indoor* et *out-door* et l'augmentation du nombre d'applications utilisées sur les appareils personnels et commerciaux conduisent à un besoin toujours croissant de transmission de données à haut débit. Parmi les nombreuses technologies concurrentes, les communications par courant porteur en ligne (CPL) ont leur place en raison des infrastructures déjà disponibles. La motivation principale de cette thèse est d'augmenter le débit et la robustesse des systèmes CPL à porteuses multiples afin qu'ils puissent être utilisés efficacement dans les réseaux domestiques et pour la domotique. Le problème de la maximisation du débit (RM en anglais *rate maximization*) pour les systèmes OFDM (en anglais *orthogonal frequency division multiplexing*) et LP-OFDM (en anglais *linear precoded OFDM*) est considéré sous les contraintes de taux d'erreur binaire (TEB) crête et moyen. Les algorithmes d'allocation sont proposés pour des systèmes réels, qui prennent en compte les gains de codage de canal dans le processus d'allocation des ressources. En outre, un nouveau schéma de minimisation du TEB, qui minimise le TEB moyen des systèmes, (MBM en anglais *mean bit error rate minimization*) est obtenu pour un débit donné et un masque de puissance imposé. Pour l'allocation des ressources dans un système à porteuses multiples, il est généralement supposé que l'information sur l'état du canal (CSI en anglais *channel state information*) est parfaitement connue à l'émission, ce qui ne correspond pas à la réalité. C'est pourquoi, nous avons également étudié des schémas d'allocation des ressources en tenant compte des effets de CSI imparfaite.

Cette thèse a été réalisée à l'Institut d'Electronique et de Télécommunications de Rennes (IETR) à l'Institut National des Sciences Appliquées (INSA-Rennes). Ce travail a été financé en partie par Orange Labs dans le contexte d'un contrat de recherche 46145507. Cette thèse a également contribué au projet ICT FP7 OMEGA (en anglais *Home Gigabit Access*), qui est un projet intégré dans le domaine de l'information et de la technologie de communication financé par l'union européenne.

L'objectif principal de cette thèse est d'augmenter le débit et la robustesse des systèmes CPL à porteuses multiples afin qu'ils puissent être utilisés efficacement dans les réseaux domestiques et pour la domotique. Le CPL a des avantages intrinsèques et il hérite également des inconvénients de son infrastructure. Le thème de ce travail de recherche est d'explorer les différentes approches de modulation et de codage de canal,

en liaison avec l'allocation des ressources, afin de fournir des systèmes CPL concurrents des autres solutions à haut débit et de faire face efficacement aux inconvénients des canaux CPL. Les objectifs de cette recherche sont également de tenir compte des limites imposées par des systèmes pratiques et de proposer les algorithmes d'allocation des bits et énergies, capables de satisfaire les besoins des systèmes de communications modernes. La portée de ce travail est énumérée dans les points suivants.

1. Le premier objectif de ce travail est d'atteindre des débits optimaux pour le réseau domestique CPL utilisant des systèmes à porteuses multiples. Les techniques OFDM et LP-OFDM sont appliquées au CPL LAN (en anglais *local area network*). Différentes contraintes d'erreurs sont utilisées pour augmenter le débit du système tout en respectant un masque de DSP (densité spectrale de puissance) et un taux d'erreur cible du système. Le codage de canal est pris en compte dans le processus d'allocation des ressources.
2. La maximisation de la robustesse (face aux diverses sources de bruit) pour le CPL LAN est également étudiée en allouant des bits et des énergies aux sous-porteuses de telle manière qu'un TEB moyen soit minimisé. Cette approche est appliquée au système OFDM classique ainsi qu'au système LP-OFDM sous une contrainte de DSP (soit une contrainte de puissance de crête). Les communications CPL doivent respecter un masque de puissance, c'est pourquoi cette contrainte de DSP est utilisée dans le processus d'allocation des ressources pour les systèmes CPL.
3. La répartition des bits et énergies est proposée pour les systèmes à porteuses multiples en tenant compte d'une CSI imparfaite à l'émetteur. Différentes approches sont étudiées pour contrer les effets des estimations bruitées dans le processus d'allocation des ressources. Les résultats obtenus dans le cas de systèmes OFDM et LP-OFDM démontrent l'intérêt de telles approches.

Chapitre 1 : Transmission des données par CPL

Introduction

L'utilisation des lignes électriques pour le transfert de l'information a été envisagée il y a environ deux siècles. Au cours des deux dernières décennies, diverses associations de grands groupes industriels ont été formées, notamment celles représentant les producteurs d'électricité. Leur but est de promouvoir la technologie CPL, d'encourager les progrès techniques et de soutenir les essais sur le terrain. L'alliance HomePlug est l'une des plus influentes de ces associations. Créée en mars 2000, elle compte plus de 70 membres. PLC forum est un autre groupe qui a été créé par les dirigeants de l'industrie européenne en 2000 pour promouvoir la technologie CPL en Europe. Dans la décennie en cours, les bandes de fréquences pour CPL ont été étendues de quelques kHz à quelques dizaines de MHz. La révolution de l'électronique numérique, comme le développement des processeurs puissants et le développement de nouvelles techniques de traitement du signal numérique et des algorithmes discrets ont permis d'utiliser les techniques de modulation modernes et de codage itératif dans les systèmes embarqués et intégrés. Aujourd'hui, le réseau électrique dessert pratiquement l'ensemble des habitations, et l'intérêt pour l'utilisation du réseau de distribution électrique est croissant. Les techniques de communication appropriées ont été intensivement étudiées et les bandes de fréquences attribuées aux systèmes CPL ont été étendues jusqu'à 30 MHz. Les caractéristiques du canal CPL ont aussi été largement documentées. De nombreuses applications et des circuits intégrés spécifiques ont également été développés pour les systèmes CPL à large bande. Très peu d'entreprises de distribution d'énergie ont commencé des activités commerciales en offrant un accès Internet à large bande via les lignes électriques, mais l'intérêt est toujours là en raison de la couverture énorme des lignes électriques dans les zones rurales. Toutefois, l'utilisation du CPL pour la domotique et le réseau domestique reste un sujet de recherche d'actualité.

Les applications de la technologie CPL

D'une manière générale, il est considéré que le réseau LV (en anglais *low voltage*) CPL a une topologie en arbre où les modems CPL sont installés aux interfaces MV/LV (en anglais *medium voltage*) et peuvent fournir des services à tous les bâtiments de la localité. Les techniques modernes et innovantes de communications numériques sont nécessaires pour optimiser l'architecture du réseau LV CPL où les caractéristiques particulières de la ligne électrique changent souvent d'un local à l'autre, en fonction du nombre de ménages par transformateur et de la distance entre le transformateur et le bâtiment des consommateurs. Dans des topologies européennes, où les distances sont importantes, les répéteurs intermédiaires sont nécessaires pour régénérer le signal d'information et fournir une couverture raisonnable à toutes les prises électriques dans les locaux du client.

Le réseau CPL *indoor* a des intérêts de recherche de plus en plus élevés. L'avantage principal offert par la ligne électrique pour des réseaux domestiques est l'infrastructure

déjà disponible. Différents dispositifs peuvent communiquer sans recourir à l'installation de câbles supplémentaires. Par exemple, ces réseaux CPL sont une solution idéale pour les applications domotiques. En outre, plusieurs ordinateurs, périphériques d'impression, scanners ou téléphones, peuvent être connectés entre eux et peuvent aussi partager l'Internet large bande en même temps.

Le canal CPL

Les principaux travaux dans ce domaine ont été menés par Philipps et Zimmermann dont les références sont les plus largement citées dans le domaine de la modélisation de canaux CPL. La réponse en fréquence d'un câble de 110 m et comportant 15 trajets, proposée par Zimmermann, est donnée par

$$H(f) = \sum_{p=1}^P g_p \cdot e^{-(a_0+a_1 f^k)d_p} \cdot e^{-j2\pi f \tau_p}, \quad (1)$$

où τ_p est le retard de trajet p , g_p est le facteur de pondération du trajet p , d_p est la distance en mètre du trajet p et $\{a_0, a_1, k\}$ sont des paramètres du modèle à ajuster. Ce modèle a été validé dans la bande de fréquences de 500 kHz à 20 MHz et est valable pour les deux environnements intérieurs et extérieurs. Les lignes intérieures sont plus courtes, mais souffrent d'une forte ramification : le nombre de trajets pertinents est généralement plus élevé tandis que l'atténuation associée à chaque trajet est plus faible.

La technologie CPL d'aujourd'hui

Différents consortiums et organismes de normalisation définissent les règles pour l'utilisation éventuelle des réseaux CPL et des appareils qui devraient être acceptés par les différents acteurs comme les fabricants, fournisseurs de services Internet, intégrateurs et opérateurs de réseaux. Certains consortiums bien connus sont énumérés ci-dessous :

- HomePlug powerline alliance,
- Universal Power Line Association,
- Consumer Electronics Power Line Communication Alliance,
- United Power Line Council,
- Continental Automated Buildings Association.

Les projets de recherche les plus significatifs du moment sont donnés dans la liste suivante.

OMEGA vise à développer une infrastructure *ultra broadband*, accessible aux clients résidentiels.

OPERA avait pour objectif de développer une technologie pour ouvrir de nouvelles lignes MV et LV pour les applications d'accès.

POWERNET avait pour principaux objectifs le développement du haut débit sur des lignes électriques cognitives (CBPL), et des équipements de communication pour l'accès et les applications intérieures.

WIRENET visait à développer un modem PLC pour la transmission de données et l'automatisation industrielle à travers une approche de modulation à bande ultra large.

Le futur du CPL

La technologie CPL a un potentiel énorme en particulier dans les domaines de la domotique et du LAN haut débit. Les communications à très haut débit par les prises électriques domestiques peuvent être utilisées, par exemple, pour partager des données entre plusieurs ordinateurs, pour permettre aux distributeurs d'électricité d'offrir l'Internet haut débit à leurs clients ou pour alerter automatiquement une agence de réparation dans le cas d'une défaillance soudaine de l'un des appareils électriques coûteux et importants.

De plus, la technologie CPL doit être considérablement renforcée afin de répondre aux attentes associées aux exigences futures du haut débit. Il est nécessaire de développer des techniques avancées de CPL pour permettre le gigabit par ligne d'énergie en optimisant les mécanismes des couches physiques, MAC et *cross-layer*. Les stratégies avancées de gestion des ressources et d'optimisation de la qualité de service doivent être prises en compte à l'aide des mécanismes d'optimisation *cross-layer*. Ces stratégies d'allocation des ressources doivent être exploitées afin de maximiser soit le débit binaire, soit la robustesse du système afin de parvenir à une performance quasi optimale.

Chapitre 2 : Spécifications du système et l'allocation des ressources

Introduction

Le principe de la modulation à porteuses multiples (MCM) est discuté dans ce chapitre, suivi par la description de l'OFDM. Par la suite, la technique d'étalement de spectre est décrite et un schéma de transmission est donné, qui combine l'OFDM et les techniques d'étalement de spectre (ou de manière équivalente les principes de précodage linéaire). Un système basé sur cette combinaison est sélectionné et les principaux avantages et motivations de ce choix sont discutés. Ce système sera appelé LP-OFDM dans la suite. Différentes études analytiques ont été effectuées pour l'allocation des ressources et l'optimisation des performances des systèmes à porteuses multiples. Diverses stratégies d'allocation des ressources sont considérées. Différents problèmes sont formulés pour ces stratégies en utilisant un certain nombre de contraintes.

Le système LP-OFDM

Dans cette thèse, nous considérons un schéma de transmission basé sur la combinaison de signaux OFDM avec les principes du précodage linéaire. Les principaux objectifs sont d'obtenir un système plus souple sans augmenter la complexité du système, tout en améliorant les performances globales du système. L'opération de précodage linéaire consiste à utiliser des matrices de précodage pour différents blocs de sous-porteuses dans le spectre multiporteuse. La complexité du système n'est pas augmentée de façon significative puisqu'un bloc précodage est simplement ajouté dans la chaîne de transmission qui introduit une complexité supplémentaire équivalente à une multiplication par une matrice de Hadamard.

Le schéma de transmission choisi peut être considéré comme une forme modifiée de la forme d'onde SS-MC-MA (en anglais *spread-spectrum multicarrier multiple-access*) initialement proposée pour les communications radio mobiles par Kaiser et Fazel. Comme dans le cas du SS-MC-MA, l'étalement pour le LP-OFDM est effectué dans la dimension fréquentielle. La composante de précodage linéaire améliore la robustesse du signal contre les interférences à bande étroite et la sélectivité en fréquence, en rendant la bande passante du signal beaucoup plus large que la bande passante des interférences. De plus, les sous-porteuses sont regroupées, ce qui permet d'augmenter le débit en particulier sous la contrainte de DSP. En outre, l'accès multiple est fourni par la dimension fréquentielle (comme dans le cas OFDMA ou SS-MC-MA) et pas dans la dimension du code (comme dans le cas MC-CDMA).

La figure 1 montre une représentation schématique d'un système LP-OFDM. La bande disponible est divisée en N sous-porteuses parallèles qui sont réparties en K blocs S_k de L sous-porteuses. La fonction de précodage est ensuite appliquée avec les séquences de précodage de longueur C , encore appelée facteur de précodage.

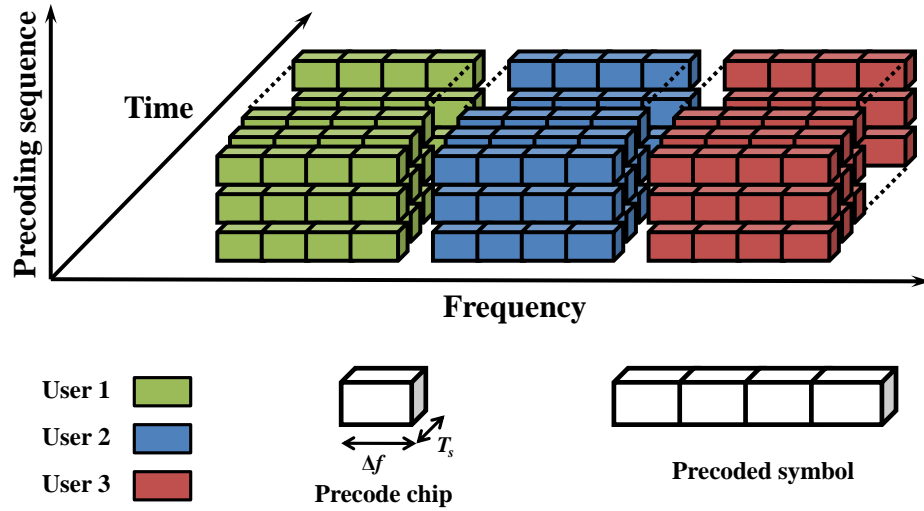


Figure 1: Le système LP-OFDM.

L'allocation des ressources

Dans les systèmes à porteuses multiples, l'allocation des bits et énergies est considérée comme un aspect fondamental. Dans les systèmes pratiques, le problème d'allocation des ressources est traité par les algorithmes de chargement des bits et énergies, qui sont utilisés pour répartir, entre les sous-porteuses, le nombre total de bits et l'énergie totale disponible, afin de maximiser la performance du système et maintenir une qualité de service requise. L'allocation des ressources peut être considérée comme un problème d'optimisation sous contrainte et est généralement divisée en deux cas : la maximisation de débit (RM) et la maximisation de la robustesse (ROM) où l'objectif est de, respectivement, maximiser le débit réalisable et la robustesse du système contre le bruit. La maximisation de la marge (MM) est le scénario le plus commun de maximisation de la robustesse où la marge du bruit du système est maximisée. Le problème d'optimisation peut être formulé sous la contrainte de puissance totale ainsi que sous la contrainte de DSP. Dans cette thèse, nous allons discuter seulement les formulations sous la contrainte de DSP, contrainte correspondant au masque de puissance imposé dans les systèmes de communication CPL. Contrairement à la contrainte de puissance totale, la puissance résiduelle d'une sous-porteuse est d'aucune utilité pour les autres sous la contrainte de DSP. Par conséquent, l'utilisation efficace de l'énergie devient encore plus cruciale. Quant à la contrainte de taux d'erreur, elle dépend de la modulation et du codage de canal considéré.

Le problème RM

Tout d'abord, nous discutons le problème le plus commun d'optimisation des systèmes à porteuses multiples qui est la maximisation du débit. Pour un système OFDM, le problème de la maximisation du débit sous une contrainte de DSP et d'un TES (taux

d'erreur symbole) cible peut être défini comme

$$\begin{cases} \max \sum_{i=1}^N \log_2 \left(1 + \frac{1}{\gamma_m \Gamma} |H_i|^2 \frac{E_i}{N_0} \right) \\ \text{subject to } E_i \leq \hat{E} \end{cases} . \quad (2)$$

L'objectif de ce problème consiste à distribuer des bits et des énergies entre les sous-porteuses tout en maximisant le débit total d'un système OFDM. Toutefois, nous notons que dans ce problème RM, le nombre de bits attribués à chaque sous-porteuse dépend uniquement de la puissance d'émission disponible pour la sous-porteuse en question (i.e. il est indépendant de la puissance d'émission disponible pour les autres sous-porteuses).

Le problème RoM

Le schéma de maximisation de la robustesse le plus connu est la maximisation de la marge (ou de minimisation de puissance). Dans ce schéma, la marge du système γ_m est optimisée pour un débit cible et un taux d'erreur donné sous la contrainte de DSP. Il peut être facile d'observer que γ_m ne peut être extrait simplement à partir de (2), on tient alors compte d'une marge de bruit distincte pour chaque sous-porteuse, γ_i , qui peut être définie comme

$$\gamma_i = \frac{1}{\Gamma N_0} \frac{E_i |H_i|^2}{2^{b_i} - 1}. \quad (3)$$

L'objectif de cette allocation étant de maximiser la marge, toutes les ressources d'énergie sont exploitées. Ainsi, $E_i = \hat{E}$, ce qui signifie que le signal est transmis en limite de DSP. Le problème de maximisation de la marge est

$$\begin{cases} \max \frac{1}{\Gamma N_0} \frac{\hat{E} |H_i|^2}{2^{b_i} - 1}, \forall i \\ \text{subject to } \sum_{i=1}^N b_i \leq \hat{R} \end{cases} \quad (4)$$

L'objectif est de maximiser la marge de bruit de chaque sous-porteuse individuellement tout en réalisant un débit cible de \hat{R} bits. La solution est obtenue en distribuant judicieusement les bits entre les sous-porteuses.

Chapitre 3 : Maximisation du débit

Introduction

Nous proposons d'intégrer le codage de canal dans le processus d'allocation des ressources. Pour améliorer les performances des systèmes à porteuses multiples CPL et démontrer l'efficacité du système LP-OFDM dans des scénarios codés, un schéma de codage de canal adéquat est sélectionné. Le schéma de codage de canal sélectionné est intégré dans les chaînes de communications OFDM et LP-OFDM. Les algorithmes d'allocation des bits et des puissances sont présentés pour les systèmes à porteuses multiples codés et les performances du LP-OFDM codé sont comparées avec l'OFDM codé en utilisant le même schéma de codage de canal. Les algorithmes d'allocation des ressources proposés sont assez souples et peuvent être utilisés pour n'importe quel schéma de codage de canal. En outre, le débit d'un système à porteuses multiples est maximisé sous la contrainte de TEB moyen. Différentes sous-porteuses d'un symbole OFDM sont autorisées à être affectées par des valeurs différentes de TEB, et la limite de taux d'erreur est imposée sur l'ensemble de chaque symbole OFDM/LP-OFDM. Cela signifie que le TEB d'un symbole OFDM/LP-OFDM ne doit pas dépasser le TEB cible. Cette approche donne un degré de liberté supplémentaire aux stratégies d'allocation des ressources pour la maximisation du débit sous la contrainte de DSP. En outre, nous présentons aussi les algorithmes d'allocation des bits et puissances pour la maximisation du débit OFDM et LP-OFDM dans le contexte CPL et sous les contraintes de DSP et de TEB moyen.

RM avec codage de canal dans l'allocation

L'algorithme d'allocation des ressources est modifié pour tenir compte des gains de codage. L'algorithme proposé peut être utilisé en combinaison avec un schéma de codage de canal. Les gains de codages peuvent être constants ou variables et dépendre des ordres de modulation, et doivent être connus. Afin de tenir compte du schéma de codage de canal dans la chaîne de communication, on a besoin de développer un algorithme d'allocation des ressources qui peut prendre en compte les gains de codage de canal. La stratégie de répartition des ressources pour le LP-OFDM codé est donnée comme

$$\begin{aligned} \bar{R}_k = & \lfloor L(2^{R_k/L - \lfloor R_k/L \rfloor} - 1) \rfloor \times (\lfloor R_k/L \rfloor + 1) \\ & + (L - \lfloor L(2^{R_k/L - \lfloor R_k/L \rfloor} - 1) \rfloor) \times \lfloor R_k/L \rfloor \end{aligned} \quad (5)$$

Maintenant, nous pouvons assigner un ordre de modulation propre à chaque séquence de précodage. La puissance d'émission, E_c^k , attribuée à ces séquences de précodage est donnée comme

$$E_c^k = (2^{b_c^k} - 1) \frac{\Gamma}{L^2} N_0 \sum_{i \in S_k} \frac{1}{|H_i|^2}. \quad (6)$$

Cet algorithme peut être généralisé pour tout schéma de précodage et tout schéma de codage de canal. Pour $L = 1$, cet algorithme distribue les bits et les puissances aux

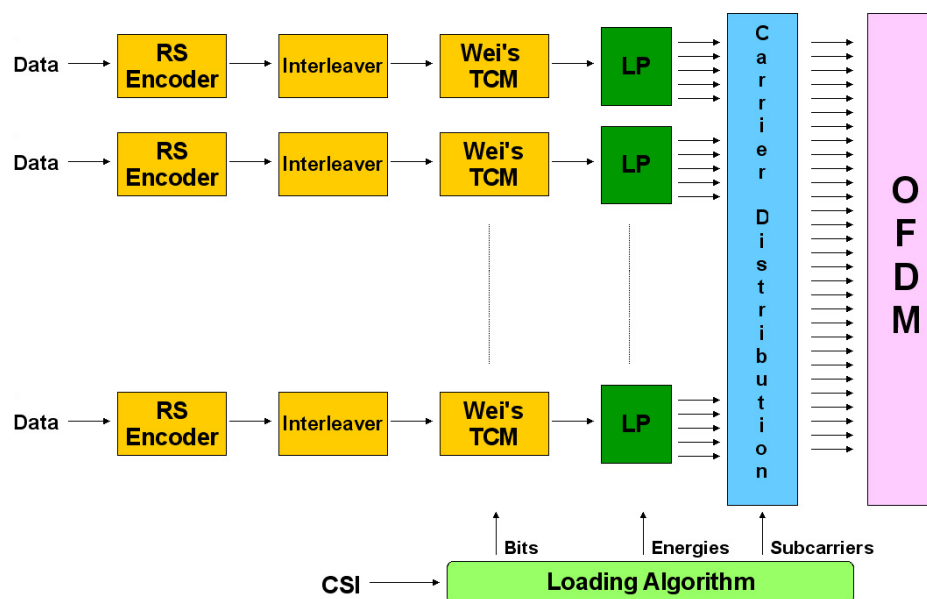


Figure 2: LP-OFDM codé.

sous-porteuses de la même manière que les bits et les puissances sont distribués dans le système OFDM conventionnel.

Le schéma de codage

Le schéma de codage adapté doit avoir des gains de codage importants et une mise en œuvre de complexité raisonnable. Sélectionnée sur ces bases, la chaîne de codage choisie est composée d'un codage interne en treillis de Wei à 4 dimensions (4D) avec 16-états, et d'un codage Reed Solomon (RS) externe. La structure de système LP-OFDM codé est montrée dans la figure 2.

Les résultats de simulations

La figure 3 montre le débit total atteint par symbole OFDM/LP-OFDM en fonction du gain moyen du canal. Les performances du système LP-OFDM sont comparées avec l'OFDM à différents gains moyens de canal pour les deux implémentations codées et non codées. On peut observer que le système proposé offre de meilleures performances que les systèmes existants. La figure 4 donne le pourcentage d'augmentation du débit obtenu avec le système LP-OFDM codé en comparaison avec l'OFDM codé et non codé pour différentes valeurs de gain moyen du canal.

RM sous la contrainte de TEB moyen

Nous proposons les algorithmes discrets et adaptatifs pour l'OFDM et le LP-OFDM sous les contraintes de DSP et de TEB moyen. L'algorithme proposé pour le sys-

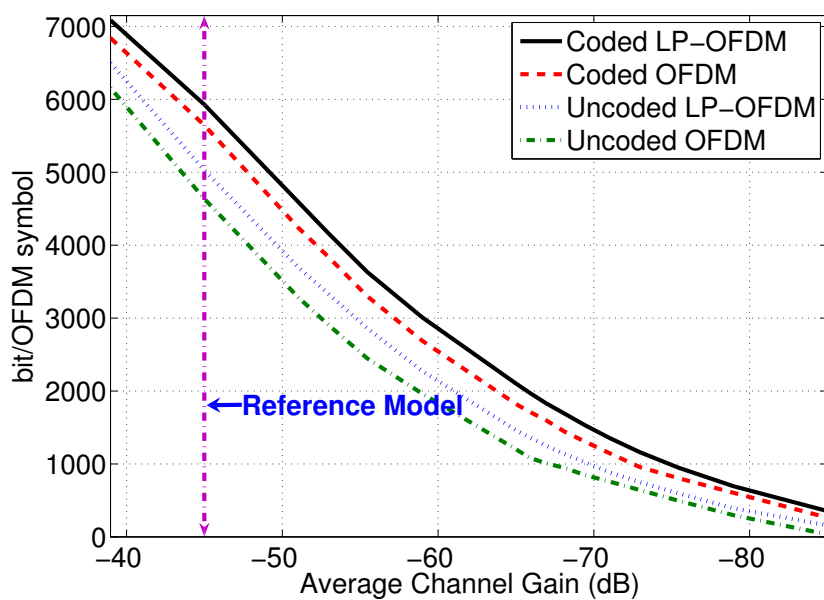


Figure 3: Débit vs gain du canal moyen.

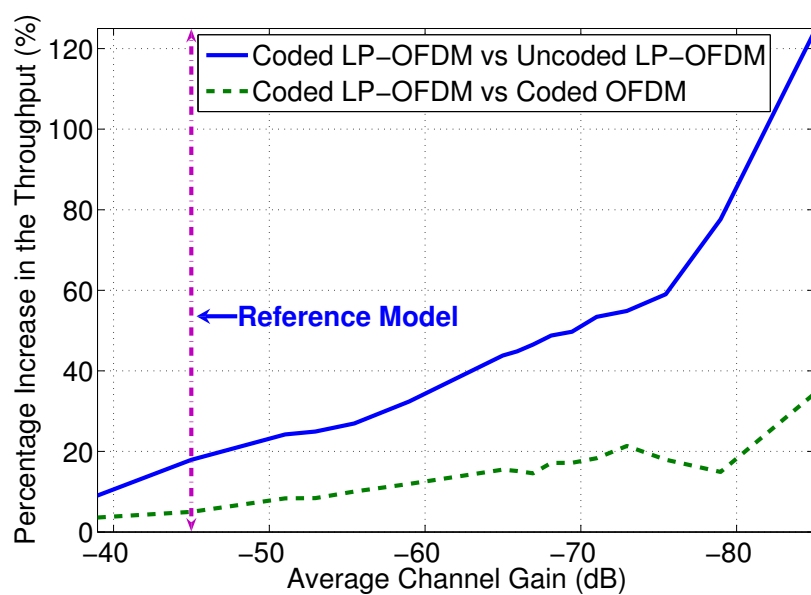


Figure 4: Pourcentage d'augmentation du débit.

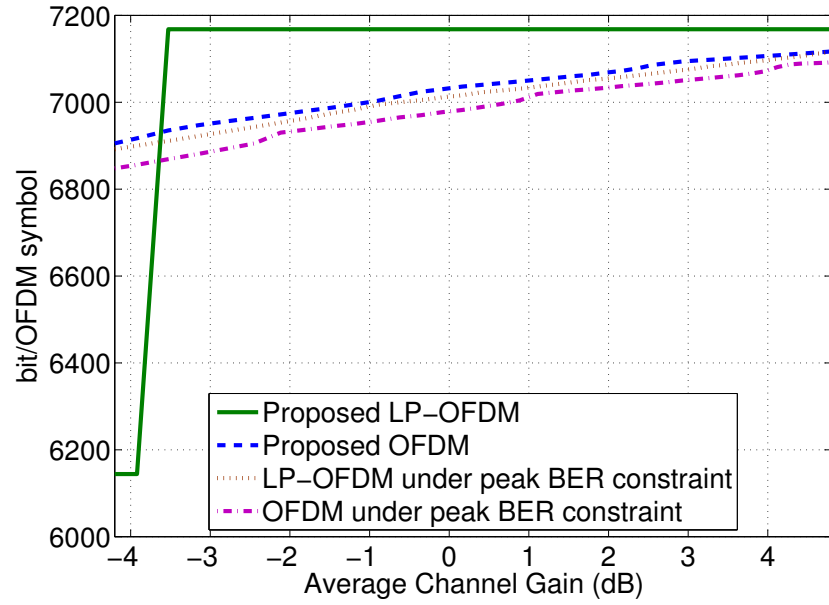
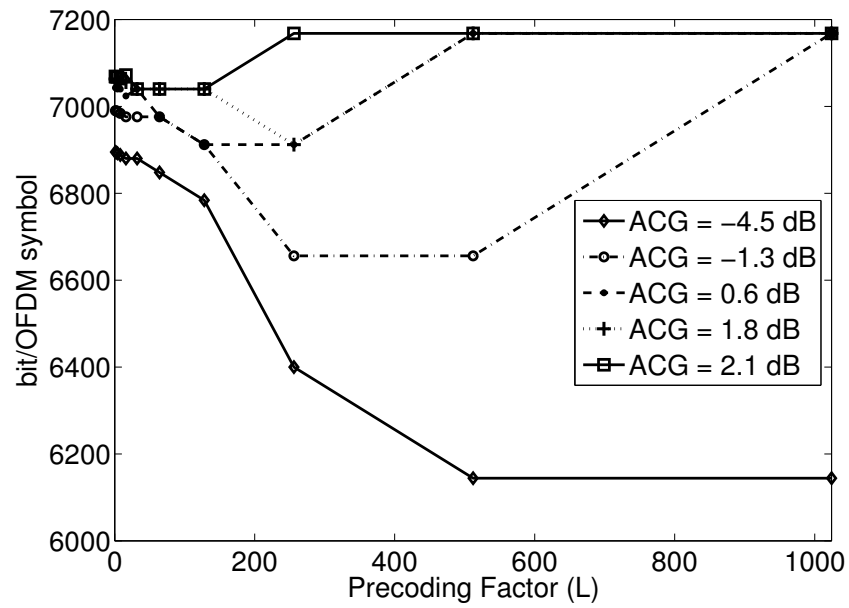


Figure 5: Débit vs gain moyen du canal

Figure 6: L vs gain moyen du canal.

tème OFDM est une version modifiée de l'algorithme de Wyglinski. Cette approche est également étendue au système LP-OFDM. Les avantages de ces systèmes sont observées dans le contexte CPL.

Les résultats des simulations

Dans la figure 5, les débits des systèmes proposés sont comparés à ceux du LP-OFDM et de l'OFDM sous la contrainte de TEB crête. Il est clair que l'OFDM atteint un débit plus élevé pour les faibles SNR (en anglais *signal-to-noise-ratio*) et le LP-OFDM donne de meilleurs résultats à fort SNR. La valeur optimale du facteur de précodage est obtenue en exécutant des simulations réalisées pour différentes valeurs possibles de L .

Chapitre 4 : Minimisation du TEB moyen

Introduction

Dans ce chapitre, une nouvelle approche de maximisation de la robustesse, appelée la minimisation de TEB moyen (MBM), est introduite, où le TEB moyen du système est minimisé pour un débit cible et un masque de puissance imposé. Les études analytiques de minimisation du TEB moyen des systèmes à porteuses multiples sont effectuées pour la première fois. Premièrement, le système OFDM conventionnel est considéré. Une étude analytique est effectuée pour obtenir la répartition des bits et des énergies optimales, qui minimise le TEB moyen du système. Ensuite, le problème de MBM est également étudié pour le LP-OFDM. En outre, une étude initiale sur MBM est exécutée pour le LP-OFDM en tenant compte du schéma de codage de canal dans le processus d'allocation des ressources.

MBM pour les systèmes OFDM

Le problème de MBM pour les systèmes OFDM est défini comme suit

$$\begin{cases} \min \frac{\sum_{i=1}^N P_i^b \cdot b_i}{\sum_{i=1}^N b_i}, \\ \text{subject to } E_i \leq \hat{E}, \text{ and } \sum_{i=1}^N b_i = R, \forall i \quad 1 \leq i \leq N, \end{cases} \quad (7)$$

L'allocation de bit et de puissance optimale, pour ce problème, peut être donnée par

$$\begin{cases} b_i^* = \frac{R}{N} + \log_2 \left(\frac{3}{2} \frac{E_i}{N_0} |H_i|^2 \right) - \frac{1}{N} \sum_{i=1}^N \log_2 \left(\frac{3}{2} \frac{E_i}{N_0} |H_i|^2 \right) \\ E_i^* = \hat{E}, \forall i \end{cases} \quad (8)$$

Dans l'algorithme proposé, au lieu d'initialiser toutes les sous-porteuses par 0 ou par b_{\max} bits, nous utilisons l'étude analytique réalisée pour trouver un raccourci vers la solution optimale. Cette approche analytique permet de réduire la complexité des systèmes de façon significative (en diminuant le nombre d'itérations) et donne exactement la même valeur de TEB moyen. La figure 7 montre le TEB moyen obtenu du système par rapport à différentes valeurs de débit cible pour les deux allocations, i.e. MM et MBM. On peut constater que le débit obtenu avec l'allocation proposée est supérieur à celui obtenu avec la répartition MM. Par exemple, la répartition classique MM donne un TEB moyen de 10^{-6} pour un débit cible de 5017 bits par symbole OFDM et la répartition proposée donne le même TEB pour un débit cible de 5089 bits par symbole OFDM.

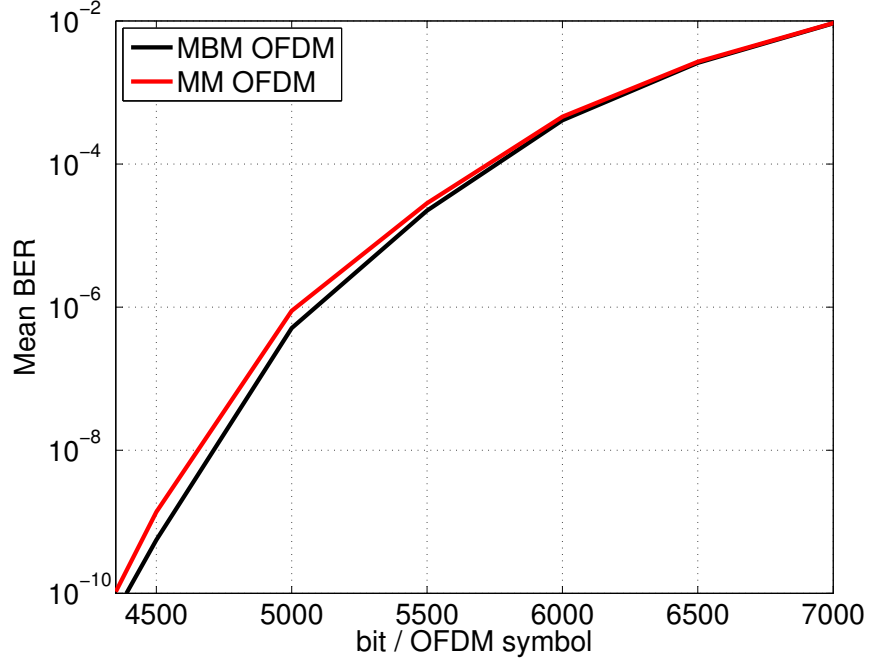


Figure 7: MM-OFDM vs MBM-OFDM.

MBM pour les systèmes LP-OFDM

Le problème MBM pour le LP-OFDM multibloc, composé de K blocs de longueur L (i.e. $K = N/L$) peut être donné par

$$\begin{cases} \min \sum_{k=1}^K 2 L \operatorname{erfc} \left(\sqrt{\frac{\alpha'_k}{2^{\frac{R_k}{L}} - 1}} \right) \\ \text{subject to } \sum_{c_k=1}^L E_c^k = \hat{E} \forall k, \sum_{k=1}^K R_k = R \end{cases} \quad (9)$$

On observe que ce problème est semblable à (7), si l'on remplace b_i par $\frac{R_k}{L}$ et α_i par α'_k . Par conséquent, en utilisant l'analogie entre les deux problèmes, la solution optimale peut être donnée par

$$R_k^* = \frac{R}{K} - \log_2 \left(\sum_{i \in S_k} \frac{1}{|H_i|^2} \right) + \frac{1}{K} \sum_{k=1}^K \log_2 \left(\sum_{i \in S_k} \frac{1}{|H_i|^2} \right). \quad (10)$$

L'équation (10) donne le nombre de bits pris en charge par chacun des blocs. La stratégie de répartition proposée fonctionne en deux étapes. Dans la première étape, le nombre de bits de chaque bloc est obtenu et ensuite le nombre optimal de séquences

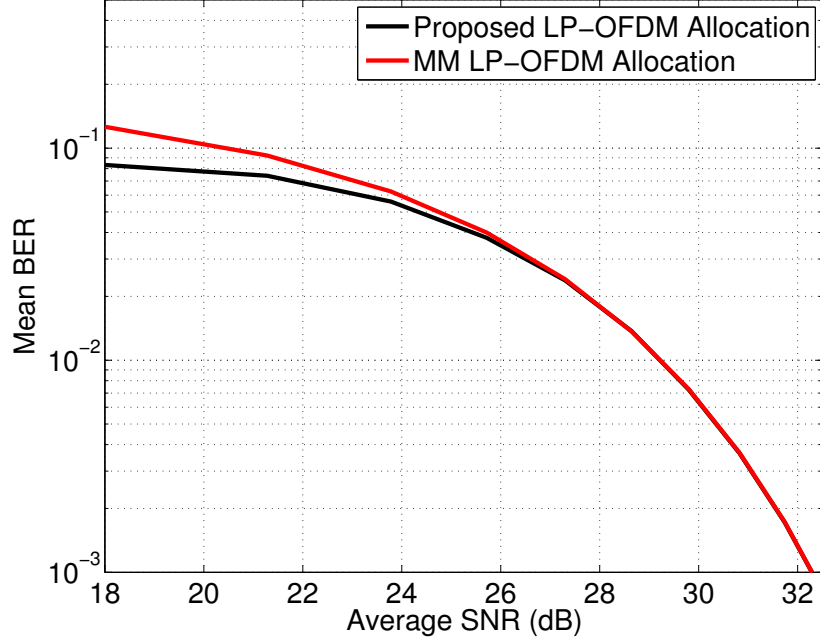


Figure 8: MM-LP-OFDM vs MBM-LP-OFDM.

de précodage utiles pour chaque bloc est calculé en utilisant

$$C^* = m \left[e^{\frac{R - 0.415}{1.4427}} - 1 \right]. \quad (11)$$

La répartition des bits et énergies entre les séquences de précodage d'un bloc est donnée comme

$$\begin{cases} E_c = \frac{\hat{E}}{C}, \forall c \\ b_c = \frac{R_k}{C}, \forall c \end{cases} \quad (12)$$

La figure 8 montre le TEB moyen en fonction du SNR à un débit cible de 4000 bits/symbole OFDM. Les performances de la répartition proposée sont comparées avec celles de la répartition MM pour le LP-OFDM. En outre, il est démontré que les performances du système LP-OFDM proposé sont meilleures que celle obtenues avec la répartition MM, en particulier pour les SNR faibles.

MBM pour les systèmes LP-OFDM codés

Nous effectuons une première étude sur la minimisation de TEB moyen d'un système LP-OFDM en tenant compte du schéma de codage de canal dans le processus

d'allocation des ressources. Cette étude est basée sur la technique d'optimisation graphique pour la minimisation du TEB moyen. Des codes convolutifs avec décision souple sont utilisés dans cette étude initiale. La même approche d'optimisation graphique peut également être étendue pour d'autres schémas de codage de canal. Les polynômes du codeur convolutif sélectionné sont en notation octale [133,171] et la longueur de contrainte est 7.

Jusqu'à présent, nous avons étudié les problèmes d'allocation des ressources dans l'hypothèse de la connaissance parfaite de canal à l'émetteur. Comme, il est bien connu que le récepteur ne dispose que très rarement d'une CSI parfaite, l'étude d'allocation des bits et des puissances avec des estimations bruitées est menée dans le chapitre suivant.

Chapitre 5 : RM avec CSI imparfaite

Dans ce chapitre, nous considérons le problème de la maximisation du débit pour les systèmes à porteuses multiples, en tenant compte d'une CSI imparfaite. Les algorithmes d'allocation sont proposés et considèrent le bruit d'estimation avant d'allouer des bits et des puissances aux différentes sous-porteuses. Ces algorithmes *sous-chargent* le système pour les valeurs élevées de la MSE (en anglais *mean square error*) d'estimation des coefficients du canal, afin de maintenir une valeur acceptable du TEB moyen. Au contraire, un algorithme qui ne tient pas compte des erreurs d'estimation, peut surcharger le système et augmenter par la suite le TEB moyen du système. En vue d'intégrer les effets de la CSI imparfaite dans le processus d'allocation des ressources, il faut trouver de nouvelles expressions du taux d'erreur qui sont modifiées en raison des estimations bruitées du canal. Nous considérons ce problème en utilisant deux approches différentes. Dans la première approche, on trouve l'expression généralisée du taux d'erreur pour tous les ordres de modulation. Cela signifie que nous n'avons qu'une seule expression du taux d'erreur pour toutes les tailles de constellation. Dans une autre approche, des expressions individuelles du taux d'erreur sont obtenues pour chaque ordre de modulation. Les algorithmes d'allocation des bits proposés sont basés sur les deux approches considérées, pour l'OFDM et le LP-OFDM, et offrent de meilleures performances de TEB moyen en comparaison des solutions existantes.

Le modèle d'erreur considéré

Nous utilisons le modèle d'erreur indiqué dans la figure 9. Ici, X_i est le symbole modulé sur une sous-porteuse i , X_i' est le symbole modulé après interaction avec le canal H_i , N_0 est le bruit blanc additif gaussien, Y_i est le symbole modulé bruité, et Y_i' est le symbole reçu après avoir été égalisé par le canal estimé \hat{H}_i . Nous supposons qu'aucune erreur ne se produit lorsque le canal estimé est renvoyé à l'émetteur, donc nous avons la même estimation du canal à l'émetteur et au récepteur. Le bruit d'estimation peut être caractérisé classiquement comme un bruit gaussien additif. Le gain du canal est estimé, $\hat{H}_i = H_i + e_i$, où le bruit d'estimation est une variable aléatoire gaussienne complexe de moyenne nulle et de variance σ_e^2 , égale au MSE de l'estimateur de canal.

L'allocation GERE

Dans la première approche, appelée GERE (en anglais *generalized error rate expression approach*), on trouve l'expression généralisée du taux d'erreur pour tous les ordres de modulation QAM qui tient compte de la CSI imparfaite. Cette approche est basée sur les travaux effectués par Ye [120]. Dans leur article, les effets de la CSI imparfaite ont été envisagés pour le système OFDM conventionnel. Nous étendons cette étude pour le système LP-OFDM et nous proposons les algorithmes d'allocation des bits et des puissances pour les deux systèmes OFDM et LP-OFDM. Ces algorithmes

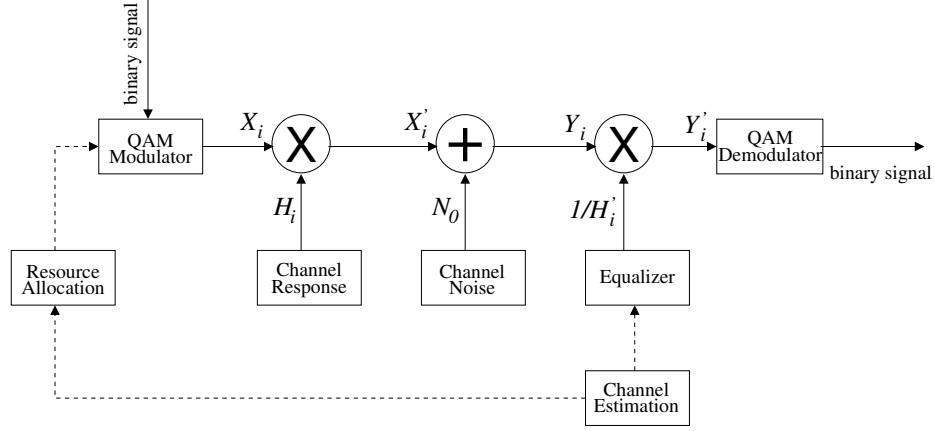


Figure 9: Le modèle d'erreur considéré.

discrets maximisent le débit du système pour un masque de puissance donné et un taux d'erreur cible en prenant en compte les effets d'estimation bruitée. L'expression du TEB \dot{P}_c^k pour une séquence de précodage c dans un bloc donné k de longueur L , en tenant compte de l'estimation du canal imparfaite, peut être donné comme

$$\dot{P}_c^k = c_1 \frac{2^{\frac{R_k}{L}} - 1}{x + \left(2^{\frac{R_k}{L}} - 1\right)} \exp \left\{ -\frac{y}{x + \left(2^{\frac{R_k}{L}} - 1\right)} \right\}, \quad (13)$$

où

$$x = c_2 \frac{\sigma_e^2}{1 + \sigma_e^2} \frac{E_k}{LN_0}, \quad y = c_2 \frac{E_k}{N_0} \sum_{i \in S_k} \frac{1}{|s_i|^2}, \quad (14)$$

et

$$s = \frac{1}{1 + \sigma_e^2} \dot{H}, c_1 = 0.2, c_2 = 1.6, \quad (15)$$

où R_k et E_k sont, respectivement, le nombre total de bits et la puissance disponible pour le bloc k . Dans cette approche, d'une part le nombre de bits par bloc est trouvé de façon itérative, et d'autre part ces bits sont répartis entre les différentes séquences de précodage d'un bloc donné. La figure 10 montre les performances des trois allocations différentes. On peut observer que les allocations proposées sont robustes contre le bruit d'estimation et fournissent une performance TEB moyen avantageuse par rapport à l'allocation itérative OFDM, qui ne prend pas en compte les effets de CSI imparfaite. La figure 11 compare les performances de débit des trois allocations.

L'allocation IERE

Dans cette approche, appelée IERE (en anglais *individual error rate expression approach*), nous obtenons des expressions de TES pour chaque ordre de modulation

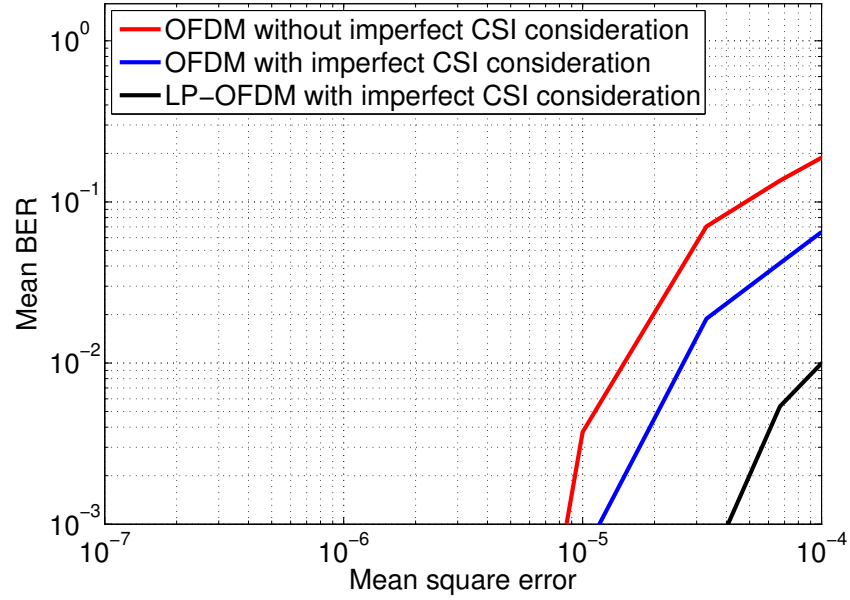


Figure 10: TEB moyen vs MSE.

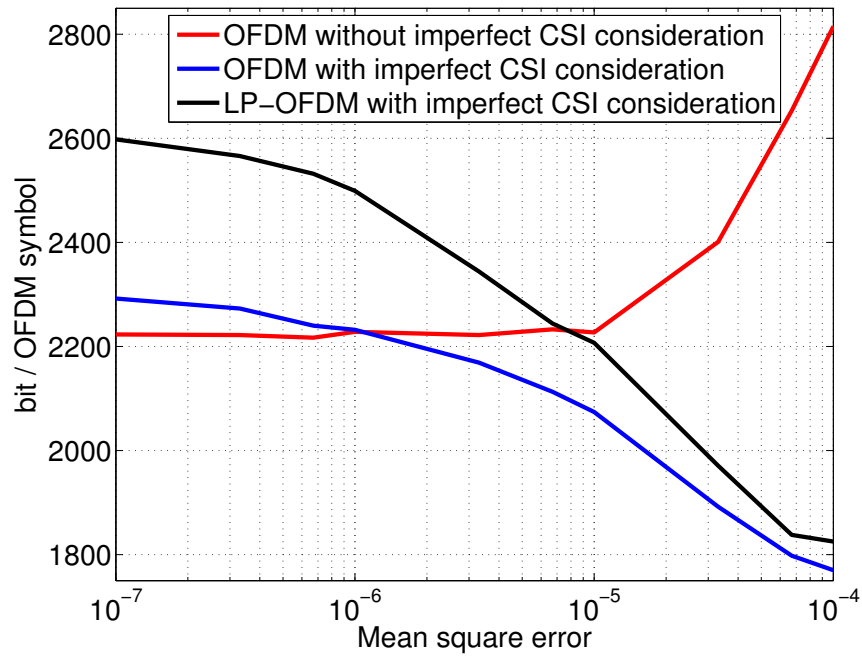


Figure 11: bit/OFDM sym vs MSE.

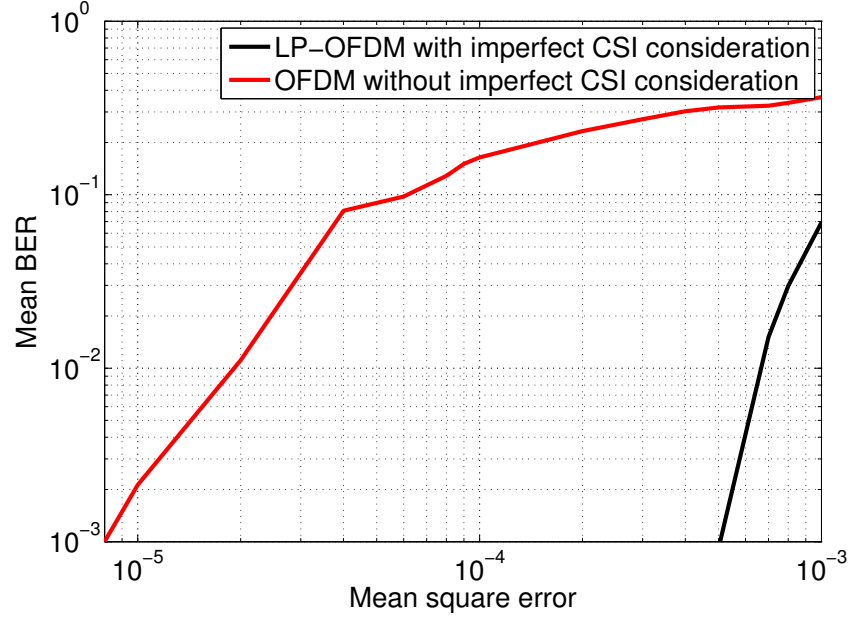


Figure 12: TEB moyen vs MSE.

qui prennent en compte les effets des estimations bruitées. La probabilité d'erreur, P^m , pour chaque point de la constellation avec une constellation QAM impaire, en présence d'un bruit d'estimation de canal, peut être donnée par

$$P^m = N^m Q \left[\sqrt{\frac{3\text{SNR}}{M-1}} \left(1 - \frac{4\sqrt{2}\alpha |X_i|}{d\sqrt{13M - 20\sqrt{2M} + 16}}} \right) \right], \quad (16)$$

et pour une constellation QAM paire, P^m peut être donnée par

$$P^m = N^m Q \left[\sqrt{\frac{3\text{SNR}}{M-1}} \left(1 - \frac{\sqrt{2}\alpha |X_i|}{d(\sqrt{M}-1)} \right) \right]. \quad (17)$$

La probabilité d'erreur globale sur une sous-porteuse est

$$P = \sum_m \text{Prob}(X_i = X_{i,m}) \cdot P^m. \quad (18)$$

L'algorithme proposé utilise des expressions de TES différentes pour différentes tailles de constellation. Le système est sous-chargé pour les valeurs élevées de MSE afin de maintenir un TEB moyen du système et la robustesse du système est améliorée sans compromettre de manière significative le débit du système.

La figure 12 montre la performance des deux allocations différentes. On peut observer que l'allocation proposée est robuste contre le bruit d'estimation et fournit de meilleures performances en terme de TEB moyen par rapport à l'allocation itérative

OFDM, qui ne prend pas en compte les effets de CSI imparfaite. L'allocation proposée offre une meilleure performance de TEB moyen même à des valeurs beaucoup plus élevées de MSE.

Conclusion

Cette thèse a principalement étudié la répartition des ressources diverses et des stratégies d'optimisation dans le but d'améliorer le débit et la robustesse des systèmes à porteuses multiples CPL, afin qu'ils puissent être utilisés efficacement dans les réseaux domestiques et pour la domotique. Des études théoriques ont été effectuées pour améliorer l'allocation des bits et des puissances dans le cas de systèmes OFDM et LP-OFDM. Plusieurs nouvelles idées ont été présentées comme l'intégration du schéma de codage dans le processus d'allocation des ressources, la maximisation du débit sous la contrainte de TEB moyen, la maximisation de la robustesse en termes de réduction de TEB moyen et l'allocation des ressources en tenant compte des effets de CSI imparfaite.

Au chapitre 1, nous avons présenté un aperçu général de la technologie CPL. Le chapitre 2 a été divisé en deux grandes parties. La première partie est consacrée aux systèmes à porteuses multiples en général. Différents schémas d'accès multiple ont également été expliqués et différentes combinaisons de l'OFDM et de l'étalement de spectre ont été illustrées. En fin de compte, le système sélectionné, le LP-OFDM, est détaillé et les avantages de ce schéma flexible ont été abordés, avantages dus principalement à la présence d'une composante de précodage linéaire. Dans la seconde partie de ce chapitre, nous avons présenté un aperçu général de la répartition des ressources et l'optimisation des systèmes OFDM conventionnels.

Le chapitre 3 est principalement centré sur le problème de maximisation des débits. Ce chapitre a été également divisé en deux grandes parties. La première partie a examiné le problème RM pour le système LP-OFDM sous la contrainte de TEB crête. Dans cette partie, une nouvelle stratégie d'allocation des ressources a été conçue lorsque le codage de canal est incorporé dans les algorithmes d'allocation. Dans la seconde partie du chapitre 3, le problème de maximisation de débit a été considéré sous la contrainte de TEB moyen. Au lieu de fixer le même taux d'erreur sur toutes les sous-porteuses/séquences de précodage, nous avons permis aux différentes sous-porteuses/séquences de précodage d'être affectées par des valeurs différentes de taux d'erreur et nous avons imposé la contrainte de taux d'erreur sur un ensemble de symboles OFDM/LP-OFDM.

Le chapitre 4 introduit une toute nouvelle méthode de maximisation de la robustesse, où le TEB moyen du système est minimisé afin d'améliorer la robustesse du système contre les diverses sources de bruit. Ce chapitre a été divisé en trois parties. Dans la première partie, l'étude analytique de MBM a été effectuée pour les systèmes OFDM conventionnels. La seconde partie du chapitre 4 a étendu l'étude de MBM au système LP-OFDM. Une étude théorique a été effectuée pour la distribution optimale des bits et puissances entre les séquences de précodage. En outre, l'étude analytique a été étendue afin d'optimiser le nombre de séquences de précodage utiles dans un bloc donné du système LP-OFDM pour un débit cible et sous la contrainte de DSP. Une étude initiale a été effectuée pour intégrer les effets du codage de canal dans le processus d'allocation des ressources du MBM en utilisant des techniques d'optimisation

graphique. A partir d'un cas d'école, cette étude a été étendue au système mono bloc LP-OFDM.

Au chapitre 5, nous avons poursuivi l'étude de la répartition des ressources en considérant une CSI imparfaite. Ici, pour la première fois, nous avons introduit les allocations RM LP-OFDM en tenant compte des effets de CSI imparfaite. Deux approches différentes ont été examinées pour contrer les effets néfastes des estimations bruitées. Ces allocations sous-chargent le système en présence de MSE élevés. La première approche, GERE, se compose d'une expression des taux d'erreur généralisée pour tous les ordres de modulation considérée. La deuxième approche, IERE, se compose d'expressions individuelles de taux d'erreur pour chaque ordre de modulation.

Diverses contributions de cette thèse ont été publiées dans les actes d'un colloque national et de six conférences internationales. Un article est soumis à une revue internationale. En outre, les travaux sur la maximisation de la robustesse vont être soumis dans la revue IEEE Transactions on Communications. Au cours de cette thèse, nous avons également collaboré très activement avec des partenaires industriels. En particulier la thèse a contribué à deux projets différents, un projet de recherche externe avec Orange Labs et le projet OMEGA, un projet intégré du 7^{me} PCRD financé par la Commission Européenne.

List of Figures

1.1	Outdoor PLC network.	13
1.2	Indoor PLC network.	14
1.3	Frequency response of 15-paths reference channel model for PLC. . . .	15
1.4	Length profiles of the attenuation of power line links.	15
1.5	Transmit PSD mask from HPAV specification.	17
2.1	Time response of a multi path channel.	28
2.2	Time and frequency domain representation of an OFDM signal. . . .	30
2.3	OFDM communication chain.	32
2.4	Mono block configurations.	39
2.5	Multi block configurations.	41
2.6	LP-OFDM system representation.	43
2.7	LP-OFDM single user transmitter.	44
2.8	Performance evaluation of uncoded QAM with convolutionally coded QAM.	49
2.9	Performance evaluation of uncoded QAM with convolutionally coded QAM.	49
2.10	SNR gap for various QAM modulation orders with target BER and target SER criteria.	50
2.11	Comparison of bit allocation for finite and infinite granularity of modulation in the case of bit rate maximization under PSD constraint. . .	54
2.12	Comparison of various bit allocation algorithms for margin maximization/total power minimization for same target bit and error rate. . . .	57
2.13	Comparison of bit allocation for finite and infinite granularity of modulation in the case of margin maximization under PSD constraint. . . .	58
2.14	Comparison of noise margin for finite and infinite granularity of modulation in the case of margin maximization under PSD constraint. . . .	59
3.1	Wei's 4D 16-states trellis code.	73
3.2	Trellis diagram of the considered convolutional coder [103].	74
3.3	Mapping of 2-dimensional cosets [103].	75
3.4	Constellation labels for $b = 2$ and $b = 4$ [103].	76
3.5	Constellation labels for $b = 5$ [103].	78

3.6	BER performance of the selected channel coding scheme over AWGN channel.	79
3.7	SNR gap evaluation for the selected channel coding scheme.	79
3.8	Uncoded LP-OFDM transmitter structure.	82
3.9	Coded LP-OFDM transmitter structure.	83
3.10	Developed communication system chain for simulation purposes. . . .	84
3.11	Achieved throughputs at various channel gains where $L = 32$ for LP-OFDM systems.	86
3.12	Transmit power distribution comparison where $L = 32$ for LP-OFDM systems.	86
3.13	Percentage increase in the throughput.	87
3.14	Throughput comparison of the proposed allocation for OFDM and the allocation proposed by Wyglinski at various average channel gains. . .	92
3.15	Throughput comparison of proposed allocations with OFDM and LP-OFDM allocations under peak BER constraint at various average channel gains.	92
3.16	Precoding factor vs bit rate at various average channel gains.	94
3.17	Power distribution comparison of allocation schemes under mean and peak BER constraints.	95
4.1	Mean BER performance comparison of MM and MBM allocations for various target bit rates.	102
4.2	Mean BER performance comparison of MM and MBM allocations for higher target bit rates.	103
4.3	Bit allocation comparison of MM and MBM allocations for a target bit rate of 4500 bit/OFDM symbol.	104
4.4	Mean BER comparison of the proposed allocations with Margin Maximization allocations for different average SNR, for $R = 4000$ bit/OFDM symbol.	109
4.5	Mean BER comparison of the proposed allocations with Margin Maximization allocations for various bit rates at average SNR = 12 dB. . .	110
4.6	First derivatives of BER with respect to transmit power versus total available power for different modulation orders.	112
4.7	Considered part of first derivatives of BER with respect to transmit power versus total available power for different modulation orders. . .	114
4.8	Results obtained from the iterative MBM algorithm.	115
4.9	Bit distribution for the proposed MBM allocation for mono block LP-OFDM.	116
4.10	Power distribution for the proposed MBM allocation for mono block LP-OFDM.	116
5.1	MCM subcarrier estimation error model.	124
5.2	Mean BER comparison for different values of mean square error. . . .	129
5.3	Bit rate comparison for different values of mean square error.	130

5.4	Goodput comparison for different values of mean square error.	130
5.5	Power distribution comparison.	131
5.6	Mean BER comparison for different values of mean square error. . . .	137
5.7	Bit rate comparison for different values of mean square error.	137
5.8	Goodput comparison for different values of mean square error.	138
A.1	Effects of imperfect CSI on 32-QAM constellation with Gray coding. .	150
A.2	4 internal points of 32-QAM.	152
A.3	4 corner points of internal square.	153
A.4	8 middle points of internal square.	153
A.5	8 corner points of circumference.	154
A.6	8 middle points of circumference.	155

List of Tables

1.1	Parameters of the 15-path model.	16
1.2	Attenuation parameters corresponding to the length profiles.	16
1.3	Comparison of PHY and MAC characteristics of existing systems. . . .	18
2.1	Puncturing sequences to generate different code rates.	48
3.1	Relation between 4-dimensional and 2-dimensional cosets.	75
3.2	Determining the top two bits of X and Y	77
3.3	Computation times in milliseconds, 1024 subcarriers, $P_T = 10^{-7}$ (Intel core 2, 2.4-GHz processor).	93
4.1	Results obtained for the textbook case.	113

List of Acronyms and Abbreviations

ADSL	Asynchronous Digital Subscriber Line
ANSI	American National Standards Institute
BER	Bit Error Rate
CABA	Continental Automated Buildings Association
CDMA	Code Division Multiple Access
CEPCA	Consumer Electronics Power Line Communication Alliance
COST	Committee on Science and Technology
CSI	Channel State Information
CSMA-CA	Carrier Sense Multiple Access with Collision Avoidance
DECT	Digital Enhanced Cordless Telecommunications
DHS	Digital Home Standard
DMT	Digital MultiTone
DS-CDMA	Direct Sequence-Code Division Multiple Access
DSL	Digital Subscriber Line
DVB-T	Digital Video Broadcast-Terrestrial
EDF	French Energy Company
EMC	Electromagnetic Compatibility
ETSI	European Telecommunications Standards Institute
FDMA	Frequency Division Multiple Access
FFT	Fast Fourier Transform
FMT	Filtered Multitone
FTTH	Fiber To The Home
GERE	Generalized Error Rate Expression
GSM	Global System for Mobile communications
HAN	Home Access Network
HD	High Definition
HPAV	HomePlug AV
HV	High Voltage
HWO	Hybrid Wireless Optics
ICI	Inter Carrier Interference
IEEE	Institute of Electrical and Electronics Engineers
IERE	Individual Error Rate Expression

IETR	Institute of Electronics and Telecommunications of Rennes
IFFT	Inverse Fast Fourier Transform
ISI	Inter Symbol Interference
ISO	International Organization for Standardization
ITU	International Telecommunication Union
J-PLC	Japan-Power Line Communications
LAN	Local Area Network
LP-OFDM	Linear Precoded Orthogonal Frequency Division Multiplexing
LTE	Long Term Evolution
LV	Low Voltage
MAC	Media Access Control
MBM	Mean BER Minimization
MCM	MultiCarrier Modulation
MIMO	Multiple Input, Multiple Output
MM	Margin Maximization
MV	Medium Voltage
OFDM	Orthogonal Frequency Division Multiplexing
OFDM/OQAM	OFDM carrying Offset QAM
OMEGA	Home Gigabit Access
OSI	Open Systems Interconnection
OVSF	Orthogonal Variable Spreading Factor
PAPR	Peak-to-Average Power Ratio
PLC	Power Line Communication
PLCA	Power Line Communications Association
PSD	Power Spectral Density
PSTN	Public Switched Telephone Network
PUA	PLC Utilities Alliance
QAM	Quadrature Amplitude Modulation
QoS	Quality of Service
RM	Rate Maximization
RoM	Robustness Maximization
SER	Symbol Error Rate
SNR	Signal-to-Noise Ratio
SS-MC-MA	Spread Spectrum-MultiCarrier-Multiple Access
TDMA	Time Division Multiple Access
UBB	Ultra BroadBand
UPA	Universal Power Line Association
UPCL	United Power Line Council
VDSL	Very High Bitrate Digital Subscriber Line
VOD	Video On Demand
VoIP	Voice Over Internet Protocol
Wi-Fi	Wireless Fidelity
WiMAX	Worldwide Interoperability for Microwave Access

Introduction

In recent years, the thriving growth of indoor and outdoor communication networks and the increase in number of data heavy applications used on personal and commercial devices are driving an ever increasing need for high speed data transmission. Among many competing technologies, power line communication (PLC) has its unique place due to already available power supply grids in both indoor and outdoor environments. The PLC technology exploits power supply grid to carry communication signals. In the PLC technology, high frequency communication signal (i.e. modulated carrier) is superimposed on the power supply grid already containing the electrical signal at 50 or 60 Hz depending upon the country. This superimposition is obtained by a process of inductive or capacitive coupling, which allows the data transfer on power lines. The coupler should ensure an optimal galvanic separation between power lines and communication devices, and acts as a high-pass filter on the receiver to differentiate the information signals from power signals.

Considering last mile communications, PLC appears to be a promising alternative to conventional technologies such as digital subscriber line (DSL) particularly in rural or underdeveloped areas where the conventional telephone line is still not available to a large population at the global level. But the coverage of power line grid is far more superior to telephone networks. Furthermore, PLC is also a suitable candidate for local area networks (LAN) and home automation. Many home appliances and equipments need to be permanently connected to the power outlet and the same outlet may also be used for communication purposes in PLC networks. It leads to a number of possible services and applications for home automation and enables the home appliances to interconnect with each other. Some of the devices may also be connected to the Internet through a suitable backbone network such as optical fiber. The wireless technologies are strong competitors to the PLC technology, but the coexistence of both technologies is likely to be seamed in future communication systems because of their unique characteristics.

This thesis was carried out at the Institute of Electronics and Telecommunications of Rennes (IETR) in the National Institute of Applied Sciences (INSA-Rennes). This work was partly funded by Orange Labs under a research contract 46145507. This thesis has also contributed to the OMEGA (Home Gigabit Access) project [1], which is an integrated project in the domain of information and communication technology and is funded by the European commission under the seventh research framework programme (FP7). During this project, we collaborated with 20 European partners

from industry and academia, including France Télécom R&D, Siemens AG, Thomson, Infineon, Telefonica, University of Oxford and University of Udine.

The aim of the OMEGA project is to develop an ultra broadband (UBB) infrastructure accessible to the most of the residential customers by exploiting UBB home access networks (HAN). This new infrastructure will enable the users to communicate at a transmission rate of 1 Gb/s via heterogeneous communication technologies, including power line communications, ultra wideband communications and optical fiber communication. The prime focus of this project is to study and implement sophisticated physical, media access control (MAC) and cross layer mechanisms to encounter noisy indoor environments in wireline and wireless context. Some of OMEGA prime objectives are to find a convergent technology independent MAC layer, to develop a combination of “no new wires” technologies in order to improve quality of service (QoS). Thus, OMEGA targets to make the information and communication services “just another utility”, as for example water, gas and electricity. With the success of OMEGA, it will be possible for a common user to access high bit rate information and communication services from his home, such as high-definition (HD) video, enhanced interactivity, 3D gaming, e-health applications and virtual reality.

For PLC technology, OMEGA aims to evaluate the possibility for employing higher bandwidth (up to 100 MHz) than existing PLC systems and sophisticated transmission schemes in order to maximize the useful bit rate. OMEGA also targets to measure and model the wireline channel through channel sounding techniques and to improve the transmission effectiveness in the presence of impulsive noise to deliver an improved QoS. Furthermore, OMEGA also promises to implement a secure and reliable network having backward compatibility with the existing networks such as HomePlug AV (HPAV).

Motivation and scope of the work

The primary motivation of this thesis is to increase the bit rate and the robustness of multicarrier PLC systems so that they can be efficiently used in home networking and automation. As it was stated earlier, PLC has some inherent advantages and in addition to this, it also inherits some built-in drawbacks from its already available infrastructure. The theme of this research work is to explore the different modulation and coding approaches in conjunction with various resource allocation and optimization schemes to bring PLC capabilities at par with other high bit rate alternatives and to cope efficiently with inherent disadvantages of power supply grid. Last but not the least, the objectives of this research also demand to take into account the limitations imposed by practical systems and to propose discrete bit and power loading algorithms capable of fulfilling growing needs of modern communication systems.

The scope of this work is enumerated in the following:

1. The first objective of this work is to achieve optimal bit rates for indoor PLC network using multicarrier systems. Conventional orthogonal frequency division

multiplexing (OFDM) and linear precoded OFDM (LP-OFDM) are applied to PLC LAN. Different error constraints are used to increase the system throughput while respecting a power spectral density (PSD) mask and a target error rate of the system. The channel coding gain is taken into account in the resource allocation process. This part mainly discusses following questions:

- I** How the channel coding gain can be integrated into the resource allocation process.
 - II** Does the linear precoding gain have any effect on the channel coding gain.
 - III** What are the impacts of mean bit error rate (BER) constraint on the bit rate maximization of multicarrier systems.
2. The aspect of the robustness (against various noise sources) improvement for PLC LAN is also taken into consideration by allocating bits and powers to subcarriers in such a way that a minimum mean BER is obtained. This approach is applied to conventional OFDM as well as to LP-OFDM systems under a PSD constraint (i.e. peak power constraint). Coded and uncoded modulation schemes are evaluated in combination with these strategies. Following questions are answered in this aspect:
- IV** How the robustness of the system may be enhanced using mean BER approach.
 - V** How the mean BER approach can be implemented taking into account the channel coding gain in the resource allocation process.
3. Bit and power allocation schemes are proposed for multicarrier systems taking into account the imperfect channel state information (CSI) at the transmitter. The system is underloaded for higher estimation noise so that the mean BER performance can be maintained at a reasonable level. Different approaches are investigated to counter the effects of noisy estimations in the resource allocation process and these approaches are applied to conventional OFDM and LP-OFDM systems for demonstrating their performance at system level. This part mainly raises following issues:
- VI** What are the effects of imperfect CSI on the performance of adaptive multicarrier systems.
 - VII** How different approaches can be implemented in order to reduce the effects of noisy estimations on system performance.

Outline of the thesis and scientific contributions

This doctoral dissertation investigates various resource allocation and optimization strategies to increase the overall performance of PLC networks. The performance of

PLC networks might be measured in terms of bit rate, noise margin or mean BER of the system. These resource allocation and optimization approaches are treated for both uncoded and coded scenarios. Novel discrete bit loading algorithms are also proposed for practical systems. For optimal allocation of bit and power to different subcarriers in a multicarrier system, it is generally supposed that perfect CSI is available at the transmitting side (i.e. estimation noise is absent). Here, optimization studies are performed for both scenarios i.e. with and without the assumption of perfect CSI at the transmitter. In this dissertation, the simulation results are presented to verify theories and analytical studies.

Chapter 1 specifies some of the fundamental aspects of PLC. A brief history of PLC is outlined followed by a discussion on applications of the PLC technology. The characteristics of the power line grid are described in general followed by a short analysis of the considered PLC channel model. Finally, the recent progress in the domain of PLC is considered. Various associations and consortiums are discussed related to the standardization and regulation of the PLC technology. Recent research projects are also presented here, with a special emphasis on the OMEGA project, to which this thesis contributes. The future possibilities and applications of the PLC technology are also considered in this chapter.

Chapter 2 presents various multicarrier system configurations. An overview of conventional OFDM systems is given. The spread spectrum principle is also elaborated in this chapter. Different transmission schemes, consisting of the combination of spread spectrum with OFDM, are analyzed. Finally, the considered system in this thesis is presented. This chapter also discusses the resource allocation and optimization in general. An introduction to Shannon theoretical capacity is given followed by the description of fundamentals of resource allocation and optimization for multicarrier systems. Different resource allocation strategies are considered. Firstly, the bit rate maximization problem is explained in the context of conventional multicarrier systems. Subsequently, the problem of robustness maximization is explored and some existing robustness maximization algorithms are also simulated.

Chapter 3 is devoted to bit rate maximization (RM) aspect of multicarrier systems. Firstly an overview of bit rate maximization is given. Then bit rate maximization problem is studied for two different constraints. One is the peak BER constraint where a target BER is respected for each subcarrier, this is also the target BER of the entire system. The other one is the mean BER constraint, where instead of fixing BER on each subcarrier, the mean BER of an OFDM symbol is taken into account and different subcarriers are allowed to be affected by different BER values. In this chapter, we also introduce a new idea of integrating the channel coding gains in the resource allocation process for bit rate maximization of OFDM and LP-OFDM systems. Bit and power loading algorithms are proposed that take into account channel coding gains in the resource allocation process. A concatenated channel coding scheme, consisting of the

combination of an outer Reed-Solomon (RS) code and an inner multidimensional trellis code, is selected for PLC systems.

Chapter 4 introduces a new robustness maximization (RoM) approach where the robustness of the system is enhanced by allocating bits and powers to subcarriers in such a way that the error rate of an entire OFDM symbol is minimized for a given target bit rate. This new approach is termed as mean BER minimization (MBM). Analytical studies are performed for OFDM and LP-OFDM systems to minimize the mean BER of the system for a target bit rate and a given PSD mask. Moreover, using these analytical studies the bit and power loading algorithms are also proposed for practical systems that minimize mean BER of the system using discrete modulations. An initial study on MBM LP-OFDM optimization is also performed taking into account the channel coding gain in the resource allocation process.

Chapter 5 takes into account the problem of noisy estimations. In resource allocation, it is generally supposed that the channel has been perfectly estimated and according to the channel responses on different subcarriers, bits and powers are allocated. For example, different constellations of quadrature amplitude modulation (QAM) can be used to assign different numbers of bits to subcarriers. In practice, perfect CSI is rarely achieved. In this chapter we study two different approaches for taking into account the imperfect CSI in resource allocation algorithms in order to underload the system at high mean square errors (MSE) of channel estimator for the sake of better mean BER performance. An algorithm, which does not take into account the estimation errors, can overload the system which subsequently degrades the mean BER performance.

Finally, in the general conclusion of the thesis, we summarize this dissertation and draw some perspectives for this work. Some recommendations are also proposed for future research works.

List of Publications

Journal Papers

- J1.** F. S. Muhammad, A. Stephan, J-Y. Baudais and J-F. H  lard “Analysis of Mean Bit Error Rate Minimization for Orthogonal Frequency Division Multiplexing,” submitted to *Wiley InterScience International Journal of Communication Systems*, 2010.
- J2.** J-Y. Baudais, F. S. Muhammad, and J-F. H  lard “Robustness maximization of parallel multichannel systems under peak-power and bit rate constraints,” to be submitted to *IEEE Transactions on Communications*, 2010.

International Conferences

- C1.** F. S. Muhammad, J-Y. Baudais and J-F. Hélard “Bit rate maximization for LP-OFDM with noisy channel estimation,” in *Proc. IEEE International Conference on Signal Processing and Communication Systems (ICSPCS)*, pp. 1-6, USA, Sep. 2009.
- C2.** F. S. Muhammad, J-Y. Baudais and J-F. Hélard “Rate maximization loading algorithm for LP-OFDM systems with imperfect CSI,” in *Proc. IEEE Personal, Indoor and Mobile Radio Communications Symposium (PIMRC)*, Japan, Sep. 2009.
- C3.** F. S. Muhammad, A. Stephan, J-Y. Baudais and J-F. Hélard “Bit rate maximization loading algorithm with mean BER-constraint for linear precoded OFDM,” in *Proc. IEEE International Conference on Telecommunications (ICT)*, pp. 281-285, Morocco, May 2009.
- C4.** F. S. Muhammad, A. Stephan, J-Y. Baudais and J-F. Hélard “Mean BER minimization loading algorithm for linear precoded OFDM,” in *Proc. IEEE Sarnoff Symposium (SARNOFF)*, pp. 1-5, USA, Apr. 2009.
- C5.** F. S. Muhammad, J-Y. Baudais, J-F. Hélard and M. Crussière “A coded bit-loading linear precoded discrete multitone solution for power line communication,” in *Proc. IEEE Workshop on Signal Processing Advances in Wireless Communications (SPAWC)*, pp. 555-559, Brazil, Jul. 2008.
- C6.** F. S. Muhammad, J-Y. Baudais, J-F. Hélard and M. Crussière “Coded adaptive linear precoded discrete multitone over PLC channel,” in *Proc. IEEE International Symposium on Power Line Communications and Its Applications (ISPLC)*, pp. 123-128, Korea, Apr. 2008.

National Conferences

- N1.** F. S. Muhammad, J-Y. Baudais and J-F. Hélard “Minimisation du TEB moyen d’un système OFDM precodé,” in *Proc. Colloque Groupe de recherche et d’étude de traitement du signal (GRETSI)*, pp. 1-4, France, Sep. 2009.

Chapter 1

Data transmission through PLC

Contents

1.1	History of power line communication	8
1.2	Application of power line technology	10
1.2.1	The power line grid	12
1.2.2	The power line channel	14
1.3	PLC technology of today	18
1.3.1	Consortiums	18
1.3.2	The OMEGA project	21
1.4	Future of PLC	23
1.5	Conclusion	24

1.1 History of power line communication

Power line communication has been around for quite some time now. The idea of using electrical lines for the transfer of information is almost two centuries old [2]. The first attempt to remotely measure the voltage levels of batteries at an unmanned site in the London-Liverpool telegraph system was made in 1838 by Edward Davy [3]. The first PLC patent on electricity meter with power line signaling was filed by Joseph Routin and C. E. L. Brown [4] in 1897. In 1905, Chester Thoradson [5] patented the remote reading of electricity meters using an additional signaling wire. The first automatic electromechanical meter repeaters were produced in 1913 and the application of thermionic valves on metering was started in 1927. 1936 was the year when indirectly heated cathode valves were used for the first time and when batteries were no more needed. The miniature valves were first utilized in 1947 followed by the transistor in 1960, which reduced the system size quite significantly. In 1967, the emergence of the integrated circuit and in 1980, the appearance of microprocessor influenced the PLC systems considerably.

In the 1980s, the PLC technology was gradually opened to the public through home automation. Various industries marketed PLC modules to drive all types of electrical devices inside a building or a house. These systems allowed different networked devices to communicate without having additional wires. The most common domestic applications were the On/Off switching of lights, the heating system temperature controllers, and the security monitoring of the premises. Although the use of power lines for home automation is still in its infancy, the PLC technology has now gone beyond this kind of low bit rate applications and is moving towards high bit rate communications. Indeed, with the increasing demand of domestic Internet connections, the PLC has become a new strategic priority in recent years. It is now becoming difficult to maintain a list of players in the field as they have proliferated. The main advantage of PLC technology, as highlighted by many, is the density and ubiquity of electricity infrastructure. The electricity distribution network is not only present outside and inside of buildings along an extremely dense mesh, but it is actually much more widespread across the globe as compared to the telephone network. As we know that reducing deployment costs is a key factor in the development of new communication networks, therefore it is not surprising that today the world is looking at the PLC technology. However, because of its hostile propagation properties, which are not suitable for data transmission, manufacturers have long shunned the PLC technology. It is only with the recent progress made in the areas of digital communication and signal processing combined with the rise in telecommunication market that the PLC technology is gaining new interests.

In the last two decades, various alliances and associations of major industrial groups have been formed including those representing electricity generators. Their purpose is to promote PLC technology, encourage technical advances and support the field tests. International HomePlug alliance is one of the most influential of these associations, which was created in March 2000 and has over 70 members, including Électricité de France (EDF), France Télécom, Motorola, Sony and Mitsubishi just

to name a few [6]. PLC forum is another group that was established by European industry leaders in 2000 to promote the PLC technology in Europe [7]. Its North American counterpart named Power Line Communications Association (PLCA) and Japan's popular J-PLC (Japan-Power Line Communications), emerged in 2001 and 2003, respectively. In Europe, another organization, the PLC Utilities Alliance (PUA), supports the development of the PLC technology. It was also founded by huge European power industries, but their main focus is marketing instead of the technology itself.

At the same time, many tests have been performed in large scale to assess the feasibility of the PLC technology and subsequent implementation challenges. One of the first tests was performed by Swiss in 2001 in Freiburg under the supervision of office of communications, in which the electromagnetic disruption caused by the PLC was measured. The Israeli department of electricity named public utility authority launched a large scale test in Zaragoza (Spain) on 300 buildings and 20,000 houses involving the installation and configuration of 140 processors. The results were very promising leading to a commercial offer from Mitsubishi in the cities of Barcelona, Madrid and Zaragoza. The German company MVV has also implemented several PLC access networks on experimental basis in the cities of Hamburg, Mannheim and Magdeburg, allowing over 3,000 subscribers to test high speed communications over low voltage lines. Finally in France, EDF through its specialized subsidiary EDEV-CPL (created in 2003) participated in various research projects of PLC deployment. In collaboration with the General Council of La Mancha, EDF has worked on an ambitious project to equip the region of Cherbourg and Saint-Lô in July 2003. Similarly, in the department of Hauts-de-Seine, a study has been conducted since the beginning of 2004 together with two access providers Tiscali and Tele2.

SmartLabs Inc introduced a home automation networking technology in 2001 known as INSTEON [8]. The main objectives of this technology were sensing applications and domestic control. It is based on the X10 standard. INSTEON technology follows a dual-band mesh topology and enables simple devices to be networked together using power lines and/or RF. This technology is less susceptible to noise and interferences than other single band networks. The 131.65 kHz band is allocated to PLC and the binary phase shift keying (BPSK) is selected as modulation scheme. INSTEON also includes error detection and correction. It also has backward compatibility with X10 and offers an instantaneous data rate of about 12.9 kb/s and a continuous data rate of 2.8 kb/s. INSTEON devices are also peers, in which each device can transmit, receive, and repeat messages of the INSTEON protocol without any additional network devices or software. The main applications of INSTEON include control systems, home sensors, energy savings, and access control.

In the current decade, the frequency bands for PLC have been extended from a few kHz to ten's of MHz. The revolution in the digital electronics such as the development of powerful processors, new techniques of digital signal processing and discrete algorithms have made it possible to use higher modulation orders and iterative error correcting techniques in embedded and integrated systems. Now it is possible to have

broadband communications over power lines using extended frequency bands and latest advances in digital technologies. Also the outdated regulations have slowed down the use of megahertz frequencies in PLC. However, the development of Internet has stimulated the inventions of new ways to transmit information to each household. Nowadays, the electricity network covers almost all households, and using the public electricity and indoor distribution networks for broadband communication has therefore gained ground. The suitable communication techniques have been intensively investigated; here, also the development of wireless communication is acknowledged. Recently, in the research community the study of PLC systems has been extended up to 30 MHz and PLC channel characteristics have also been widely researched. Many application-specific integrated circuits (ASICs) have also been developed for the broadband PLC systems. Very few power distribution companies started commercial activities to offer broadband Internet access through power lines but the interest is still there due to the wide coverage of power lines in rural areas. However, the utilization of PLC for home automation and networking remains a very interesting topic for research. In 2002, several HomePlug compliant home networking products were presented in the USA, and during the following year in Europe. HomePlug 1.0 specification is described in detail in [9].

1.2 Application of power line technology

Power line communication is considered as a promising solution for high bit rate communications, multimedia distribution and high speed Internet access while exploiting already available power supply grids without any need of infrastructure development [10]-[13]. PLC can play its vital role in those areas where Internet services are not available through public switch telephone network (PSTN) or wireless networks such as wireless fidelity (WiFi) and worldwide interoperability for microwave access (WiMAX). There is a strong dearth and need for harmonization of broadband PLC technology with existing wireless systems to have an optimal coexistence. An electromagnetic compatibility (EMC) issues for the use of high frequency bands in PLC is the topic of high research interests in recent times.

One of the most striking examples is undoubtedly the domestic Internet usage. This sector is one of those who have experienced the strongest growth in terms of number of subscribers for instance in France from a few tens of thousands in 1998 to over 95% of French population at the end of 2007 [1]. In this domain, demands and supplies have continued to evolve according to an evident trend of increasing volume and speed of information transfer. In this race of more and more high bit rate requirements, the different players and service providers are now offering many high speed and market oriented services such as digital TV, telephone, voice over Internet protocol (VoIP) and video on demand (VOD).

The other existing high bit rate wired solutions are DSL and fiber to the home (FTTH). Both of these solutions cost much higher than the capillary (already built) power line network. On one hand, FTTH is a very expensive solution from an instal-

lation point of view while on the other hand DSL is not so cheap to attract investors to make a try. In available wireless options, WiMAX might be a promising candidate but it also requires a significant amount of work in terms of antenna tower installations for wireless backhauls. Furthermore, these installations can raise environmental issues in rural areas where the broadband is primarily required to solve the problem of digital divide. The solution of these fundamental problems can be found in PLC technology, which is not only cheap and practical but also does not require exceedingly high cost for installation. Due to these considerations, PLC is gaining more and more research interest every day and several projects/research teams have addressed the challenges associated with electromagnetic compatibility [14]-[16], channel modeling [17]-[19], transmission/reception [20]-[24], networking [25]-[27], and optimal allocation of resources [28]-[30].

With the end of telecommunication monopolies in 1998, the dramatic changes occurred in the scene of telecommunication advancement and services. The significant advances in the field of transmission/reception techniques, digital modulation, source and channel coding, detection techniques and multiple input and multiple output technology (MIMO) [31] made it possible to provide high quality broadband communication services using PLC. Low-voltage (LV) power grid has been proposed to provide high speed Internet access to domestic customers as an alternative to conventional solutions for instance FTTH, asynchronous DSL (ADSL), cable modems and other wireless technologies. Generally speaking, it is considered that LV PLC networks have a physical tree topology where PLC modems are installed at medium-voltage/low-voltage (MV/LV) transformer and can provide services to all buildings of the locality, as shown in Fig. 1.1. It is needed to optimize the architecture of the LV PLC network for particular characteristics of the power line grid that changes from one premises to another, depending upon the number of households per transformer and the distance between the transformer and the consumer building. In European topologies, where longer distances are involved, intermediate repeaters are required to regenerate the information signal for providing reasonable coverage to all power outlets at customer premises.

Indoor PLC network enjoy increasingly high research interests. The main advantage offered by power line based home networks is the already available infrastructure of wires and outlets, therefore they don't require new cable installations. Different devices can communicate on their own. For instance, these networks give a perfect solution to the idea of home automation. Furthermore several computers, printing devices, scanners, telephones, can be connected together while all of them may also share the broadband Internet at the same time. An example of indoor PLC network is shown in Fig. 1.2.

The outdoor network is connected to the telecommunication backbone network via a coupler and a base station placed at MV/LV transformer. This base station converts data received from the global network (such as Internet) to a suitable format for power lines. It also collects information from the local loop and transfers it to the

other parts of the global network via conventional transport networks. All users of a neighbourhood are linked to the base station via a single branch of the grid.

1.2.1 The power line grid

The internationally uniform hierarchical structure of power line grid is as follows [32]:

- High voltage (HV, above 36 kV) lines are used to connect power-generating station to a substation. These lines form the backbone of power distribution network and generally have the voltages in the range of 155,000 to 765,000 volts. Due to their highly noisy behaviour, HV lines are not used for information transfer and are normally substituted by an alternative solution such as fiber optic. The research work to develop equipment capable of transmitting data over noisy HV lines is underway.
- Medium voltage (MV, ranging from 1 kV to 36 kV) lines are routed from a substation to a neighbouring transformer. These lines have manageable voltage ranges from 7,000 to 15,000 volts. HV lines form the backbone of an electric utilities data over power line infrastructure. These lines constitutes a fine meshed network, bring electrical power into cities, towns, and villages.
- Low voltage (LV, below 1 kV) lines connect the neighbouring transformer to the premises. The voltage is stepped down to 230 volt (or 120 volt, depending upon the country), which is used within homes and small businesses. Therefore it is the LV line, which is brought to the consumer. The LV grid represents a very fine-meshed network, precisely adapted to the density of consumer loads.

As shown in Fig. 1.1, power is distributed to the consumer premises from an MV/LV transformer using either underground or aerial cables. These cables are terminated on a panel board where different electric appliances and sockets are connected through wiring. In Europe, an MV/LV transformer generally provides power to hundreds of household customers. Typically, from 3 to 10 service cables emerge from one transformer substation, which form a tree-like structure. Three phases are provided. The voltage from phase to phase is 400 volts while the voltage from phase to neutral (ground) is 230 volts. All three phases and neutral are routed (except in some countries where only one phase and the neutral are provided) to the consumer's panel board, therefore the service cables include 4 conductors.

In the United States, power distribution works in a different way. The MV distribution circuit consists of a three phase main trunk. A two-phase or one-phase tap may extend to load premises depending upon the load value. In close proximity, single-phase transformer provides the low voltage that is directly connected to the customer's panel board. Due to this, the length of the LV component is generally less than 300 m, consisting of 1 to 10 customers per transformer. Common loads use 120 volts whereas heavy loads are connected to 240 volts.

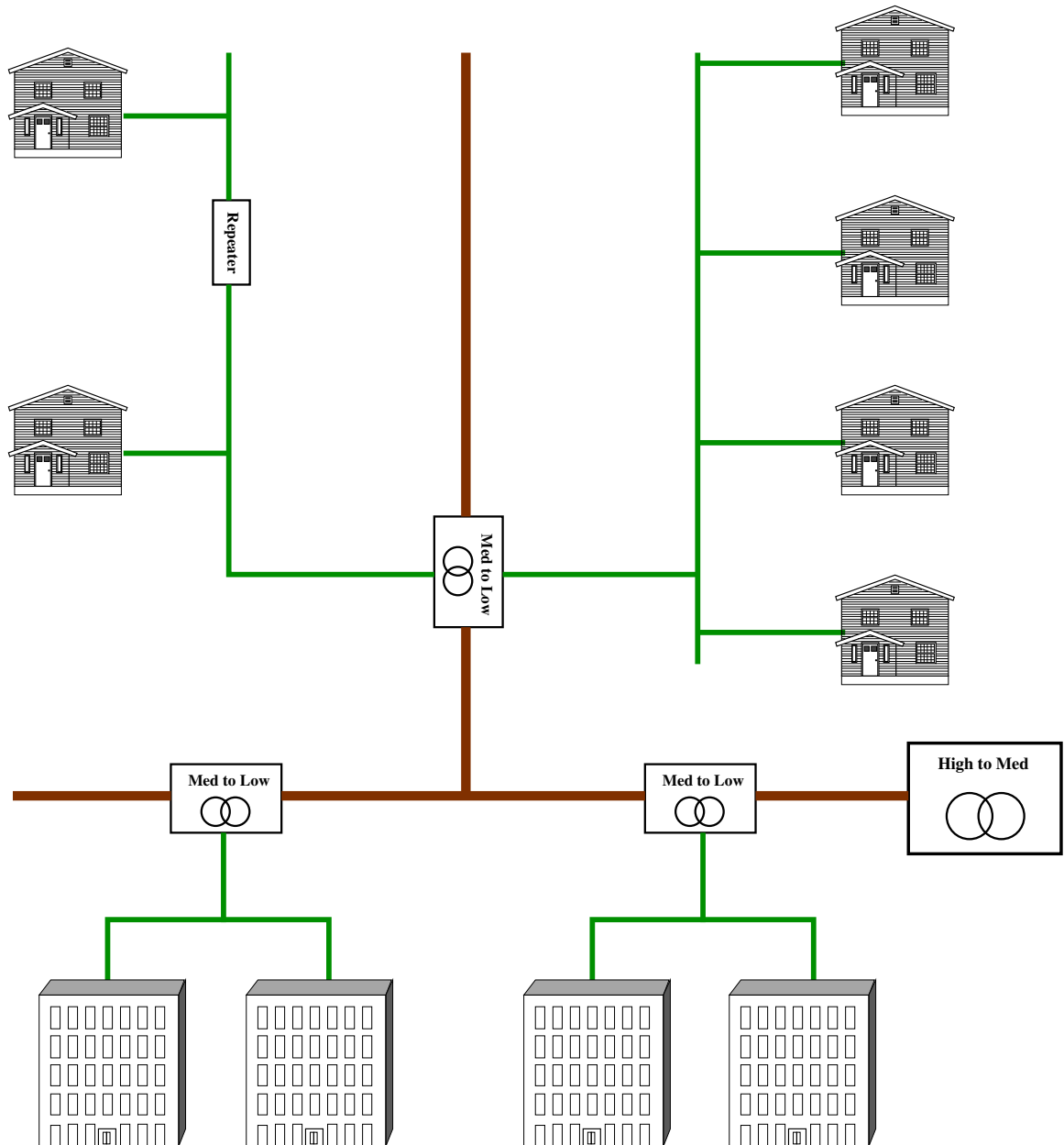


Figure 1.1: Outdoor PLC network.

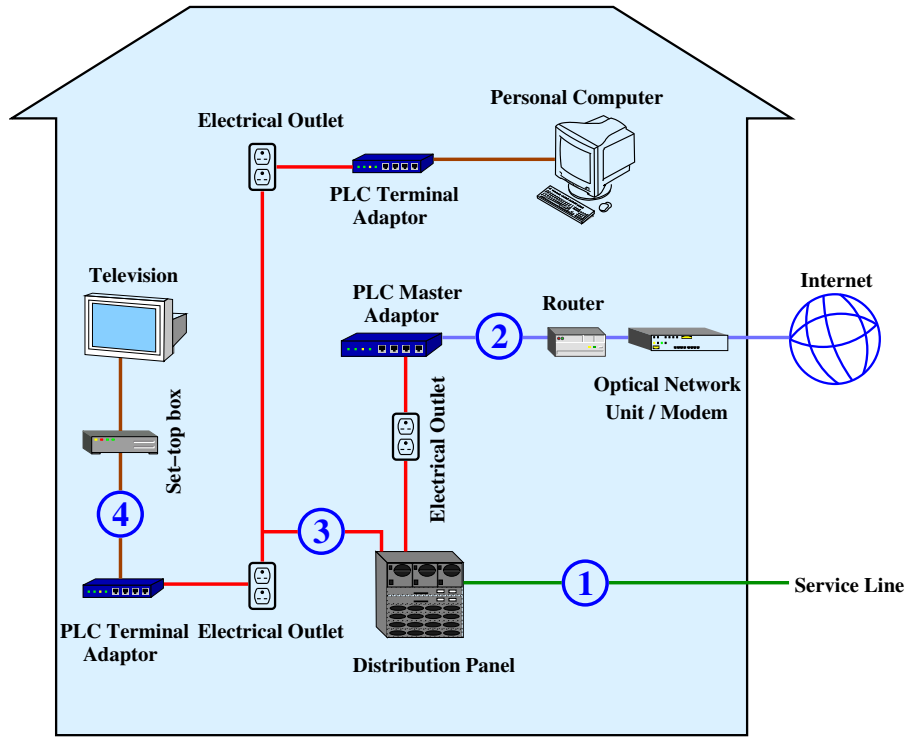


Figure 1.2: Indoor PLC network.

1.2.2 The power line channel

We need suitable channel models to really evaluate the performance of a PLC system. These channel models may include different classes of channel frequency response and a comprehensive noise scenario. Generally, in many different domains of telecommunication, we have some universally recognized channel models. For instance, for mobile radio communications, Committee on Science and Technology (COST) models have a universal acceptance. Similarly, for DSL communications, American National Standards Institute (ANSI) and European Telecommunications Standards Institute (ETSI) standards have world-wide recognition. Critically speaking, we do not have any standardized channel model for PLC systems.

In the process of channel modeling for PLC systems, we encounter many crucial hurdles. PLC networks differ significantly in topology, structure, and physical properties from classical media such as twisted pair cable, coaxial, and fiber-optic cables. Therefore, PLC systems have to face rather hostile characteristics [33]. PLC signals suffer from reflections caused by impedance mismatches at line discontinuities. Thus the PLC channel is characterized by a multipath environment with frequency-selective fading. Generally, the channel transfer function has a lowpass characteristic, with deep notches at some points. The number of branches is directly proportional to attenuation as some transmitted power is absorbed at each tap. The time domain signal is dispersed due to multipath reflections. This dispersion is characterized by

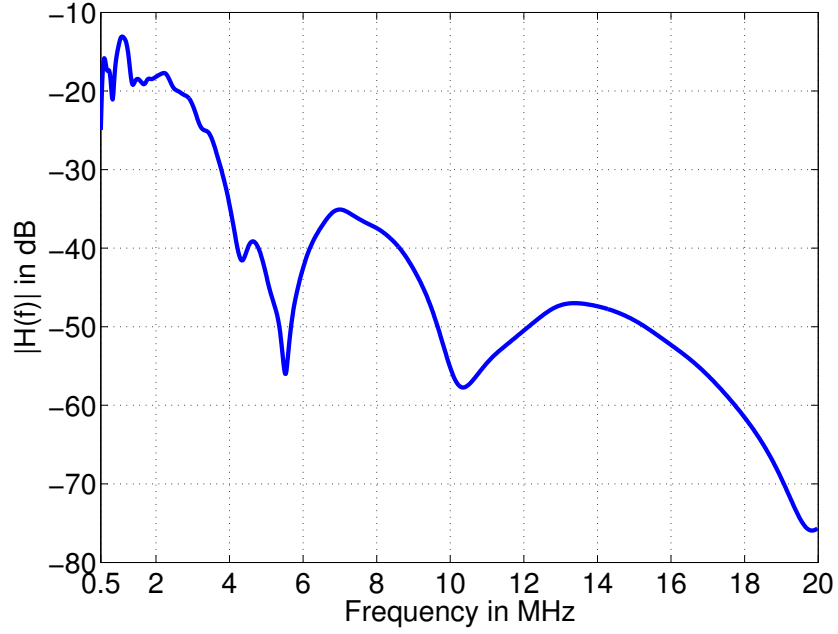


Figure 1.3: Frequency response of 15-paths reference channel model for PLC.

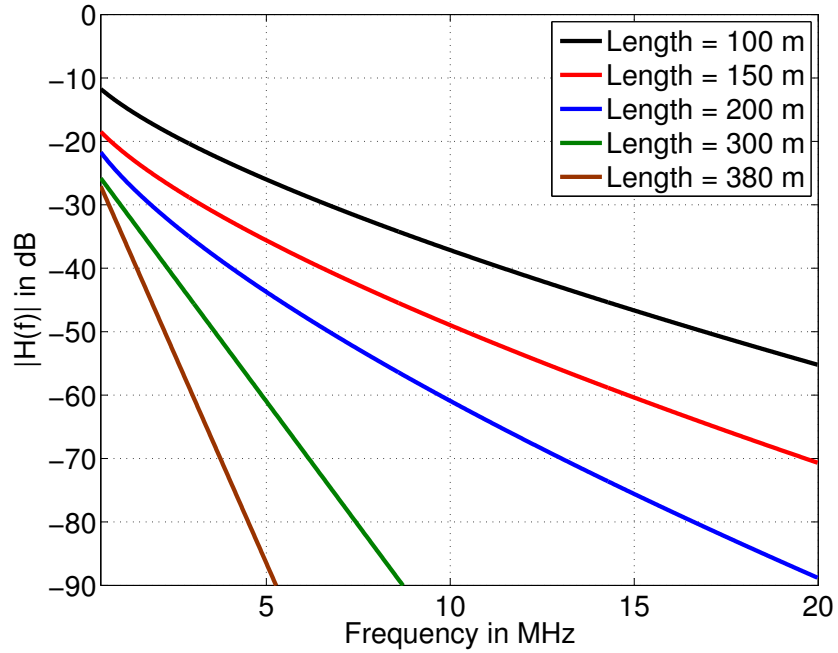


Figure 1.4: Length profiles of the attenuation of power line links.

Table 1.1: Parameters of the 15-path model.

attenuation parameters					
$k = 1$		$a_0 = 0$		$a_1 = 2.5 \cdot 10^{-9}$	
path-parameters					
p	g_p	$d_p(m)$	p	g_p	$d_p(m)$
1	0.029	90	9	0.071	411
2	0.043	102	10	-0.035	490
3	0.103	113	11	0.065	567
4	-0.058	143	12	-0.055	740
5	-0.045	148	13	0.042	960
6	-0.040	200	14	-0.059	1130
7	0.038	260	15	0.049	1250
8	-0.038	322			

Table 1.2: Attenuation parameters corresponding to the length profiles.

$class$	g_p	$a_0[m^{-1}]$	$a_1[s/m]$	k
100m	1	$9.40 \cdot 10^{-3}$	$4.20 \cdot 10^{-7}$	0.7
150m	1	$1.09 \cdot 10^{-2}$	$3.36 \cdot 10^{-7}$	0.7
200m	1	$9.33 \cdot 10^{-3}$	$3.24 \cdot 10^{-7}$	0.7
300m	1	$8.40 \cdot 10^{-3}$	$3.00 \cdot 10^{-9}$	1
380m	1	$6.20 \cdot 10^{-3}$	$4.00 \cdot 10^{-9}$	1

the delay spread, which is defined as the total time interval taken by signal reflections (with significant power) in arriving at the receiver from the transmitter. Intersymbol interference that is generated by time dispersion might be compensated by using suitable equalization algorithms at the receiver.

The PLC channel may be considered as quasi static, as the frequency responses are slowly time varying but at certain times may vary abruptly due to changes in impedances at the terminal. This problem is generally caused by switching (ON/OFF) power supplies, frequency converters, fluorescent lamps and television sets etc. Therefore, the channel state must be regularly monitored at transmitter and receiver.

The elementary work in this field was done by Philipps [34] and Zimmermann [35] and they are the references the most widely quoted in the domain of PLC channel modeling. The frequency response of 110 m link 15-paths reference model proposed by Zimmermann is given by

$$H(f) = \sum_{p=1}^P g_p \cdot e^{-(a_0 + a_1 f^k) d_p} \cdot e^{-j2\pi f \tau_p}, \quad (1.1)$$

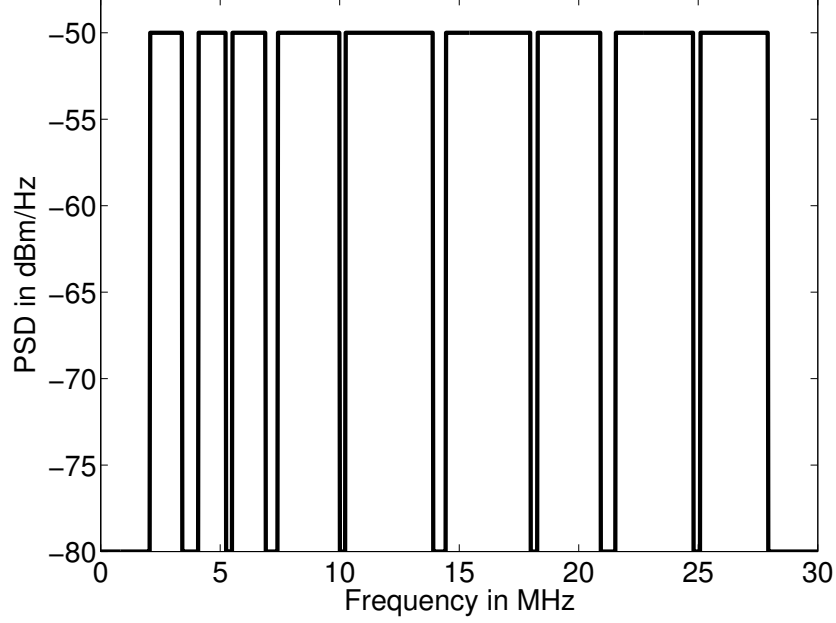


Figure 1.5: Transmit PSD mask from HPAV specification.

where $\tau_p = \frac{d_p \sqrt{\epsilon_r}}{c_0}$ is the delay of path p , d_p is the distance in meters of path p , ϵ_r is the relative permittivity of the insulating material, c_0 is the speed of light, g_p is the weighting factor of path p and $(a_0 + a_1 f^k)$ are model parameters to be adjusted. The parameters of the 15-path model are listed in Table 1.1. This model was validated in the frequency range of 500 kHz to 20 MHz. It is valid for both outdoor and indoor PLC channels. The indoor lines are shorter, but they suffer from strong branching: the number of relevant paths is then usually higher while the attenuation associated with each path is smaller.

Length profiles of the attenuation of power line links, i.e. neglecting the impacts of notches, as proposed in [35], are shown in Fig. 1.4 and the corresponding parameters are listed in Table 1.2. These profiles are used to compare the performance of PLC systems at various distances.

A PSD mask is shown in Fig. 1.5 from HPAV specification, where 4 or 5 additional subcarriers on either side of the each notch are set to zero amplitude in order to guarantee that the energy inside the licensed band will be at least 30 dB lower than the normal transmit power. It is due to this tightly imposed PSD mask that a PSD constraint is used in the resource allocation process for PLC systems. Generally, a high background noise level of -110 dBm/Hz is considered for indoor PLC networks [13].

Table 1.3: Comparison of PHY and MAC characteristics of existing systems.

	Panasonic	HPAV	UPA
Modulation	wavelet OFDM	windowed OFDM	windowed OFDM
Channel coding	RS-CC, LDPC	Parallel-concatenated turbo convolutional code & windowed OFDM	RS + 4D-TCM concatenation
Mapping	PAM 2-32	QAM 2, 4, 8, 16, 64, 256, 1024	ADPSK 2-1024
FFT/FB size	512 (extendable to 2048)	3072	2048
Max number of carriers	NC	1536	1536
Sample frequency	62.5 MHz	75 MHz	NC
Frequency band	4-28 MHz (2-28 MHz optional)	2-28 MHz	0-30 MHz (0-20 MHz optional)
Information Rate	NC	150 Mb/s	158 Mb/s
Power Spectral Density	NC	-56 dBm/Hz	-56 dBm/Hz
Media Access Method	TDMA-CSMA/CA	TDMA-CSMA/CA	ADTDM

1.3 PLC technology of today

Standardization is one of the most important issues that has to be dealt for any nascent technology. Various consortiums and standardization bodies define rules and regulations for possible utilization of PLC networks and appliances that should be acceptable to different actors such as manufacturers, Internet service providers, network integrators and operators. Table 1.3 summarizes various characteristic parameters of some well known existing systems. Defined bandwidth and imposed power levels on the transmitted signals are quite significant parameters and have a considerable influence on system performance.

1.3.1 Consortiums

For better treatment of standardization and compatibility issues and to share their views and interests, various companies have come together under one roof.

1.3.1.1 HomePlug powerline alliance

It is an initiative led by industry leaders at all levels of value chain, from technology to services and content. The main purpose of this alliance is to develop the specifications for high bit rate PLC home networking products and to devise the command and control between different platforms inside the home and to bring broadband Internet to all homes. There are more than 75 registered industrial partners in this alliance. The HomePlug power line alliance has catalyzed the demands of HomePlug enabled appliances and services through market sponsorship and public educational programs.

HPAV specification was defined in order to provide proper bandwidth for demanding applications such as high definition video and other multimedia applications. It uses 1536 subcarriers in the frequency band of 2-28 MHz, as shown in Table 1.3. Parallel-concatenated convolutional codes are used in conjunction with windowed OFDM for better error correction performance. It is backward compatible with HomePlug 1.0 specification.

1.3.1.2 UPA

Universal Power Line Association (UPA) was founded in 2004 to integrate PLC into the telecommunications landscape. Main UPA objectives are:

- To define world-wide standards for PLC,
- To take special measures for providing credible, unifying and consistent communication on PLC,
- To have a global view of the market and embracing all type of applications and to ensure speedy world-wide deployment of PLC networks.

UPA is also working in collaboration with European project OPERA. UPA also promotes DS2 chipsets and has developed digital home standard (DHS) with a target to provide comprehensive specifications to silicon vendors for integrated circuit designing for video, data and voice transmission through PLC. UPA specification uses 1536 subcarriers for a 30 MHz band, as shown in Table 1.3. It uses a concatenated channel coding scheme consisting of an outer RS code and an inner 4-dimensional (4D) 16-states trellis code. We also select this powerful combination of an RS and an multidimensional trellis code in this dissertation, and this combination will be detailed later in this thesis.

1.3.1.3 CEPCA

Consumer Electronics Power Line Communication Alliance (CEPCA) also supports advancement in high bit rate PLC technology in order to develop a new generation of consumer electronic appliances. It mainly comprises of leading Japanese manufacturers such as Panasonic, Mitsubishi and Sony etc. The main objective of CEPCA is to make the coexistence of different PLC systems possible and to incorporate CEPCA

specifications into international standards. The main parameters of the system proposed by Panasonic are also summarized in Table 1.3. Wavelet OFDM was chosen by Panasonic due to the lack of guard interval in this technique, which may subsequently reduce the system overhead.

1.3.1.4 Other alliances

Some of the other popular alliances are:

- United Power Line Council (UPCL), an association of Canadian organizations associated to HomePlug.
- Continental Automated Buildings Association (CABA), a North American industry association dedicated to the advancement of intelligent home and intelligent building technologies.

1.3.1.5 Projects

The most popular current research projects are given in the following:

- OMEGA is an integrated project in the domain of information and communication technology and is funded by the European commission under the seventh research framework programme (FP7). There are 20 European partners in this project from industry and academia, including France Télécom R&D, Siemens AG, Thomson, IETR, Infineon, Telefonica, University of Oxford and University of Udine. This thesis has also contributed to the OMEGA project. The aim of the OMEGA project is to develop a ultra broadband infrastructure accessible to most of the residential customers by exploiting UBB home access networks.
- OPERA was a 4 year research and development project funded by the European commission. It was completed in two phases, OPERA 1 in framework programme 6 (FP6) and OPERA 2 in FP7. The major objective of OPERA was to select a technology baseline and to develop a new open technology over medium voltage and low voltage lines for access applications.
- POWERNET was also a research and development project under framework programme 6 and had funding from European commission. Its prime objectives were to develop cognitive broadband over power lines (CBPL) communication equipment both for access and indoor applications.
- WIRENET was also a European project under framework programme 5. The aim of WIRENET was to develop a PLC modem for data transmission and industrial automation through an approach of ultra wide band modulation.

1.3.2 The OMEGA project

1.3.2.1 Main objectives

The OMEGA project targets to develop an inter-MAC convergence layer situated between MAC and network layers of the Open System Interconnection (OSI) reference model, of the international organization for standardization (ISO), for efficient cooperation and compatibility among various communication technologies. Thus, it opens the way for an entirely new approach as it is the first research effort concerning the convergence of such diverse wireless (radio and hybrid wireless optics (HWO)) and wired (PLC) technologies in highly demanding applications of multimedia and high bit rate home area networks. This project will create a new method of inter-MAC convergence and will identify the benefits and limitations of this approach in terms of reliability, performance, backward compatibility, stability, cost and potential impacts on existing standards. It aims to develop a future-proof scalable inter-MAC layer, which will be located at the heart of the OMEGA network. PLC benefits from the already available power line grid for high bit rate and robust communication and therefore easily fulfils the main criterion for OMEGA i.e. ‘no new wires’. In a very high bit rate services environment, a single in-home access point is not enough, and PLC has the capability to easily connect different segments of the considered infrastructure but has to be considerably enhanced to provide such services. At the time of this thesis, only available products in Europe are limited to tens of Mb/s (HomePlug 1.0). HPAV and OPERA target to increase it to 200 Mb/s but even better performances are required to integrate PLC in high bit rate home area networks.

1.3.2.2 Use of high bandwidth

The OMEGA initially focuses on the possibility of high bandwidth communications. Existing systems use the frequency from 2 to 30 MHz. Measurements and modeling of the channel up to 100 MHz has been undertaken in order to increase discrete bit rates. The consequent impacts on electro-magnetic compatibility constraints and the required digital signal processing have been investigated. New transmission techniques have been tested to enhance spectral efficiency of the system in conjunction with improved modulation and coding schemes. Effects caused by channel distortion, impulsive noise and other impairments and practical issues (such as imperfect channel estimation) on the studied schemes have been investigated. These new systems must be compatible with existing PLC systems, therefore all new schemes are backward compatible. The relevant regulation and specification associations are used to disseminate the novel high bit rate and robust techniques to guarantee broader acceptability of the new concepts originated during the project. New cognitive MAC approach for guaranteeing compatibility between different protocols is evaluated. In lower frequency bands (i.e. below 30 MHz), the new system is backward compatible with HPAV systems with full interoperability. For higher frequency bands (i.e. above 30 MHz), the proposed system is coexistent with other competing non HPAV systems. In all cases, for resource sharing and for a given quality of service, comprehensive strate-

gies are studied. OMEGA partners actively participate in the standardization and regularization efforts in the major international regulatory bodies such as Institute of Electrical & Electronics Engineers (IEEE) and ETSI. OMEGA is making all necessary efforts to implement coexistence mechanisms to enable its global recognition.

1.3.2.3 Channel modeling

It is essential to characterize and model the domestic power line channel consisting of power grids to assess the possibilities of performance improvements of HPAV in terms of bit rates and quality of service. Extensive characterization of PLC channel has been made in both point-to-point and point-to-multipoint scenarios starting from 0.1 MHz to 100 MHz [36]. These measurements are carried out using a multi-point channel sounder, which uses a number of waveform generator acquisition devices for precise results. Reference channel modes, both deterministic and statistical, are obtained from these measurements. To carry out realistic measurements, an emulator has been built with the PLC hardware prototype. A comprehensive study has been performed on the compatibility issues associated with the interaction of electric and magnetic fields of power lines with the environment. It considers the low frequency electromagnetic fields coupled with delicate home appliances as well as the effects of natural and domestic electromagnetic interference to PLC. Theoretical studies have been performed for this analysis using numerical modeling in conjunction with a number of experiments including measurements on low frequency fields.

1.3.2.4 Use of innovative technologies

Sophisticated modulation schemes are explored based on multi-carrier and spread-spectrum approaches. Accurate channel estimations and equalizations are performed to get the bit rate much closer to the Shannon capacity. Impulsive noise mitigation techniques are incorporated to counter any unforeseeable noises. Combined modulation and user multiplexing schemes (such as orthogonal frequency division multiple access (OFDMA), time division multiple access (TDMA) or code division multiple access (CDMA)) are investigated to exploit multi-user/multi-point channel diversity. Single link resource allocations, including dynamic allocation of codes, time slots, and carriers are considered. Spectrum sensing algorithms (such as carrier sense multiple access with collision avoidance (CSMA-CA)) are investigated along with algorithms for spectrum management and electromagnetic compatibility. Multiple user resource allocations (bits, carriers, codes, etc.) in a multi-user environment are carried out to enhance the system performance in terms of the capacity and the robustness of the system. A PLC prototype architecture is defined by using work from the modeling and measurement tasks with OMEGA system and inter-MAC layer requirements. Hardware implementations of developed algorithms will be implemented using fixed point conversion and performance verification after cost evaluation and the development of test environments (i.e. throughput, latency, BER and signal-to-noise (SNR) monitoring). This prototype will comprise of multiple PLC nodes able to transmit si-

multaneously. The system performance will be compared with the specifications. The complete system will be integrated with the inter-MAC layer and platform demonstration.

1.4 Future of PLC

PLC technology has enormous potential particularly in the domains of home automation and high bit rate LAN. Very high speed communication through domestic power outlets can be used, for instance, to share various accessories and data among a number of computers, to allow power distributors to offer broadband Internet to their customers and even to automatically alert a repairing agency in the case of a sudden failure of any of the expensive and important home appliances. PLC technology can also be used by power suppliers to remotely manage loads and efficiently control rolling power-cuts or enable power-hungry devices only during off-peak hours. In a future smart home, we can imagine to be benefited by number of useful applications that are not so easy to experience in current times. For instance, smart coffee machines may be set to turn on just before the alarm-clock, intelligent air conditioners may use thermostats in different rooms to regulate the airflow into each room through adaptive-speed fans situated at the ventilation ducts and a smart pressing iron may automatically be turned off when the home alarm system is armed, when it is left vertical for a given amount of time or when the lights are turned off. All these and many other intelligent home automation applications may be realized using simple control circuits, once the PLC technology is fully ready to be deployed.

In addition to this, the PLC technology needs to be significantly enhanced in order to fulfil the common expectations associated with the future broadband requirements. It is needed to develop advanced PLC techniques to enable Gigabit rates through power lines by optimizing the physical, MAC and cross-layer mechanisms. For physical layer, the focus should be on developing a wide band transmission interface with backward compatibility with the current HPAV specifications. New modulation and transmission schemes such as OFDM carrying offset QAM (OFDM/OQAM) and Filtered Multitone (FMT), advanced filter bank modulation techniques, linear precoded OFDM based on the combination of multicarrier and spread spectrum techniques should be evaluated in order to achieve bit rates in multiples of Gb/s. Furthermore, new and powerful channel coding schemes must be considered in the PLC context to achieve the system capacity close to the Shannon limit. Enhanced signal processing techniques such as accurate channel estimation, efficient equalization methods, quasi perfect synchronization, adequate and fair spectrum management and effective impulsive noise mitigation techniques may increase the system performance significantly. Considering MAC layer, the technology-dependent medium access controls are studied (in the context of the OMEGA project) to analyze and subsequently optimize the performance of each transmission technique. A customized and enhanced mesh mechanism is to be elaborated for seamless handovers between heterogeneous technologies. Advanced resource management and quality of service optimization strategies have to

be taken into account under the context of cross layer mechanisms. These resource allocation strategies must be exploited to maximize either the bit rate or the robustness of the system in order to achieve near optimal performance. In short, the focus of ongoing studies should be to enhance the existing PLC technology by exploring and efficiently combining the novel techniques in order to achieve challenging goal of Gigabit communications over power lines.

1.5 Conclusion

In this first chapter, we have presented a general overview on PLC technology to make the reader familiar with the fundamental characteristics of the PLC technology. Due to already available power supply grids, PLC has its unique position in both indoor and outdoor environments. High frequency communication signal (i.e. modulated carrier) is superimposed on the power supply grid already containing the electrical signal at 50 or 60 Hz depending upon the country. This thesis focuses on very high bit rate communications over power lines and proposes various resource allocation and optimization strategies for both coded and uncoded multicarrier systems with and without the assumption of perfect channel knowledge at the transmitter.

This chapter discussed a brief history of the PLC technology. Some fundamental aspects of the PLC technology were also specified. A brief description of the standard power line grid was given followed by a short analysis of the considered PLC channel model. The current progress on the canvas of the PLC technology was then summarized with introduction of various consortiums and associations working for the development and standardization of the communication over wirelines. Some important research projects were listed and the role and objectives of the OMEGA project, to whom this thesis also contributes, were explained in detail. Finally, the future trends in the PLC technology were discussed with some unique ideas that demonstrate the futuristic home automation applications. The contribution of the OMEGA project to the future of the PLC technology was also presented. Different resource allocation strategies for multicarrier systems will be elaborated in following chapters. The next chapter comprehensively discusses the fundamentals of resource allocation and optimization for multicarrier systems. An overview of the conventional OFDM is given before the presentation of the spread spectrum principle and its combinations with multicarrier technique.

Chapter 2

System specifications and resource allocation

Contents

2.1	Introduction	26
2.2	System specifications	26
2.2.1	OFDM	27
2.2.2	Spread spectrum OFDM	34
2.2.3	Multiple access schemes	36
2.2.4	System selection	42
2.3	Resource allocation for multicarrier systems	45
2.3.1	Theoretical capacity	47
2.3.2	Fundamentals of multicarrier resource allocation	50
2.3.3	Rate maximization	52
2.3.4	Robustness Maximization	54
2.4	Conclusion	60

2.1 Introduction

The ability to adaptively modulate different subcarriers is a very useful advantage obtained through multicarrier communication. Multicarrier modulation (MCM) is considered one of the leading transmission technologies in both wired and wireless communication arena. The principle of MCM is discussed in this chapter followed by the description of the idea of OFDM. Subsequently, the spread spectrum technique is described and an introduction of transmission schemes is given, which are resulted through a combination of OFDM and spread spectrum techniques (or equivalently linear precoding principles). A scheme based on these combinations is selected and the main advantages and motivations to this choice are discussed. This system will be known as linear precoded OFDM (LP-OFDM) in the following.

The resource allocation on different subcarriers and the performance optimization on the basis of given constraints, have become an important research topic in recent years. CSI can be made available at the transmitter by sending adequate feedback information from the receiver. The channel knowledge is exploited by adaptive and variable modulation at different subcarriers to increase either the capacity or the robustness of the transmission system. Generally, each subcarrier is assigned a suitable transmit power, driven by the SNR, and is loaded with a given modulation, such as different modulation orders of QAM. Various analytical studies have been performed for the resource allocation and performance optimization of multicarrier systems. This chapter extensively discusses the resource allocation and optimization for multicarrier systems. Various resource allocation strategies are considered. Different problems are formulated for these strategies using a number of constraints.

2.2 System specifications

In this section, we will discuss transmission techniques, which are considered in this thesis. First of all an introduction to MCM is given and specifically the principles of OFDM are described in detail. As it was discussed in the first chapter, we consider a transmission technique consisting of the combination of OFDM and spread spectrum. We explain the functionality and principles of these hybrid techniques in this section. After an introduction to OFDM modulation, we discuss the linear precoding techniques (also known as spread spectrum in wireless mobile networks) in general followed by a discussion on advantages and disadvantages of different transmission techniques obtained through the combination of OFDM and spread spectrum. Finally, a particular combination of OFDM and spread spectrum is selected due to its suitability to PLC networks and its capability to enhance the system performance significantly in terms of increased bit rate and better system robustness against noise.

2.2.1 OFDM

Multicarrier modulation has its roots in the concept of frequency division multiplexing (FDM). It was proposed by Doelz [37] for the first time in 1950 but was implemented in real systems, after various improvements, almost 40 years later as the recent developments in semiconductor and circuit miniaturization technologies have reduced the cost of the hardware and signal processing needed for multicarrier modulation systems [38]-[40]. In recent times, a global acceptance has occurred for OFDM utilization as a leading technology for high bit rates. Particularly, a number of standards for wireless and wired communications have chosen OFDM to significantly improve the performance of modern communication systems. This includes digital video broadcasting-terrestrial (DVB-T), long term evolution (LTE), WiMAX and IEEE 802.11a for wireless communication and DSL for wired communication. OFDM is a special form of MCM with densely spaced subcarriers and overlapping spectra. It is quite appropriate for high bit rate communications and for channels involving frequency selective fading. The idea of dividing frequency selective wide band channels into a number of narrow band subchannels, non-selective in frequency, is the core reason that makes the system robust against large delay spreads by maintaining the orthogonality of subcarriers in frequency domain. Furthermore, the brilliant idea of introducing cyclic redundancy at the transmitter fairly lessens the system complexity to only fast Fourier transformation (FFT) processing and a simple one-tap equalizer per subcarrier is needed at the receiver if the maximum delay spread is less than the guard interval duration. Last but not least, the ability to adaptively modulate different subchannels is one of the main reasons behind its acceptance as a leading transmission technology.

2.2.1.1 OFDM principle

The fundamental principle of OFDM is to split a high-rate data stream into several parallel streams of lower rate and transmit each of them on a different subcarrier. First of all, a brief overview of frequency selective channels is given [41]-[43]. The low-pass received signal $y(t)$ can be given as,

$$y(t) = \int_{-\infty}^{\infty} h(\tau)x(t - \tau)d\tau + n(t), \quad (2.1)$$

where $x(t)$ is the transmitted signal, $h(t)$ is the channel impulse response. Whenever the transmitted signal bandwidth $[-\frac{f_x}{2}, \frac{f_x}{2}]$ is greater than the channel coherence bandwidth f_c , frequency selectivity occurs. The channel coherence bandwidth is inversely related to the delay spread σ_d [41]. In the case of frequency selective channel, the frequency components of $x(t)$ with frequency separation exceeding f_c tend to have different channel gains. In Fig. 2.1, time impulse response of a given channel is shown. For broadband signals, the sampling rate T is quite small in comparison to σ_d and therefore they tend to be affected by frequency selectivity. The multipath channel model can be given by,

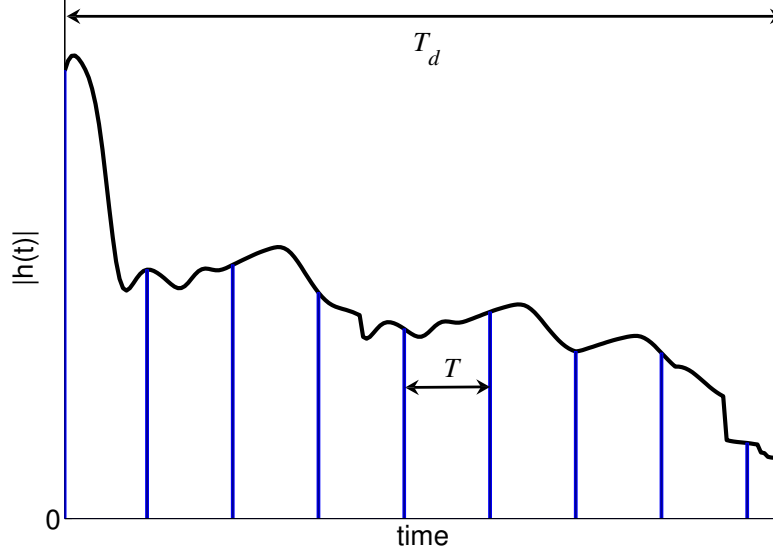


Figure 2.1: Time response of a multi path channel.

$$h(t) = \sum_{p=1}^{p_M} \alpha_p e(t - \tau_p), \quad (2.2)$$

where $e(t)$ is the transmission filter. $(\alpha)_{p=1,2,\dots,p_M}$ and $(\tau)_{p=1,2,\dots,p_M}$ are the gains and delays associated with each path, respectively. Generally, propagation measurements are carried out to evaluate the variance of channel gain and time delays. Equalization operation (or retrieving $x(t)$ from (2.1)) is one of the main parameters describing the performance of transmission schemes. Mostly, this difficulty is due to the frequency selectivity behaviour of the channel. Furthermore, complexity of an equalizer increases with the channel memory. Therefore the hardware and power consumption cost of such an equalizer is very high, particularly in the case of high bit rate communication. To significantly simplify the equalization task, OFDM converts the channel convolutional effect of (2.1) into the multiplicative one. For that purpose, OFDM adds cyclic prefix intelligently to circularize the channel effect. Since, the circular convolution can be diagonalized in an FFT basis [44], therefore the multipath time domain channel is converted to a number of frequency flat fading channels. Furthermore, due to the low implementation cost of digital FFT modulator, the overall cost of OFDM systems is minimized.

Considering N serial data symbols with a symbol duration T_d , using an OFDM scheme these symbols are transmitted simultaneously on N different subcarriers. The modified symbol duration is now $T_s = N \times T_d$ for the same total bit rate as with single carrier modulation. In time domain, the resultant signal consists of symbols of duration T_s obtained from N overlapping sinusoids of different frequencies. By

increasing the number of subcarriers, the symbol duration can be made much greater than the delay spread of the channel impulse response, which reduces the inter-symbol-interference (ISI). In frequency domain, by increasing the number of subcarriers, the channel responses of individual subchannels can be made quite narrower and eventually be considered as flat channel response. In this way, the signal distortions introduced by the channel can be fairly limited.

Historically, FDM systems were proposed to reduce overlapping between subcarriers by increasing the frequency spacing Δf between them. However, this solution, which allows ICI minimization, is not interesting in terms of spectral efficiency and a spectral band larger than the band of a single-carrier system may be required. A better and now commonly used approach is to use orthogonal overlapping subcarriers in time and frequency. Through this innovative approach the spectral efficiency of OFDM can be optimized. It was the combination of orthogonal subcarriers with FDM techniques that gave birth to the first OFDM system in 1960s [45].

The orthogonality of OFDM is related to the pulse shaping function. Several pulse shaping functions have been proposed in the literature [46] and among them the rectangular function is the most widely accepted. This function can be seen as a rectangular window, with duration T_s equal to the OFDM symbol duration. In frequency domain, it can be represented by a sinc function ⁽¹⁾ for each subcarrier of the generated signal. A minimum spacing between adjacent subcarriers is required in order to attain the frequency orthogonality between the signals on N subcarriers. For the rectangular pulse shaping, this minimum subcarrier spacing can be expressed as,

$$\Delta f = \frac{1}{T_s}. \quad (2.3)$$

Fig. 2.2 shows an OFDM signal in time and frequency domain. In time domain, OFDM signal can be seen as compound function consisting of various overlapping sinusoids with a time period equal to the inverse of the corresponding subchannel frequency. However, in frequency domain, the OFDM signal is represented by a series of sinc functions separated by Δf . It must be noted here that in a frequency selective channel, the greater the number of subcarriers is, the flatter is the OFDM spectrum for a given subcarrier.

Due to their distinct characteristics, the identification and extraction of different subcarriers is possible everywhere in the spectrum that helps in adapting the system according to the dimension of the given spectrum. This flexibility in the spectrum management is very advantageous as it is quite possible to assign different modulation orders (i.e. different numbers of bits) and different transmit powers to distinct subcarriers. The main idea is to adapt the transmitted signal according to the propagation channel under the assumption of all or partial knowledge of the channel state. It is exactly what our proposed resource allocation and optimization algorithms will

⁽¹⁾ $\text{sinc}(x) = \sin(\pi x)/\pi x$ the term sinc is a contraction of the function's full Latin name, the *sinus cardinalis* or cardinal sine

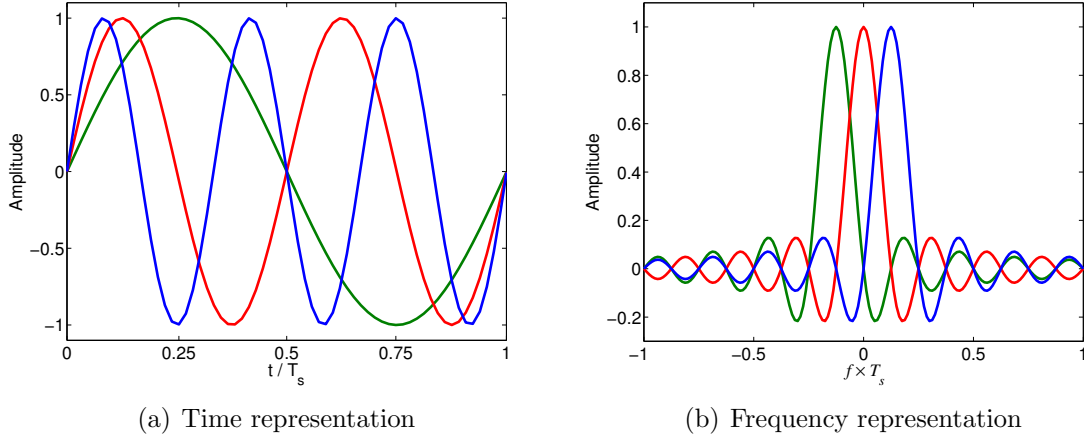


Figure 2.2: Time and frequency domain representation of an OFDM signal.

exploit in order to either increase the bit rate of the system or enhance the system robustness by suitably allocating bits and powers to different subcarriers.

2.2.1.2 The interest of adding channel coding and interleaving

The OFDM technique successfully counters the problem of channel selectivity, however it does not reduce fading. The amplitude of each carrier is usually affected by a Rayleigh law, or a Rice law in the presence of a direct path. Here, an efficient channel coding scheme has to play a vital role. The principle of coded OFDM systems is to link different symbols through a coding procedure and to transmit elementary signals at distant locations of the time-frequency domain. It can also be achieved by simple convolutional coding with soft decision Viterbi decoding, in combination of time and frequency interleavers.

The diversity obtained through the interleaving process has immense significance. It is quite important for the efficient functioning of the Viterbi decoder that successive samples at its input are affected by independent Rayleigh laws. In practical systems, the distortions to which these samples are subjected have a strong time/frequency correlation. If the receiver is static, the frequency domain diversity is sufficient in order to guarantee the proper system functioning. Due to a few microseconds spread of the channel response, flat fadings over a few megahertz are very unlikely. Looking at the system from this point of view shows the presence of multipath as a form of diversity and should be considered as a positive element.

2.2.1.3 Signal characteristics

Considering an OFDM signal with N distinct subcarriers of frequencies $f_i = f_0 + i\Delta f$, $i \in [1 : N]$ used for transmitting N symbols x_i in parallel. x_i are complex symbols represented by finite alphabet corresponding to a given digital modulation,

for example QAM. Using a rectangular function $\Pi(t)$ as pulse shaping function and applying the criterion of orthogonality $\Delta f = 1/T_s$, the normalized expression for a simplified OFDM signal (i.e. without taking into account the guard interval) generated for an interval $[0 : T_s]$ can be given as

$$s(t) = \frac{1}{N} \sum_{i=1}^N \Re \left\{ x_i \Pi(t) e^{2\pi j (f_0 + \frac{i}{T_s}) t} \right\}. \quad (2.4)$$

Supposing $f_c = f_0 + N/2T_s$ is the central frequency of the signal, we get

$$s(t) = \Re \left\{ \Pi(t) e^{2\pi j f_c t} \sum_{i=1}^N \frac{x_i}{\sqrt{N}} e^{2\pi j (i - \frac{N}{2}) \frac{t}{T_s}} \right\}. \quad (2.5)$$

In other way, we can write this expression as,

$$s(t) = \Re \left\{ \tilde{s}(t) \Pi(t) e^{2\pi j f_c t} \right\}, \quad (2.6)$$

where $\tilde{s}(t)$ is the complex envelope of signal $s(t)$ before being windowed by $\Pi(t)$. Its spectrum is limited to interval $[-N/2T_s : N/2T_s]$, $\tilde{s}(t)$ can be sampled at a frequency $f_e = N/T_s$ without any spectral folding. The obtained samples can be written as,

$$\begin{aligned} \tilde{s}_n &= \sum_{i=1}^N \frac{x_i}{\sqrt{N}} e^{2\pi j (i - \frac{N}{2}) \frac{n}{N}} \\ &= (-1)^N \underbrace{\sum_{i=1}^N \frac{x_i}{\sqrt{N}} e^{2\pi j \frac{in}{N}}}_{\text{DFT}^{-1}}. \end{aligned} \quad (2.7)$$

It shows that an OFDM signal can be generated using an inverse discrete Fourier transform (IDFT). A direct discrete Fourier transformation (DFT) of received signal is used on the receiver to extract the transmitted symbols. Recent advances in the domain of Fourier transformations (such as specific digital signal processor (DSP) for FFT and inverse FFT (IFFT)) have made it possible to implement such operations quite efficiently and at a very low cost. The multiplication by (-1) is performed for re-centering of the spectrum around the zero frequency in order to obtain the transmitted signal in baseband representation. It is therefore, we capture the first intermediate frequency OFDM signal at the output of IFFT i.e. the analytical OFDM signal is calculated for $f_c = 0$. A matrix representation of this analytical OFDM signal can be written as,

$$\mathbf{s} = \mathbf{F}^{-1} \mathbf{x}, \quad (2.8)$$

where $\mathbf{s} = [s_1 \ s_2 \ \cdots \ s_N]^T$ is the time sampled vector of an OFDM symbol, $\mathbf{x} = [x_1 \ x_2 \ \cdots \ x_N]^T$ is the vector of modulated symbols transmitted at each subcarrier and \mathbf{F} is an $N \times N$ Fourier matrix defined as,

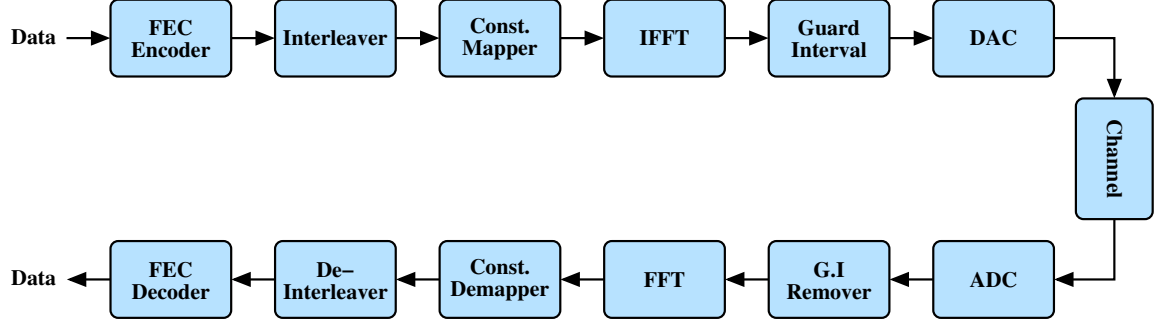


Figure 2.3: OFDM communication chain.

$$\mathbf{F} = \begin{bmatrix} 1 & 1 & \cdots & 1 \\ 1 & e^{-\frac{2\pi j}{N}} & \cdots & e^{-\frac{2\pi j(N-1)}{N}} \\ \vdots & \vdots & \ddots & \vdots \\ 1 & e^{-\frac{2\pi j(N-1)}{N}} & \cdots & e^{-\frac{2\pi j(N-1)^2}{N}} \end{bmatrix}. \quad (2.9)$$

\mathbf{F} is a unitary matrix and therefore $\mathbf{F}^{-1} = \mathbf{F}^H$.

2.2.1.4 ISI and ICI minimization

ISI and ICI are the major issues, which must be considered by OFDM system designers. Generally, a trade-off is sorted out between bit rate and these interferences. As discussed earlier, ISI can be asymptotically limited by increasing the symbol duration T_s . In practical systems, the symbol duration cannot be increased indefinitely due to the limits imposed by channel coherence time. Here, the guard interval has to play its role. The guard interval can be defined as the space between consecutive symbols. ISI occurs when echoes of one symbol interfere with the other. Introducing a time interval between adjacent symbols allows these echoes to settle down before the next symbol arrived. During this interval no useful data is transmitted. The duration of guard interval T_g must be greater than or equal to the maximum delay spread τ_{max} of the impulse response. It must be noted here that introduction of the guard interval should not change the subcarrier spacing. However it increases the OFDM symbol duration to $T_s + T_g$, which leads to a loss of orthogonality between subcarriers at the transmitter. It is very crucial to have this orthogonality at the receiver to extract the transmitted symbol without them being affected by ICI. However, this problem can be solved if each of the sinusoids, constituting an OFDM symbol at the rectangular window (on which FFT is applied), includes an integer number of periods. It can be achieved by making the guard interval repetitive at the end of the symbol. One disadvantage of this method is that it leads to a loss in spectral efficiency equivalent to $T_s/(T_s + T_g)$ and therefore symbol dimensions should be minimized.

Furthermore, an OFDM signal can also be adapted in order to be backward compatible with other technologies. It means that we can use different numbers of sub-

carriers for the same bandwidth. The bandwidth occupied by the transmitted OFDM signal can be precisely adapted to the channel bandwidth by forcing some subcarriers to zero at the extremes of the frequency band. Fig. 2.3 depicts the functionality of an OFDM communication chain.

2.2.1.5 Pros and Cons of OFDM

OFDM systems, like every real life system, have some advantages as well as some undesirable features. Here we will discuss the pros and cons of OFDM with a critical point of view. Firstly we will look at the advantages of OFDM systems.

1. Due to the introduction of redundancy, the complexity (for a certain delay spread) of an OFDM system does not increase with the sampling rate as much as in the case of a single carrier system. It is because of the increased length of the equalizer due to the reduction in the sampling rate. The length of the equalizer increases quadratically with the inverse of the sampling rate while the OFDM complexity increases a bit more than the linear growth in some cases [47, 48]. It is very advantageous for making high bit rate modems. OFDM employs simple equalizers whereas a matrix inversion is used for single carrier equalizers. For an impulse response shorter than the guard interval, each constellation has to be multiplied by the channel frequency coefficient. Zero forcing (ZF) or minimum mean square error (MMSE) equalizations are generally performed.
2. Simple methods such as learning sequences [49, 50] or blind estimation methods [51, 52] are conventionally used to determine channel attenuations in the frequency domain. For turbo estimation, the time and frequency autocorrelation function of the channel can also be taken into account [53].
3. Flexible spectrum adaptation can be implemented for instance notch filtering.
4. It is quite possible to assign different modulation orders (i.e. different numbers of bits) and different transmit powers to distinct subcarriers in order to enhance the system performance in terms of bit rate and robustness of the system.
5. Subcarriers frequency overlapping allows better spectral efficiency in comparison of frequency division multiple access (FDMA) systems.

The few disadvantages of OFDM systems are listed in the following.

1. A high input back-off ratio can be generated at the transmitter amplifier if a baseband signal is transmitted experiencing significant amplitude fluctuations. Generally, non-linear distortions are introduced by power amplifiers and they severely affect the subcarriers orthogonality. Formally, it is known as peak to average power ration (PAPR) and has become an interesting topic of research [54, 55].

2. OFDM is not very robust against frequency off-set and the distortions caused by problems in synchronization [56].
3. OFDM is sensitive to Doppler spread.
4. The introduction of guard intervals causes some loss in the spectral efficiency.
5. The application of OFDM is limited to the systems where the channel length is smaller than the cyclic prefix. The orthogonality between subcarriers is only approximative if it is not the case. ICI is generally resulted for such systems, which may be countered by applying a shortening filter at the receiver [59].

2.2.2 Spread spectrum OFDM

In this section, we will discuss the spread spectrum principle and characteristics of various transmission schemes derived by combining OFDM with the spread spectrum.

2.2.2.1 Spread spectrum principle

The idea of spread spectrum, arguably, was first conceived by a Hollywood actress, Hedy Lamarr, and a pianist, George Antheil, in their US patent, titled “secret communication system” [60]. Initially, this brilliant idea was not taken seriously by both industrial and research communities and the first major application of spread spectrum technique arose in 1960s when US national aeronautics and space administration agency (NASA) used this method to precisely evaluate the range to deep space probes. Subsequently, US also started using this technique for military purposes due to its anti-jamming and hard-to-intercept characteristics. It was also used by the military for applications involving radio links in hostile environments.

Due to enormous growth in mobile radio communications in recent times, spread spectrum has been used in various commercial applications such as mobile networks and wireless personal area networks. The most important applications include multiple access, interference rejection, multipath reception, accurate universal timing, high resolution ranging and multipath reception. Spread spectrum has been adapted by many communication standards, such as the digital cellular standard IS-95 (or interim standard 95) [61], IEEE 802.11, IEEE 802.15.4, satellite navigation systems such as global positioning system (GPS) and universal mobile telecommunication systems (UMTS), which use a wideband code division multiple access (W-CDMA) [62].

The basic idea behind spread spectrum is to spread a signal over a wide frequency band much greater than the minimum bandwidth required to transmit the information successfully. A given value of C can be transmitted either through a narrow band W with a strong SNR or through a wide band using a low SNR that is the case for spread spectrum. Different procedures can be implemented to carry out the spreading operation. Some of these procedures are outlined below:

- In direct-sequence spread spectrum (DS-SS), the signal is spread over a continuous bandwidth by combining it with a continuous vector of pseudo-random

codes consisting of various chips. The duration of one chip is quite shorter than the duration of one bit.

- Frequency-hopping spread spectrum (FH-SS) is quite similar to DS-SS and uses a pseudo-random sequence for signal spreading. But the signal is hopped over multiple subcarriers (having bandwidths equal to the bandwidth of the transmitted signal) instead of spreading over a continuous bandwidth. This technique is very robust against narrowband interference and is quite difficult to intercept. A popular example is the Bluetooth 1.2 that uses FHSS to solve interference problems with many other standards that also operate in the 2.4-2.4835 GHz frequency band.
- In time-hopping spread spectrum (TH-SS), the pseudo-random code turns the carrier on and off.
- Chirp spread spectrum encodes information using linear frequency modulated chirp pulses. Chirp is a sinusoid whose frequency varies over a certain amount of time. Contrary to previous methods, any pseudo-random sequence is not added to the signal.

The DS-SS technique is the most popular, particularly for systems combining multicarrier with spread spectrum. The transmitted data is multiplied by a pseudo-random noise sequence whose values are normally $-1, +1$. Let T_d represent the data symbol duration and T_c the chip duration. Thus, the bandwidth $B_c = 1/T_c$ of the transmitted DS-SS signal is much larger than the bandwidth $B_d = 1/T_d$ of the message data to transmit. Subsequently, in the considered scenario, the processing gain PG can be derived from the ratio of these two bandwidths as

$$P_G = \frac{B_c}{B_d} = \frac{T_d}{T_c} = L, \quad (2.10)$$

where L is the length of pseudo-random codes sequence, i.e. the number of used chips per sequence. The PSD of the transmitted signal is thus attenuated by a factor of P_G . At the receiver side, the original data can be exactly reconstructed by multiplying it by the same pseudo-random sequence. This process, known as “despreading”, mathematically constitutes a correlation of the transmitted pseudo-random sequence with the pseudo-random sequence that the receiver knows the transmitter is using. The despreading works correctly if the transmit and receive sequences are well synchronized. A judicious selection of pseudo-random codes with good cross and autocorrelation facilitates the synchronization process [63].

The spread spectrum techniques are widely used in different communication systems and standards due to the multiple advantages they offer. Since the transmitted signal PSD is attenuated by a factor of P_G , other communication systems can use the same frequency bands. In addition, these techniques offer a low probability of intercept since the signal can be seen as noise-like by other users, and only users having the correct synchronous pseudo-random sequence can intercept the communication.

Moreover, the transmitted signal is robust against narrowband interference because these interfering signals are spread by the despreading process at the receiver. Last but not least, the ability of spread spectrum to provide multiple access is one of its major advantages. In other words, we can make multiple users to receive and transmit simultaneously on the same frequency bands by using different spreading codes for each user.

2.2.3 Multiple access schemes

The task of sharing available resources among different users has the utmost importance in modern communication systems. For effectively performing this task, many multiple access techniques have been proposed. The most popular of them are FDMA, TDMA and CDMA.

In FDMA, the spectrum is divided into several subcarriers, which are assigned to different users. It can be implemented quite easily since different users can be separately identified using simple filters at the receiving side. The limit on the maximum number of users sharing a given band is one of the drawbacks of FDMA technique. Actually, the increase in the number of users can decrease the individual bandwidth of each user that must be sufficiently large to counter strong attenuations in the transmitted signal.

In TDMA, the signal is divided into various short time slots in order to allow multiple users to share the same frequency band. Different users use their own time slots to rapidly send their information in short successions, one after the other. TDMA requires perfect synchronization between all transmitters and receivers and therefore are more delicate to implement. Some modern systems employing TDMA include digital enhanced cordless telecommunications (DECT) and global system for mobile communications (GSM).

CDMA allows multiple users to transmit information simultaneously on the same time slot and on the same frequency band. Communication signals from different users are identified by pseudo-random codes known at the transmitter as well as at the receiver. The combination of direct-sequence (DS) principle and CDMA is known as DS-CDMA. DS-CDMA requires a suitable selection of pseudo-random codes with sophisticated cross and auto-correlation. Orthogonal codes, such as Walsh-Hadamard codes [64], orthogonal variable spreading factor (OVSF) codes and complementary series of Golay codes [65], can be used to obtain optimal performance for synchronous communication systems. Non-orthogonal codes with excellent cross and auto-correlation, such as Kasami [66] and Gold [67], may be used for asynchronous communication systems. DS-CDMA systems enjoy many advantages including enhanced robustness against interferences, adaptive data rates and simple frequency planning. On the other side, the system may also encounter several drawbacks in a multi-user scenario with limited bandwidth:

- Multiple access interference (MAI), for higher number of simultaneously active users.

- High receiver complexity due to the use of adaptive filters and significant signalling overhead.
- Single-tone and multitone interference, when spreading operation is insufficient for interference suppression, notch filtering has to be performed at the receiver, further increasing the complexity of the already complex receiver.

It must be noted that DS-CDMA system needs accurate power control. Actually, if rigorous power control is not performed, it may lead to the monopoly of any one user (with very strong power level) to the entire spectrum when multiple users access the same spectrum simultaneously.

2.2.3.1 Principle of the combination

The combination of spread spectrum with OFDM can give rise to a large number of variants, grouped together under the generic name multicarrier spread spectrum (MC-SS). A number of advantages offered by OFDM and spread spectrum and their successful implementations in recent communication systems have motivated many researchers to work on different combination strategies of these techniques. Therefore, different strategies for combining OFDM with DS-CDMA have been proposed [68]–[72]. The spread spectrum technique can be implemented before or after the FFT operation. In this dissertation, we take into account only the cases where the spread spectrum is carried out before the FFT operation. The transmitted MC-SS symbol has more or less the same structure as of the conventional OFDM symbol where different subcarriers are orthogonal to each other. The cyclic prefix is also applied in MC-SS systems in the same manner as in the conventional OFDM.

Contrary to the case of OFDM where information symbols are simply distributed to different subcarriers during one OFDM symbol period, the MC-SS allocates multiple subcarriers (or symbol periods) to different chips of CDMA symbol. This process is known as chip mapping. The fundamental concept behind chip mapping is to have a diversity gain and to consequently improve the system performance by transmitting the same data over a whole code that provides a time or frequency diversity gain depending on the configuration. Moreover, the spreading component provides an additional degree of freedom by adding a code dimension in the system. In MC-SS systems, it is possible for multiple users to simultaneously transmit data on the same spectrum using its CDMA component. It is not possible in OFDM and may cause a loss in spectral efficiency or in time. Furthermore, the code dimension enhances the system optimization and resource allocation flexibility and better optimization strategies may be sorted out in comparison to OFDM.

Various MC-SS schemes can be obtained depending upon how the codes are distributed and how the multiple access between users and the data multiplexing of each user is carried out. The multiple access among different users can be implemented in time, frequency or code dimensions. Furthermore, the data of each user can also be multiplexed in any of these dimensions. If the signal is frequency spread, the combination is known as F-CDM (F-CDMA) and when the signal is time spread, the

combination is referred as T-CDM (or T-CDMA). Moreover, different subcarriers can be grouped together in multiple smaller blocks with a particular multiplexing and spreading technique. Thus, these systems may be divided in two broad categories, mono block systems (where all subcarriers are grouped in only one block) and multi block systems.

2.2.3.2 Mono block systems

Consider an OFDM system with N subcarriers. The spreading code length is L and all subcarriers are grouped in a single block. As discussed earlier, the multiple access can be provided in time, frequency or code dimension. In CDMA, different users are allocated a given number of codes for each generated CDMA symbol. The remaining time and frequency dimensions may be used by each user for multiplexing and chip transmission. Various chip mapping schemes can be used and the spreading in the frequency dimension is the most common that is known as F-CDMA. The signal is generated from a serial combination of conventional DS-CDMA and OFDM. Chips of spread information are transmitted in parallel on different subcarriers, as shown in Fig. 2.4(a). It is alternatively referred as multicarrier code division multiple access (MC-CDMA) in mobile radio communications. The prime positives of this scheme are a good spectral efficiency, improved frequency diversity (due to frequency spreading) and low complexity receivers.

Moreover, spreading may also be carried out in the time direction. This scheme is known as T-CDMA, as shown in Fig. 2.4(b). In mobile radio communications, this technique is alternatively referred as multicarrier direct-sequence code division multiple access (MC-DS-CDMA). Similar to the case of F-CDMA, L is considered to be equal to N . The MC-DS-CDMA signal can be generated by a serial-to-parallel conversion of data symbols into N sub-streams, followed by a DS-CDMA implemented on each individual sub-stream. Therefore, all chips of a CDMA symbol are transmitted on the same subcarrier but on different OFDM symbols. The prime advantage of this scheme is the improved time diversity gain due to the time spreading. Till now, we discussed schemes where either the time spreading or the frequency spreading was performed. However, it is quite possible to perform spreading in both dimensions at the same time. This idea is known as two-dimensional spreading and has been discussed in [73].

In TDMA schemes, each user is assigned multiple OFDM symbols and in one symbol duration only one user can transmit its information, as shown in Fig. 2.4(c). In the given case, the chip mapping is implemented in the frequency dimension and the code dimension is used by a given user for multiplexing purposes. This scheme is known as F-CDM/TDMA.

In FDMA schemes, each user is assigned multiple subcarriers. These subcarriers are dedicated to only one user and therefore cannot be used by other users as shown in Fig. 2.4(d). In the given case, the chip mapping is implemented in the time dimension, and the code dimension is used by the same user for data multiplexing purposes. This scheme is known as T-CDM/FDMA.

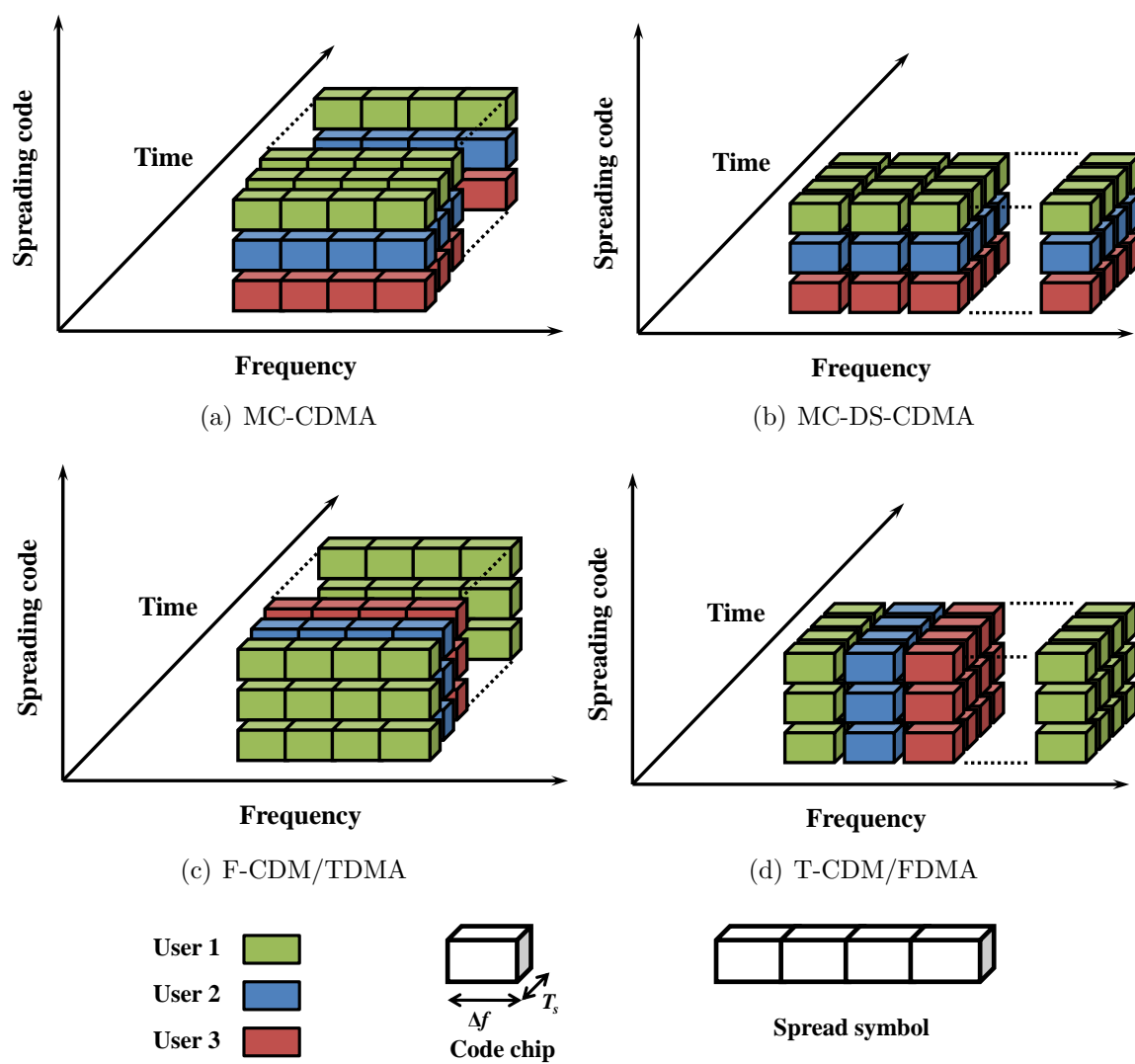


Figure 2.4: Mono block configurations.

2.2.3.3 Multi block systems

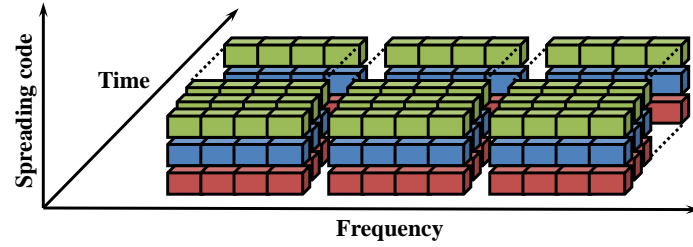
An extension of previous systems can be made by allowing multiple blocks of subcarriers to transmit simultaneously. This additional flexibility, obtained due to the better exploitation of the frequency axis, gives birth to systems consisting of a unique characteristic of dual parallelization on the frequency axis: frequency division multiplexing between subcarriers of a given block FDM (A) and frequency multiplexing between different blocks of subcarriers BDM (A). In the previous discussion, the spreading code length was considered to be equal to the total number of subcarriers i.e. $L = N$. In a more general approach L may not be necessarily equal to N . Furthermore, various system parameters may be modified for better compatibility of MC-SS signal with the channel. For example, the code length L can be reduced to make the system more flexible and to reduce the receiver complexity. Therefore, various multi block MC-SS configurations can be developed by combining N subcarriers into B smaller blocks of length $L = N/B$. A different multiplexing scheme may be employed for each block.

When multiple access is performed in the code dimension, the spreading can be carried out in the frequency dimension, as discussed earlier for MC-CDMA systems. The data multiplexing for each user may be performed in both time and frequency dimensions as depicted in Fig. 2.5(a). This system is quite similar to MC-CDMA systems but L is no more equal to N . It should be noted that all users can transmit their data simultaneously using all subcarriers and the number of multiplexed data per user in the frequency dimension is equal to the number of blocks B . This scheme is known as BDM & TDM/F-CDMA. Furthermore, the spreading can also be carried out in time direction, in this way a multiple block FDM/T-CDMA scheme is obtained.

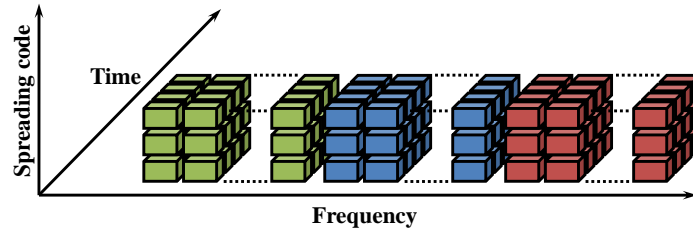
For frequency division multiple access scenario, various configurations can be developed. One approach is to assign one block of subcarriers to each user. Moreover, we obtain a T-CDM & FDM/BDMA scheme when spreading is performed in time direction, as shown in Fig. 2.5(b). Systems BDM & F-CDM/TDMA and BDM & FDM/T-CDMA, as shown in Fig. 2.5(c) and 2.5(d) respectively, are direct multi block extensions of mono block systems discussed previously. It shows that they result simply from frequency multiplexing of various blocks of combinations shown in Fig. 2.4.

All MC-SS schemes discussed until now, employ the spreading either in frequency or in time dimension and therefore are known as one-dimensional spreading. However, such MC-SS scheme can also be developed that perform spreading in time and frequency dimension simultaneously. It is known as two-dimensional spreading and can be carried out either by a two-dimensional code or two cascaded one-dimensional codes. An efficient method for performing two-dimensional spreading is to use one-dimensional code concatenated with a two-dimensional interleaver [68].

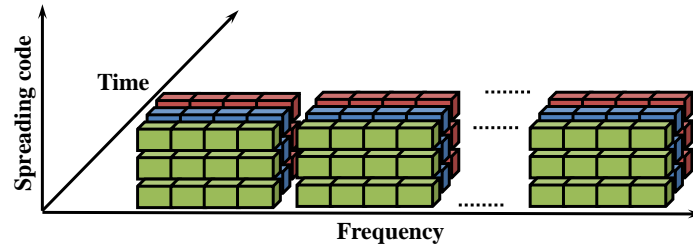
It will be further detailed in Section 2.2.4 that the selected modulation scheme in this dissertation for PLC systems is a modified version of SS-MC-MA scheme, known as linear precoded orthogonal frequency division multiplexing (LP-OFDM). In this scheme, SS-MC-MA principles are applied using a frequency-hopping technique.



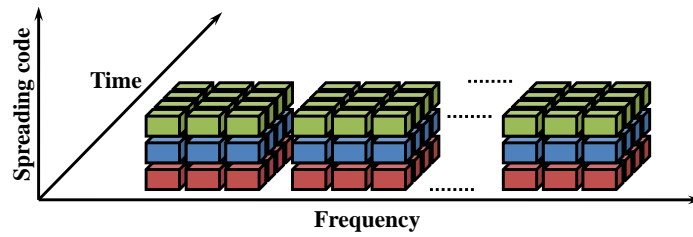
(a) BDM & TDM/F-CDMA



(b) T-CDM & FDM/BDMA



(c) BDM & F-CDM/TDMA



(d) BDM & FDM/T-CDMA

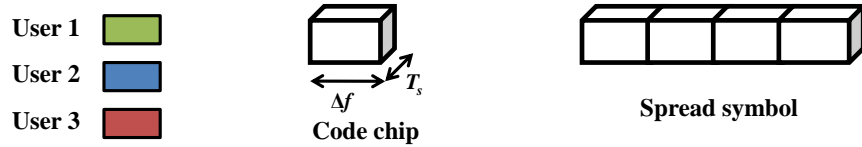


Figure 2.5: Multi block configurations.

The prime positives of LP-OFDM, which justify the selection of this scheme for PLC applications, are also explained in the following section.

2.2.4 System selection

In this section, we come to the point for which we presented all these techniques. The goal is to choose the best suited technique to the requirements of the considered system. As discussed earlier, the allowed frequency band is almost 20 MHz and therefore a multi block system should be considered. Note that a multi block system permits a more adaptable chip allocation on the time-frequency code than a mono block system. Furthermore, the selected system must be having a good compatibility with PLC channel characteristics. Therefore, the judiciously selected system, on one hand, should be able to employ an adaptive allocation strategy to distribute the available resources between multiple users and subcarriers and on the other it should fairly improve the bit rate and the system robustness against various noise and interference sources. Moreover, for practical implementations, the system complexity aspects must also be taken into account.

2.2.4.1 Selection of LP-OFDM

In this dissertation, we consider a transmission scheme based on the combination of OFDM waveform with spread spectrum principles, or equivalently linear precoding techniques. The main objectives are to obtain a more flexible system with reduced system complexity and to enhance the overall system performance. The strategy to combine spread spectrum with OFDM was originally proposed for multi-user scenario, however it can be easily employed in all single-user systems as well. Linear precoding operation consists of using precoding matrices for various blocks of subcarriers in the multicarrier spectrum [74]-[75]. The system complexity is not significantly increased for practical purposes as a precoding block is simply added in the transmission chain that introduces an additional complexity equivalent to one Hadamard matrix multiplication.

The selected transmission scheme, known as LP-OFDM in the following, can be seen as a modified form of SS-MC-MA waveform originally proposed for mobile radio communications by Kaiser and Fazel [76]. As was the case for SS-MC-MA, the spreading for LP-OFDM scheme is performed in the frequency dimension after taking into account the frequency selectivity and quasi static nature of the PLC channel in an indoor environment. The spreading component enhances the robustness of the waveform against narrowband interference and frequency selectivity by making the signal bandwidth much larger than the interference and coherence bandwidth. It also accumulates energies of many subcarriers by grouping them together which is useful in increasing the throughput especially under PSD constraint. Furthermore, multiple access is provided through the frequency dimension (as in OFDMA or SS-MC-MA) rather than the code dimension (as in MC-CDMA).

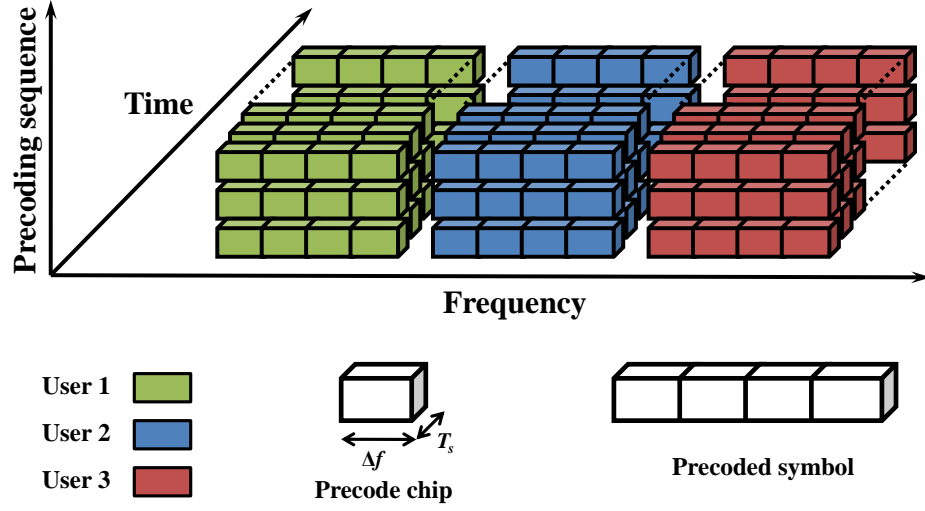


Figure 2.6: LP-OFDM system representation.

Fig. 2.6 shows a schematic representation of an LP-OFDM system. The entire bandwidth is divided into N parallel subcarriers which are split up into K blocks S_k of L subcarriers, where k signifies the block number. The precoding function is then applied block-wise by mean of precoding sequences of length C , also known as precoding factor. Note that the subcarriers in a given block are not necessarily adjacent. Each user u of the network is being assigned a set B_u of subsets S_k . We emphasize that $\forall u$, B_u are mutually exclusive subsets. Each user communicates on a specific set of subcarriers. Linear precoding is implemented in the frequency dimension therefore each user benefits from the linear precoding component by multiplexing its transmit symbols. Inserting an interleaver, before the OFDM modulator, allows each user to take advantage of the independence associated to the total frequency band of the transmitted signal. In a general approach, the generated symbol vector at the output of the OFDM modulator, for a single block LP-OFDM system, can be written as

$$s = F^H M X. \quad (2.11)$$

Vector s is L -dimensional, where L is the number of used subcarriers. $X = [x_1, \dots, x_C]^T$ is the output of the serial-to-parallel conversion of the C QAM modulated symbols to be transmitted. M represents the precoding matrix of size $L \times C$ applied to X , which precodes C symbols over L subcarriers. This precoding matrix is composed of orthogonal Hadamard matrices. Finally, F^H represents the Hermitian of the unitary Fourier matrix of size $L \times L$ that realizes the multicarrier modulation. The number of precoding sequences used to spread information symbols on one subset S_k is denoted by C^k , with $0 \leq C^k \leq L$, since we assume orthogonal sequences. A certain amount of transmit power E_c^k is assigned to each precoding sequence c^k associated to a given modulated symbol of b_c^k bits.

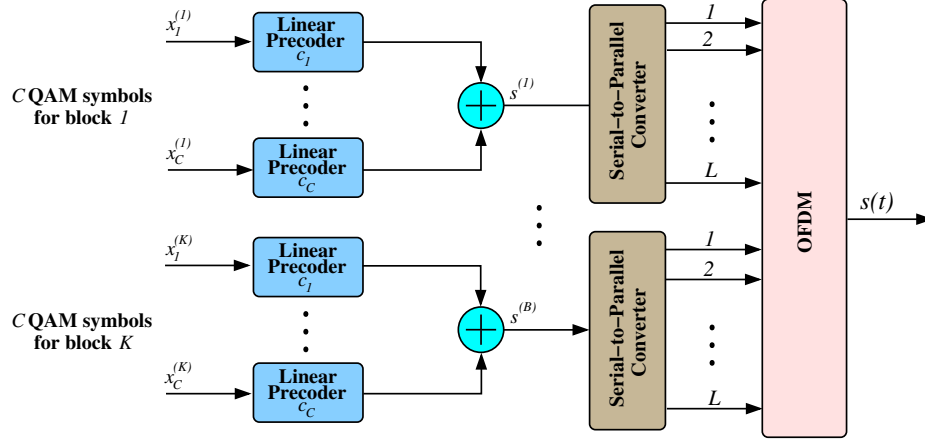


Figure 2.7: LP-OFDM single user transmitter.

In short, the proposed LP-OFDM scheme exploits the advantages of linear precoding and OFDM combination. The linear precoding in the frequency dimension improves the signal robustness against frequency selectivity. It also counters the effects of narrowband interference. Moreover, ISI and ICI can be avoided in both MC-CDMA and LP-OFDM systems, resulting in simple detection techniques and it can also be exploited to reduce the PAPR of the OFDM system [77].

Furthermore, the considered LP-OFDM technique has a number of advantages over MC-CDMA. Actually, it is generally known that spreading may introduce some typical interferences between spreading sequences when orthogonality is not perfect. Therefore, MC-CDMA systems have to encounter multiple access interference (MAI) while the proposed LP-OFDM system is free of MAI. Rather, the LP-OFDM system encounters some self-interference that is occurred by signal superposition from the same user. This self-interference may be easily compensated by a simple detection with only one complex coefficient per subcarrier. Moreover, some research studies may also be performed for suitable division of subcarriers and linear precoding sequences among different blocks and users of LP-OFDM to minimize the self-interference effects [78, 79]. Furthermore, each subcarrier is exclusively dedicated to one user at a given time in LP-OFDM that allows low complexity channel estimation. On the other hand, for MC-CDMA systems, the channel estimation has to encounter signal superposition from various users that are faded individually on same subcarriers if signals have been sent from different places, for instance uplink applications. This process significantly increases the channel estimation complexity [68].

The LP-OFDM system provides additional degree of freedom through linear precoding sequences for performance optimization and resource allocation strategies, thus increasing their flexibility and their performance. These degrees of freedom include the linear precoding factor, the number of useful precoding sequences and the subcarrier division among different blocks. Another positive of the proposed system is that

it provides a range of bit rates using high flexibility produced by combined assignment of the coding rates and the number of useful precoding sequences.

2.2.4.2 Signal characteristics

The structure of an LP-OFDM transmitter is shown in Fig. 2.7 with L precoding sequences, K blocks and C useful precoding sequences. It permits each user to simultaneously transmit C data symbol streams per block. The resulted C parallel converted data symbols of a given block k in a vectorial form may be given as,

$$x^{(k)} = [x_1^{(k)}, \dots, x_c^{(k)}, \dots, x_C^{(k)}]^T. \quad (2.12)$$

These data symbols are then multiplied by an orthogonal code of length L (such as Walsh-Hadamard code) represented as $c_c = [c_{1,c} \dots c_{l,c} \dots c_{L,c}]^T$. c_c consists of vectors of the precoding sequences matrix of size $L \times C$ and given by

$$C = [c_1 \dots c_c \dots c_C]. \quad (2.13)$$

The same linear precoding matrix C can be used for all blocks. These modulated precoding sequences are then synchronously added, which results in the transmission vector per block and can be given as

$$s^{(k)} = Cx^{(k)}, \quad (2.14)$$

where $s^{(k)} = [s_1^{(k)}, \dots, s_l^{(k)}, \dots, s_L^{(k)}]^T$. These transmission vectors (obtained from various blocks) are then fed to the OFDM modulator for further processing.

2.3 Resource allocation for multicarrier systems

In multicarrier system design, bit and power allocation is considered as a fundamental aspect. In practical systems, the problem of resource allocation is dealt with the help of bit and power loading algorithms, which are used to distribute the total number of bits and the total available power among different subcarriers in an optimal way to maximize the system performance and to maintain a requested quality of service. The resource allocation can be seen as a constraint optimization problem [80] and is generally divided into two cases: rate maximization (RM) [81] and robustness maximization (RoM) [82] where the objective is to maximize the achievable data rate and the system robustness against noise, respectively. Margin maximization (MM) is the classical and the most common scenario of robustness maximization where the system's noise margin is maximized. The optimization problem can be formulated under total power constraint [81] as well as under PSD constraint [13]. In this thesis, we will only discuss the formulations subject to PSD constraint. In contrast to total power constraint, the residual power of one subcarrier is of no use for the others under PSD constraint. Therefore the task of efficient utilization of power becomes even

more sophisticated. The maximum error rate constraint depends upon the considered modulation and channel coding scheme.

Under PSD constraint and for a given target error rate, the resource allocation generally gives either the maximum bit rate for a given system margin or the maximum system margin for a target bit rate. MM optimization problem is also known in the literature as the problem of power minimization under fixed bit and error rate. CSI must be known in advance at the transmitter and receiver to adaptively modulate different subcarriers. Wireless channel is generally time varying and therefore the same modulation order is commonly used by all subcarriers. Wireline channel, on the other hand, is either quasi-static or very slow time-varying, therefore CSI can be sent to the transmitter through a feedback channel. In common wireline channels (e.g. channels in DSL and PLC etc.) the capability of MCM to adaptively load different bits and powers to different subcarriers is well exploited. Increase in the number of required subcarriers and the growth in the total number of users in commercial applications have led to the demands of very sophisticated and efficient loading algorithms. There is a high research and commercial interest in the development of high performance bit and power loading algorithms, which can efficiently boost the system performance without significantly increasing the system complexity. This exciting field is becoming more and more challenging with every passing day.

We can find many loading algorithms proposed for DSL [81]-[83] and PLC systems [30, 84] in the existing literature. These algorithms generally deal with either the RM or the MM problem. The resource allocation is normally classified into two stages. The first stage consists of the analytical study of the optimization problem and assumes infinite granularity of the modulation. This analytical study generally uses numerical methods that employ Lagrange multipliers to solve the optimization problem. Other analytical approaches for optimization may also be found in the literature. These methods generally result in real numbers for optimum bit allocation and thus are for the theoretical purposes only [85, 86]. The second stage is the practical implementation of the theoretical study obtained from the first stage. It uses discrete modulations and quantization techniques are applied while still providing a solution near to the optimal one. This stage provides a sub-optimal solution because of the use of finite granularity of modulation and therefore this stage normally includes a bit-rounding step. A combinatorial structure is imposed in the loading optimization problem by the integer-bit constraint. A greedy and iterative method may be used in this stage to obtain the optimum discrete bit allocation. Some analytical studies may also be performed to reduce the complexity of this greedy solution [87]. In this dissertation, we consider only the single user case i.e. a point-to-point link is assumed between a PLC-based transmitter and a receiver. A single user resource allocation scheme is an essential part of a practical system consisting of multiple users and applications.

2.3.1 Theoretical capacity

Claude E. Shannon [88] presented the maximum digital information that can be transmitted in a non-dispersive channel environment, with an attenuation factor α and in the presence of additive white Gaussian noise (AWGN) with a noise power N_0 . This classical work of Shannon states that reliable communications over a channel can be achieved only for those information rates which are less than a certain threshold rate, Shannon capacity. Shannon capacity depends upon the frequency band W and the available transmit power E_s and can be given as

$$C_{Shannon} = W \log_2 \left(1 + \frac{\alpha E_s}{N_0} \right) = W \log_2 (1 + \text{SNR}), \quad (2.15)$$

where $C_{Shannon}$ is presented in b/s and $\alpha E_s/N_0$ is the available SNR. The objective of the modern research in modulation and channel coding schemes is to approach the Shannon limit as closer as possible but it is universally accepted that we can never exceed the limit defined by Claude Shannon in 1940 through his extremely rigorous mathematical analysis. It is generally considered that the Shannon limit is only achievable if we employ a channel coding scheme with infinite complexity and immeasurable coding/decoding delays. It is quite obvious that in real systems, this scenario is not possible where practical suboptimal channel coding schemes are used. Therefore the bit rate that can be achieved in practical scenarios is always lower than the Shannon capacity. Using Shannon limit, the capacity can be given in b/s/Hz as,

$$C = \log_2 (1 + \text{SNR}). \quad (2.16)$$

A parameter Γ , called as the SNR gap (also known as the normalized SNR), is used to evaluate the relative performance of a modulation scheme versus the theoretical capacity of the channel. SNR gap is defined by the power (in dB) required to transmit a given modulation order at a given error rate minus the power (in dB) given by Shannon limit to transmit the same number of bits. The SNR gap (in dB) for any given modulation scheme requiring SNR_{dB} to transmit b bit can be given as

$$\Gamma_{\text{dB}} = \text{SNR}_{\text{dB}} - 10 \log_{10} (2^b - 1), \quad (2.17)$$

where linear calculations results in the following expression for Γ ,

$$\Gamma = \frac{\text{SNR}}{2^b - 1}. \quad (2.18)$$

The SNR gap is calculated using the “gap approximation” analysis [89, 90], based on the target error probability P^s , the channel coding gain γ_c , and the system noise margin γ_m . For uncoded QAM with null system margin, Γ can be given as [89]

$$\Gamma \approx \frac{1}{3} \left[Q^{-1} \left(\frac{P^s}{4} \right) \right]^2, \quad (2.19)$$

where Q^{-1} , the inverse of the well-known Q-function, is given as

Table 2.1: Puncturing sequences to generate different code rates.

code rate	puncturing sequence
1/2	1
	1
2/3	10
	11
3/4	110
	101
4/5	1111
	1000
5/6	11010
	10101
6/7	111010
	100101

$$Q(x) = \frac{1}{\sqrt{2\pi}} \int_x^\infty e^{-y^2/2} dy. \quad (2.20)$$

For coded QAM systems with a specified system margin, Γ can be written as,

$$\Gamma = \frac{1}{3} \left[Q^{-1} \left(\frac{P^s}{4} \right) \right]^2 \frac{\gamma_m}{\gamma_c}. \quad (2.21)$$

The system noise margin γ_m is the immunity provided by system designers against the SNR degradation and the various noise sources. High values of noise margin guarantee the promised error rate for a given modulation order even in highly noisy environments but on the other hand it also increases the total power required for the target error rate. Using a channel coding scheme, with a coding gain γ_c , reduces the power required to transmit target number of bits at the desired error rate. Therefore, the higher the coding gain is, the closer is the transmission rate to the Shannon capacity.

In Fig. 2.8 and 2.9, the performance of uncoded QAM is compared with the convolutionally coded QAM. Gray coding is applied to both the uncoded and coded QAM as the default source coding scheme. The simulations are run for a target BER of 10^{-5} and a non-systematic convolutional encoder is used with a constraint length 7 and polynomials $g^1 = 171_8$ and $g^2 = 133_8$. Different code rates are obtained by using different puncturing sequences. These puncturing sequences are given in Table 2.1 [91].

The value of the SNR gap can be evaluated using the error rate curves for a given operating point that can either be a target BER or a target symbol error rate (SER). In Fig. 2.10, the practical spectral efficiency of different QAM modulation orders is presented for a target BER of 10^{-5} and a target SER of 10^{-5} . It should be noted that the spectral efficiency curves given in this figure are derived from well known

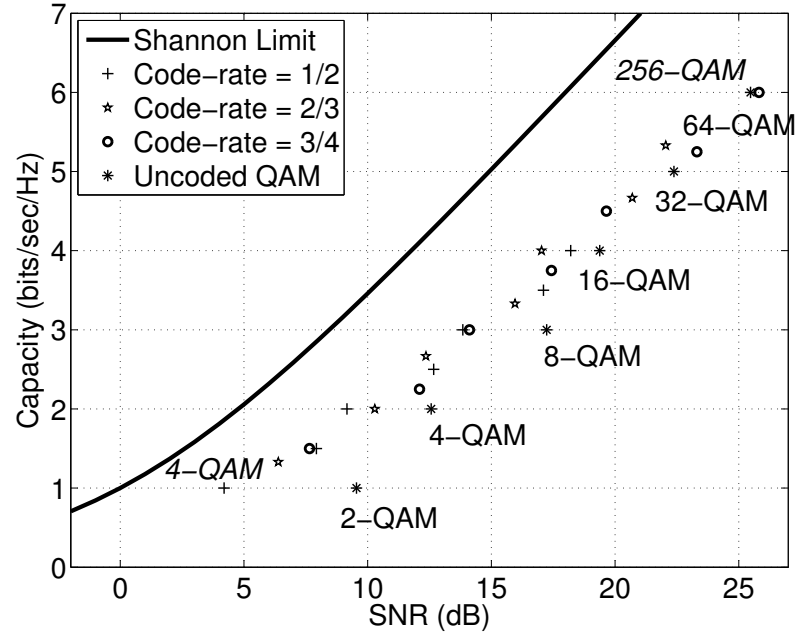


Figure 2.8: Performance evaluation of uncoded QAM with convolutionally coded QAM.

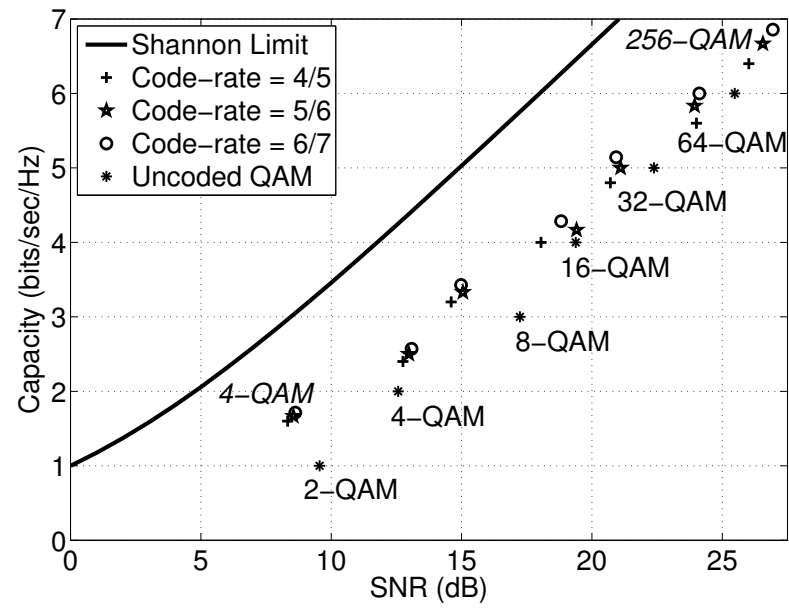


Figure 2.9: Performance evaluation of uncoded QAM with convolutionally coded QAM.

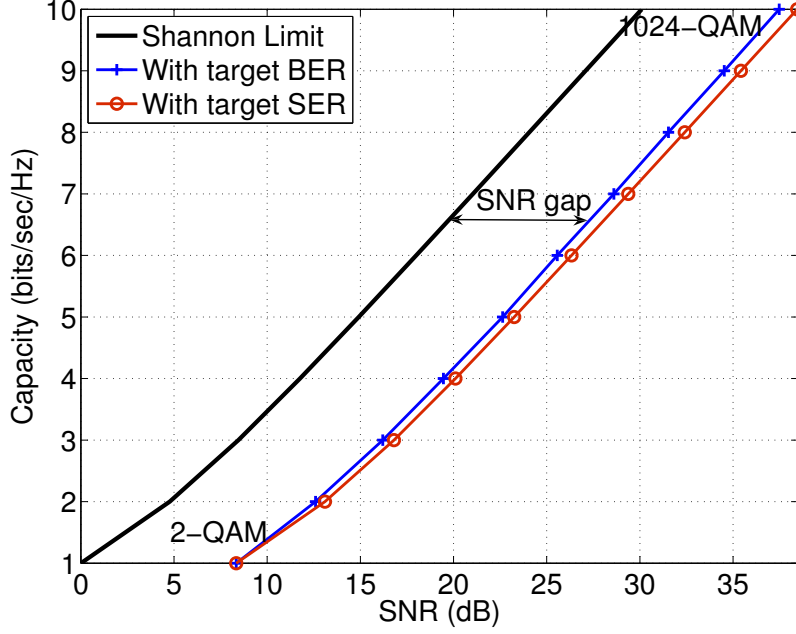


Figure 2.10: SNR gap for various QAM modulation orders with target BER and target SER criteria.

capacity approximations [41]. We observe that for a given SER, Γ has the same value for all the modulation orders taking into account the capacity approximations. This constant value of Γ is very advantageous in the implementation of bit and power loading algorithms as we do not need to change the value of Γ for different subcarriers and one variable is reduced from the objective function of optimization. This is one of the main reason of almost universal acceptance of constant SER approach in the existing analytical studies on resource allocation and optimization for multicarrier systems. For a target BER, on the other hand, Γ is no more constant and it somewhat decreases for higher modulation orders. For instance, at target BER of 10^{-5} , $\Gamma = 8.34$ dB for 2-QAM and $\Gamma = 7.37$ dB for 1024-QAM, and this slight difference (i.e. of almost 1 dB) in the value of Γ creates a significant difference in the performance of resource allocation algorithms. It must be noted here that for higher value of target BER this difference becomes even more significant. On the other hand, $\Gamma = 8.34$ dB for all the constellation sizes of QAM for a target SER of 10^{-5} . Although it is not commonly used, the advantages of using target BER approach will be discussed in following chapters.

2.3.2 Fundamentals of multicarrier resource allocation

In MCM, the entire bandwidth is divided into N orthogonal, narrowband subcarriers with generally equal bandwidth. A rate function $R(E_i, P)$ can be defined for each

subcarrier i that gives the number of bits b_i that can be transmitted using power E_i while respecting a maximum error rate P (generally speaking $P_i = P \forall i$). The rate function also takes into account the applied modulation and coding schemes, which is supposed to be the same for all the subcarriers (of course the modulation orders and the coding rate may vary for different subcarriers). Inversely, a power function $E(b_i, P)$ can be defined which suggests the power required to transmit b_i bits while respecting a maximum tolerable error rate. Considering QAM, the number of bits that can be carried for a known SNR is given as

$$b_i = \log_2 \left(1 + \frac{E_i |H_i|^2}{\Gamma N_0} \right), \quad (2.22)$$

where H_i is the complex frequency response of subcarrier i and N_0 is the noise power spectral density. In classical resource allocation problems, an additional margin γ_m is added to the SNR gap Γ (as explained in (2.21)). This margin ensures that the target error rate is achieved even if the noise level is increased by a factor of γ_m . The number of bits that can be carried by a symbol can then be written as

$$b_i = \log_2 \left(1 + \frac{E_i |H_i|^2}{\gamma_m \Gamma N_0} \right). \quad (2.23)$$

Therefore, by increasing the value of γ_m we can improve the system robustness against noise, and hence have the new operating point of the QAM constellations at a distance of $(\Gamma + \gamma_m)$ dB from the Shannon limit. This idea of noise margin has been discussed thoroughly in the existing literature on the optimization of the system robustness and will be challenged with a new approach of robustness optimization in the following chapters.

The transmit power required to transmit b_i number of bits for a known channel response and a target error rate is given as

$$E_i = (2^{b_i} - 1) \frac{\gamma_m \Gamma N_0}{|H_i|^2}. \quad (2.24)$$

A communication system is mainly limited by the allocated frequencies and the transmit power. All the systems are assigned limited frequency bands to reduce interference with each other. System standards also impose power constraints to respect medical regulations and avoid interferences. PLC communications suffer from both limited bandwidth and strict power limitations in terms of PSD. Furthermore, the available optimization parameters also vary depending upon the considered multicarrier scheme. For instance, in OFDM systems, different numbers of bits and different transmit powers can be attributed to different subcarriers depending upon the channel strength on the subcarrier. LP-OFDM systems provides additional degrees of freedom to resource allocation strategies due to its linear precoding component, such as optimal number of linear precoding sequences in a block, optimal number of useful precoding sequences in a block and optimal allocation of subcarriers among different blocks of LP-OFDM system.

In the following, we discuss the common resource allocation strategies for multi-carrier systems. We chose the conventional OFDM system for the detailed description of optimum distribution of bit and power to different subcarriers. This OFDM system will be considered as a reference system for our studies in this dissertation, as it has been largely implemented in practical PLC modems. For a given OFDM system with N subcarriers the total bit rate obtained from all the subcarriers can be given as

$$R_{OFDM} = \sum_{i=1}^N b_i = \sum_{i=1}^N \log_2 \left(1 + \frac{E_i |H_i|^2}{\gamma_m \Gamma N_0} \right). \quad (2.25)$$

This defines the function of optimization for which, we will apply different optimization schemes. The power constraint can either be imposed in terms of total power constraint E_T (i.e. $\sum_i E_i \leq E_T$) or in terms of PSD (or peak power) constraint that is $E_i \leq \hat{E}$, where \hat{E} is the maximum authorized power, as discussed in Section 1.2.2. The total power constraint has been thoroughly discussed in the existing literature. It is under this constraint that the well known water filling solution was first proposed for rate maximization [92]. In this study, we consider the PSD constraint instead of total power constraint that is imposed by the transmission standards. Thus, the PSD constraint will be applied to various optimization studies carried out in this work.

In the following, we will make distinction between the theoretical solutions obtained from the optimization study where the number of bits are presented in real numbers and the practical solutions for real systems where the transmitted bits are presented in integer values imposed by the finite granularity of QAM. The former scenario will be referred as infinite granularity and the latter one as finite granularity.

2.3.3 Rate maximization

First of all, we discuss the most common optimization problem for multicarrier systems that is the maximization of bit rate. For an OFDM system, the problem of bit rate maximization under a PSD constraint and for a target SER can be defined as

$$\begin{cases} \max \sum_{i=1}^N \log_2 \left(1 + \frac{1}{\gamma_m \Gamma} |H_i|^2 \frac{E_i}{N_0} \right) \\ \text{subject to } E_i \leq \hat{E} \end{cases} \quad (2.26)$$

The objective of this problem is to distribute bits and powers among different subcarrier in such a way that the total bit rate of an OFDM system is maximized. However, we note that in this RM problem, the number of bits at each subcarrier solely depends upon the transmit power available at the same subcarrier (i.e. independent of the transmit power available at other subcarriers). Therefore, no water filling solution can be applied in this case. The bit and power allocation is performed in two steps. Firstly, we find out the optimal solution consisting of real values for number of bits and in the second step, this solution is rounded to integer values.

2.3.3.1 Infinite granularity solution

When the number of bits per subcarrier can have real values, all the available power on each subcarrier, of course, will be used to maximize the bit rate of the system. Thus, the solution of bit rate maximization for OFDM under PSD constraint and with a target SER using infinite granularity of modulation can be given as

$$\begin{cases} b_i = \log_2 \left(1 + \frac{1}{\gamma_m \Gamma} |H_i|^2 \frac{E_i}{N_0} \right), \forall i, \\ E_i = \hat{E}, \forall i. \end{cases} \quad (2.27)$$

Here, the real capacity of the QAM shown in Fig. 2.10 is obtained. It must be noted that for a total power constraint the solution of bit rate maximization is entirely different from that of a PSD constraint, as discussed in [92].

2.3.3.2 Finite granularity solution

The solution of rate maximization problem for finite granularity is also as straightforward as for infinite granularity, if not more. Actually, the number of bits for each subcarrier can be obtained through a simple rounding operation performed on the real valued solution obtained previously. It is recommended to use the floor operation (instead of a ceil operation) to respect the limitations imposed on transmit power and maximum acceptable SER. Therefore, using (2.25) and (2.27), the finite granularity bit and power allocation for RM-OFDM problem can be given by

$$\begin{cases} \ddot{b}_i = \lfloor b_i \rfloor, \forall i, \\ \ddot{E}_i = \gamma_m \Gamma \frac{N_0}{|H_i|^2} \left(2^{\ddot{b}_i} - 1 \right), \forall i, \end{cases} \quad (2.28)$$

where \ddot{x} specifies that x is a non-negative integer valued number. It should be noted here that \ddot{E}_i in (2.28) is always less than the PSD limit \hat{E} . For the sake of simplicity and to provide an additional noise margin, each subcarrier is assigned all the available transmit power. Fig. 2.11 explains the difference between the resultant bit allocation for finite and infinite granularity of modulation, considering a textbook case consisting of 100 subcarriers. The subcarriers are sorted in descending order of their channel gain for the sake of simplicity and to enhance the graphical readability. In the background different broken line curves show the capacity achieved for various PSD limits. The blue curve shows the bit rate achieved for the applied PSD limit. This PSD limit is supposed to be flat i.e. $\hat{E}_i = \hat{E} \forall i$. The staircase curve shows the bit rate when discrete modulation is taken into account i.e. the finite granularity. In this case we can observe some loss of bit rate due to quantization. It shows that OFDM allocation is not efficiently exploiting the available power in order to maximize the bit rate. Furthermore, some subcarriers with poor channel gain cannot even transmit a single bit if the PSD limit is very low. The ability of LP-OFDM to better exploit the available energy resources will be demonstrated in the next chapter.

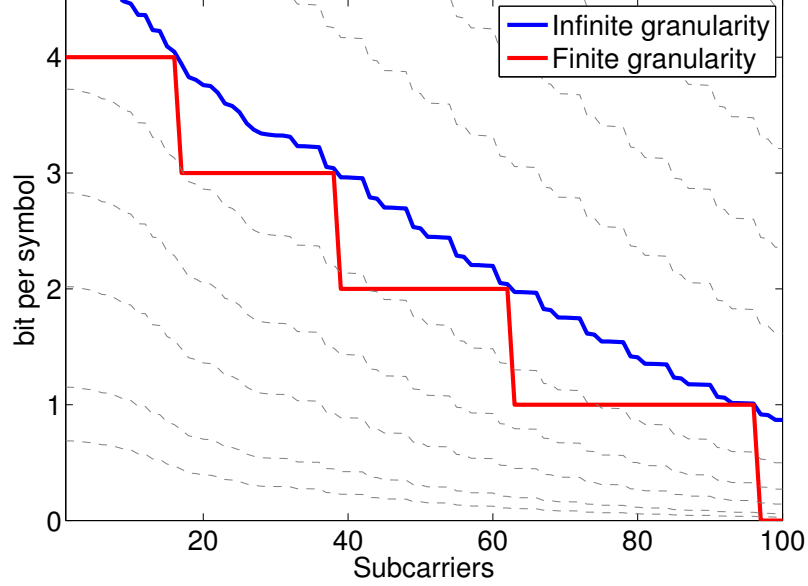


Figure 2.11: Comparison of bit allocation for finite and infinite granularity of modulation in the case of bit rate maximization under PSD constraint.

2.3.4 Robustness Maximization

The most common robustness maximization scheme is the noise margin maximization (or power minimization). In this scheme, the system's noise margin γ_m is maximized for a target bit rate and a given error rate under PSD constraint. It can be easily observed that γ_m cannot be extracted simply from (2.25), therefore we take into account the separate noise margin for each subcarrier γ_i , which can be defined as

$$\gamma_i = \frac{1}{\Gamma N_0} \frac{E_i |H_i|^2}{2^{b_i} - 1}. \quad (2.29)$$

The objective of this scheme is to have the maximum possible noise margin, therefore all the power resources must be exploited. Thus, $E_i = \hat{E}$, which signifies that the signal will be transmitted just under the PSD limit. The problem of margin maximization then can be given as

$$\begin{cases} \max \frac{1}{\Gamma N_0} \frac{\hat{E} |H_i|^2}{2^{b_i} - 1}, \forall i \\ \text{subject to } \sum_{i=1}^N b_i = \hat{R} \end{cases} \quad (2.30)$$

The objective is to maximize the noise margin of each subcarrier individually while achieving a target bit rate \hat{R} . The solution is obtained by wisely distributing different bits among subcarriers. Thus, the solution of this problem is to give the optimal

bit allocation, whereas the optimal power distribution is performed by using all the available power under the limit of the imposed PSD mask.

2.3.4.1 Infinite granularity solution

Similar to our approach in the case of bit rate maximization, firstly we discuss the case of margin maximization for infinite granularity of modulation and then for discrete modulations. The problem of margin maximization can be expressed as the problem of $\frac{1}{\gamma_m}$ minimization. The solution of this optimization problem is found by applying Lagrange multiplier method. Lagrangian associated with this problem can be written as

$$L(b_i, \lambda) = \Gamma N_0 \frac{2^{b_i} - 1}{\hat{E} |H_i|^2} + \lambda \sum_{i=1}^N b_i - \lambda \hat{R}, \quad \forall i, \quad (2.31)$$

where λ is the Lagrange multiplier. Taking derivative of Lagrange function leads to the expression of b_i in function of the multiplier λ

$$b_i = \log_2 \left(-\frac{\lambda}{\ln 2} \frac{\hat{E} |H_i|^2}{\Gamma N_0} \right). \quad (2.32)$$

Now, by using the constraint equation we can easily extract the Lagrange multiplier,

$$\lambda = -\ln 2 \frac{\Gamma N_0}{\hat{E}} \frac{2^{\frac{\hat{R}}{N}}}{\left(\prod_{i=1}^N |H_i|^2 \right)^{\frac{1}{N}}}. \quad (2.33)$$

Once we have found the Lagrange multiplier, it is easy to find the optimal bit allocation by putting it back in the constraint equation. Thus, the optimal bit and power allocation for margin maximization can be summarized as follows

$$\begin{cases} b_i = \frac{\hat{R}}{N} + \log_2(|H_i|^2) - \frac{1}{N} \sum_{i=1}^N \log_2(|H_i|^2), \forall i, \\ E_i = \hat{E}, \forall i. \end{cases} \quad (2.34)$$

It must be noted here that the subcarriers carrying negative values of b_i should be excluded from the allocation process as it may lead to absurd results. They are therefore separated from the lot and the resource allocation calculation is performed on the rest of subcarriers. It must also be noted that the obtained solution is exactly the same as is obtained in the case of total power minimization for target bit rate [93]. Thus, for infinite granularity of modulation the margin maximization is equivalent to the total power minimization for a given bit rate.

2.3.4.2 Finite granularity solution

Contrary to the case of bit rate maximization, the finite granularity allocation for MM case cannot be attained by applying a simple rounding operation of infinite granularity allocation. In fact, if we perform a rounding operation on infinite granularity allocation, the resulting bit rate becomes less than the target value and the constraint is no more respected. It leads us to a separate study of margin maximization for finite granularity of modulation. If \ddot{b}_i is the integer number of bits allocated to subcarrier i , the noise margin $\ddot{\gamma}_i$ associated to this subcarrier can be given as

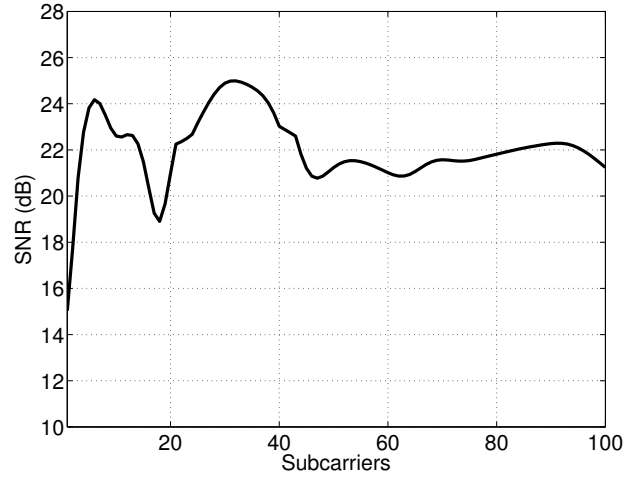
$$\ddot{\gamma}_i = \frac{1}{\Gamma N_0} \frac{E_i |H_i|^2}{2^{\ddot{b}_i} - 1}. \quad (2.35)$$

Therefore, the MM problem for finite granularity can be given as

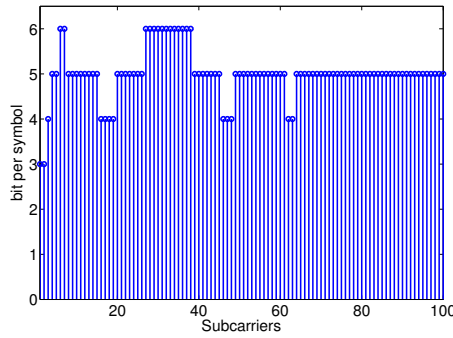
$$\begin{cases} \max \frac{1}{\Gamma N_0} \frac{\hat{E} |H_i|^2}{2^{\ddot{b}_i} - 1}, \forall i \\ \text{subject to } \sum_{i=1}^N \ddot{b}_i = \hat{R} \end{cases}. \quad (2.36)$$

This type of problem can be simply resolved by implementing a greedy algorithm consisting of an iterative procedure in which we attain the optimal solution by maximizing the local function step by step. In the case of MM problem the local optimization function is the noise margin associated to each subcarrier. The greedy algorithm, applied to the problem, thus distribute the bits one by one to the subcarrier in such a way that each new bit is assigned to the subcarrier that has the maximum value of noise margin after this new allocation. It must be noted that the bit allocation to one subcarrier does not affect the noise margins of other subcarriers. It shows that noise margins of each subcarrier is independent of others, which confirms that the optimization problem can be effectively resolved through the greedy approach. It must be noted here that due to the finite granularity the optimal noise margins obtained through this iterative approach will be different from one another.

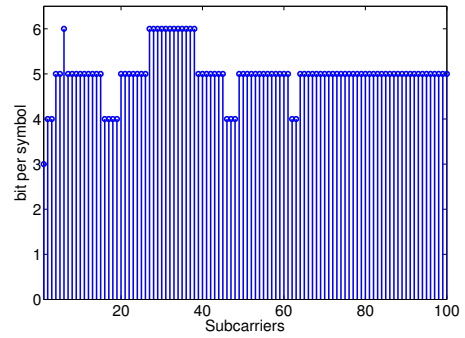
As an iterative solution is proposed for this problem, it can also be shown that to distribute B bits on N subcarriers, the greedy algorithm can be executed from an initial allocation $\hat{B} \neq B$ to attain the optimal solution. It implicates that it is possible to start the iterative procedure from an allocation having a bit rate well under or above the target bit rate. Particularly, it is possible to start the greedy algorithm with zero bit on all subcarriers as well as maximum allowed modulation order on all subcarriers. One interesting idea is to use the bit allocation attained in (2.34) after rounding operation as the starting point to reach quickly at the optimal solution. The sum of total number of bits on all subcarriers is calculated in each iteration. If it is less than the target bit rate, one bit is added in the system and if it is greater than the target bit rate, one bit is extracted from the system. When the target bit rate is achieved, the iterative procedure is ended.



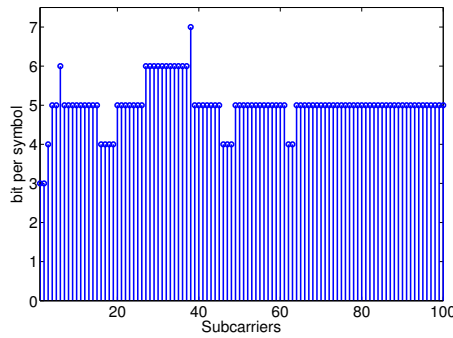
(a) Channel frequency response



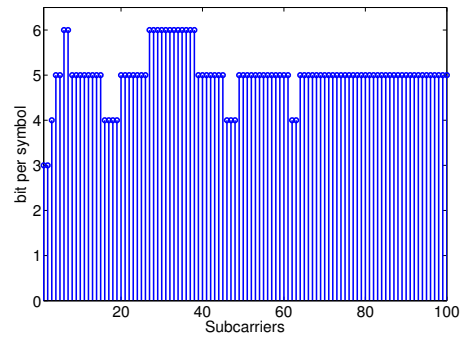
(b) Hughes-Hartogs allocation



(c) Chow's allocation



(d) Czylwik's allocation



(e) Campello's allocation

Figure 2.12: Comparison of various bit allocation algorithms for margin maximization/total power minimization for same target bit and error rate.

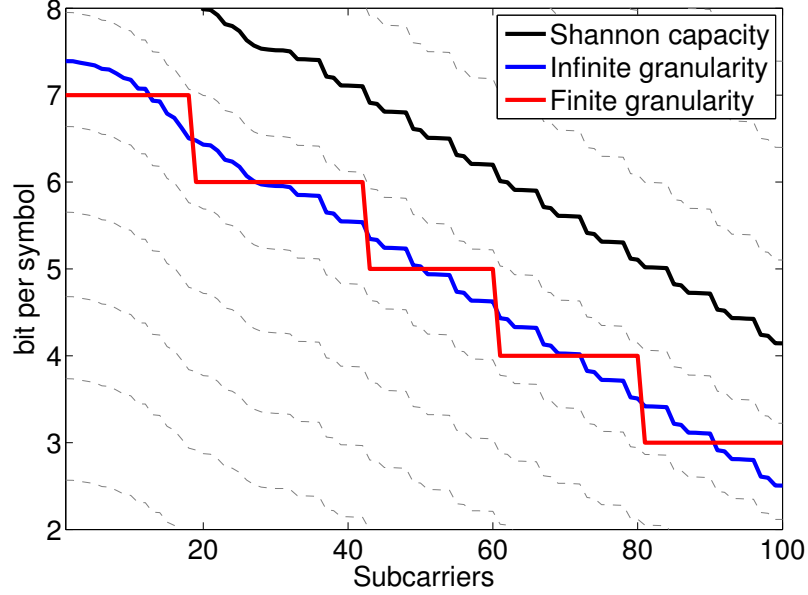


Figure 2.13: Comparison of bit allocation for finite and infinite granularity of modulation in the case of margin maximization under PSD constraint.

Various margin maximization/total power minimization algorithms are studied and the bit allocations obtained from these algorithms are shown in Fig. 2.12. The same channel transfer function is used for all these algorithms and it is also shown in the figure. Hughes-Hartogs [92] applied the greedy algorithm in margin maximization problem for the first time for multicarrier systems. This multicarrier loading algorithm implements the water-filling solution adapted to QAM by using the SNR gap approximation to relate capacity to the achievable bit rate. Chow's algorithm [83] was originally developed for DMT in ADSL systems. In the literature, it is considered as the first sub-optimal solution to the bit loading problem in multicarrier systems, which discusses implementation issues. Czylik's algorithm [94] minimizes the total transmit power for a given bit rate. Campello also proposed in his paper [95] an optimal and efficient algorithm for practical systems. Since it uses the gap approximation, its results are similar to Hughes-Hartogs method. However, the way of doing the adaptation is quite different with a lower number of operations that means faster implementation.

The greedy algorithm for the noise margin maximization can be given as follows:

MM FOR OFDM USING QAM()

- 1 Initialize $\ddot{b}_i = 0$ or $\ddot{b}_i = \lfloor b_i^* \rfloor, \forall i$
- 2 **while** $\sum_i \ddot{b}_i \neq \hat{R}$
- 3 **do if** $\sum_i \ddot{b}_i < \hat{R}$
- 4 **then** $i = \arg \max_i \ddot{\gamma}_i(\ddot{b}_i)$

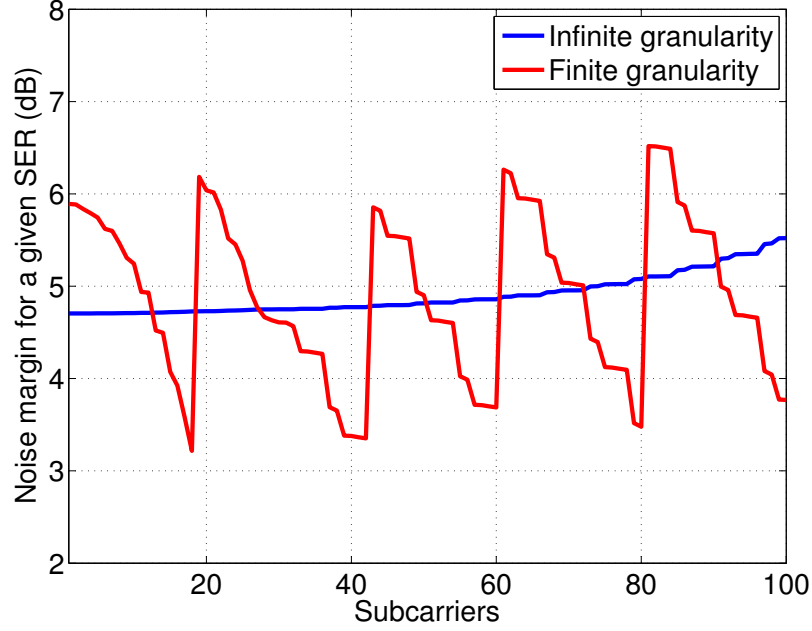


Figure 2.14: Comparison of noise margin for finite and infinite granularity of modulation in the case of margin maximization under PSD constraint.

```

5          $\ddot{b}_i = \ddot{b}_i + 1$ 
6     else  $i = \arg \min_i \ddot{\gamma}_i (\ddot{b}_i)$ 
7          $\ddot{b}_i = \ddot{b}_i - 1$ 
8     end if
9 end while

```

The above algorithm is deduced from well known Hughes-Hartogs algorithm and has been modified to respect the PSD constraint. It should be noted that the initial state for this algorithm may be zero for all subcarriers as well as the state derived from (2.34). The bit and power allocation for noise margin maximization using finite granularity of modulation can be given as

$$\begin{cases} \ddot{b}_i, \text{ obtained through the greedy approach, } \forall i, \\ \ddot{E}_i = \hat{E}, \forall i, \end{cases} \quad (2.37)$$

Contrary to the case of infinite granularity of modulation, the optimal allocation obtained for the MM problem in the case of finite granularity is not similar to that of the allocation obtained for the total power minimization for the same target bit rate.

Fig. 2.13 presents the difference between the results obtained from bit allocations for margin maximization considering finite and infinite granularity of modulation. As in the case of bit rate maximization, the subcarriers are sorted in descending order of their channel gain to enhance the graphical readability. In the background different

broken line curves show the capacity achieved at different PSD limit. The solid black curve shows the Shannon capacity achieved for the imposed PSD limit. The blue curve shows the bit allocation for applied PSD limit using infinite granularity of modulation. The staircase curve shows the bit allocation when finite granularity of modulation is taken into account for noise margin maximization under given bit rate and error rate constraints. Fig. 2.14 shows the margins obtained through these bit allocations. It must be noted that the noise margins obtained in the case of infinite granularity of modulation do not change significantly for different subcarriers and are a little bit higher for lower number of bits per subcarrier. On the other hand, the noise margins obtained for discrete modulations vary considerably depending upon the SNR available on the subcarrier and the number of bits allocated to it. It shows that in the case of finite granularity, some of the subcarriers are more vulnerable to the noise than the others. It may therefore be concluded that OFDM is not very efficient for margin maximization under PSD constraint. The better performance of LP-OFDM in margin maximization will be demonstrated in the next chapter.

2.4 Conclusion

In this chapter, various multicarrier system configurations were discussed. The principle of MCM was explained followed by the description of the idea of OFDM. Signal characteristics of OFDM were also explained and different interferences encountered by OFDM systems were studied. The pros and cons of OFDM communication were taken into consideration with a critical point of view. The principle of spread spectrum was then introduced followed by a brief survey on different multiple access schemes. Various combinations of spread spectrum with OFDM were then elaborated in mono block and multi block scenarios. Finally the description of the chosen transmission scheme was given and the reasons for the selection of this transmission scheme were discussed. The signal characteristics of the selected scheme were also presented.

Furthermore, we presented a general overview of the resource allocation and optimization for conventional multicarrier systems. Due to quasi static nature of the power line channel, the resource allocation can be efficiently performed for the PLC systems without significantly compromising on the system complexity since the channel can be known at the transmitter through the simple feedback from the channel estimator. After an introduction of the theoretical capacity of the communication system, the fundamentals of multicarrier resource allocation were discussed followed by detailed analyses of bit rate maximization and robustness maximization problems both for finite and infinite granularities of modulation. Simulation results from various studied bit and power loading algorithms were also presented. The resource allocation strategies considered in this chapter did not take into account the channel coding scheme. This aspect of the resource allocation will be discussed in the following chapters. The next chapter discusses the bit rate maximization problem for two different error rate constraints under PLC context. The results are presented for both OFDM and LP-OFDM systems in coded and uncoded scenarios.

Chapter 3

Bit rate maximization

Contents

3.1	Introduction	62
3.2	RM under peak BER constraint	63
3.2.1	RM for uncoded LP-OFDM	64
3.2.2	Mono block resource allocation	66
3.2.3	Multi block resource allocation	69
3.2.4	RM for coded LP-OFDM	70
3.2.5	Coded LP-OFDM resource allocation	81
3.3	RM under mean BER constraint	88
3.3.1	OFDM systems	88
3.3.2	LP-OFDM systems	90
3.3.3	Results	91
3.4	Conclusion	94

3.1 Introduction

After having presented the selected LP-OFDM system in the previous chapter, here we discuss the bit rate maximization strategies under PSD constraint for LP-OFDM systems in PLC context. It must be noted here that in this thesis, to better concentrate on the resource allocation at subcarrier level only single user scenarios are considered i.e. a point-to-point link is assumed between a transmitter and a receiver. A single user resource allocation scheme is the constituent part of a complete multi user scenario. It should also be noted that our colleagues in IETR are working on the multi user problem notably Ali Maiga [96]. Two new error rate constraints are used in order to obtain better throughputs for modern multicarrier PLC systems in comparison of existing solutions. Firstly, a resource allocation problem is considered for a peak BER constraint, i.e. the target BER is fixed for each subcarrier and all subcarriers must respect the given BER value. In this manner, the target BER is equal to the BER value on any given subcarrier. This approach is slightly different from the classical peak SER approach, where instead of fixing SER, the target BER is fixed on each subcarrier. The bit and power loading algorithms are presented for LP-OFDM systems using peak BER approach.

Furthermore, to enhance the performance of multicarrier PLC systems and to demonstrate the validity of efficient performance of the proposed LP-OFDM system in coded system scenarios, an adequate channel coding scheme is selected. The selected channel coding scheme is incorporated in the communication system chains of OFDM and LP-OFDM systems. We propose a new idea of integrating channel coding gains into the resource allocation process. To the best of author's knowledge, this idea has never been used in the existing literature for bit rate maximization purposes. A very few scientific publications may be found in the existing literature that discuss the idea of integrating channel coding scheme in the resource allocation process but only for power minimization in conventional OFDM systems [97]. Here, we consider the resource allocation problem for bit rate maximization of both OFDM and LP-OFDM systems that integrate the channel coding gains in bit and power loading algorithms.

In this dissertation, the bit and power loading algorithms are presented for coded multicarrier systems and the performance of the proposed coded LP-OFDM system is compared with the coded OFDM system using the same channel coding scheme. The proposed resource allocation algorithms are quite flexible in their approach and may be used for any efficient channel coding scheme. The results are shown only for the selected channel coding scheme on both systems in order to perform fair evaluations of their performances. Communication system chains are also developed in order to efficiently simulate these systems with sufficient number of transmitted symbols that are required to validate the statistical criteria for the target BER.

Moreover, in our second approach, the bit rate of a multicarrier system is maximized under the constraint of mean BER of an entire OFDM symbol. In this way, different subcarriers in a given OFDM symbol are allowed to be affected by different BER values and the error rate limit is imposed on an entire OFDM symbol. It means that mean BER of an OFDM/LP-OFDM symbol must not exceed the target BER.

We get the same BER performance as was achieved in the case of peak BER constraint since the only difference between these two approaches is the hierarchical level at which the error rate limit is imposed. In the case of peak BER approach, this limit is imposed on each QAM symbol. As we know, there are a number of QAM symbols in the considered multicarrier systems. Therefore, instead of imposing the error rate limit on each QAM symbol, the BER limit is put on a group of QAM symbols (i.e. an OFDM/LP-OFDM symbol).

Under PSD constraint, the transmitted power on each subcarrier has to be less than a defined value. In practical systems, where discrete modulation orders are used, different constellation sizes require different levels of transmitted power in order to respect a given BER as shown in Fig. 2.10. It is quite common to encounter such problems where an increase in the constellation size (for instance from 16-QAM to 32-QAM) requires a transmit power level that is more than the imposed peak power limit and when the constellation size is decreased (i.e. from 32-QAM to 16-QAM) in order to respect the imposed PSD limit, the allowed power is not utilized completely which leads to a decrease in the achievable value of the maximized bit rate. That is why, we observe a significant difference between bit rates obtained for infinite granularity of modulation and those obtained by using practical discrete modulations, as shown in Fig. 2.11. This problem may be compensated by using different value of BER on each subcarrier under PSD constraint and by imposing an error rate limit on the entire OFDM/LP-OFDM symbol. This approach gives an additional degree of freedom to resource allocation strategies for bit rate maximization under PSD constraint. Moreover, we also present the practical bit and power loading algorithms for bit rate maximization of OFDM and LP-OFDM systems in PLC context under PSD and mean BER constraints.

3.2 RM under peak BER constraint

In this section, we will consider a number of resource allocation strategies for bit rate maximization. Conventionally, to achieve a target error rate, SER is fixed on each subcarrier which is equal to the global SER of an OFDM symbol, since all QAM constellation sizes have the same value of the SNR gap at the same SER, as it is clear from the approximation given in (2.19). Generally the error rate limit is imposed by upper layers of the network (i.e. transport and application layers) and this limit is happened to be in terms of BER and not in SER, since the symbols at MAC and physical layers are definitely different from the symbols at the upper layer. Thus, working under the constraint of BER instead of SER is an interesting idea. Conventionally, in theoretical studies of resource allocation, an approximate relation is used between SER and BER [98] which leads to violations of error rate constraint in some cases, as discussed in [99]. In this section, we consider resource allocation strategies based on BER constraint. One solution is to fix the BER on each subcarrier instead of fixing the SER. The other solution is to respect the target error rate in terms of mean BER of OFDM/LP-OFDM symbol and allow different

subcarriers to be affected by different values of BER. The former scenario is discussed in this section while the latter one will be discussed in Section 3.3. The resultant maximized bit rate is slightly different under peak BER constraint as compared to bit rate maximization under peak SER constraint. Therefore, we will not discuss the maximization strategy for the case of conventional OFDM, as it has been already discussed in Section 2.3.3 for the classical case of RM under peak SER constraint.

3.2.1 RM for uncoded LP-OFDM

After presenting various optimization schemes for conventional OFDM systems, here we discuss bit rate maximization scheme for the selected LP-OFDM system in order to achieve high bit rate for indoor PLC environment. The single user resource allocation problem for OFDM systems may be dealt in two steps. In the first step, a single user, single block LP-OFDM will be considered and finite and infinite granularity scenarios will be analysed. After getting the optimal solutions for single user and single block scenario, these results will be extended for a multi block LP-OFDM system. Firstly, an overview on the theoretical system capacity is given for a multi block uncoded LP-OFDM system followed by a discussion on allocation strategies.

3.2.1.1 Mutual information for LP-OFDM

The mutual information between transmitted and received signals is needed in order to obtain the objective function (i.e. the capacity) required for the treatment of resource allocation and optimization of LP-OFDM systems before adding and after removing the linear precoding components.

$$y = \frac{1}{\sqrt{L}} M^H G H \mathfrak{N} + \frac{1}{\sqrt{L}} M^H G b, \quad (3.1)$$

where G is the equalization matrix, \mathfrak{N} is the chip mapping matrix and M is the precoding matrix of dimension $L \times C$ as defined in (2.13).

In order to reduce the receiver complexity, we consider simple equalization schemes in our study. Zero forcing (ZF) and minimum mean square error (MMSE) detection techniques have been used. The role of ZF technique is to apply channel inversion and to eliminate multiple access interferences by maintaining orthogonality among the linear precoded data but at the cost of increased noise. The MMSE equalizer provides a trade-off between the interference minimization and the noise increasing factor. The associated equalization coefficients g_i with both techniques for subcarrier i , are given as

$$\text{ZF} \quad g_i = \frac{1}{H_i} \forall i, \quad (3.2)$$

$$\text{MMSE} \quad g_i = \frac{\bar{H}_i}{|H_i|^2 + \frac{N_0}{P_i}} \forall i. \quad (3.3)$$

It is well known that MMSE equalization performs better than ZF equalization, but the application of MMSE gives significantly complex mutual information expression in comparison with ZF technique [100] and the analysis to achieve required optima becomes a highly tedious task due to the complexity involved in the objective function. Moreover, for strong SNRs, the performance of ZF technique is comparable to MMSE detection. Therefore, in this thesis we selected the ZF detection in order to obtain practically implementable algorithms. Thus in the following, G is the diagonal matrix and $G = H^{-1}$.

3.2.1.2 Mono block systems

The mono block system is an elementary part of a complete multi block LP-OFDM system. This system consists of just one block of subcarriers. By applying a ZF equalization on the received vector at the output of OFDM demodulation, we get

$$y = x + \frac{1}{\sqrt{L}} M_{L,C}^H H^{-1} \acute{b}. \quad (3.4)$$

It must be noted here that vectors x and y are of size C . Furthermore, x and y are jointly Gaussian random variables, therefore the mutual information expression between them is written as [101]

$$I = \frac{1}{2} \log_2 \det [I_c - R_{X,Y} R_Y^{-1}], \quad (3.5)$$

where $R_{X,Y}$ is the covariance matrix of x and y and R_Y is the auto-covariance matrix of y . I_c is the identity matrix. The calculation of the mutual information, by solving (3.5) leads to,

$$I_{mono} = \frac{1}{2} \sum_{c=1}^C \log_2 \left(1 + \frac{L^2}{\sum_{i=1}^L \frac{1}{|H_i|^2}} \frac{E_c}{N_0} \right), \quad (3.6)$$

where E_c is the transmit power available at the precoding sequence c . As we know, for a given block, a QAM symbol is spread on all of its subcarriers, thus each subcarrier transmits a number of QAM symbols (of course not entire QAM symbols but only small parts of multiple QAM symbols) simultaneously. Therefore, the sum of transmit powers on individual precoding sequences must not exceed the PSD limit \hat{E} in order to avoid regulatory violations. This condition may be given as

$$\sum_{c=1}^C E_c \leq \hat{E}. \quad (3.7)$$

Therefore, in LP-OFDM systems we consider transmit power per precoding sequence E_c instead of the classical concept of the transmit power per subcarrier used in the conventional OFDM systems.

3.2.1.3 Multi block systems

A multi block dimension is added in the elementary system to obtain a multi block system. Therefore the mutual information can be written as the sum of mutual informations of multiple single block systems. Thus, we obtain

$$I_{multi} = \sum_{k=1}^K \sum_{c=1}^{C_k} \log_2 \left(1 + \frac{L^2}{\sum_{i \in S_k} \frac{1}{|H_i|^2}} \frac{E_c^k}{N_0} \right), \quad (3.8)$$

where S_k signifies a given a set of subcarriers in block k , C_k are the used number of precoding sequences in block k and E_c^k is the transmit power available on precoding sequence c of block k . It must be noted that if we select $L = C = 1$ and $K = N$, the obtained results give the mutual information for conventional OFDM systems implemented using ZF detection. It may be found from (3.6) and (3.8) that the performance of the conventional OFDM system is better than that of the performance of LP-OFDM in the case of infinite granularity of modulation. However, we will show in the following that in the case of practical finite granularity of modulation, LP-OFDM outperforms OFDM. The constraint of peak power constraint for LP-OFDM systems may be given as,

$$\sum_{c=1}^{C_k} E_c^k \leq \hat{E} \quad \forall k. \quad (3.9)$$

As discussed earlier, in this chapter we consider the resource allocation and optimization problem under the constraint of PSD and peak BER. We explained in Section 2.3.1 that the SNR gap does not hold a constant value for different modulation orders under peak BER constraint and slightly decreases for higher modulation orders. For the sake of simplicity, we ignore this slight variation in the analytical study of bit rate maximization and the variable values of the SNR gap are compensated algorithmically in the practical solution proposed for discrete modulations. Therefore, SNR gap is treated as constant in this analytical study for all modulation orders for a given BER.

3.2.2 Mono block resource allocation

In the previous section, we have introduced the mutual information expressions, which will be used in this work as the reference. All the resource allocation strategies are considered to be working under PSD constraint. The bit rate maximization problem

for a single block LP-OFDM system can be given as

$$\begin{cases} \max \sum_{c=1}^C \log_2 \left(1 + \frac{1}{\Gamma} \frac{L^2}{\sum_{i=1}^C \frac{1}{|H_i|^2}} \frac{E_c}{N_0} \right) \\ \text{subject to } \sum_{i=1}^C E_c \leq \hat{E} \end{cases}, \quad (3.10)$$

where E_c is the transmit power for precoding sequence c and it can be observed from the above equation that the sum of the transmit powers associated with different precoding sequences of the considered block must not exceed the imposed PSD limit. The optimal solution of b_c bits and E_c power level have to be allocated to precoding sequences c of the given block in order to maximize the bit rate of the mono block LP-OFDM system. For the infinite granularity of modulation $b \in \mathbb{R}$ and for the finite granularity of modulation for practical purposes (i.e. discrete modulations) $b \in \mathbb{N}$. Firstly, we will treat the bit rate maximization problem for infinite granularity of modulation and then we will extend this theoretical study for discrete modulations to be implemented in practical systems. It must be noted here that the target error rate is represented by the SNR gap expression discussed in Section 2.3.1. To increase the readability of equations, let,

$$\chi = \frac{L^2}{\sum_{i=1}^C \frac{1}{|H_i|^2}} \frac{1}{\Gamma N_0}. \quad (3.11)$$

In order to obtain the optimal power distribution among different precoding sequences, we may apply the method of Lagrange multiplier. Lagrangian of the considered optimization problem can be given as

$$L(E_c, \lambda) = \sum_{c=1}^C \log_2(1 + \chi E_c) + \lambda \sum_{c=1}^C E_c - \lambda \hat{E}. \quad (3.12)$$

The simultaneous treatment of these equations results in the following optimal solution for the transmit power allocation between different precoding sequences

$$E_c = \frac{\hat{E}}{C}, \quad (3.13)$$

which shows that the optimal power allocation is to distribute the transmit power uniformly among all precoding sequences of the given block. As it was discussed earlier that all the precoding sequences of LP-OFDM must respect the same error rate constraint. Therefore as a consequence of the result obtained in (3.13), the optimal

bit allocation becomes to distribute the uniform number of bits among all precoding sequences of the given block. Since in order to respect the same error rate constraint with the same transmit power, we need to transmit the same number of bits on each precoding sequence. Thus, the total number of bits per LP-OFDM symbol, using C precoding sequences, can be given as

$$R = C \log_2 \left(1 + \chi \frac{\hat{E}}{C} \right). \quad (3.14)$$

Equation (3.14) gives an expression for total number of bits per LP-OFDM symbol that is a strictly increasing function for C . Therefore, we can simply reach at the optimal solution for number of useful precoding sequences in the given block. The use of orthogonal precoding sequences imposes a limit on the maximum number of precoding sequences in a block and that is the number of subcarriers in the given block. Thus, optimal solution for bit rate maximization is to use L precoding sequences in a block i.e. $C = L$. The optimal number of bits in an LP-OFDM symbol can then be given as

$$R = L \log_2 \left(1 + \frac{1}{\Gamma} \frac{L}{\sum_{i=1}^L \frac{1}{|H_i|^2}} \frac{\hat{E}}{N_0} \right). \quad (3.15)$$

Finally, the optimal allocation strategy for different precoding sequences in the given mono block LP-OFDM system is summarized as follows

$$\begin{cases} b_c = \frac{R}{C} \\ E_c = \frac{\hat{E}}{C} \\ C = L \end{cases}. \quad (3.16)$$

For practical systems, we need to work under the constraint of discrete modulation orders, for instance QAM. One solution might be to simply round the real values of b_c into integer values for all precoding sequences. This rounding process can be executed in three different ways known as ‘*floor*’, ‘*ceil*’ and ‘*round*’ operations. Note that, to avoid any violation of PSD and error rate constraints, a ‘*floor*’ operation must be used that truncates the real valued number to the nearest integer less than or equal to the real number. The use of ‘*round*’ or ‘*ceil*’ operation may round the real valued number to the nearest integer greater than the real number and this may lead to violations of PSD or error rate constraint in some cases.

The rounding solution certainly respects the PSD constraint but on the other hand may cause a significant loss of several bits. An optimal solution for this problem has been proposed in [13] where it was shown that the optimal bit distribution is to

allocate $\lfloor R/L + 1 \rfloor$ bits to n precoding sequences and $\lfloor R/L \rfloor$ bits to the remaining $L - n$ precoding sequences, where n is an integer and is given by

$$n = \lfloor L (2^{R/L - \lfloor R/L \rfloor} - 1) \rfloor. \quad (3.17)$$

The final bit and power allocation scheme for mono block LP-OFDM systems may be summarized as

$$\begin{cases} b_c = \left\lfloor \frac{R}{L} \right\rfloor + 1 & \forall c \in [1 : n], \\ b_c = \left\lfloor \frac{R}{L} \right\rfloor & \forall c \in [n + 1 : L], \\ E_c = (2^{b_c} - 1) \frac{\Gamma}{L^2} N_0 \sum_{i=1}^L \frac{1}{|H_i|^2}, \forall c. \end{cases} \quad (3.18)$$

The total number of bits per LP-OFDM symbol, using discrete modulations, can then be given as

$$R = \lfloor L (2^{R/L - \lfloor R/L \rfloor} - 1) \rfloor + L \lfloor R/L \rfloor. \quad (3.19)$$

3.2.3 Multi block resource allocation

For a more general case of a multi block LP-OFDM system, where K blocks of same length L are present in the system, the bit rate maximization problem under PSD constraint and for same error rate on each subcarrier can be given as

$$\begin{cases} \max \sum_{k=1}^K \sum_{c=1}^C \log_2 \left(1 + \frac{1}{\Gamma} \frac{L^2}{\sum_{i \in S_k} \frac{1}{|H_i|^2}} \frac{E_c^k}{N_0} \right) \\ \text{subject to } \sum_{c=1}^C E_c^k \leq \hat{E} \end{cases}. \quad (3.20)$$

The subcarriers must also be distributed among different subcarriers in such a way that the bit rate of an entire LP-OFDM symbol is maximized. An optimal distribution of subcarriers has been proposed in [13], where it is suggested to sort all the subcarriers in the descending order of the amplitudes of their frequency responses, before distributing them to different blocks. In order to maximize the total bit rate of a multi block LP-OFDM, we need to maximize the individual bit rate of all the constituent blocks. Therefore, the optimal allocation of bits and powers using infinite granularity of modulation can be given as

$$\begin{cases} b_c^k = \frac{R_k}{L} \\ E_c^k = \frac{\hat{E}}{L} \end{cases}, \quad (3.21)$$

where R_k is the real valued number of bits for a given block k and using (3.13), R_k can be given as

$$R_k = L \log_2 \left(1 + \frac{1}{\Gamma} \frac{L}{\sum_{i \in S_k} \frac{1}{|H_i|^2}} \frac{\hat{E}}{N_0} \right). \quad (3.22)$$

The extension of this real valued optimal solution to the integer valued practical solution can simply be obtained by applying the results obtained for mono block systems for finite granularity of modulation. In other words, the optimization procedure for bit rate maximization for mono block systems is implemented K times on K blocks of a multi block LP-OFDM system. Finally, we may write these allocations as

$$\begin{cases} b_c^k = \left\lfloor \frac{R_k}{L} \right\rfloor + 1 & \forall c \in [1 : n_k], \forall k, \\ b_c^k = \left\lceil \frac{R_k}{L} \right\rceil & \forall c \in [n_k + 1 : L], \forall k, \\ E_c^k = (2^{b_c^k} - 1) \frac{\Gamma}{L^2} N_0 \sum_{i \in S_k} \frac{1}{|H_i|^2}, & \forall c, \forall k, \end{cases}, \quad (3.23)$$

where n_k can be written as

$$n_k = \lfloor L (2^{R_k/L - \lfloor R_k/L \rfloor} - 1) \rfloor. \quad (3.24)$$

It may be observed that for $L = 1$, we find the solution obtained for the conventional OFDM system in the previous chapter. Particularly, for the conventional OFDM system, $n_k = 0$, and therefore $b_c^k = b_i$ and $E_c^k = E_i$. This method thus gives a generalized solution that can treat different variants of LP-OFDM systems with different values of the precoding factor L including $L = 1$. Bit and power loading algorithms may be devised based on the study performed in this section for both mono and multi block LP-OFDM systems to increase the system throughput significantly as will be shown in simulation results later in this chapter. Furthermore, the transmission capabilities of LP-OFDM are significantly improved in comparison with the conventional OFDM system and it may transmit sufficient number of bits even for very poor SNR.

3.2.4 RM for coded LP-OFDM

In the previous section, we discussed the bit rate maximization problem for LP-OFDM systems but without taking into account the channel coding gain in the resource allocation process. In this section, we will discuss the resource allocation and optimization problem for coded LP-OFDM systems. Firstly, a description of the selected channel coding scheme is given followed by a discussion on resource allocation strategies for coded multicarrier systems. The bit loading algorithms are proposed that may be

used for any given channel coding scheme provided that the channel coding gains are known for the target bit error rate. A brief description of the communication system chain is given that was developed in C++ in order to evaluate the performance of proposed algorithms. The selected channel coding schemes are also integrated in the developed communication chain for LP-OFDM systems. The results are presented for both OFDM and LP-OFDM systems with and without the integrated channel coding scheme.

3.2.4.1 Selected channel coding scheme

Uncoded LP-OFDM has already been discussed for resource allocation and optimization problem to handle subcarrier, precoding sequence, bit, and power resource distribution among different blocks and precoding sequences but without taking into account the channel coding scheme. Assuming perfect CSI at the transmitting side, powers and bits are efficiently distributed among precoding sequences by the loading algorithm to achieve either high throughput or high robustness. Here, we examine the performance of an LP-OFDM system exploiting a resource allocation algorithm which takes into account the channel coding scheme.

Given an adaptive LP-OFDM system, the suitable coding scheme should have large coding gains, reasonable implementation complexity and some measures of burst immunity. Selected on these bases, the chosen concatenated channel coding scheme consists of an inner Wei's 4-dimensional (4D) 16-states trellis code [102] and an outer RS code. This combination has already proved its significance in multicarrier systems and has been included in popular standards such as very high bitrate DSL (VDSL) [103]. Moreover, this particular combination has also been recommended for multicarrier PLC communications by the well known UPA [104]. The efficient performance of Wei's 4D 16-states trellis code has also been demonstrated in [105] and [106].

3.2.4.2 Wei's 4D 16-states trellis code

Trellis coded modulation enables a better trade-off between performance and bandwidth efficiency, while enjoying low-complexity Viterbi decoding. Trellis coded modulation systems achieve significant distance gains which are directly related to the number of states. However, the coding gain saturates upon approaching a certain number of states and the constellations must be changed to achieve higher gains. Multidimensional constellation then gives a potential solution. An inherent cost of 2D coded schemes is that the size of the constellation is doubled over uncoded schemes. This is due to the fact that a redundant bit is added to every signaling interval. Without that cost, the coding gain of those coded schemes would be 3 dB greater. Using a multidimensional constellation with a trellis code of rate $\frac{m}{m+1}$ can reduce that cost because fewer redundant bits are added for each 2D signaling interval. For example, that cost is reduced to about 1.5 (which is the case for the suggested coding scheme) or 0.75 dB if four-dimensional (4D) or eight-dimensional (8D) constellations are used, respectively. The trellis code considered here is a 4D 16-states code developed by

Wei [102]. This code provides a fundamental coding gain of $\gamma_{f,dB} = 4.5$ dB, computed as a 6.0 dB increase in the minimum squared distance between allowable signal sequences, less a 1.5 dB penalty incurred for a normalized redundancy of 0.5 bits per 2D symbol [106].

The innovative aspect of TCM is the concept that convolutional encoding and modulation should not be treated as separated entities, but rather as a single operation. Similarly the received signal is processed by combining the demodulation and decoding in a single step, instead of being first demodulated and then decoded. In the consequence, the parameter governing the performance of the transmission system over the channel is not the free Hamming distance of the convolutional code but rather the free Euclidean distance between the transmitted signal sequences. Thus, the optimization of the TCM design is based on the Euclidean distances rather than the Hamming distances, and the choice of the code and of the signal constellation is not performed in separate steps. Finally, the detection process involves soft rather than hard decisions. That is, instead of processing the received signal before making decisions as to which transmitted symbols they correspond to, the demodulator passes metric information to a soft Viterbi decoder directly. TCM systems achieve significant distance gains, and increasing the number of states would increase the performance of TCM. However, the returns diminish with the increase in number of states after certain level. The selected Wei's 4D 16-states trellis code is based on VDSL2 standard [103] and is performed in the following steps:

Bit extraction

Bits are extracted from the data frame buffer in the sequential order. Due to the 4-dimensional nature of Wei's trellis codes, the process of extraction is based on pairs of consecutive bits and not on individual bits. The output of the encoder is divided into two 2-dimensional symbols on two different precoding sequences (for simulation purposes, 2-dimensional symbols are split in time). If the 1st precoding sequence supports j bits and the second precoding sequence supports k bits, then $j + k - 1$ bits are extracted from the data frame buffer, causing a constellation expansion of 1 bit per 4-dimensional symbol, or $\frac{1}{2}$ bit per precoding sequence (or 2-dimensional symbol). These $j + k - 1$ bits are used to make the binary word u as shown in Fig. 3.1.

Convolutional encoding

The convolutional encoder used in Wei's 4-dimensional trellis codes is a systematic encoder (i.e. u_1 and u_2 (the least significant bits of u) are passed through unchanged) as shown in Fig. 3.1. The trellis diagram of this systematic convolutional coder is shown in Fig. 3.2.

Bit conversion

Three output bits of convolutional encoder and the 3rd least significant bit of u (i.e. u_3) are fed to the bit converter to perform logical operations in order to give two

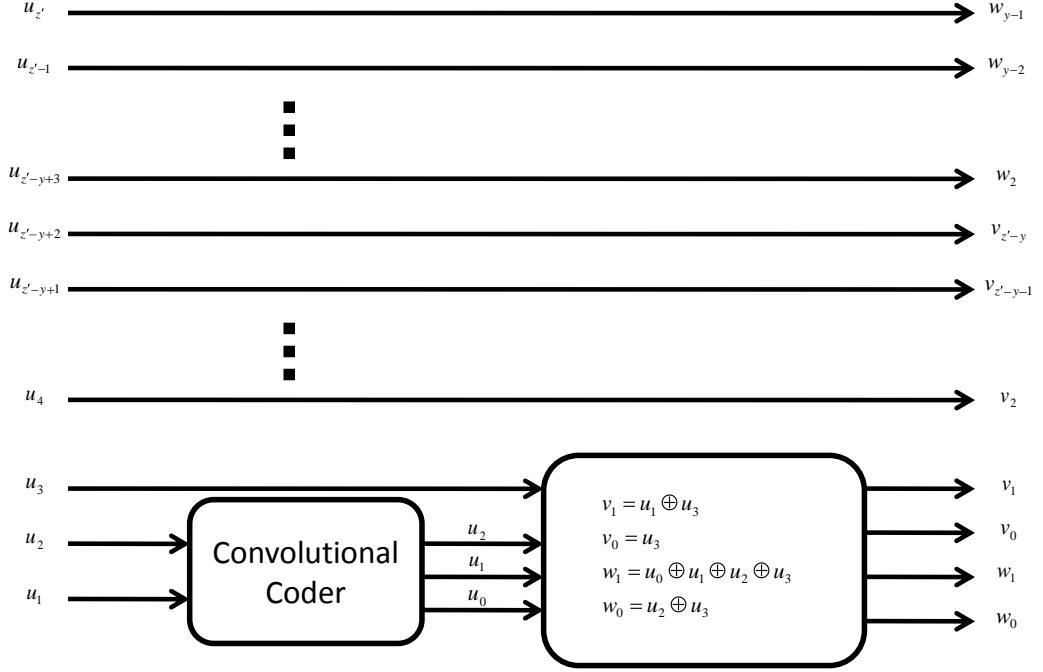


Figure 3.1: Wei's 4D 16-states trellis code.

least significant bits of both the 2 dimensional transmitted words (i.e. v_0, v_1, w_0 and w_1). The remaining bits of v and w are obtained from the less significant and more significant bits of u , respectively. v and w are transmitted through different precoding sequences after constellation mapping.

Coset partitioning and trellis diagram

Generally in trellis coded modulation schemes, the expanded constellation is labeled and partitioned into subsets, also known as “cosets”, using mapping by set-partitioning technique. The 4-dimensional cosets in Wei's 4-dimensional code are written as the union of two Cartesian products of two 2-dimensional cosets.

For example, $C_4^0 = (C_2^0 \times C_2^0) \cup (C_2^3 \times C_2^3)$. The four constituent 2-dimensional cosets, denoted by 0, 1, 2 and 3 for $C_2^0, C_2^1, C_2^2, C_2^3$, respectively, are shown in Fig. 3.3

This constellation mapping guarantees that the two least significant bits of a constellation point comprise the index i of the 2-dimensional coset C_2^i in which the constellation point is located. The bits (v_1, v_0) and (w_1, w_0) are actually the binary representations of this index.

Three bits (u_2, u_1, u_0) are used to select one of the eight possible 4-dimensional cosets. These eight cosets are known as C_4^i where i is the integer with binary representation of (u_2, u_1, u_0) . The additional bit u_3 (see Fig. 3.1) determines which one of the two Cartesian products of 2-dimensional cosets is selected from the 4-dimensional coset. The relationships between 2 and 4 dimensional cosets are given in Table 3.1.

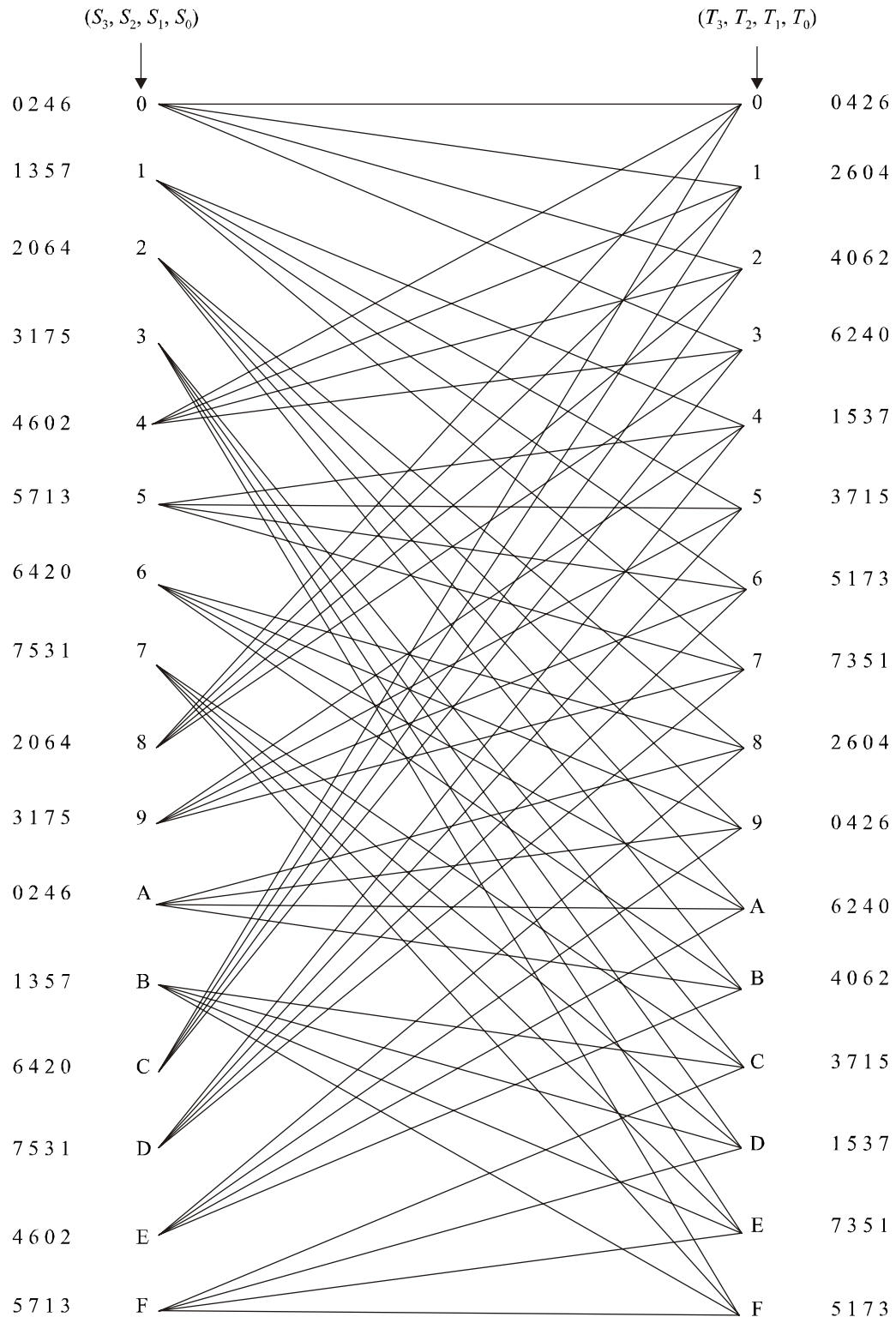


Figure 3.2: Trellis diagram of the considered convolutional coder [103].

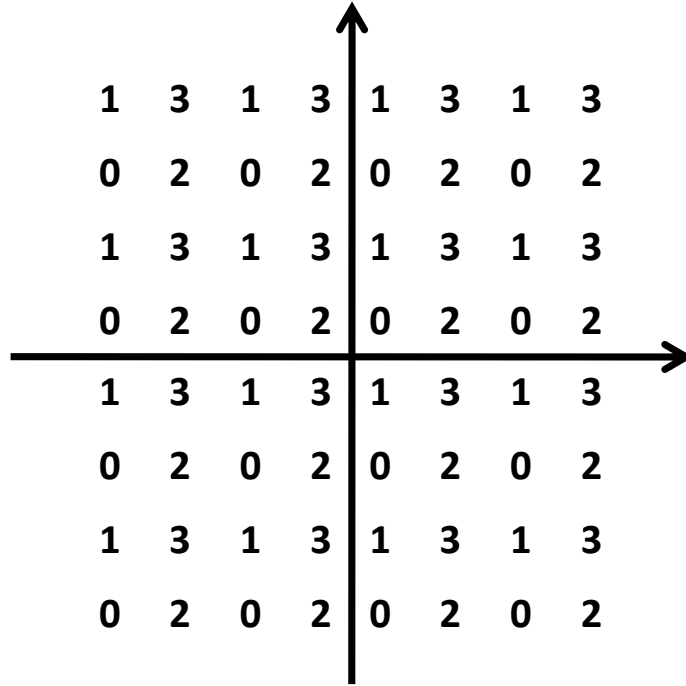


Figure 3.3: Mapping of 2-dimensional cosets [103].

Table 3.1: Relation between 4-dimensional and 2-dimensional cosets.

4-D coset	$u_3u_2u_1u_0$	v_1v_0	w_1w_0	2-D cosets
C_4^0	0 0 0 0	0 0	0 0	$C_2^0 \times C_2^0$
	1 0 0 0	1 1	1 1	$C_2^3 \times C_2^3$
C_4^0	0 1 0 0	0 0	1 1	$C_2^0 \times C_2^3$
	1 1 0 0	1 1	0 0	$C_2^3 \times C_2^0$
C_4^2	0 0 1 0	1 0	1 0	$C_2^2 \times C_2^2$
	1 0 1 0	0 1	0 1	$C_2^1 \times C_2^1$
C_4^6	0 1 1 0	1 0	0 1	$C_2^2 \times C_2^1$
	1 1 1 0	0 1	1 0	$C_2^1 \times C_2^2$
C_4^1	0 0 0 1	0 0	1 0	$C_2^0 \times C_2^2$
	1 0 0 1	1 1	0 1	$C_2^3 \times C_2^1$
C_4^5	0 1 0 1	0 0	0 1	$C_2^0 \times C_2^1$
	1 1 0 1	1 1	1 0	$C_2^3 \times C_2^2$
C_4^3	0 0 1 1	1 0	0 0	$C_2^2 \times C_2^0$
	1 0 1 1	0 1	1 1	$C_2^1 \times C_2^3$
C_4^7	0 1 1 1	1 0	1 1	$C_2^2 \times C_2^3$
	1 1 1 1	0 1	0 0	$C_2^1 \times C_2^0$

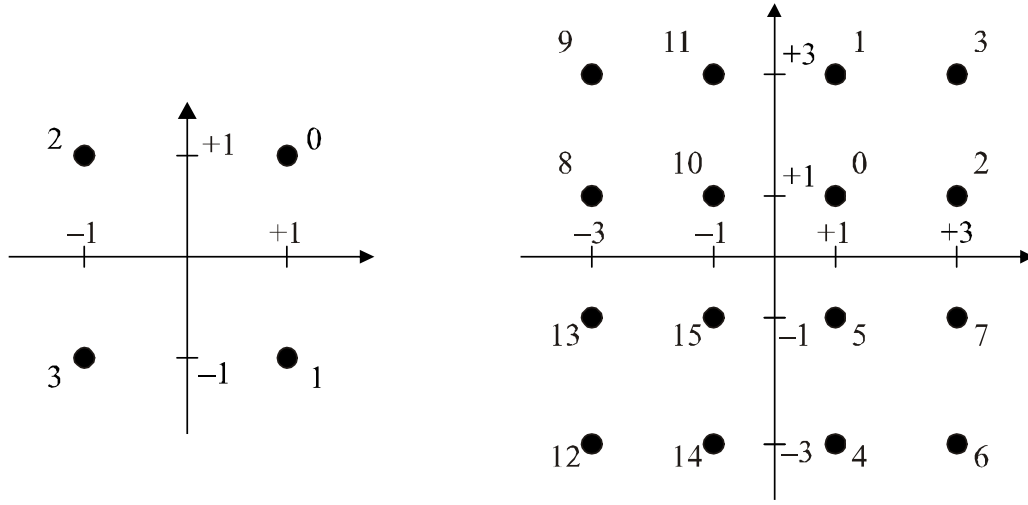


Figure 3.4: Constellation labels for $b = 2$ and $b = 4$ [103].

Bits (v_1, v_0) and (w_1, w_0) are computed from (u_3, u_2, u_1, u_0) using logical operations shown in Fig. 3.1.

Constellation mapper

QAM constellations are constructed using an algorithmic constellation mapper for a minimum of 2 bits per symbol and a maximum of 15 bits per symbol. The constellation points are denoted as (X, Y) . X and Y lie at the odd integers $\pm 1, \pm 3, \pm 5$ etc. For the sake of improved readability, each constellation point in Fig. 3.4 and 3.5 is represented by an integer whose unsigned binary representation is $(v_{b-1}v_{b-2} \cdots v_1v_0)$.

Even values of b

In the case of even constellation points, the integer values X and Y of the constellation point (X, Y) are determined from b bits $(v_{b-1}, v_{b-2}, \cdots, v_1, v_0)$ as follows. X and Y are odd integers with twos-complement binary representations $(v_{b-1}v_{b-3} \cdots v_11)$ and $(v_{b-2}v_{b-4} \cdots v_01)$, respectively. The MSBs, v_{b-1} and v_{b-2} , are the sign bits for X and Y , respectively. Fig. 3.4 shows the constellation diagrams for $b = 2$ and $b = 4$. The 6-bit constellation may be obtained from the 4-bit constellation by replacing each label n by the 2x2 block of labels:

$$\begin{array}{cc} 4n + 1 & 4n + 3 \\ 4n & 4n + 2 \end{array}$$

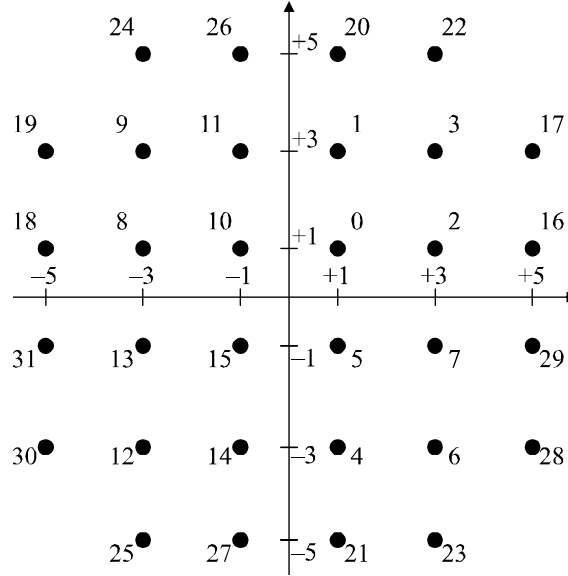
In the same way, the greater even-bit constellation may be obtained. These even-bit constellations are square in shape.

Table 3.2: Determining the top two bits of X and Y .

$v_{b-1} v_{b-2} \cdots v_{b-5}$	$X_c X_{c-1}$	$Y_c Y_{c-1}$
0 0 0 0 0	0 0	0 0
0 0 0 0 1	0 0	0 0
0 0 0 1 0	0 0	0 0
0 0 0 1 1	0 0	0 0
0 0 1 0 0	0 0	1 1
0 0 1 0 1	0 0	1 1
0 0 1 1 0	0 0	1 1
0 0 1 1 1	0 0	1 1
0 1 0 0 0	1 1	0 0
0 1 0 0 1	1 1	0 0
0 1 0 1 0	1 1	0 0
0 1 0 1 1	1 1	0 0
0 1 1 0 0	1 1	1 1
0 1 1 0 1	1 1	1 1
0 1 1 1 0	1 1	1 1
0 1 1 1 1	1 1	1 1
1 0 0 0 0	0 1	0 0
1 0 0 0 1	0 1	0 0
1 0 0 1 0	1 0	0 0
1 0 0 1 1	1 0	0 0
1 0 1 0 0	0 0	0 1
1 0 1 0 1	0 0	1 0
1 0 1 1 0	0 0	0 1
1 0 1 1 1	0 0	1 0
1 1 0 0 0	1 1	0 1
1 1 0 0 1	1 1	1 0
1 1 0 1 0	1 1	0 1
1 1 0 1 1	1 1	1 0
1 1 1 0 0	0 1	1 1
1 1 1 0 1	0 1	1 1
1 1 1 1 0	1 0	1 1
1 1 1 1 1	1 0	1 1

Odd values of b

In the case of even constellation points, the two MSBs of X and the two MSBs of Y are obtained from five MSBs of b bits ($v_{b-1}v_{b-2} \cdots v_1v_0$). Lets consider $c = \frac{(b+1)}{2}$, then X and Y have the twos-complement binary representations ($X_c X_{c-1} v_{b-4} v_{b-6} \cdots v_3 v_1 1$) and ($Y_c Y_{c-1} v_{b-5} v_{b-7} v_{b-9} \cdots v_2 v_0 1$), where X_c and Y_c are the sign bits of X and Y re-

Figure 3.5: Constellation labels for $b = 5$ [103].

spectively. The relationship between $X_c, X_{c-1}, Y_c, Y_{c-1}$ and $(v_{b-1}v_{b-2} \cdots v_{b-5})$ is shown in Table 3.2. Fig. 3.5 shows the constellation for the case $b = 5$. The 7-bit constellation may be obtained from the 5-bit constellation by replacing each label n by the 2x2 block of labels:

$$\begin{array}{cc} 4n + 1 & 4n + 3 \\ 4n & 4n + 2 \end{array}$$

In the same way, the greater odd-bit constellation may be obtained. In the selected channel coding scheme, Wei's 4D 16-states trellis code is concatenated with the well known Reed-Solomon code.

3.2.4.3 RS Codes

An RS (k, t) coder takes in k information symbol and outputs n information symbols, where $n = 2^m - 1$ with m the number of bits per symbol. Each symbol belongs to the Galois field (GF 2^m) consisting of 2^m integer elements. The second parameter (i.e. t) gives the number of symbols that can be corrected by the decoder.

The binary data at the input is first fed to an outer interleaved RS code with code length n and information length k . To correct t random errors in a block of n symbols, $n - k = 2t$ parity check symbols are required for an RS code. The RS code used here is based on a finite field (also known as Galois Field) GF(2^8), and can have 256 different values between 0 and 255. It is a shortened RS code RS(240,224), supported in many standards [107], and can correct up to 8 erroneous bytes.

Fig. 3.6 shows the BER curves for the complete channel coding selected and Fig. 3.7 presents the evaluation of the SNR gap for all used modulation orders from 4-QAM up to 1024-QAM and for a target BER of 10^{-7} .

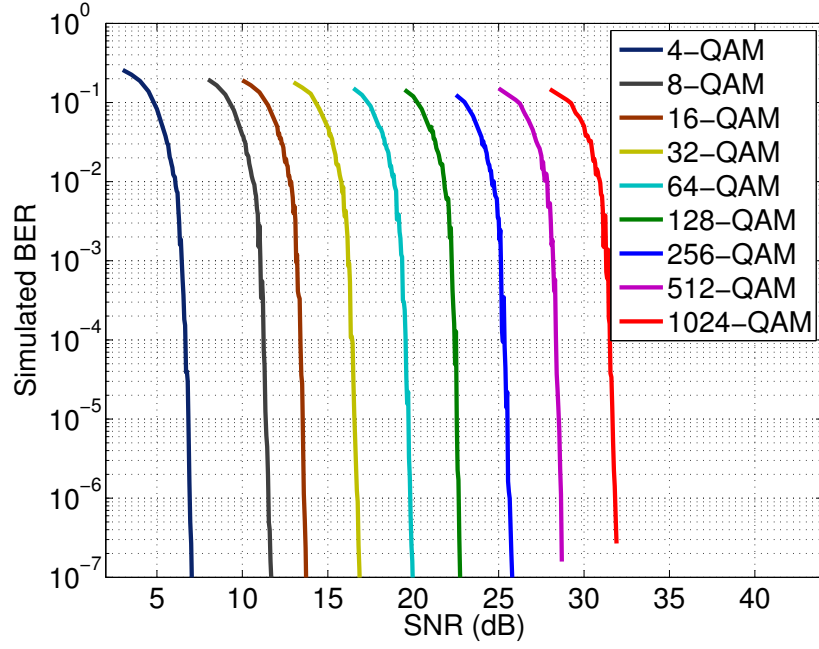


Figure 3.6: BER performance of the selected channel coding scheme over AWGN channel.

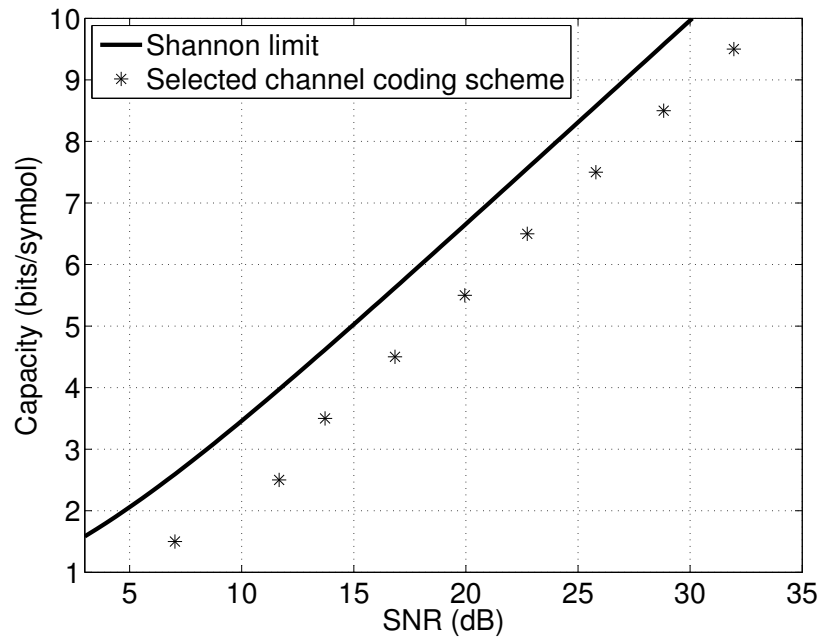


Figure 3.7: SNR gap evaluation for the selected channel coding scheme.

3.2.4.4 Theoretical coding effects on system performance

In this section, we consider the theoretical coding gain promised by the proposed concatenated channel coding scheme. In this analysis we need to deal with 2D error rates, BERs, and RS SERs, depending upon what part of the system is being considered. We use the assumptions given in [105, 106] for the sake of simplicity. Contrary to [105, 106], all calculations are made dealing only with BERs. In these assumptions, these quantities are related by constant factors, and the 2D error rate is used as a common basis. In particular, 2D SERs are converted to BERs by multiplying by one-half. Similarly, 2D SERs are converted to RS SERs by multiplying by a constant c , where c represents the average number of precoding sequences contributing bits to each RS symbol [105]. P_{bit} denotes the required BER at the output of the overall system. From [89], the probability of 2D symbol error in quadrature amplitude modulation is closely approximated by

$$P_{2D} \leq 4Q\left[\frac{d_{min}}{2\sigma}\right] \quad (3.25)$$

where d_{min} is the minimum distance between QAM constellation points at the channel output, σ is the noise variance, and $Q[\cdot]$ represents the well-known Q-function. By using the first assumption, as discussed above, the SNR gap Γ for a target BER of 10^{-7} is given as

$$\Gamma = 9.8 + \gamma_m - \gamma_c \quad (\text{dB}) \quad (3.26)$$

where γ_m is the desired margin in the system and γ_c , the coding gain for the proposed concatenated channel coding scheme, is given as

$$\gamma_c = \gamma_{tc,dB} + \gamma_{rs,dB} - \gamma_{loss,dB} \quad (\text{dB}) \quad (3.27)$$

where $\gamma_{tc,dB}$ and $\gamma_{rs,dB}$ are the gains provided by the trellis code and the RS code respectively and $\gamma_{loss,dB}$ is the loss incurred for increasing the data rate.

RS code gain $\gamma_{rs,dB}$

While assuming efficient interleaving to have random errors at the input of RS decoder and assuming that RS decoder does not attempt to correct the codeword if greater than t errors are detected, we may relate the output RS SER, P_{rs} , to the input RS SER, P_s , by

$$P_{rs} = \sum_{i=t+1}^n \binom{n-1}{i-1} P_s^i (1 - P_s)^{n-i}. \quad (3.28)$$

Given P_{bit} and knowing that $P_{2D} = 2P_{bit}$ and $P_{rs} = cP_{2D}$, we can say that $P_{rs} = 2cP_{bit}$ and by iteratively solving (3.28) for P_s , the corresponding BER at the input of RS decoder is given by

$$P_b = \frac{P_s}{2c} \quad (3.29)$$

and P_b is the BER at the output of the demodulator. Therefore an SNR gap to obtain P_b , Γ_{rs} , can be written as

$$\Gamma_{rs} = \frac{1}{3} \left(Q^{-1} \left[\frac{P_b}{2} \right] \right)^2 \quad (3.30)$$

$\Gamma_{0,P_{bit}}$ is defined as an SNR gap required by an uncoded system to achieve P_{bit} , and is given as

$$\Gamma_{0,P_{bit}} = \frac{1}{3} \left(Q^{-1} \left[\frac{P_{bit}}{2} \right] \right)^2 \quad (3.31)$$

From (3.31) and (3.30), γ_{rs} can be given as

$$\gamma_{rs} = \Gamma_{0,P_{bit}} - \Gamma_{rs} \quad (dB) \quad (3.32)$$

Trellis code gain $\gamma_{tc,dB}$

As P_b is the required BER at the input to the RS decoder and Γ_{0,P_b} and Γ_{tc,P_b} are the SNR gaps required by an uncoded and a Wei's 4D 16-states trellis coded system respectively to achieve P_b . Then the coding gain of a Wei's 4D 16-states trellis code can be given by

$$\gamma_{tc} = \Gamma_{0,P_b} - \Gamma_{tc,P_b} \quad (dB) \quad (3.33)$$

Loss of redundancy $\gamma_{loss,dB}$

If $P_{tot}^*(b)$ is the minimum amount of power required to achieve the data rate b as defined in [105], the loss for the increased data rate associated with the RS code, $\gamma_{loss,dB}$, can be given as

$$\gamma_{loss,dB} = P_{tot,dB}^* \left(\frac{nb}{k} \right) - P_{tot,dB}^*(b) \quad (3.34)$$

3.2.5 Coded LP-OFDM resource allocation

LP-OFDM resource allocation has already been discussed for PLC networks without taking into account the channel coding scheme in the resource allocation process. The resource allocation algorithm, discussed earlier for uncoded LP-OFDM, is modified to accommodate the coding gains associated to the channel coding scheme. The proposed bit and power allocation algorithm can be used in combination with any channel coding scheme, no matter it has constant or variable coding gains for different modulation orders, provided the obtained coding gains are known for all the modulation orders.

3.2.5.1 Structure of coded LP-OFDM

The structure of the considered adaptive LP-OFDM system is shown in Fig. 3.8. The entire bandwidth is divided into N parallel subcarriers which are split up into N_k sets

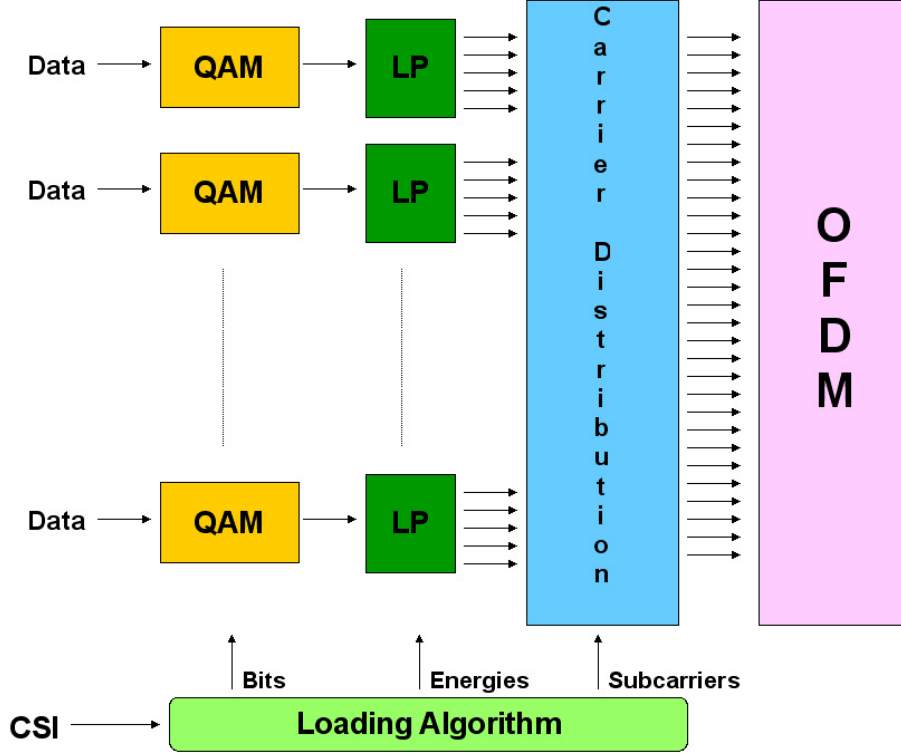


Figure 3.8: Uncoded LP-OFDM transmitter structure.

' S_k ' of L subcarriers. The precoding function is then applied block-wise by mean of precoding sequences of length L . Factor L is such that $L \ll N$, which implies that $N_k = \lfloor \frac{N}{L} \rfloor$. Note that the subsets in a given set are not necessarily adjacent.

The number of precoding sequences used to spread information symbols on one subset S_k is denoted by C_k , with $0 \leq C_k \leq L$ since we assume orthogonal sequences. A certain amount of power E_c^k will be assigned to each precoded sequence c associated to a given modulation symbol of b_c^k bits.

In Fig. 3.9, only a single output is shown for Wei's trellis encoder, because both 2D outputs are allocated to the same code. Also multiple copies of Wei's encoder is shown for the purpose of illustration whereas, in practice a single encoder is used to encode across the precoding sequences as discussed in [105, 106], where a single encoder is used to encode across the subcarriers. It will be shown in Section 3.2.5.3 that similar to independent and memoryless subchannels in a OFDM scenario, precoding sequences are also independent and memoryless in an LP-OFDM scenario. The gain obtained from the application of trellis code will therefore be the same as that obtained in an ISI free environment. On the other hand, the RS code operates on the binary stream at the input of the system, before the bit allocation block as shown in Fig. 3.9. A convolutional interleaver is used to spread the errors over a number of RS codewords. A complete communication system chain was developed in order to evaluate the performance of the proposed resource allocation algorithms. This com-

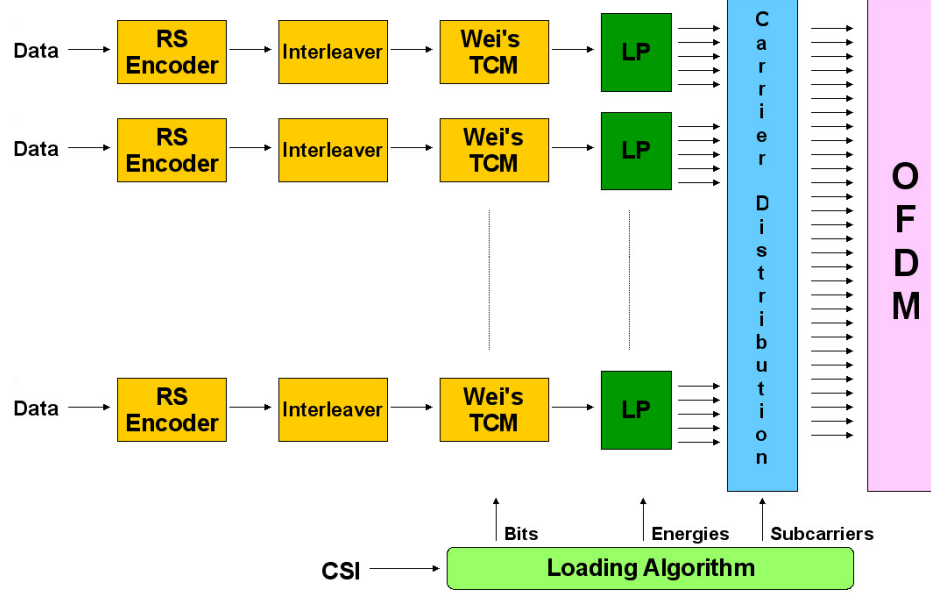


Figure 3.9: Coded LP-OFDM transmitter structure.

munication system chain contains the complete LP-OFDM system with integrated bit and power loading algorithms and the selected channel coding scheme. The developed communication system chain is shown in Fig. 3.10. This chain consists of the following important components:

1. Data generation
2. Reed Solomon encoder and decoder
3. Wei's 4D 16-states trellis encoder and decoder
4. An LP-OFDM system and power line channel

This simulation uses the bit and power vectors provided by the loading algorithm to transmit suitable number of bits on different precoding sequences with the correct transmit power. In the end of the simulation the bit error rate is computed by dividing the total number of erroneous bits by the total number of transmitted bits.

3.2.5.2 Resource allocation

In order to accommodate channel coding scheme in the communication chain, one needs to develop such a resource allocation algorithm that may take into account the channel coding gains obtained from the selected coding scheme and discussed in the previous section. We would like to reiterate the expression for achievable data rate on a given subset S_k from Section 3.2.3, which is given as

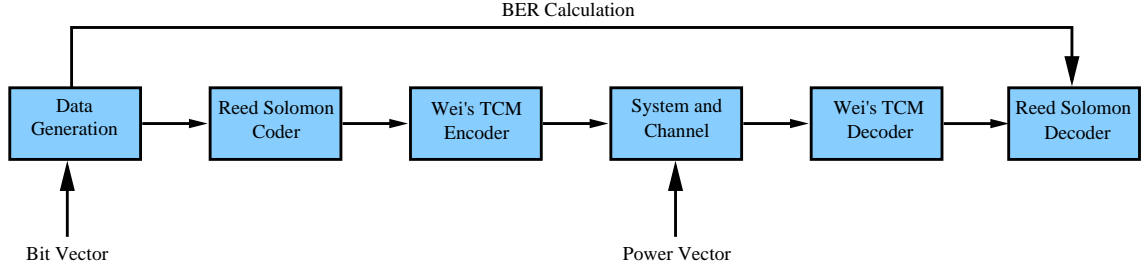


Figure 3.10: Developed communication system chain for simulation purposes.

$$\begin{aligned} \bar{R}_k = & \lfloor L(2^{R_k/L - \lfloor R_k/L \rfloor} - 1) \rfloor \times (\lfloor R_k/L \rfloor + 1) \\ & + (L - \lfloor L(2^{R_k/L - \lfloor R_k/L \rfloor} - 1) \rfloor) \times \lfloor R_k/L \rfloor \end{aligned} \quad (3.35)$$

Now we can optimally assign a particular modulation order to each code on different subsets. The transmit power, E_c^k , assigned to these codes is given as

$$E_c^k = (2^{b_c^k} - 1) \frac{\Gamma}{L^2} N_0 \sum_{i \in S_k} \frac{1}{|H_i|^2} \quad (3.36)$$

which satisfies $\sum_c E_c^k < \hat{E}$. This power allocation considers null noise margin as each code receives the exact amount of power to transmit the number of bits determined by the algorithm for a given Γ . As discussed above, Γ is generally defined for a given target SER and approximately has the constant value for all modulation orders. In this section we are going to deal with fixed target BER instead of SER. Then taking into account the coding gains and fixed BERs, Γ is no more constant for all the modulation orders. The above algorithm is modified to accommodate variable Γ for different modulation orders. The exact values of the SNR gaps for all the modulation orders are stored in a predefined table and are denoted by $\Gamma_i^{(k)}$. These values are calculated on the basis of the selected channel coding scheme and the required system margin. For a given subset S_k , initially, we can take any value for Γ , say $\Gamma_i^{initial(k)} = 1$. The closer the initial value to the exact value, the more efficient is the algorithm because a closer value helps in the rapid convergence to the optimal solution. R_k is calculated from (3.22) using $\Gamma_i^{initial(k)}$ while b_c^k and n_k from (3.23). Now the exact value of SNR gap, $\Gamma_i^{(k)}$, is taken from the table depending upon the bit vector b_c^k , and E_c^k is calculated from (3.36) using $\Gamma_i^{(k)}$. Gradually bits are added in the bit vector, b_c^k , till $\sum_i E_c^k$ exceeds the PSD limit, \hat{E} , and subsequently bits are removed to respect the PSD limit. We can summarize this approach as follows:

```

RM FOR CODED LP-OFDM()
1  Calculate  $R_k, n_k$  and  $b_c^k$  for  $\Gamma_i^{initial(k)}$ 
2  Take  $\Gamma_i^{(k)}$ , depending upon  $b_c^k$ 
3  Calculate  $E_c^k$  for  $\Gamma_i^{(k)}$ 
4  Start a counter, say  $count = 1$ 
5  while  $\sum_c E_c^k < \hat{E}$ 
6      do  $b_{n_k+count}^{(k)} += 1$ 
7           $count += 1$ 
8          Update  $E_c^k$ 
9  end while
10 while  $\sum_c E_c^k > \hat{E}$ 
11     do  $count -= 1$ 
12          $b_{n_k+count}^{(k)} -= 1$ 
13         Update  $E_c^k$ 
14 end while

```

This algorithm can be generalized for any value of the precoding factor and any channel coding scheme. For $L = 1$, this algorithm distributes bits and power to various subcarriers in the same way as bits and power are distributed in the conventional OFDM system.

3.2.5.3 Results

As discussed earlier, a communication system chain is developed in order to compare the performance of the proposed loading algorithm with existing systems. A background noise level of -110 dBm/Hz is assumed and the signal is transmitted with respect to a flat PSD of -40 dBm/Hz [13]. The maximum number of bits per symbol is limited to 10 and minimum number of bits per symbol is 2. Results are given for a fixed target BER of 10^{-7} . The optimal value of the precoding factor is obtained by running the simulations for various possible values of L , which came out to be 32 for the considered channel model. Fig. 3.11 shows the achieved bit per OFDM symbol versus the average channel gain $G = (\frac{1}{N}) \sum |H_i|^2$ which conveys the attenuation experienced by the signal through the channel. The corresponding SNR is then given by $SNR = -40 + G_{dB} + 110$. The performance of LP-OFDM is compared with OFDM at different average channel gains for both coded and uncoded implementations, where coded LP-OFDM implementation uses the proposed algorithm as discussed in Section 3.2.5.2. The OFDM system can be obtained by taking $L = 1$ in the LP-OFDM system. The simulations are run for a single user multi block scenario. The proposed adaptive coded LP-OFDM system can easily be extended to a multi user multi block scenario.

The reason for the better performance of the coded LP-OFDM system is explained in Fig. 3.12, where power distribution of the coded LP-OFDM is compared with

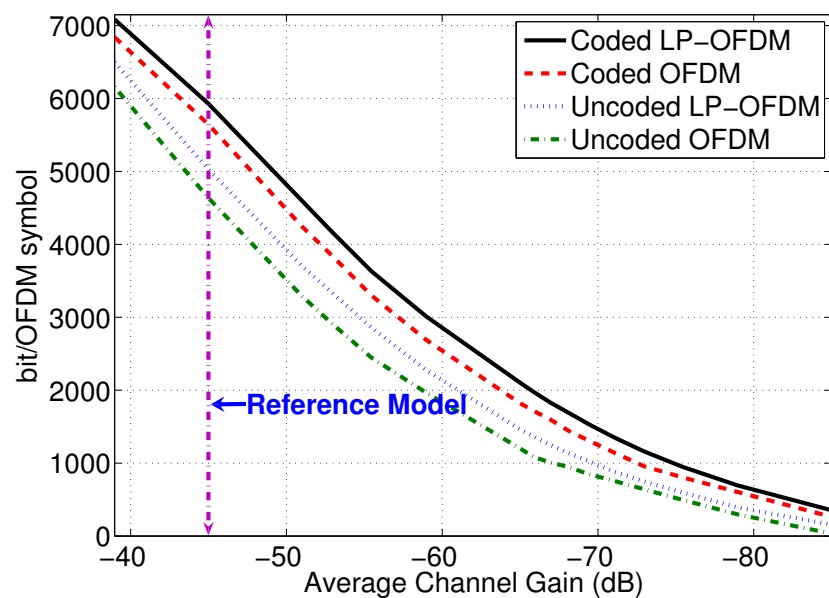


Figure 3.11: Achieved throughputs at various channel gains where $L = 32$ for LP-OFDM systems.

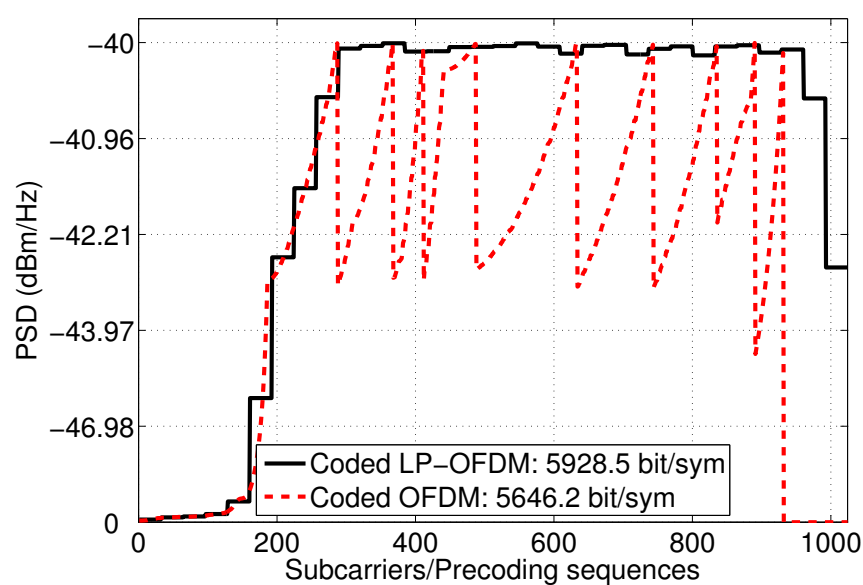


Figure 3.12: Transmit power distribution comparison where $L = 32$ for LP-OFDM systems.

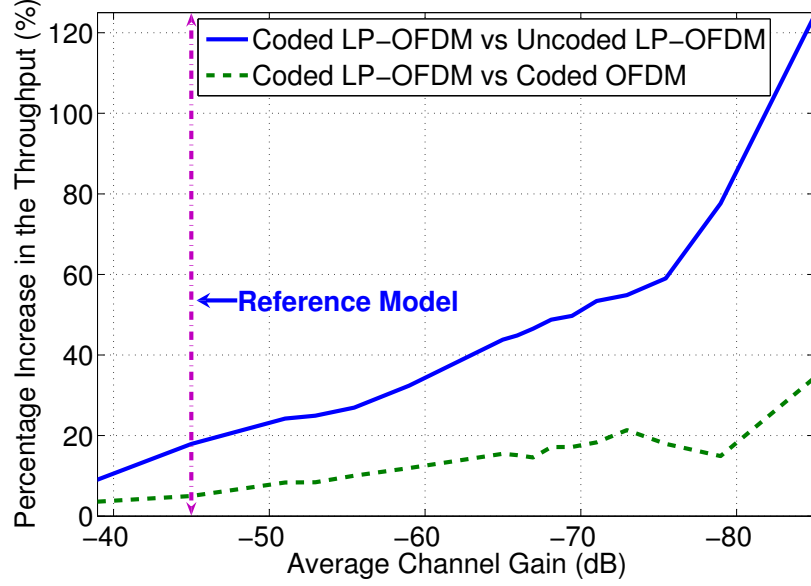


Figure 3.13: Percentage increase in the throughput.

that of the coded OFDM. The spike-shaped curve of the coded OFDM shows the transitions of the modulation orders (i.e. decreasing the constellation sizes) when no more power is available to sustain the fixed target BER. It is clear that the coded OFDM is not fully exploiting the available power on each subcarrier due to finite granularity and PSD constraints, while the precoding component of the coded LP-OFDM system accumulates the energies of a given subset of subcarriers to transmit additional bits. Both systems respect the PSD constraint of -40 dBm/Hz as defined earlier. The coded adaptive LP-OFDM system utilizes more efficiently this PSD limit in comparison with the coded OFDM system. Fig. 3.12 gives the minimal required power for the transmission of the maximum data rate. According to the PSD mask, the residual available power would not lead to any increase in the data rate.

Fig. 3.13 gives the percentage increase in the throughput obtained by coded LP-OFDM in comparison of coded OFDM and uncoded LP-OFDM for various values of average channel gain. The vertical broken line in Fig. 3.13 represents the reference power line channel model proposed by Zimmermann. As it is shown in Fig. 3.12 and 3.13 that coded LP-OFDM has the highest throughput and more efficient power utilization when compared to coded OFDM. Furthermore, it is worth noting that coded LP-OFDM is all the more interesting when the channel gain is low, i.e. the reception SNR is low. For instance, at an average channel gain of -60 dB, there is an improvement in the throughput of approximately 34.3% and 12.5% when we compare our coded LP-OFDM system with uncoded LP-OFDM and coded OFDM respectively for a fixed target BER of 10^{-7} . This improvement becomes 51% and 17.5% respectively at an average channel gain of -70 dB and is even higher at lower channel gains. Hence, we conclude that the proposed system can especially be advantageously ex-

exploited for poor SNR which is equivalent to claim that the proposed system ensures reliable communication over longer links and effectively increases the range of PLC systems.

In the next section, we discuss the bit rate maximization problem under mean BER constraint and for an imposed PSD mask. In this approach, instead of fixing the target BER on each subcarrier, the mean BER of an OFDM/LP-OFDM is constrained to achieve the target error rate and different subcarriers/precoding sequence may experience different values of BER.

3.3 RM under mean BER constraint

As discussed earlier, the bit loading is generally performed with fixed error rate on each subcarrier to attain a target error rate of the system [108]. In order to achieve a target error rate, we allow different subcarriers to carry different values of the BER, and we put a limit on the mean BER of an OFDM symbol, as proposed in [99] and [109]. This provides some flexibility to increase the throughput of the system under PSD constraint.

In this section, we propose discrete rate-adaptive loading algorithms for OFDM and LP-OFDM systems under PSD and mean BER constraints. The proposed algorithm for the OFDM system is a modified version of the algorithm of Wyglinski [99]. This modified approach is further extended to the LP-OFDM system. The advantages of these systems are observed under different scenarios in the PLC context. The uncoded QAM is selected as the modulation scheme. Firstly, we will discuss the rate maximization problem for the conventional OFDM system and then this study will be extended to LP-OFDM systems. This study may also be extended to the resource allocation algorithms that take into account the channel coding schemes and this is one of the perspectives of this dissertation.

3.3.1 OFDM systems

The proposed allocation maximizes the bit rate under PSD and mean BER constraint. Here, we consider one more time the expression of the SNR gap, Γ , from (2.19)

$$\Gamma \approx \frac{1}{3} \left[Q^{-1} \left(\frac{P^s}{4} \right) \right]^2. \quad (3.37)$$

Classically, to achieve a target error rate, SER is fixed on each subcarrier which is equal to the global SER of an OFDM symbol, because all the constellation sizes of QAM have the same value of the SNR gap at constant SER, as it is clear from approximation (3.37). But the value of the SNR gap varies with the constellation size at constant BER. For a fixed target BER and due to this dependence of the SNR gap on the number of bits per symbol, the target BER is rarely achieved as discussed in [99]. One solution is to use the peak BER constraint where BER (and not SER) is fixed on each subcarrier as discussed in the previous section, which gives

the comparable throughput as in [13, 108] but does not violate the fixed target error rate constraint. In this section, we maximize the bit rate while respecting a mean BER and PSD constraint. Thus, the allocation problem is formulated as follows

$$\begin{cases} \max \sum_{i=1}^N b_i, \\ \text{subject to } E_i \leq \hat{E} \text{ and } \frac{\sum_{i=1}^N P_i^b b_i}{\sum_{i=1}^N b_i} \leq P_T, \end{cases} \quad (3.38)$$

where \hat{E} is the given PSD limit. P_i^b is the BER of subcarrier i and P_T is the target mean BER of the system.

We consider a multicarrier system employing 6 uncoded M-QAM constellations with $M \in \{4, 8, 16, 32, 64, 128\}$. For uncoded QAM, SER is given as [41]

$$P_i^s \approx 4 Q \left(\sqrt{\frac{3\text{SNR}}{M_i - 1}} \right), \quad (3.39)$$

where P_i^s and M_i are the SER and the modulation order assigned to subcarrier i , respectively. BER is obtained from SER using the approximation $P_i^b \approx P_i^s/b_i$ [99]. Using this approximation, the second constraint of the problem described in (3.38) becomes,

$$\bar{P} = \frac{\sum_{i=1}^N P_i^s}{\sum_{i=1}^N b_i}, \quad (3.40)$$

which shows that the mean BER depends upon the sum of the SERs of all the subcarriers of a multicarrier system and not upon the individual number of bits supported by each subcarrier. Based on this result, we modify the loading algorithm proposed in [99], where rather than searching for the worst BER to reduce the constellation size, we search for the worst SER. This approach will then further be extended to an LP-OFDM system in Section 3.3.2. The algorithm can be described as follows:

RM FOR OFDM UNDER MEAN BER CONSTRAINT()

- 1 Initiate all the subcarriers with the highest modulation scheme (i.e. 128-QAM)
- 2 Calculate \bar{P} from (3.40)
- 3 **while** $\bar{P} \geq P_T$
- 4 **do** Search the subcarrier j with maximal SER: $j = \arg \max(P_i^s)$
- 5 Reduce the constellation size of the subcarrier j , null the subcarrier
- 6 if it supports 2 bits

```

7         Calculate  $\bar{P}$  from (3.40)
8     end while

```

In this way, we achieve the near optimal solution faster than that of [99], and the throughput is also higher, as it will be shown later. It is clear that the mean BER directly depends upon the sum of SERs (i.e. the product of BER and the number of bits per symbol) and does not directly depend upon the sum of BERs. In other words, reducing the constellation size of the subcarrier with the worst BER does not necessarily mean that it is the maximum decrease in the mean BER of the system. Therefore, in this allocation we reduce the constellation size of the subcarrier with the worst SER, which means that it is the maximum decrease in the mean BER of the system while still removing one bit.

3.3.2 LP-OFDM systems

As discussed earlier, an LP-OFDM system groups together multiple subcarriers. R_k is the number of bits supported by a group S_k of subcarriers. Here, we propose an allocation scheme with the same number of bits on all the precoding sequences of a group. In consequence, all the precoding sequences in a group have the same SER P_k^s and the sum of all SERs of a group can be defined as group error rate, $P_k = LP_k^s$. Note that P_k is not an SER by definition. P_k^s is the SER of all the precoding sequences of group k , and is given as

$$P_k^s = 4 Q \left(\sqrt{\frac{3 \gamma_k}{2^{R_k/L} - 1}} \right), \quad (3.41)$$

where γ_k is given as [13]

$$\gamma_k = \frac{L}{\sum_{i \in S_k} \frac{1}{|H_i|^2}} \frac{E}{N_0}. \quad (3.42)$$

Hence using (3.40), the mean BER of an LP-OFDM symbol can be given as

$$\bar{P} = \frac{\sum_{k=1}^K P_k}{\sum_{k=1}^K R_k}. \quad (3.43)$$

The allocation problem for an LP-OFDM system can be formulated as follows

$$\max \sum_{k=1}^K R_k,$$

$$\text{subject to } E_k \leq E, \text{ and } \frac{\sum_{k=1}^K P_k}{K} \leq P_T, \quad (3.44)$$

$$\sum_{k=1}^K R_k$$

where E_k is the power allocated to group k . In the proposed algorithm, we search for the worst value of P_k , and reduce the constellation sizes of all the precoding sequences of the found group. It is summarized as follows:

RM FOR LP-OFDM UNDER MEAN BER CONSTRAINT()

- 1 Initiate all the precoding sequences with the highest modulation scheme
- 2 Calculate \bar{P} from (3.43)
- 3 **while** $\bar{P} \geq P_T$
- 4 **do** Search the block of subcarriers k with the worst value of P_k
- 5 Reduce the constellation size of all precoding sequences of k , null all
- 6 precoding sequences if they support 2 bits.
- 7 Calculate \bar{P} from (3.43)
- 8 **end while**

Due to the removal of bits from all the precoding sequences of a given group, this allocation is much faster than the proposed allocation in [99] and gives higher throughput for high SNR, as it will be shown later. Constellation sizes of all the precoding sequences of a given group are reduced because the removal of bits from just one precoding sequence in a group changes negligibly the group error rate, as all the precoding sequences of a group have the same value of the transmit power. It is shown in (3.39) that SER depends upon the Q-function of SNR and due to the higher slope of the Q-function, SER of those precoding sequences, which do not have reduced constellation sizes, dominate in the group error rate. It is worthy to mention here that, the OFDM allocation can be obtained by taking $L = 1$ in the LP-OFDM allocation.

3.3.3 Results

In this section, we will present simulation results for both the proposed allocation schemes. The results will be compared with the allocation schemes proposed by Wyglinski and the ones proposed under peak error rate constraint for OFDM and LP-OFDM systems.

Fig. 3.14 shows the achieved bit per OFDM symbol versus the average channel gain, $ACG = \frac{1}{N} \sum |H_i|^2$ which conveys the attenuation experienced by the signal through the channel. The corresponding mean SNR is then given by $SNR_{dB} = -40 + ACG_{dB} + 110$. The performance of the proposed allocation for OFDM is compared with the allocation of Wyglinski at different average channel gains, particularly for poor SNR. It is shown that the proposed scheme performs better than the allocation

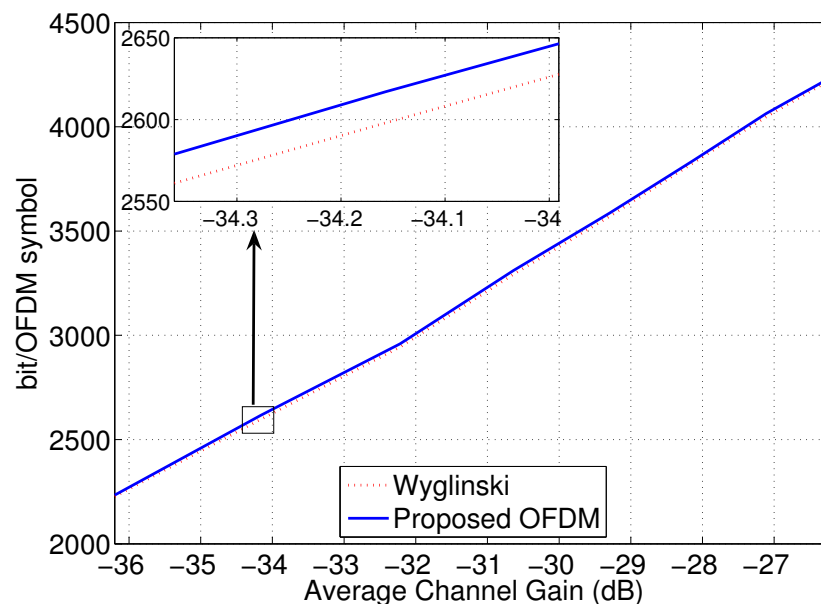


Figure 3.14: Throughput comparison of the proposed allocation for OFDM and the allocation proposed by Wyglinski at various average channel gains.

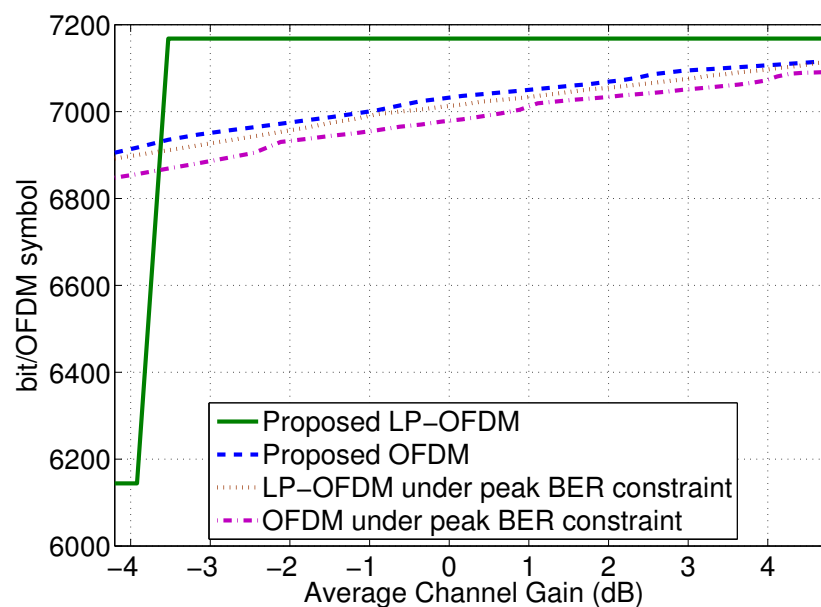


Figure 3.15: Throughput comparison of proposed allocations with OFDM and LP-OFDM allocations under peak BER constraint at various average channel gains.

Table 3.3: Computation times in milliseconds, 1024 subcarriers, $P_T = 10^{-7}$ (Intel core 2, 2.4-GHz processor).

	LP-OFDM peak BER	OFDM peak BER	Proposed LP-OFDM	Proposed OFDM	Wygliniski
Mean	5.46	21.96	0.45	41.99	43.96
Worst	30.43	34.33	1.02	176.87	194.11

of Wygliniski, as the minimum number of bits are removed before achieving P_T . This allocation is also faster as shown in Table 3.3.

In Fig. 3.15 the throughputs of the proposed allocations are compared, at higher average channel gains, with those of LP-OFDM and OFDM under peak BER constraint [13]. It is clear from the results that OFDM achieves higher throughput for poor SNR and LP-OFDM performs better at higher average channel gains. The proposed OFDM allocation performs better than the proposed LP-OFDM allocation for lower average channel gains since a uniform modulation order scheme is employed in the proposed LP-OFDM algorithm. The optimal value of the precoding factor, for the proposed LP-OFDM allocation, is obtained by running the simulations for various possible values of L , especially for higher SNRs, which is the region of high interest. The results are shown in Fig. 3.16. It can be observed that in the region where LP-OFDM performs better than OFDM, the maximum spreading always obtains the highest bit rate. Therefore L was taken as N (i.e. 1024 in this case). For the peak BER constraint LP-OFDM, the optimal value of the precoding factor, $L = 32$, is used.

Under PSD constraint, the major task is to efficiently utilize the available power, since the transmit power that is not used by a subcarrier (or a group of subcarriers) is lost and cannot be used by other subcarriers (or groups of subcarriers). It can be observed in Fig. 3.17 that, the proposed allocations with mean BER constraint utilize more efficiently the available power. The spike-shaped curve of the OFDM under peak BER constraint shows the transitions of the modulation orders (i.e. decreasing the constellation sizes) when no more power is available to sustain the target BER. LP-OFDM under peak BER constraint accumulates the energies of all the subcarriers of the group to utilize it more efficiently. It can be observed that it is using more power than OFDM, but still not utilizing it completely. LP-OFDM with mean BER constraint is using all the available power at higher channel gains and also accumulating the energies of different subcarriers to transmit more bits.

Consequently, it can be observed that the proposed OFDM allocation performs better at lower average channel gains while the proposed LP-OFDM allocation performs better at higher average channel gains. It has also been stated that the OFDM allocation can be obtained by taking $L = 1$ in the LP-OFDM allocation, therefore it might be an interesting solution to design an adaptive transmitter which decides between two optimal values of L (i.e. either 1 or N). Furthermore, a summary of mean

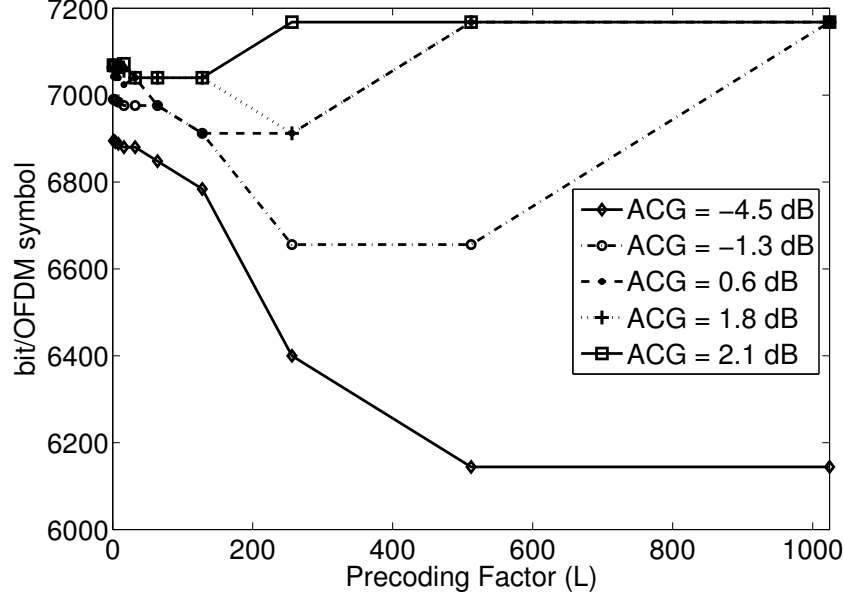


Figure 3.16: Precoding factor vs bit rate at various average channel gains.

and worst case computation times for a 1024-subcarrier system with a P_T of 10^{-7} is shown in Table 3.3. These results are obtained by running the simulations for 600 different values of ACG. It can be observed that the proposed LP-OFDM allocation is the fastest one and the proposed OFDM allocation is faster than the Wyglinski's incremental allocation. Furthermore, comparing our results with [99] implicates that the performance of the proposed allocations is better than [81].

3.4 Conclusion

Different resource allocation and optimization strategies for bit rate maximization of OFDM and LP-OFDM have been discussed in this chapter. We divided this chapter in two large sections. In the first part of this chapter, the bit rate maximization problem for OFDM and LP-OFDM systems was considered under peak BER constraint. This approach is slightly different from the classical peak SER approach, where instead of fixing SER, the target BER is fixed on each subcarrier. The resource allocation and optimization problem was discussed for both OFDM and LP-OFDM systems using peak BER approach.

Furthermore, to enhance the performance of multicarrier PLC systems and to demonstrate the validity of efficient performance of the proposed LP-OFDM system in coded systems scenarios, an adequate channel coding scheme has been selected. In order to comprehensively cover the RM problem for modern communication systems, the resource allocation problem was discussed with and without the integrated channel

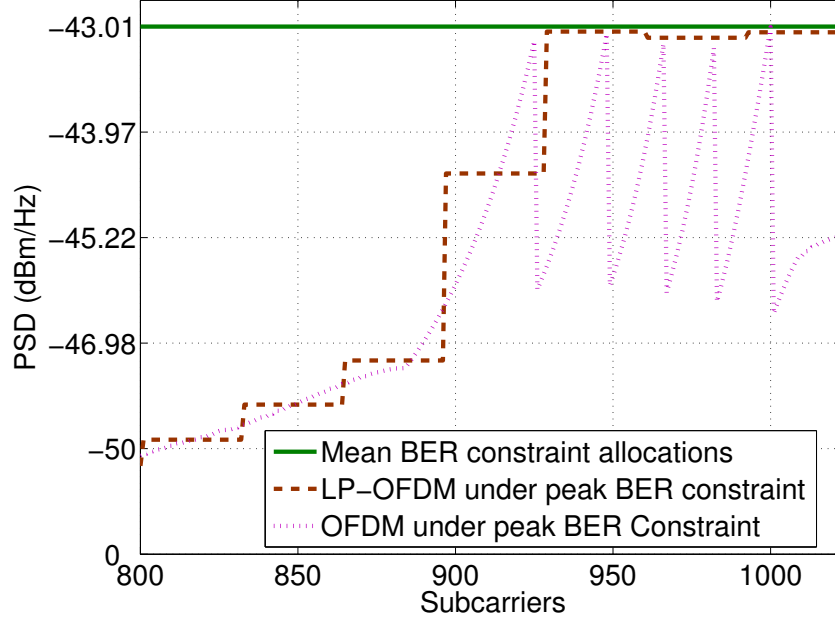


Figure 3.17: Power distribution comparison of all four considered allocation schemes at an ACG = -3.5 dB. OFDM under peak BER constraint supports 6869 bit, LP-OFDM under peak BER constraint supports 6911 bit, proposed OFDM with mean BER constraint supports 6935 bit and proposed LP-OFDM with mean BER constraint supports 7168 bit.

coding scheme. Bit and power loading algorithms were proposed that take into account the channel coding scheme in the resource allocation process.

To the best of author's knowledge, the idea of integrating channel coding gains into resource allocation process for bit rate maximization has never been used before. The only algorithm that integrates channel coding into power minimization was proposed by [97] only for conventional OFDM systems. The proposed resource allocation algorithm can handle various values of the SNR gap depending upon the constellation size of QAM modulation. The performance of the proposed system was compared with that of coded OFDM and uncoded LP-OFDM and it was shown that the proposed system was able to transmit higher rates especially for lower channel gains. The performance was compared while applying the same channel coding scheme to both systems, although the proposed resource allocation algorithms are quite flexible in their approach and may be used for any efficient channel coding scheme provided the SNR gaps of that scheme are known for all modulation orders. It was shown that using a powerful but low-complexity coding scheme with the proposed algorithm, improves the throughput of the system significantly and can especially be advantageously exploited for poor SNR. This work also contributed to an external research contract (no.46145507) with Orange Labs and a complete communication system chain was

developed for Orange Labs in “Galacsy” (a C++ based simulation system developed by France Télécom). This communication chain incorporates the proposed loading algorithm and the selected channel coding scheme in LP-OFDM system under PLC context. This first contribution has been published in the proceedings of two international conferences [110] and [111].

Furthermore, in the second part of this chapter we discussed the bit rate maximization problem under mean BER constraint. In this way, different subcarriers in a given OFDM symbol are allowed to be affected by different BER values and the error rate limit is imposed on an entire OFDM symbol. It means that mean BER of an OFDM/LP-OFDM symbol must not exceed the target error rate. We get the same BER performance as was achieved in the case of peak BER constraint but with better bit rate performance. Under PSD constraint, the transmitted power on each subcarrier must be less than the imposed limit. In practical systems, where discrete modulation orders are used, different constellation sizes require different levels of transmitted power in order to respect a given BER. That is why, we observed a significant difference between bit rates obtained for infinite granularity of modulation and those obtained by using practical discrete modulations. This problem may be compensated by using different values of BER on each subcarrier under PSD constraint and to impose a mean BER constraint on OFDM/LP-OFDM symbol. This approach gives an additional degree of freedom to resource allocation strategies for bit rate maximization under PSD constraint. In this part, we proposed bit and power loading algorithms for OFDM and LP-OFDM systems that maximize the bit rate of the system under mean BER constraint. These algorithms provide high throughputs and have low computational complexity while respecting a mean BER of an OFDM/LP-OFDM symbol. The performance of these allocations was compared with the algorithm of Wyglinski [99] and with algorithms optimizing the system bit rate under peak BER constraint. It was shown that the proposed allocation for OFDM performs better at lower channel gains and achieves higher throughput than existing algorithms. This algorithm is also faster than that of Wyglinski. Furthermore, a bit loading algorithm for LP-OFDM was also proposed which performs better at higher channel gains and has a very low implementation complexity. While comparing with the allocations under peak BER constraint, it was shown that the proposed allocations have higher throughputs under PSD constraint, as they are using the available power more efficiently. This second contribution has been published in the proceedings of an international conference [112].

In the next chapter, we discuss a new robustness maximization approach, where the mean BER of the system is minimized for a target bit rate and a given PSD mask. In this approach, the robustness of the system can be enhanced by allocating bits and powers to subcarriers in such a way that the error rate of an entire OFDM symbol is minimized for a target bit rate. Practical bit loading algorithms are also proposed for practical systems.

Chapter 4

Mean BER minimization

Contents

4.1	Introduction	98
4.2	MBM for OFDM systems	99
4.2.1	Proposed Loading Algorithm	100
4.2.2	Results	101
4.3	MBM for LP-OFDM systems	103
4.3.1	Mono block LP-OFDM	104
4.3.2	Proposed loading algorithm for mono block LP-OFDM	106
4.3.3	Multi block LP-OFDM	107
4.3.4	Proposed loading algorithm for multi block LP-OFDM	108
4.3.5	Results	109
4.4	MBM for Coded LP-OFDM	111
4.4.1	A textbook case	111
4.4.2	Algorithm for the textbook case	112
4.4.3	Mono block LP-OFDM	114
4.4.4	Results	117
4.5	Conclusion	117

4.1 Introduction

The application of RM optimization techniques to increase the system throughput, for a given error rate and an imposed transmit power constraint, has already been discussed. In parallel of RM optimization techniques, there exists another well known optimization technique that is used to enhance the system robustness against various noise sources in the transmission chain. The most popular robustness maximization (RoM) technique is margin maximization (or power minimization), where the system noise margin is maximized for a given bit and error rate [28, 29, 82].

The optimization problem is generally formulated under fixed SER on each subcarrier to attain a target error rate of the system. In this chapter, instead of fixing SER on each subcarrier we take into account the mean BER of an OFDM symbol and allow different subcarriers to be affected by different BER values. It provides additional flexibility to increase the robustness of the system under PSD constraint. The mean BER approach has been considered, in the existing literature, only for algorithmic treatment of bit rate maximization in [99, 109], and no analytical study has been performed. Looking at the robustness maximization problem from a different angle leads to a new approach, where the robustness of the system can be enhanced by allocating bits and powers to subcarriers in such a way that the error rate of an entire OFDM symbol is minimized for a given target bit rate. In this chapter, a new robustness maximization approach, hereafter known as mean BER minimization (MBM) is introduced, where the mean BER of the system is minimized for a target bit rate and a given PSD mask. Analytical studies are carried out for the first time to minimize the mean BER of multicarrier systems.

This new robustness maximization approach is based on the well known measure of the system robustness i.e. the error rate of the transmitted bits. In this chapter, we assume perfect channel knowledge at the transmitter and the delay of the CSI feedback is also neglected due to the quasi static nature of the power line channel. QAM modulation is the selected modulation scheme. We divide this chapter in three large sections. Firstly, the conventional OFDM system is considered. An analytical study is performed to obtain optimal bit and power distribution that minimizes the mean BER of the system. Discrete bit and power loading algorithms are proposed for practical systems.

In the second section, the MBM problem is studied for LP-OFDM systems. A theoretical analysis is performed by dividing LP-OFDM systems into mono block and multi block systems. Practical resource allocation algorithms are devised for real-life systems. The performance of the proposed system is compared with the MM LP-OFDM allocation. Furthermore, an initial study of MBM allocation is performed for LP-OFDM systems taking into account the channel coding scheme in the resource allocation process. Different future prospects of this study are also discussed. Simulation results are presented for mono block LP-OFDM systems that integrate the effects of channel coding into bit and power loading algorithms. Finally, we conclude this chapter.

4.2 MBM for OFDM systems

Classically, to achieve a target error rate, SER is fixed on each subcarrier which is equal to the global SER of an OFDM symbol, since all QAM constellation sizes have the same value of SNR gap at the same SER, as it is clear from the approximation (2.19). In another approach, the BER rather than SER is fixed on each subcarrier as proposed in [111]. In this section, we perform theoretical study of a new approach where rather than fixing the BER at each subcarrier, mean BER of a complete OFDM symbol is considered. The mean BER of an OFDM symbol is given as [99]

$$\bar{P} = \frac{\sum_{i=1}^N P_i^b \cdot b_i}{\sum_{i=1}^N b_i}, \quad (4.1)$$

where P_i^b is the BER for subcarrier i .

The MBM problem for OFDM systems is defined as follows

$$\begin{cases} \min \frac{\sum_{i=1}^N P_i^b \cdot b_i}{\sum_{i=1}^N b_i}, \\ \text{subject to } E_i \leq \hat{E}, \text{ and } \sum_{i=1}^N b_i = R, \forall i \ 1 \leq i \leq N, \end{cases} \quad (4.2)$$

Using approximation $P_i^b \approx P_i^s/b_i$ [99], the MBM problem for OFDM systems with uncoded QAM modulation can be written as [41]

$$\min \ 2 \sum_{i=1}^N \text{erfc} \left\{ \sqrt{\frac{\alpha_i}{2^{b_i} - 1}} \right\}, \quad (4.3)$$

where $\alpha_i = \frac{3}{2} \frac{E_i}{N_0} |H_i|^2$, with N_0 the noise power, and H_i the gain of subcarrier i . Under PSD constraint, the residual power of one subcarrier can not be used by other subcarriers, therefore to minimize the mean BER of the system, all available power on each subcarrier should be used, thus $E_i = \hat{E}$. The optimization problem can be solved by applying Lagrange multiplier method to (4.3), which follows

$$L(b_i, \lambda) = 2 \sum_{i=1}^N \text{erfc} \left\{ \sqrt{\frac{\alpha_i}{2^{b_i} - 1}} \right\} - \lambda \left(\sum_{i=1}^N b_i - R \right). \quad (4.4)$$

To eliminate Lagrange multiplier, we differentiate (4.4) with respect to b_i and approximate $2^{b_i} - 1 \approx 2^{b_i}$, which results in

$$\sqrt{\frac{\alpha_i}{2^{b_i}}} \exp \left(\frac{-\alpha_i}{2^{b_i}} \right) = u\lambda, \quad (4.5)$$

where $u = \frac{\sqrt{\pi}}{2 \ln 2}$. By using Lambert W function [113]⁽¹⁾, we can write

$$\frac{-2\alpha_i}{2^{b_i}} = W(-2u^2\lambda^2), \quad (4.6)$$

therefore

$$b_i = \log_2 \left[\frac{-2\alpha_i}{W(-2u^2\lambda^2)} \right]. \quad (4.7)$$

By using b_i in the constraint (4.2), we get

$$W(-2u^2\lambda^2) = -2 \cdot 2^{\frac{-R}{N}} \cdot \left(\sum_{i=1}^N \alpha_i \right)^{\frac{1}{N}}, \quad (4.8)$$

using $W(-2u^2\lambda^2)$ in (4.7) we find

$$b_i^* = \frac{R}{N} + \log_2 \left(\frac{3}{2} \frac{E_i}{N_0} |H_i|^2 \right) - \frac{1}{N} \sum_{i=1}^N \log_2 \left(\frac{3}{2} \frac{E_i}{N_0} |H_i|^2 \right). \quad (4.9)$$

Equation (4.9) gives the optimal distribution of bit b_i^* for different subcarriers. The optimal distribution of power E_i^* is to use all available power on a given subcarrier, as the residual power of a subcarrier can not be used by another subcarrier under PSD constraint. Therefore,

$$E_i^* = \hat{E}, \forall i. \quad (4.10)$$

The analytical study of the mean BER minimization produces comparable results to margin maximization allocation. Here, we propose a novel bit loading algorithm for practical applications. This loading algorithm uses the result obtained from the analytical study to find the discrete allocation faster than the iterative approach.

4.2.1 Proposed Loading Algorithm

The proposed bit and power loading algorithm minimizes the mean BER of OFDM systems for a target bit rate and a given PSD mask. In an iterative optimal solution, the algorithm is started either by assigning 0 bit to all subcarriers or by allocating the maximum number of allowed bits per QAM symbol b_{max} to each subcarrier. In each iteration one bit is added (or subtracted in the latter case) to the subcarrier that gives the minimum value of mean BER for OFDM systems. In this manner, we obtain an allocation that iteratively minimizes the mean BER of the system for a target bit rate. This computationally heavy greedy approach can be summarized as:

⁽¹⁾If $x \cdot \exp(x) = y$, then $x = W(y)$

ITERATIVE MBM ALLOCATION FOR OFDM()

```

1  Initialize  $b_i = 0$  or  $b_i = b_{max} \forall i$ 
2  while  $\sum_{i=1}^N b_i \neq R$ 
3      do if  $\sum_{i=1}^N b_i < R$ 
4          then  $\hat{i} = \arg \min \bar{P}(b_i + 1)$ 
5               $b_{\hat{i}} = b_{\hat{i}} + 1$ 
6          else  $\hat{i} = \arg \max \bar{P}(b_i - 1)$ 
7               $b_{\hat{i}} = b_{\hat{i}} - 1$ 
8          end if
9  end while

```

In the proposed algorithm, instead of initializing all subcarriers by 0 or b_{max} , we use the analytical study performed in Section 4.2 to find a shortcut to the optimal solution. This analytical approach reduces the system complexity significantly (by decreasing the number of iterations) whereas achieving exactly the same mean BER performance. The proposed algorithm can be given as:

PROPOSED MBM ALLOCATION FOR OFDM()

```

1  Initialize  $b_i = \lfloor b_i^* \rfloor$  from (4.9)  $\forall i$ 
2  while  $\sum_{i=1}^N b_i < R$ 
3      do  $\hat{i} = \arg \min \bar{P}(b_i + 1)$ 
4           $b_{\hat{i}} = b_{\hat{i}} + 1$ 
5      end while
6   $E_i = \hat{E} \forall i$ 

```

4.2.2 Results

In this section, we present simulation results, comparing the performance of MM and MBM allocations. As a reference, we use the iterative MM allocation discussed in [29, 100]. For MBM allocation, the analytical approach has been chosen to rapidly reach the optimal solution. The results obtained with the iterative greedy approach for MBM are not shown as they are strictly identical to the results obtained with the analytical study. For MBM allocations, we suppose a null system margin. The required error rate does not have any effect on MM allocations, therefore we calculate the MM allocation for any given value of SER. After deciding the bit and power distributions we calculate the mean BER for both allocation schemes. For a fair comparison, all the available transmit power on each subcarrier is utilized for both allocation schemes. The generated OFDM signal consists of $N=1024$ subcarriers

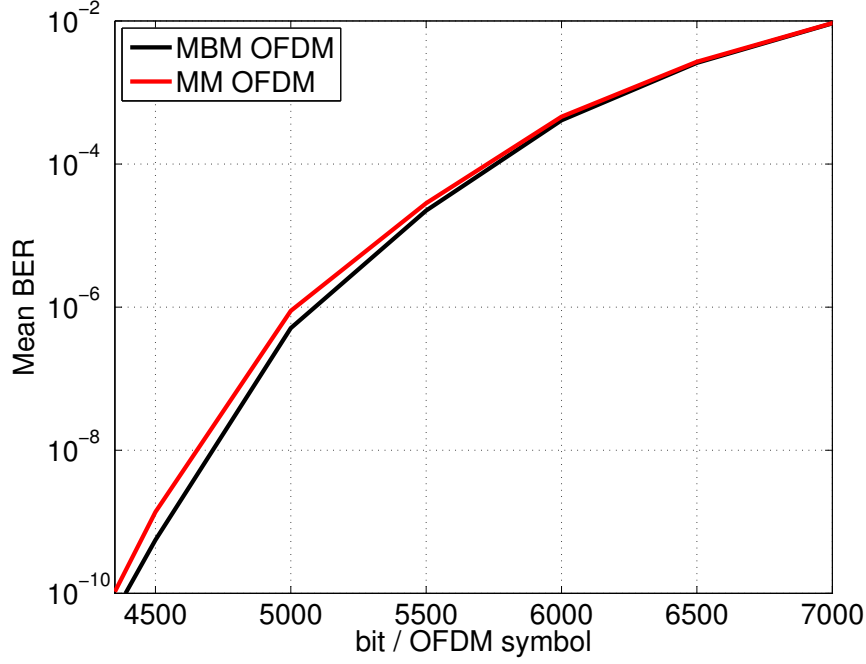


Figure 4.1: Mean BER performance comparison of MM and MBM allocations for various target bit rates.

transmitted in the band [500;20,000] kHz. The subcarrier spacing is 19.043 kHz. It is assumed that the synchronization and channel estimation tasks have been successfully performed.

Fig. 4.1 shows the obtained mean BER of the system versus different values of target bit rate for both MM and the proposed MBM allocation. It can be seen that the mean BER performance of the proposed allocation is better than the MM allocation. For instance, the classical MM allocation is achieving a mean BER of 10^{-6} for a target bit rate of 5017 bit/OFDM symbol whereas the proposed MBM OFDM allocation is respecting the same mean BER for a target bit rate of 5089 bit/OFDM symbol. A zoomed version of these results is shown in Fig. 4.2 to view the mean BER performance at higher target bit rates. The mean BER performance of the proposed allocation is better than MM allocation, since bits are allocated to minimize the mean BER of the system and we get a different bit allocation as it can be seen in Fig. 4.3.

In Fig. 4.3 the numbers of bits (i.e. different QAM sizes) assigned to each subcarrier are shown for a target bit rate of 4500 bit/OFDM symbol. It can be observed that both allocations are achieving the target bit rate in different manners i.e. by assigning not necessarily the same number of bits to the same subcarrier. Furthermore for this target bit rate, the proposed MBM allocation is achieving a mean BER of 5.5×10^{-10} while the MM allocation is achieving a mean BER of 1.3×10^{-9} .

The proposed MBM allocation does not impose any limit on the peak BERs of individual subcarrier and therefore it provides an additional degree of freedom. This

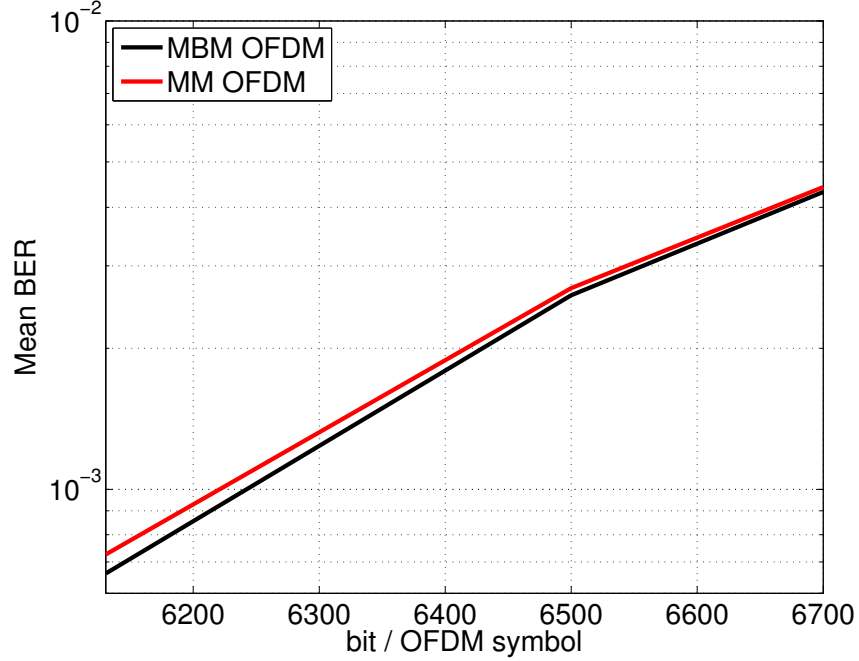


Figure 4.2: Mean BER performance comparison of MM and MBM allocations for higher target bit rates.

additional degree of freedom is judiciously exploited to attain better robustness for PLC multicarrier systems in the proposed resource allocation algorithm. On the contrary, the conventional MM allocation imposes a peak error rate constraint on each subcarrier. The effect of this peak error rate constraint becomes cumulative due to the presence of already imposed PSD constraint. The proposed allocation, while respecting the same PSD constraint, allows better mean BER performance.

In the next section, we will discuss the newly devised MBM problem for LP-OFDM systems. Discrete bit and power loading algorithms are also proposed for practical PLC systems for a given bit rate and under PSD constraint.

4.3 MBM for LP-OFDM systems

Here, we extend the study of the MBM problem for LP-OFDM systems and additional degree of freedom of LP-OFDM systems, provided by the linear precoding component, is exploited to attain even better mean BER performance for multicarrier PLC systems.

The performance optimization problem of MBM for an LP-OFDM system is divided into two cases. Firstly, only a mono block scenario is considered and subsequently a generalized multi block scenario is studied. Discrete bit and power loading algorithms are also proposed for practical PLC systems.

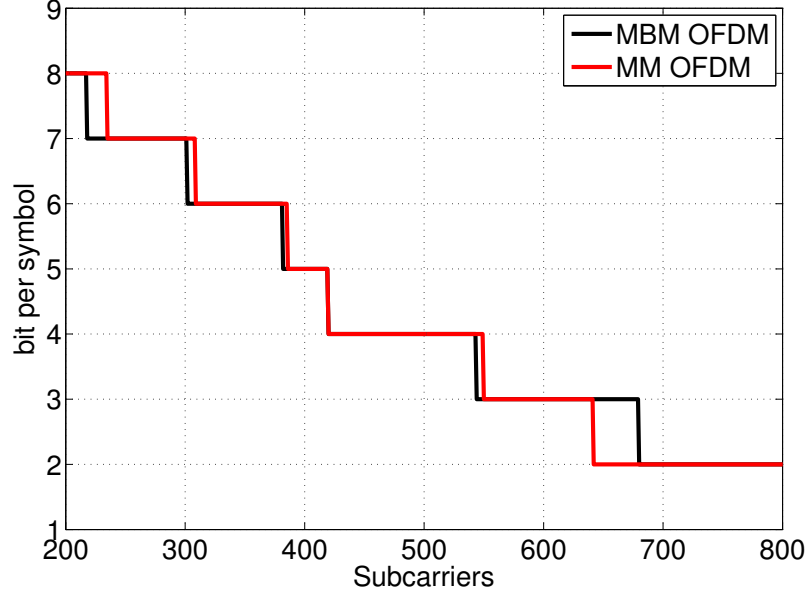


Figure 4.3: Bit allocation comparison of MM and MBM allocations for a target bit rate of 4500 bit/OFDM symbol, MBM OFDM is achieving a mean BER of $5.5 \cdot 10^{-10}$ while the MM OFDM achieves a mean BER of $1.3 \cdot 10^{-9}$.

4.3.1 Mono block LP-OFDM

The MBM problem for a mono block LP-OFDM system can be described as follows

$$\left\{ \begin{array}{l} \min \frac{\sum_{c=1}^C P_c b_c}{C}, \\ \sum_{c=1}^C b_c \\ \text{subject to } \sum_{c=1}^C E_c = \hat{E}, \text{ and } \sum_{c=1}^C b_c = R_k, \end{array} \right. , \quad (4.11)$$

where C is the number of useful precoding sequences in a block, P_c is the BER associated to precoding sequence c , b_c is the number of bits allocated to precoding sequence c , E_c is the power assigned to precoding sequence c , \hat{E} is the defined PSD limit and R_k is the target bit rate of the considered block. The problem can be simplified as follows,

$$\min \sum_{c=1}^C 2\text{erfc} \left(\sqrt{\frac{\alpha_k E_c}{2^{b_c} - 1}} \right) \quad (4.12)$$

where $\alpha_k = \frac{3}{2} \cdot \frac{L^2}{\sum_{i=1}^L \frac{1}{|H_i|^2}} \cdot \frac{1}{N_0}$.

The Lagrangian of this problem can be written as

$$L(E_c, b_c, \lambda, \mu) = \sum_{c=1}^C 2\text{erfc} \left(\sqrt{\frac{\alpha_k E_c}{2^{b_c} - 1}} \right) + \lambda \left(\hat{E} - \sum_{c=1}^C E_c \right) + \mu \left(R_k - \sum_{c=1}^C b_c \right). \quad (4.13)$$

After differentiating with respect to E_c and b_c , respectively, equating with zero, and considering, $2^{b_c} - 1 \approx 2^{b_c}$, Lagrange multipliers are given as

$$\lambda = -2 \sqrt{\frac{\alpha_k}{\pi}} \frac{e^{-\frac{\alpha_k E_c}{2^{b_c}}}}{\sqrt{E_c 2^{b_c}}} \quad (4.14)$$

$$\mu = 2 \ln 2 \sqrt{\frac{\alpha_k E_c}{\pi}} \frac{e^{-\frac{\alpha_k E_c}{2^{b_c}}}}{\sqrt{2^{b_c}}}. \quad (4.15)$$

And by simultaneously solving (4.14) and (4.15), we get

$$\begin{cases} E_c = \frac{\hat{E}}{C}, \forall c \\ b_c = \frac{R_k}{C}, \forall c \end{cases} \quad (4.16)$$

It is interesting to note that the optimal solution of bit and power distribution for mono block LP-OFDM is to equally distribute bits and powers among all precoding sequences. Now the only parameter that may be optimized in order to obtain minimum mean BER for mono block LP-OFDM system is the number of useful precoding sequences C in the given block. Taking $b_c = \frac{R}{C}$, and $E_c = \frac{\hat{E}}{C}$, in (4.12), the optimization problem can be written as

$$\min C \cdot \text{erfc} \left(\sqrt{\frac{3(2^R - 1)m}{2C(2^{\frac{R}{C}} - 1)}} \right), \text{ for } 1 \leq C \leq L \quad (4.17)$$

where

$$\alpha_k \cdot \hat{E} = \frac{3}{2} (2^R - 1) m,$$

where m is a constant multiplier, which shows that $\alpha_k \cdot \hat{E}$ must be a multiplicative factor of $\frac{3}{2} (2^R - 1)$. To find the optimal value of C , which minimizes the mean BER, we differentiate (4.17) with respect to C , in order to find critical points. Then by using the linear regression, the optimal value, C^* , is obtained

$$C^* = m \left[e^{\frac{R - 0.415}{1.4427}} - 1 \right]. \quad (4.18)$$

Equation (4.18) gives the optimal number of precoding sequences of a block to be used for data transmission.

4.3.2 Proposed loading algorithm for mono block LP-OFDM

The proposed pragmatic solution is the discrete bit loading algorithm, where for a target bit rate and a given block length, L , we find the optimal number of useful precoding sequences. For infinite granularity of modulation, the optimal solution is to distribute R/C^* bits to C^* precoding sequences of the given block. In the case of integer bit allocation, we need to find a suboptimal solution that allocates discrete bits to all precoding sequences. For this purpose, we use the analytical study performed in the previous section and allocated $\lfloor R/C^* \rfloor + 1$ bits to n precoding sequences and $\lfloor R/C^* \rfloor$ bits to the remaining $C^* - n$ precoding sequences. Since we have a target throughput R , n should respect the equation $n(\lfloor R/C^* \rfloor + 1) + (C^* - n)\lfloor R/C^* \rfloor = R$. Thus, we find

$$n = R - C^* \lfloor R/C^* \rfloor. \quad (4.19)$$

Consequently, the integer bit allocation solution for a single-block system is given by

$$\begin{cases} b_c = \lfloor R/C^* \rfloor + 1, & \forall c \in [1 : n] \\ b_c = \lfloor R/C^* \rfloor, & \forall c \in [n + 1 : C^*]. \end{cases} \quad (4.20)$$

Now we need to distribute the transmit power among different precoding sequences of the given block in such a way that it is proportional to the number of bits assigned, in order to keep the error rate of all precoding sequences in a reasonable range. For this purpose, we use the following power allocation, which allocates the transmit power among different precoding sequences according to the number of bits assigned,

$$E_c = \frac{(2^{b_c} - 1)}{C^*} \hat{E}. \quad (4.21)$$

The algorithm can be described as follows:

MBM FOR MONO BLOCK LP-OFDM()

- 1 Compute C^* from (4.18)
- 2 **if** $C^* < 1$
- 3 **then** $C^* = 1$
- 4 **else if** $C^* > L$
- 5 **then** $C^* = L$
- 6 **end if**
- 7 **end if**
- 8 Calculate n from 4.19
- 9 Calculate b_c from 4.20
- 10 Calculate E_c from 4.21

This algorithm performs a faster allocation of bits and transmits powers and performs better than OFDM allocation and MM allocation under difficult conditions. It also has significantly low computational complexity, as no iterative procedure is used. Now we will extend this analysis to a multi block system in order to fully exploit the additional degree of freedom provided by the linear precoding component of LP-OFDM systems.

4.3.3 Multi block LP-OFDM

The MBM problem for a multi block LP-OFDM system consisting of K blocks of length L (i.e. $K = \frac{N}{L}$) can be given as

$$\left\{ \begin{array}{l} \min \frac{\sum_{k=1}^K P_k R_k}{\sum_{k=1}^K R_k} \\ \text{subject to } \sum_{c_k=1}^{C_k} E_c^k = \hat{E} \forall k, \sum_{k=1}^K R_k = R \end{array} \right. , \quad (4.22)$$

where c_k is a given precoding sequence in block k , P_k is the BER of block k , R_k is the number of bits supported by block k , C_k is the number of useful precoding sequences in block k , E_c^k is the transmit power available for precoding sequence c_k and b_c^k is the number of bits supported by precoding sequence c_k . As we know from (4.16), for a given block $b_c^k = \frac{R_k}{C_k}$, and $E_c^k = \frac{\hat{E}}{C_k}$, therefore the problem can be redefined as

$$\min \sum_{k=1}^K 2 \cdot C_k \operatorname{erfc} \left(\sqrt{\frac{\alpha_k \hat{E}}{C_k \left(2^{\frac{R_k}{C_k}} - 1 \right)}} \right). \quad (4.23)$$

C_k is generally equal to L for high SNR values therefore by approximating $C_k \approx L$, and $\alpha'_k = \frac{\alpha_k \hat{E}}{L}$, the MBM problem for multi block LP-OFDM becomes

$$\left\{ \begin{array}{l} \min \sum_{k=1}^K 2 L \operatorname{erfc} \left(\sqrt{\frac{\alpha'_k}{2^{\frac{R_k}{L}} - 1}} \right) \\ \text{subject to } \sum_{c_k=1}^L E_c^k = \hat{E} \forall k, \sum_{k=1}^K R_k = R \end{array} \right. . \quad (4.24)$$

It can be observed that, this problem is similar to (4.3), if we replace b_i by $\frac{R_k}{L}$ and α_i by α'_k . Therefore, by using the analogy between the two problems, the optimal solution for (4.24) can be given as

$$R_k^* = \frac{R}{K} - \log_2 \left(\sum_{i \in S_k} \frac{1}{|H_i|^2} \right) + \frac{1}{K} \sum_{k=1}^K \log_2 \left(\sum_{i \in S_k} \frac{1}{|H_i|^2} \right). \quad (4.25)$$

Equation (4.25) gives the number of bits supported by each block. The proposed allocation strategy works in two steps. In the first step, numbers of bits of each block are obtained and then the optimal number of useful precoding sequences for each block is calculated using (4.18). The proposed bit and power loading algorithm, based on this strategy, is discussed in the next section.

4.3.4 Proposed loading algorithm for multi block LP-OFDM

Here, we propose an iterative algorithm which allocates bits to the block, which has the best mean BER (i.e. the minimum value of P_k^b). Similar to the case of OFDM, here each block uses all available transmit power no matter what is the constellation size. In this manner, we find the target bit rate of each block. The second step consists in finding the optimal number b_c of bits that should be allocated to each precoding sequence in order to achieve the block throughput R_k , as explained in Section 4.3.1. The proposed algorithm for a multi block LP-OFDM system can be described as follows:

MBM FOR MULTI BLOCK LP-OFDM()

```

1  Initialize  $R_k = \lfloor R_k^* \rfloor \ \forall k$  from (4.25)
2  while  $\sum_{k=1}^K R_k < R$ 
3      do  $k = \arg \min_k P_k^b(R_k)$ 
4           $R_k = R_k + 1$ 
5  end while
6  for  $k \leftarrow 1$  to  $K$ 
7      do Calculate  $C^{k*}$  from 4.18
8          if  $C^{k*} < 1$ 
9              then  $C^{k*} = 1$ 
10             else if  $C^{k*} > L$ 
11                 then  $C^{k*} = L$ 
12             end if
13         end if
14         Calculate  $n^k$  from 4.19
15         Calculate  $b_c^k$  from 4.20
16         Calculate  $E_c^k$  from 4.21
17  end for
```

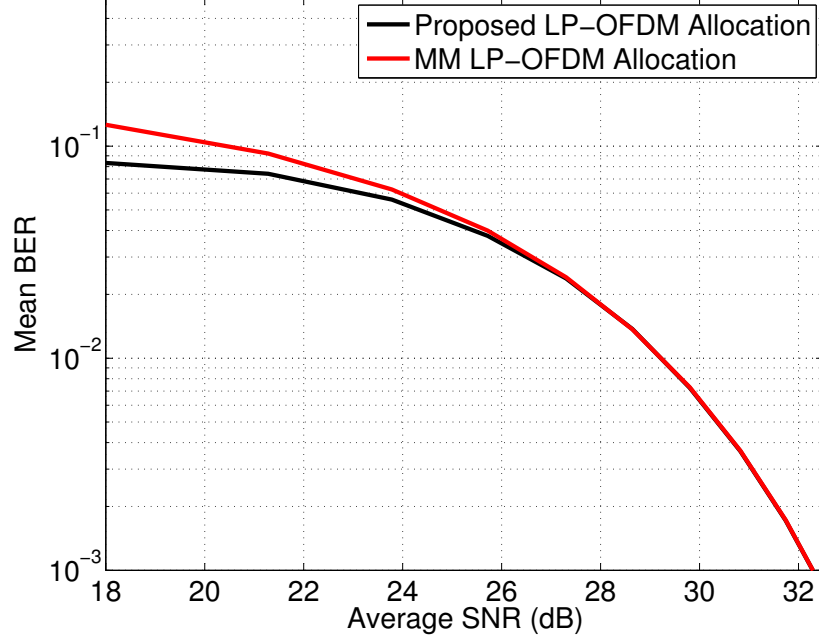


Figure 4.4: Mean BER comparison of the proposed allocations with Margin Maximization allocations for different average SNR, for $R = 4000$ bit/OFDM symbol.

This algorithm uses the analytical study performed in Section 4.3.3 for speedy convergence to the optimal solution. Therefore, the theoretical study significantly reduces the system complexity in terms of the number of iterations required to reach the optimal solution. In the second step, bits and powers are calculated for all precoding sequences of the given block. This step does not involve any iterative procedure for a given block. In the next section, various simulation results are presented comparing the performance of the proposed system with the existing robustness maximization schemes.

4.3.5 Results

Here, we present simulation results comparing the performances of MM and MBM allocations for LP-OFDM systems. We use the MM allocation proposed in [29]. For MBM allocation, a null system margin is considered. The required error rate does not have any effect on MM allocations, therefore we calculate the MM allocation for any given value of SER. After deciding bit and power distributions we calculate the mean BER for both allocation schemes. For a fair comparison, all available transmit power on each block is utilized for both allocation schemes. The generated signal is a baseband signal produced by dividing 20 MHz band of Zimmermann channel into 1024 subcarriers. The maximum number of bits per symbol is limited to 15 and the value of L for LP-OFDM systems is taken as 32.

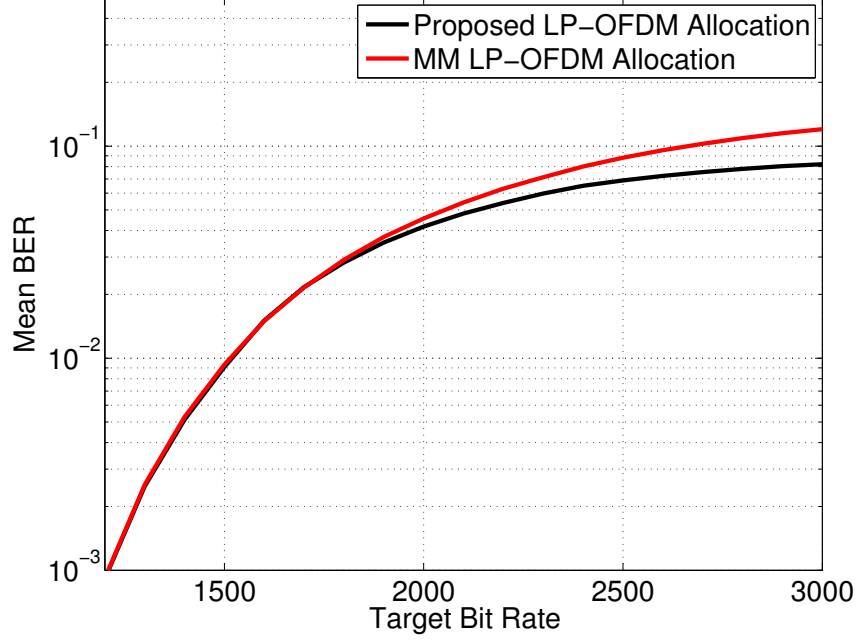


Figure 4.5: Mean BER comparison of the proposed allocations with Margin Maximization allocations for various bit rates at average SNR = 12 dB.

Fig. 4.4 shows the achieved mean BER versus the average SNR at a fixed target bit rate of 4000 bit/OFDM symbol. The performance of the proposed allocation is compared with the MM allocation for LP-OFDM. Furthermore, it is shown that the performance of the proposed LP-OFDM solution is better than the MM allocation, especially for poor SNRs. At strong SNRs, both LP-OFDM allocations perform equally well. The proposed LP-OFDM allocation performs better than MM allocation at low average SNR, as it uses the optimal number of useful precoding sequences, while the MM LP-OFDM allocation always uses all the precoding sequences of a block i.e. L . For high average SNR, the calculated optimal value of the number of useful precoding sequence C^* is equal to L . It might be further optimized by using the optimal block length, which might be a promising prospect for future work.

Fig. 4.5 compares the performance of both allocations for different values of target bit rates at a low value of average SNR (i.e. 12 dB). The results show that the proposed LP-OFDM allocation performs better than MM LP-OFDM. It signifies that the proposed MBM LP-OFDM allocation is more robust for low values of SNR.

In this section, we consider the MBM problem for LP-OFDM system and propose the bit allocation algorithm, which minimizes the mean BER of the system for a fixed target bit rate and a given PSD mask. The proposed algorithm provides better results than the MM allocation, while both are serving the purpose of robustness maximization of the system. Furthermore, the proposed algorithm uses different numbers of useful precoding sequences as an additional degree of freedom for optimization. It is

shown that the proposed allocation for LP-OFDM performs better at lower average SNR and for higher target bit rates.

In the next section, we consider the MBM problem for LP-OFDM system while taking into account the channel coding gains in the resource allocation process. An initial study is performed for coded LP-OFDM systems using simple convolutional codes as the selected channel coding scheme.

4.4 MBM for Coded LP-OFDM

In this section, an initial study on mean BER minimization is performed for LP-OFDM systems taking into account the channel coding scheme into the resource allocation process. This study is based on the graphical optimization technique for mean BER minimization. Simple soft decision convolutional codes are used in this initial study. The same approach of the graphical optimization may also be extended for other channel coding schemes. The polynomial for the selected convolutional coder is [133,171] and the constraint length is 7. Fig. 2.8 shows the BER performance of the selected convolutional codes on Gaussian channel.

4.4.1 A textbook case

In order to find out the optimal resource allocation for coded LP-OFDM, firstly we find the optimal power distribution that achieves a minimum mean BER with only two modulation orders on L precoding sequences. Therefore, this study leads to systems having two consecutive QAM orders on different precoding sequences in a block. In the studied case, m precoding sequences support b_1 bits and n precoding sequences support b_2 bits. The expression for mean BER is then given as

$$\bar{P} = \frac{m \times P(e_1) \times b_1 + n \times P(e_2) \times b_2}{m \times b_1 + n \times b_2}, \quad (4.26)$$

with

$$m \times b_1 + n \times b_2 = R, \quad (4.27)$$

where $P(e_1)$ and $P(e_2)$ are BERs for m and n precoding sequences for transmit powers e_1 and e_2 respectively and R is the target bit rate. By using Lagrange multiplier method, we can determine the optimal power distribution, for a known bit distribution of a given block, that minimizes the mean BER of the system. Lagrangian associated with this problem can be given as

$$L(e_i, \lambda) = \bar{P} + \lambda \times (m \times e_1 + n \times e_2 - \hat{E}), \quad (4.28)$$

where λ is the Lagrange multiplier. The derivatives of Lagrangian can be given as

$$\frac{\partial L}{\partial e_1} = \frac{m \times \partial P(e_1) \times b_1}{\partial e_1 \times R} + \lambda \times m = 0, \quad (4.29)$$

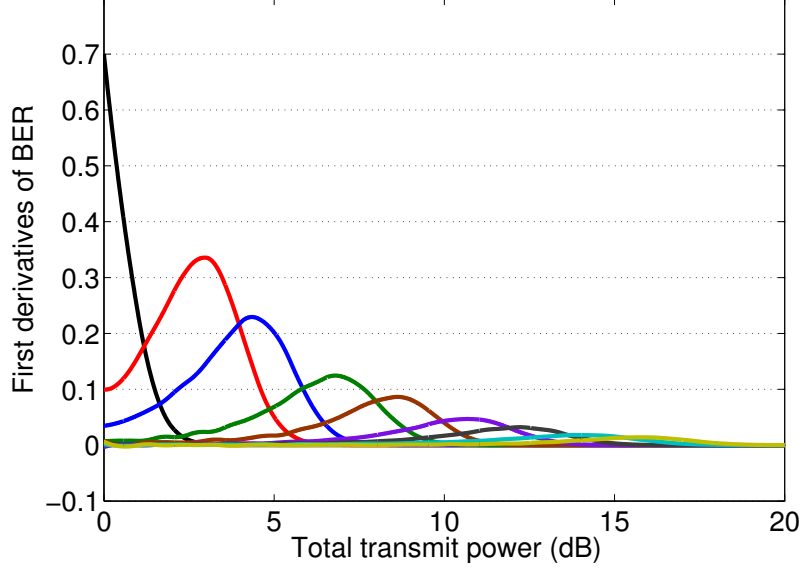


Figure 4.6: First derivatives of BER with respect to transmit power versus total available power for different modulation orders.

and

$$\frac{\partial L}{\partial e_2} = \frac{n \times \partial P(e_2) \times b_2}{\partial e_2 \times R} + \lambda \times n = 0, \quad (4.30)$$

where

$$\frac{\partial L}{\partial \lambda} = m \times e_1 + n \times e_2 - \hat{E} = 0. \quad (4.31)$$

By simultaneously treating (4.29) and (4.30), we obtain

$$\dot{\lambda} = -\frac{\partial P(e_1) \times b_1}{\partial e_1} = -\frac{\partial P(e_2) \times b_2}{\partial e_2}, \quad (4.32)$$

where the following constraint must be satisfied

$$m \times e_1 + n \times e_2 = \hat{E}. \quad (4.33)$$

It must be noted here that for each value of $\dot{\lambda}$, we have an optimal power distribution (e_1, e_2) that guarantees the minimum value of mean BER. In order to respect the imposed PSD constraint, the sum of powers must be less than \hat{E} , as shown in (4.33).

4.4.2 Algorithm for the textbook case

The textbook case algorithm can be summarized as follows:

Table 4.1: Results obtained for the textbook case.

Given bit distribution	
$b_1 = 7$	$b_2 = 6$
$m = 6$	$n = 26$
Obtained results	
$e_1 = 11.495$ dB	$e_2 = 10.598$ dB
$\bar{P} = 2.81 \times 10^{-3}$	

THE TEXTBOOK CASE ALGORITHM()

```

1   $i = \min \left( \max \left\{ -\frac{\partial P(e_1) \times b_1}{\partial e_1} \right\}, \max \left\{ -\frac{\partial P(e_2) \times b_2}{\partial e_2} \right\} \right)$ 
2   $I = \min \left( \text{length} \left\{ -\frac{\partial P(e_1) \times b_1}{\partial e_1} \right\}, \text{length} \left\{ -\frac{\partial P(e_2) \times b_2}{\partial e_2} \right\} \right)$ 
3  while  $i < I$ 
4      do Calculate  $e_1$  and  $e_2$ 
5          if  $m \times e_1 + n \times e_2 = \hat{E}$ 
6              then Calculate  $\bar{P}$ 
7              else  $i = i + 1$ 
8          end if
9  end while
```

In order to implement such an algorithm, firstly we need the curves of first derivatives as shown in Fig. 4.6 for a normalized noise power of 0 dB. For all modulation orders greater than 2 (i.e. $M > 2$), these curves have a peak value. We can therefore divide these curves into two parts; before and after the peak value. The first part of the curve (i.e. before the peak value) corresponds to very high values of BER, thus it can be rejected. The zone of interest therefore lies on the right hand side of the peak value. The curves presenting the zone of interest are shown in Fig. 4.7. For a target bit rate of 198 bits, and $L = 32$, obtained results from this algorithm are shown in Table 4.1.

In order to verify the obtained optimization results from Lagrange multiplier method and to generalize these results for mono block LP-OFDM systems, we use a simple iterative algorithm. This algorithm can be summarized as:

ITERATIVE MBM ALGORITHM()

```

1  for  $i \leftarrow 1$  to  $\text{length}(e_1)$ 
2      do for  $j \leftarrow 1$  to  $\text{length}(e_2)$ 
3          do if  $m \times e_1(i) + n \times e_2(j) == \hat{E}$ 
4              then Calculate  $\bar{P}$ 
5          end if
6      end for
7  end for
```

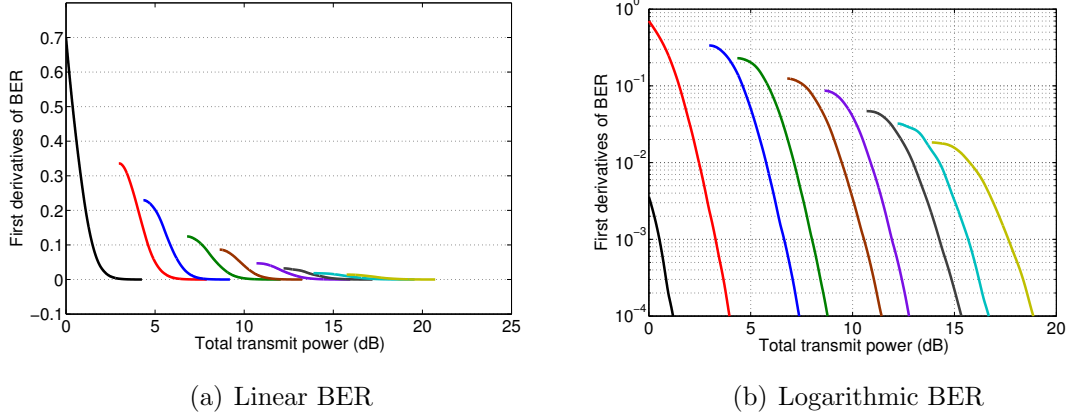


Figure 4.7: Considered part of first derivatives of BER with respect to transmit power versus total available power for different modulation orders.

This algorithm consists of two BER functions $P_1 = f(e_1)$ and $P_2 = f(e_2)$, where $m \times e_1 + n \times e_2 = \hat{E}$. Two respective minima of these two curves give the same value of BER that is the minimized mean BER of the system and corresponding power values are also at the required optima. The result of this algorithm is presented in Fig. 4.8 and it corresponds to the result obtained from the theoretical study. It also justifies the feasibility of the method of Lagrange multiplier for the MBM problem.

4.4.3 Mono block LP-OFDM

After studying a simple textbook case where we determined the optimal power for only two possible modulation orders scenario, here we generalize the MBM problem for mono block LP-OFDM systems. No advance knowledge of bit distribution is considered in this case. Rather, a target bit rate has to be respected under PSD constraint. The mean BER, then, can be given as

$$\bar{P} = \frac{m_1 P(e_1) \times b_1 + \cdots + m_i \times P(e_i) \times b_i + \cdots + m_n \times P(e_n) \times b_n}{R}, \quad (4.34)$$

with

$$m_1 \times b_1 + \cdots + m_i \times b_i + \cdots + m_n \times b_n = R, \quad (4.35)$$

where m_i represents the number of precoding sequences having the same modulation order. The Lagrangian of this problem can be given as

$$L(e_i, \lambda) = \bar{P} + \lambda \times (m_1 \times b_1 + \cdots + m_i \times b_i + \cdots + m_n \times b_n - \hat{E}), \quad (4.36)$$

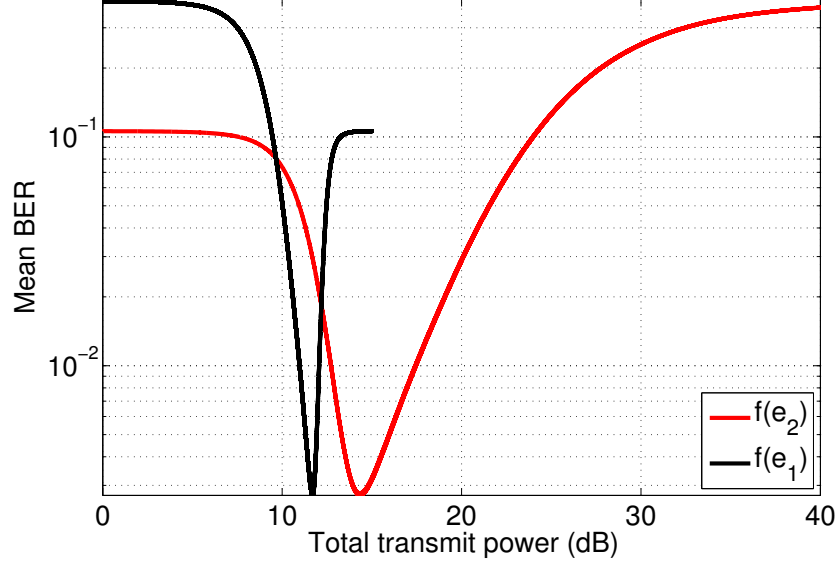


Figure 4.8: Results obtained from the iterative MBM algorithm.

and Lagrangian derivatives can be written as for all $i \in [1; n]$

$$\frac{\partial L}{\partial e_i} = \frac{m_i \times \partial P(e_i) \times b_i}{\partial e_i \times R} + \lambda m_i = 0. \quad (4.37)$$

By differentiating with respect to Lagrange multiplier, we obtain

$$\frac{\partial L}{\partial \lambda} = m_1 \times e_1 + \dots + m_i \times e_i + \dots + m_n \times e_n - \hat{E} = 0, \quad (4.38)$$

and by replacing $\lambda \times R$ by λ' , we obtain

$$\lambda' = -\frac{\partial P(e_1) \times b_1}{\partial e_1} = \dots = -\frac{\partial P(e_i) \times b_i}{\partial e_i} = \dots = -\frac{\partial P(e_n) \times b_n}{\partial e_n} \quad (4.39)$$

$$\Rightarrow m_1 \times e_1 + \dots + m_i \times e_i + \dots + m_n \times e_n = \hat{E}. \quad (4.40)$$

The optimal power distribution can be obtained by using (4.39) for mono block LP-OFDM systems under an imposed PSD constraint. The problem of bit distribution is solved in an iterative fashion. At each iteration, we calculate the mean BER for all possible distributions using the optimal power distribution discussed above. The bit distribution, that gives the minimum value of mean BER, is selected. This process is continued until we achieve the target bit rate. The PSD constraint is verified at each iteration.

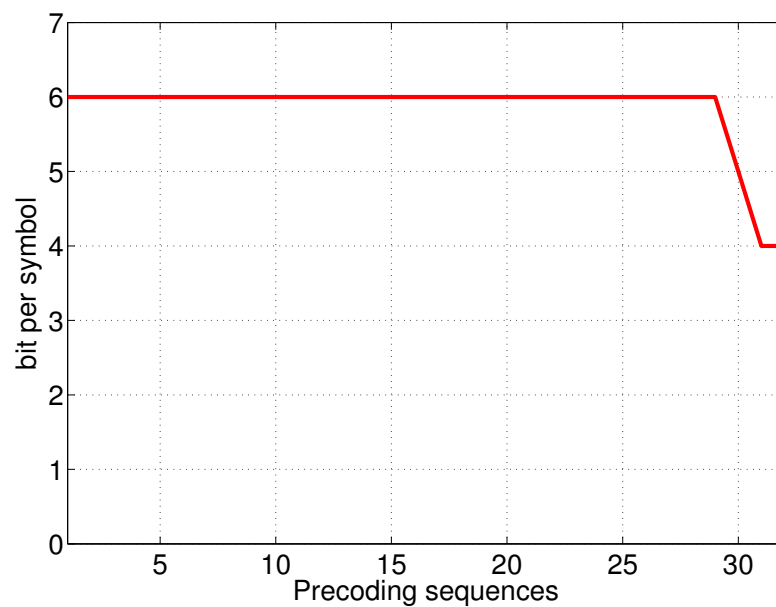


Figure 4.9: Bit distribution for the proposed MBM allocation for mono block LP-OFDM.

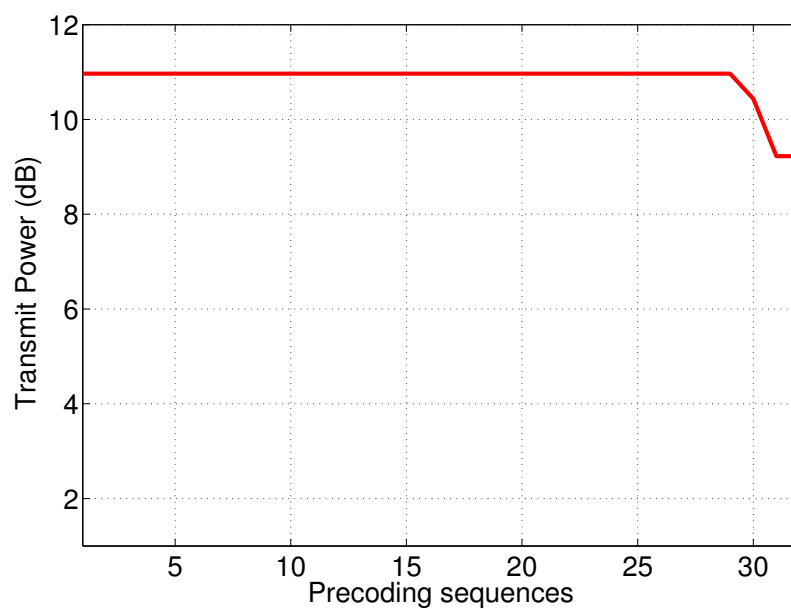


Figure 4.10: Power distribution for the proposed MBM allocation for mono block LP-OFDM.

4.4.4 Results

Here, we present results of simulations carried out to verify the performance of the initial study on the MBM problem for LP-OFDM systems taking into account the channel coding in the resource allocation process. In the simulation, the precoding factor L is 32 and the normalized noise power is 0 dB. Fig. 4.9 shows the optimal bit distribution for the defined parameters, obtained through the proposed algorithm. Fig. 4.10 presents the optimal power distribution for the found bit distribution. The minimized mean BER obtained from this simulation is 3.36×10^{-4} .

It must be noted here that the presented analysis is an initial study on the MBM for LP-OFDM systems taking into account the channel coding in resource allocation process. There are many future prospects of this study. Some of them are listed below:

1. The study may be extended for multi block LP-OFDM systems.
2. In the mean BER approach, different channel coding schemes possess significantly different behaviours. Therefore, this study may be extended for other channel coding schemes. The same graphical optimization approach may be used for this purpose.
3. Performance comparison may be done with other robustness optimization schemes that take into account the channel coding in the resource allocation process. To the best of author's knowledge, no such robustness optimization scheme exists that integrates convolutional codes into the resource allocation process.
4. Other parameters of LP-OFDM systems may also be optimized such as the number of useful precoding sequences.

After this initial study, we can observe the feasibility of the MBM allocation for LP-OFDM systems taking into account the resource allocation process. The channel coding gain may be used in the resource allocation process to cumulate the advantages offered by the precoding component.

4.5 Conclusion

In this chapter, we considered the robustness maximization problem for OFDM and LP-OFDM systems. A new approach for robustness maximization was proposed. In this approach, instead of fixing SER on each subcarrier, the mean BER of an OFDM symbol is taken into account and different subcarriers are allowed to be affected by different BER values. It provides additional flexibility to increase the robustness of the system under PSD constraint. Bits and powers are allocated to different subcarriers/precoding sequences in such a way that the mean BER of the system is minimized. The mean BER approach has been considered only for algorithmic treatment of bit rate maximization in [99, 109]. To the best of author's knowledge, no theoretical

analysis has been performed, using mean BER approach, that maximizes the robustness of the system. Detailed analytical studies are performed in order to develop the theoretical framework for this new approach.

We divided this study in three large sections. First of all, the mean BER minimization was performed for conventional OFDM systems. Theoretical analysis was presented, for the first time, for conventional OFDM systems in order to obtain the infinite granularity bit and power allocation that optimally minimizes the mean BER of OFDM systems. Discrete bit and power loading algorithms were also presented for practical PLC systems. The proposed MBM allocation does not impose any limit on the peak BERs of individual subcarrier and therefore it provides an additional degree of freedom. This additional degree of freedom is judiciously utilized in order to attain better mean BER performance for multicarrier PLC systems. On the contrary, conventional MM allocations impose a peak error rate constraint on each subcarrier. Effects of this peak error rate constraint become cumulative due to the presence of already imposed PSD constraint. The proposed allocation, while respecting the same PSD constraint, allows better mean BER performance. This contribution is under review for a possible publication in an international journal [114].

In the second section, the MBM problem was considered for LP-OFDM systems. Detailed analytical study was performed for LP-OFDM systems and real valued optimal solutions are obtained for bit and power distribution among different precoding sequences in order to obtain the minimized BER of the system. The additional degree of freedom provided by the linear precoding component of LP-OFDM systems was exploited in order to get better mean BER performance. Analytical study was also performed to optimize the number of useful precoding sequences. Discrete bit and power loading algorithms were also proposed for practical systems. Complete communication chain was developed, with integrated resource allocation algorithms, to evaluate the performance of proposed schemes. It was shown that proposed algorithms perform better than MM LP-OFDM allocations for low SNR values. This contribution has been published in the proceedings of a national [115] and an international conference [116].

Furthermore, we extended the study of MBM problem for LP-OFDM systems taking into account the channel coding in the resource allocation process. An initial study was performed in this context for integrated convolutional codes. This initial study is based on the graphical optimization technique for mean BER minimization. The same approach of the graphical optimization may also be extended for other channel coding schemes such as turbo codes and low density parity check (LDPC) codes. We started from a textbook case and extended this study to mono block LP-OFDM systems. The method of Lagrange's multiplier was used in order to obtain the optimal solution. Theoretically obtained results were verified by implementing an iterative algorithm. We also proposed a discrete loading algorithm for mono block LP-OFDM that works in combination with the convolutional code and the soft-decision Viterbi decoder. Simulation results were presented and future prospects of this study were highlighted.

Until now, we studied the resource allocation problems under the assumption of perfect channel knowledge at the transmitter. As, it is well known that perfect CSI is rarely achieved, the study of bit and power loading for noisy estimations are carried out in the next chapter.

Chapter 5

Bit rate maximization with imperfect CSI

Contents

5.1	Introduction	122
5.2	Considered error model	123
5.3	Impacts on allocations	124
5.4	Allocation based on generalized error rate expressions .	125
5.4.1	OFDM allocations	125
5.4.2	LP-OFDM allocations	126
5.4.3	Results	128
5.5	Allocations based on individual error rate expressions .	132
5.5.1	Modified SER expressions	132
5.6	Proposed LP-OFDM allocation	135
5.6.1	Results	136
5.7	Conclusion	139

5.1 Introduction

In this chapter, we consider the bit rate maximization strategies under PSD constraint for both OFDM and LP-OFDM systems in PLC context but with the assumption of imperfect CSI. Most of the previous works on constrained resource allocation and optimization have been done under perfect instantaneous CSI at the transmitter. However, in a system with a high number of subcarriers, using pilots and/or feedback per subcarrier can require excessive overhead and even then, the full perfect CSI is rarely achieved. To overcome this problem, we need such bit and power loading algorithms that can take care of the noisy estimations at the transmitter. The perfect CSI assumption is also unrealistic since perfect CSI is exceptionally obtained due to channel estimation errors and channel feedback delays.

As we discussed earlier, the resource allocation and optimization lie in the heart of modern communication systems. However, to achieve the performance advantages of adaptive modulation, conventionally accurate CSI is required at the transmitter. In PLC context, due to harsh channel characteristics, the estimated channel response may be noisy. Some researchers have studied the performance when imperfect or partial CSI is available, and some of them have proposed possible solutions for the imperfect CSI case [117]-[124]. Adaptive transmission based on imperfect or partial CSI for multiple-antenna OFDM systems has also been studied [125]-[128]. The impact of imperfect CSI was also studied in [120] and [121] for the constant bit rate case. A low-complexity ordered subcarrier selection algorithm was proposed in [117], and the robustness of this algorithm against Doppler was studied. In [119], channel prediction is employed to mitigate the impact of outdated CSI for the constant bit rate case. A statistical adaptive modulation scheme based on the long-term channel statistics (partial CSI) was proposed in [123]. In [124], optimal power loading algorithms based on average and outage capacity criteria were pursued when partial CSI was available at the transmitter.

The resource allocation is generally performed on the transmitting side. According to the channel responses on different subcarriers, bits and powers are allocated, such as various constellations of QAM are used to assign different numbers of bits per subcarrier. In this chapter, we consider the bit rate maximization problem for multicarrier systems, taking into account the imperfect CSI. The bit loading algorithms which are proposed consider the estimation noise before allocating bits and powers to different subcarriers. These algorithms underload the system for higher values of mean square error (MSE) of the estimator, in order to sustain an affordable value of the mean BER. On the contrary an algorithm, which does not take into account the estimation errors, can overload the system and subsequently increases the mean BER of the system. In order to incorporate the effects of imperfect CSI in the resource allocation process, one needs to find the modified error rate expressions that are changed due to noisy channel estimations. We consider the RM problem with imperfect CSI consideration using two different approaches. The considered approaches use the statistical information about the estimation errors to maintain the mean BER level and in result slightly reduce the spectral efficiency of the system. In the first approach,

we find the generalized error rate expression for all considered modulation orders. It means that we have just one modified error rate expression for all constellation sizes that take into account the effects of imperfect CSI. In another approach, individual error rate expressions are devised for each QAM modulation order with the aim of countering the effects of erroneous estimations.

Bit loading algorithms are proposed, based on two considered approaches, for OFDM and LP-OFDM systems that provide better mean BER performance in comparison of existing solutions that do not take into account the noisy estimations. Firstly, we will consider the impacts of imperfect CSI on resource allocation in general. The considered error model is then discussed. Subsequently, the analytical study of the resource allocation problem is considered taking into account the effects of imperfect CSI using the first approach, as discussed earlier. Discrete bit and power loading algorithms are also proposed for practical systems. Moreover, the analytical study for resource allocation is also performed for the RM problem under imperfect CSI assumption using the second approach of individual error rate expression for each QAM modulation order. Analytical formulae are derived for all QAM modulation orders with the aim of countering the adverse effects of noisy estimations. Discrete bit and power loading algorithms are also proposed for practical systems using this approach. Simulation results are presented for both approaches to evaluate the performance of proposed algorithms in comparison with conventional systems. Finally, we conclude this chapter.

5.2 Considered error model

The classical allocations do not change the number of bits on a given subcarrier in case of noisy estimations. In the proposed algorithm, we underload the system, which means that less numbers of bits are allocated to various subcarriers in order to maintain the mean BER of the system. It is supposed that the estimation noise is included at the receiver and no noise is added when this information is sent back to the transmitter through a feedback channel. Therefore we have the same estimated channel at both sides of the communication system. The well known power line channel is used for simulations and because of its quasi static nature, delays in the CSI are neglected. In this section, we describe the considered error model in order to properly understand adverse effects of noisy estimations. We use the error model described in [118] and a modified version of this model is shown in Fig. 5.1 with additional resource allocation component.

Here X_i is the modulated symbol at subcarrier i , X_i' is the modulated symbol after interacting with the channel gain H_i , N_0 is the additive white Gaussian noise, Y_i is the noisy modulated symbol, and Y_i' is the received symbol after being equalized by the estimated channel gain \hat{H}_i . We suppose that no error occurs when the estimated channel is fed back to the transmitter, therefore we have the same estimated channel at the transmitter and the receiver. This estimated channel can be different from the actual channel in case of noisy estimations.

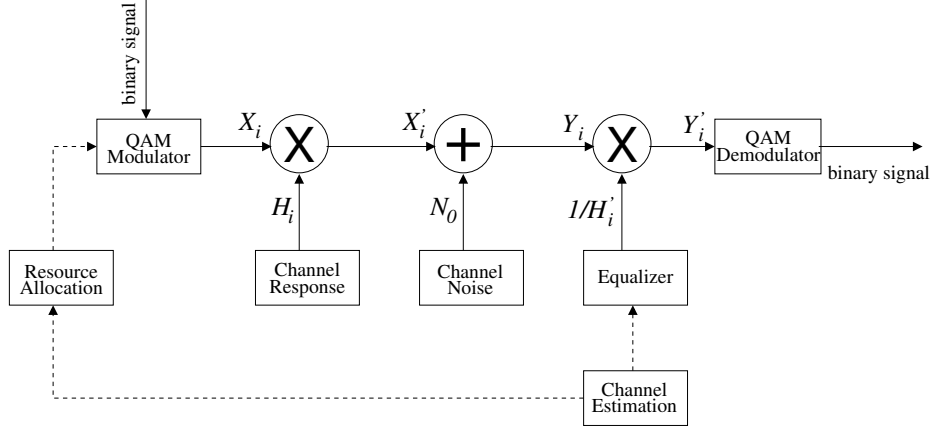


Figure 5.1: MCM subcarrier estimation error model.

The estimation noise can be classically characterized as additive Gaussian noise [122]. The estimated channel gain is $\hat{H}_i = H_i + e_i$, where estimation noise is a complex Gaussian random variable with zero mean and a variance, σ_e^2 , equal to the MSE of the channel estimator. It is also considered that \hat{H}_i is the only known information about the current CSI of the i^{th} subcarrier. The considered approaches use the statistical information about the estimation errors to maintain the mean BER level and in result slightly reduce the spectral efficiency of the system.

5.3 Impacts on allocations

Conventionally, imperfect CSI is not taken into account and therefore the mean BER performance of the multicarrier system may be severely affected for the higher values of the estimation noise variance. In this section, we discuss the effects of noisy estimations on multicarrier systems. Here, we would like to reiterate the expression for the number of bits supported for a given value of SNR from Section 2.3.2. For a known channel response, the number of bits b_i supported by subcarrier i can be given as [89]

$$b_i = \log_2 \left(1 + \frac{E_i}{N_0} \frac{|H_i|^2}{\Gamma} \right), \quad (5.1)$$

where $\frac{E_i}{N_0}$ is the SNR. The SNR gap, Γ , for any uncoded QAM with a target SER P , and for a null system margin, is given as [89]

$$\Gamma \approx \frac{1}{3} \left[Q^{-1} \left(\frac{P}{4} \right) \right]^2. \quad (5.2)$$

It can be seen in (5.2) that Γ depends upon the error rate of the system, and it has approximately the same value for different modulation orders of QAM for a given

error rate. In an allocation where the effects of imperfect CSI are not considered, the bits are allocated to different subcarriers in an iterative fashion by using (5.1), as Γ is known in advance. But in practice, where perfect CSI is rarely achieved, the value of Γ which was calculated in advance remains no more valid. Therefore, the bits may be wrongly allocated to subcarriers, which results in the increase of BER at the receiver. This anomaly in the mean BER performance of the system may only be dealt if expressions of error rates (subsequently expressions of the SNR gap) are modified in such a way that they compensate the effects of imperfect CSI. This is exactly what we do in this chapter. We consider two different approaches, which take into account noisy estimations in resource allocation process. In the following, we describe these approaches one by one.

5.4 Allocation based on generalized error rate expressions

In the first approach, hereafter known as generalized error rate expression approach (GERE), we find the generalized error rate expression for all modulation orders of QAM that take into account the imperfect CSI. This approach is based on the work carried out by Ye et al [122]. In their paper, the effects of the imperfect CSI were considered for the conventional OFDM system.

We extend this study for LP-OFDM systems and we propose simple bit and power loading algorithms for both OFDM and LP-OFDM systems. Firstly, we consider the case of the conventional OFDM system. Theoretical expressions are described for the conventional OFDM system followed by the description of the proposed bit and power loading algorithm for the conventional OFDM under PLC context, where the bit rate of the system is maximized for a given PSD mask and a target error rate taking into account the effects of imperfect CSI. This study is then extended to LP-OFDM systems in order to exploit the system resources more efficiently. Discrete bit and power loading algorithms are proposed for practical LP-OFDM systems that maximize the bit rate of LP-OFDM systems for a given PSD mask and a target error rate taking into account the effects of noisy estimations. Finally, the mean BER performance of proposed systems is compared with classical systems that do not take into account the effects of imperfect CSI.

5.4.1 OFDM allocations

Practically speaking, it is impossible to obtain the perfect CSI. The classical allocations do not change the number of bits on a given subcarrier in case of noisy estimations. In the proposed algorithm, we underload the system, which means that less numbers of bits are allocated to various subcarriers in order to sustain the mean BER of the system. We propose an allocation, where without significantly compromising on the spectral efficiency, the robustness of the system is increased against the estimation noise.

The expression of bit error rate \dot{P} , taking into account the imperfect channel estimation, can be given as [122]

$$\dot{P} = c_1 \frac{2^b - 1}{x + (2^b - 1)} \exp \left\{ -\frac{y}{x + (2^b - 1)} \right\}, \quad (5.3)$$

where

$$x = c_2 \frac{\sigma_e^2}{1 + \sigma_e^2} \frac{E_s}{N_0}, \quad y = c_2 |s|^2 \frac{E_s}{N_0}, \quad (5.4)$$

and

$$s = \frac{1}{1 + \sigma_e^2} \dot{H}, c_1 = 0.2, c_2 = 1.6, \quad (5.5)$$

where σ_e is the estimation noise variance and c_1 and c_2 are empirical values defined in [122]. We consider an OFDM system with N subcarriers and the highest modulation order is limited to $2^{b_{\max}}$. The target bit error rate per subcarrier is expected to be 10^{-3} . The proposed algorithm for OFDM systems can be described as follows:

RM FOR OFDM WITH IMPERFECT CSI CONSIDERATION USING GERE()

```

1  for  $i = 1 : N$ 
2      do
3          Initiate  $b_i = b_{\max}$ 
4          Calculate  $\dot{P}$  from (5.3)
5          while  $\dot{P} > 10^{-3}$ 
6              do
7                   $b_i = b_i - 1$ 
8                  Calculate  $\dot{P}$  from (5.3)
9              end while
10 end for
```

In this way, a resource allocation is obtained that underloads the system for high values of MSE in order to sustain the mean BER performance of the multicarrier system. Contrary to the conventional OFDM allocations, this loading algorithm takes into account the effects of imperfect CSI. In the following, we consider the resource allocation problem for LP-OFDM systems taking into account the noisy estimations.

5.4.2 LP-OFDM allocations

The rate maximization problem for LP-OFDM systems has been discussed previously but without taking into account the effects of imperfect CSI. Here, we propose a bit and power allocation algorithm for LP-OFDM systems that maximizes the bit rate of the system for a given error rate and a defined PSD limit but also takes into account the noisy channel estimations using GERE approach. We consider an LP-OFDM

system with N subcarriers, precoding factor L and number of blocks K . The highest modulation order is limited to $2^{b_{\max}}$ and the target bit error rate per block is expected to be 10^{-3} . The expression of BER \dot{P}_c^k for a precoding sequence c in a given block k of length L , taking into account the imperfect channel estimation, can be given as

$$\dot{P}_c^k = c_1 \frac{2^{\frac{R_k}{L}} - 1}{x + \left(2^{\frac{R_k}{L}} - 1\right)} \exp \left\{ -\frac{y}{x + \left(2^{\frac{R_k}{L}} - 1\right)} \right\}, \quad (5.6)$$

where

$$x = c_2 \frac{\sigma_e^2}{1 + \sigma_e^2} \frac{E_k}{LN_0}, \quad y = c_2 \frac{E_k}{N_0} \sum_{i \in S_k} \frac{1}{|s_i|^2}, \quad (5.7)$$

and

$$s = \frac{1}{1 + \sigma_e^2} \dot{H}, c_1 = 0.2, c_2 = 1.6, \quad (5.8)$$

where R_k and E_k are the total number of bits and the total transmit power available to block k , respectively. Here, we use the optimal allocation obtained in Section 3.2.1 for infinite granularity of modulation. Thus, $b_c^k = \frac{R_k}{L}$ and $E_c^k = \frac{E_k}{L}$, where b_c^k and E_c^k are the number of bits and transmit power allocated to precoding sequence c , respectively. We propose a bit and power loading algorithm for practical systems (i.e. finite granularity of modulation). In this approach, firstly numbers of bits per block are found in an iterative fashion and then these bits are distributed, among different precoding sequences of a given block, in the following manner:

$$b_c^k = \begin{cases} \lfloor R_k/L \rfloor + 1 & (1 \leq i \leq n_c^k) \\ \lfloor R_k/L \rfloor & (n_c^k < i \leq L) \end{cases} \quad (5.9)$$

where

$$n_c^k = \lfloor L(2^{R_k/L - \lfloor R_k/L \rfloor} - 1) \rfloor. \quad (5.10)$$

After deciding the suitable number of bits for all precoding sequences, the transmit power is divided among different precoding sequences in the following manner

$$E_c^k = \frac{(2^{b_c^k} - 1)}{\sum_{c=1}^L (2^{b_c^k} - 1)} E^k. \quad (5.11)$$

The proposed algorithm for LP-OFDM systems can be described as follows:

RM FOR LP-OFDM WITH IMPERFECT CSI CONSIDERATION USING GERE()

```

1  for  $i = 1 : K$ 
2      do
```



```

3      Initiate  $R_k = Lb_{\max}$ 
4      Calculate  $\dot{P}_c^k$  from (5.6)
5      while  $\dot{P}_c^k > 10^{-3}$ 
6          do
7               $R_k = R_k - 1$ 
8              Calculate  $\dot{P}_c^k$  from (5.6)
9          end while
10     Calculate  $n_c^k$  from (5.10)
11     Calculate  $b_c^k$  from (5.9)
12     Calculate  $E_c^k$  from (5.11)
13 end for

```

This algorithm allocates bit and power to various precoding sequences of the LP-OFDM system, taking into account the effects of noisy channel estimation. It underloads the system for higher MSEs to sustain a mean BER of the system and fairly increases the system robustness against imperfect CSI without significantly compromising on the system throughput.

5.4.3 Results

In this section, we present the results of simulations carried out for the performance evaluation of proposed algorithms in comparison of the iterative RM allocation that does not take into account the effects of imperfect CSI. A complete communication system chain is developed, based on the error model described in Section 5.2. Fig. 5.2 shows the mean BER performance of all three allocations for different values of MSE. It can be observed that the proposed allocations are robust against the estimation noise and provide sustainable BER performance as compared to iterative OFDM allocation, which does not take into account the effects of imperfect CSI. It may further be seen that the proposed LP-OFDM allocation outperforms both the OFDM allocations and provides reasonable BER performance even at much higher values of MSE. For instance, iterative OFDM allocation without imperfect CSI consideration, for MSEs higher than 8×10^{-6} results in mean BERs higher than 10^{-3} , while for an MSE = 4×10^{-5} the mean BER is around 10^{-1} . The proposed LP-OFDM allocation provides a mean BER of 10^{-2} even at an MSE of 1×10^{-4} .

Fig. 5.3 compares the throughput performance of all three allocations for different values of MSE. The proposed allocations perform better than the conventional iterative OFDM allocation for lower MSEs but underloads the system for higher values of estimation noise variance, as expected. The classical iterative OFDM is achieving higher bit rate for an MSE greater than 8×10^{-6} , but as discussed earlier the mean BER performance of this allocation is collapsing for these MSEs. Thus these higher throughputs are of no use. Instead it is more useful to underload the system at this stage to maintain the mean BER performance and it is exactly what our proposed allocations are doing. In order to clearly demonstrate the better performance of pro-

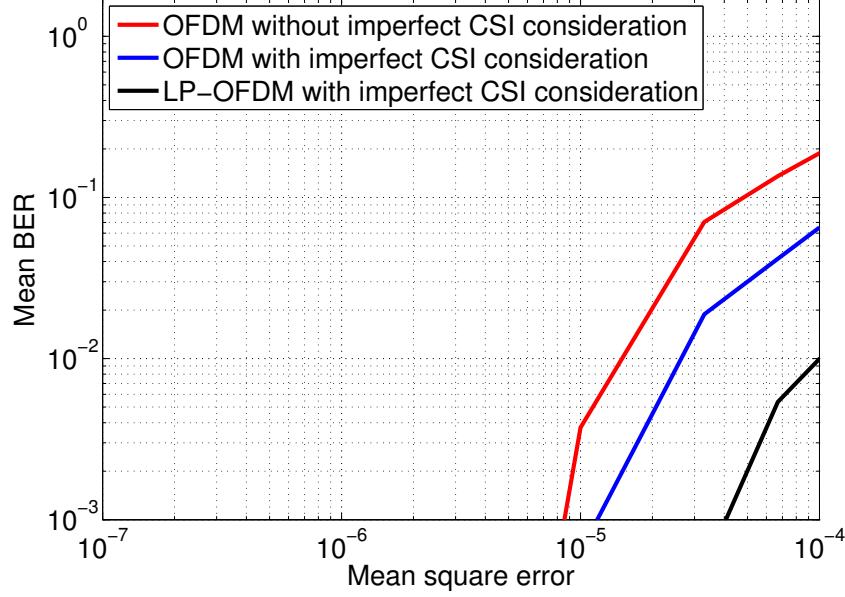


Figure 5.2: Mean BER comparison for different values of mean square error.

posed algorithms, we introduce a new parameter that is known as goodput r of the system in the following and is given as

$$r = \begin{cases} (10^{-3} - \bar{P}) \times R & \text{if } \bar{P} \leq 10^{-3} \\ 0 & \text{if } \bar{P} > 10^{-3} \end{cases}, \quad (5.12)$$

where \bar{P} is the mean BER of the system shown in Fig. 5.2 and R is the achieved system bit rate per OFDM/LP-OFDM symbol shown in Fig. 5.3.

Fig. 5.4 compares the goodput performance of all three allocations for different values of MSE. Proposed allocations outperform the conventional OFDM allocation that does not take into account the effects of imperfect CSI. The proposed LP-OFDM allocation performs significantly better than other two allocations in terms of the goodput. It delivers better goodput of the system even for high values of estimation noise. Although, proposed allocations underload the system for high values of MSE but their mean BER performance is better than that of the conventional OFDM system. It is due to this better mean BER performance that proposed systems outperform the conventional OFDM system in terms of the system goodput. At lower MSEs, the proposed LP-OFDM allocation provides much higher bit rate than OFDM allocations as it accumulates energies of multiple subcarriers by grouping them together. Therefore, the proposed LP-OFDM allocation utilizes the available power more efficiently than OFDM allocations. Even under high values of MSE, it provides significantly sustainable BER performance with fairly reasonable bit rate. The reason for this better performance can be easily understood from power distribution diagram.

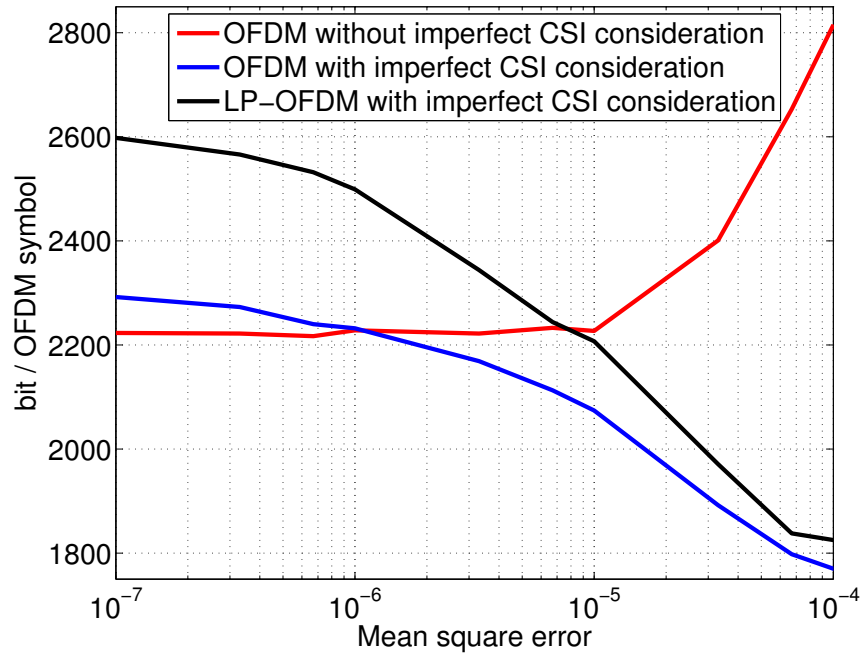


Figure 5.3: Bit rate comparison for different values of mean square error.

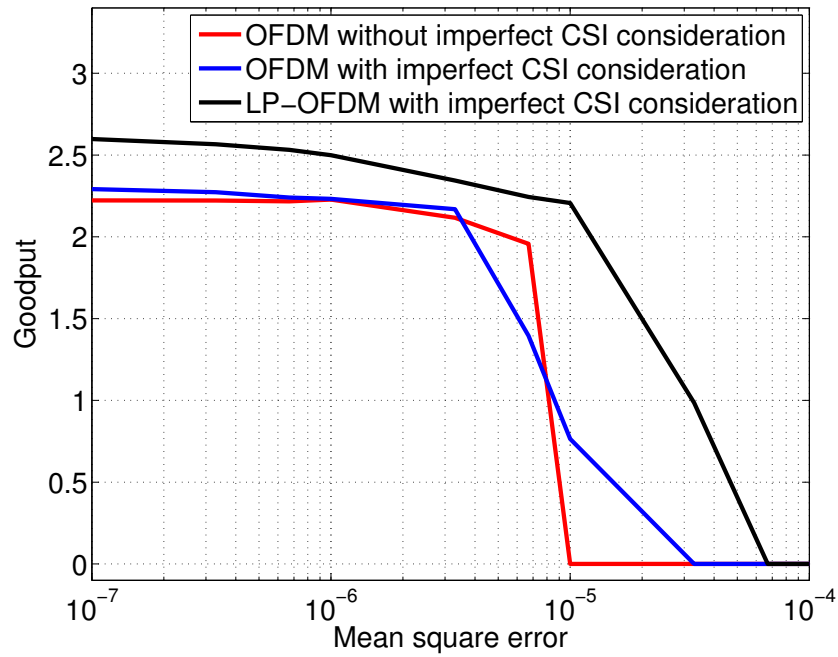


Figure 5.4: Goodput comparison for different values of mean square error.

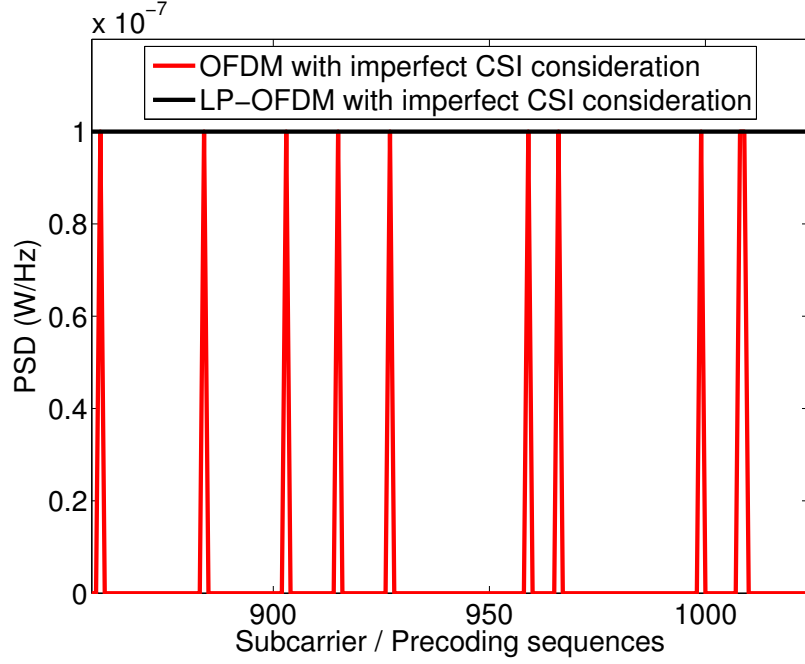


Figure 5.5: Power distribution comparison.

Fig. 5.5 compares the power distribution of OFDM and LP-OFDM allocations for higher frequency range. The spike-shaped curve of the OFDM allocation shows the transitions of the modulation orders when no more power is available to sustain the target BER. Under PSD constraint, the major task is to efficiently utilize the available power, since the transmit power that is not used by a subcarrier (or a group of subcarriers) is lost and cannot be used by other subcarriers (or groups of subcarriers). The LP-OFDM allocation accumulates the energies of all subcarriers of the group to utilize it more efficiently, which can be seen in the greater area under the curve. It can be observed that it uses more power than OFDM, almost all available power for the system has been utilized. It accumulates the energies of different subcarriers to transmit more bits. Thus higher bit rates are obtained.

In the next section, we discuss another approach for taking care of noisy estimations in resource allocation and optimization of multicarrier systems. Contrary to GERE approach, in the next section, we obtain individual error rate expressions for each QAM modulation order to get even better mean BER performance at high values of MSE.

5.5 Allocations based on individual error rate expressions

In this second approach, hereafter known as individual error rate expression approach (IERE), we obtain individual SER expressions for each QAM modulation order that take into account the effects of noisy estimations. This approach is based on the work carried out by Leke and Cioffi [118]. In their paper, the effects of the imperfect CSI were considered for the conventional OFDM system and only even QAM constellations were considered. We extended this study for LP-OFDM systems and considered both even and odd QAM constellations. The modified SER expressions are devised for different QAM modulation orders. These expressions are used in the proposed resource allocation algorithm to underload the system at higher MSEs for the sake of better mean BER performance. An algorithm which does not take into account the estimation errors, can overload the system, which subsequently degrades the mean BER performance.

5.5.1 Modified SER expressions

As discussed earlier, the perfect channel estimation is not possible. Here, we devise the new SER expressions taking into account the imperfect CSI⁽¹⁾. We use the same error model described in Section 5.2. X_i is the modulated symbol at subcarrier i , X_i' is the modulated symbol after interacting with the channel gain H_i , Y_i is the noisy received modulated symbol, and Y_i' is the symbol obtained after the equalization by the estimated channel gain \hat{H}_i . The decoding error can be avoided if the following inequality is satisfied (in the absence of noise)

$$\max \left| \frac{H_i - \hat{H}_i}{\hat{H}_i} \right| \cdot |X_i| < \frac{d}{2}, \quad (5.13)$$

where d is the minimum distance between constellation points. The maximum value of this expression occurs at $X_{i,\max}$. For odd QAM constellations

$$X_{i,\max} = \left[\left(\sqrt{\frac{9M}{8}} - 1 \right) \cdot \frac{d}{2}, \left(\sqrt{\frac{M}{2}} - 1 \right) \cdot \frac{d}{2} \right], \quad (5.14)$$

where M is the modulation order. For even QAM constellations [118]

$$X_{i,\max} = \left[\left(\sqrt{M} - 1 \right) \cdot \frac{d}{2}, \left(\sqrt{M} - 1 \right) \cdot \frac{d}{2} \right]. \quad (5.15)$$

In [118] only even QAM constellations were treated. Here, we consider all possible QAM constellations (including the particular case of 8-QAM). The probability of

⁽¹⁾The detailed analysis for modified error rate expressions is given in Appendix A

error, P^m , for each constellation point with an odd QAM constellation, in presence of channel noise, can be given as

$$P^m = N^m Q \left[\sqrt{\frac{3\text{SNR}}{M-1}} \left(1 - \frac{4\sqrt{2}\alpha |X_i|}{d\sqrt{13M-20\sqrt{2M}+16}} \right) \right], \quad (5.16)$$

and for an even QAM constellation, P^m can be given as

$$P^m = N^m Q \left[\sqrt{\frac{3\text{SNR}}{M-1}} \left(1 - \frac{\sqrt{2}\alpha |X_i|}{d(\sqrt{M}-1)} \right) \right], \quad (5.17)$$

where N^m is the number of nearest neighbours to the constellation point $X_{i,m}$ on i^{th} subcarrier and α is a measure of the accuracy in channel identification. For an odd QAM constellation, α can be given as

$$\alpha = \sqrt{\frac{\text{MSE} \left(13M - 20\sqrt{2M} + 16 \right)}{8}}, \quad (5.18)$$

and for an even QAM constellation, α can be given as

$$\alpha = \sqrt{2\text{MSE}} (\sqrt{M} - 1). \quad (5.19)$$

The overall probability of error on a subcarrier can be given as

$$P = \sum_m \text{Prob}(X_i = X_{i,m}) \cdot P^m. \quad (5.20)$$

The modified SER, P , expressions obtained from this analysis are given below. For $M = 4$

$$P = 2Q \left[(1 - \alpha) \cdot \sqrt{\text{SNR}} \right]. \quad (5.21)$$

For $M = 8$ with $\beta = \sqrt{\frac{3\text{SNR}}{7}}$

$$P = Q \left[(1 - \alpha) \cdot \beta \right] + \frac{3}{2} Q \left[\left(1 - \frac{\alpha}{\sqrt{5}} \right) \cdot \beta \right]. \quad (5.22)$$

For $M = 16$ with $\beta = \sqrt{\frac{\text{SNR}}{5}}$

$$P = Q \left[(1 - \alpha) \beta \right] + \frac{3}{2} Q \left[\left(1 - \frac{\sqrt{5}\alpha}{3} \right) \beta \right] + Q \left[\left(1 - \frac{\alpha}{3} \right) \beta \right]. \quad (5.23)$$

For $M = 32$ with $\beta = \sqrt{\frac{3\text{SNR}}{31}}$

$$P = \frac{1}{2}Q[(1-\alpha)\beta] + Q\left[\left(1 - \frac{\sqrt{5}\alpha}{\sqrt{17}}\right)\beta\right] + \frac{1}{2}Q\left[\left(1 - \frac{\alpha}{\sqrt{17}}\right)\beta\right] \\ + \frac{3}{4}Q\left[\left(1 - \frac{\sqrt{13}\alpha}{\sqrt{17}}\right)\beta\right] + \frac{1}{4}Q\left[\left(1 - \frac{3\alpha}{\sqrt{17}}\right)\beta\right]. \quad (5.24)$$

For $M = 64$ with $\beta = \sqrt{\frac{\text{SNR}}{21}}$

$$P = \frac{1}{32}Q[(1-\alpha)\beta] + \frac{1}{4}Q\left[\left(1 - \frac{\alpha}{7}\right)\beta\right] + \frac{1}{4}Q\left[\left(1 - \frac{3\alpha}{7}\right)\beta\right] + \frac{1}{2}Q\left[\left(1 - \frac{\sqrt{5}\alpha}{7}\right)\beta\right] \\ + \frac{1}{2}Q\left[\left(1 - \frac{\sqrt{13}\alpha}{7}\right)\beta\right] + \frac{1}{2}Q\left[\left(1 - \frac{\sqrt{17}\alpha}{7}\right)\beta\right] + \frac{5}{8}Q\left[\left(1 - \frac{5\alpha}{7}\right)\beta\right] \\ + \frac{3}{8}Q\left[\left(1 - \frac{\sqrt{29}\alpha}{7}\right)\beta\right] + \frac{3}{8}Q\left[\left(1 - \frac{\sqrt{37}\alpha}{7}\right)\beta\right]. \quad (5.25)$$

For $M = 128$ with $\beta = \sqrt{\frac{3\text{SNR}}{127}}$

$$P = \frac{1}{16}Q[(1-\alpha)\beta] + \frac{1}{4}Q\left[\left(1 - \frac{\alpha}{\sqrt{17}}\right)\beta\right] + \frac{1}{4}Q\left[\left(1 - \frac{\alpha}{\sqrt{5}}\right)\beta\right] \\ + \frac{1}{8}Q\left[\left(1 - \frac{\alpha}{\sqrt{85}}\right)\beta\right] + \frac{1}{8}Q\left[\left(1 - \frac{3\alpha}{\sqrt{85}}\right)\beta\right] + \frac{1}{4}Q\left[\left(1 - \frac{\sqrt{13}\alpha}{\sqrt{85}}\right)\beta\right] \\ + \frac{3}{8}Q\left[\left(1 - \frac{\sqrt{5}\alpha}{\sqrt{17}}\right)\beta\right] + \frac{1}{4}Q\left[\left(1 - \frac{\sqrt{29}\alpha}{\sqrt{85}}\right)\beta\right] + \frac{1}{4}Q\left[\left(1 - \frac{\sqrt{37}\alpha}{\sqrt{85}}\right)\beta\right] \\ + \frac{1}{8}Q\left[\left(1 - \frac{7\alpha}{\sqrt{85}}\right)\beta\right] + \frac{1}{4}Q\left[\left(1 - \frac{\sqrt{41}\alpha}{\sqrt{85}}\right)\beta\right] + \frac{1}{4}Q\left[\left(1 - \frac{3\alpha}{\sqrt{17}}\right)\beta\right] \\ + \frac{1}{4}Q\left[\left(1 - \frac{\sqrt{53}\alpha}{\sqrt{85}}\right)\beta\right] + \frac{9}{32}Q\left[\left(1 - \frac{\sqrt{13}\alpha}{\sqrt{17}}\right)\beta\right] + \frac{3}{16}Q\left[\left(1 - \frac{\sqrt{61}\alpha}{\sqrt{85}}\right)\beta\right] \\ + \frac{3}{16}Q\left[\left(1 - \frac{\sqrt{73}\alpha}{\sqrt{85}}\right)\beta\right]. \quad (5.26)$$

The SER expressions for higher modulation orders can also be derived using this analysis. It can be observed from (5.18) and (5.19) that α is directly proportional to MSE. Therefore, as expected, in devised SER expressions for higher MSE, higher values of SNR are required to attain the same target error rate. For an allocation which does not take into account the imperfect CSI, the SNR required to attain a given error rate does not change and therefore the mean BER performance degrades for higher MSEs. These modified SER expressions are used in the proposed loading algorithm, which takes into account the imperfect channel estimation.

5.6 Proposed LP-OFDM allocation

The classical allocations do not consider the noisy estimation to change the allowed number of bits on a given subcarrier. In the proposed allocation the system is under-loaded (less numbers of bits are allocated to subcarriers) in order to maintain the mean BER of the system. A bit and power loading algorithm is proposed that increases the system robustness against noisy estimations without significantly compromising on the system throughput. It is supposed that the estimation noise is included at the receiver and no noise is added when this information is sent back to the transmitter through a feedback channel. Therefore we have the same estimated channel at both sides of the communication system. The well known power line channel is used for simulations and the feedback delay of the CSI is neglected because of the quasi static nature of the power line channel.

Here, we propose a bit and power allocation algorithm for an LP-OFDM system that maximizes the bit rate of the system for a given error rate and a defined PSD limit but also takes into account the noisy channel estimation. We consider an LP-OFDM system with N subcarriers, precoding factor L and number of blocks K . The highest modulation order is limited to 2^7 and the minimum number of bits supported is 2. The target bit error rate is expected to be 10^{-3} . Here, we propose a resource allocation algorithm where all precoding sequences in a given block are allocated the same number of bits and therefore are assigned equal transmit power, thus $b_c^k = R_k/L$ and $E_c^k = E_k/L$ where b_c^k is the number of bits supported by precoding sequence c^k of block k , R_k is the number of bits in block k , E_c^k is the transmit power allocated to precoding sequence c^k of block k and E_k is the total transmit power available to block k . Here, we reiterate the expression for the signal to noise ratio for a precoding sequence c^k of a block k ,

$$\text{SNR}_c^k = \frac{E_k}{N_0} \frac{L}{\sum_{i \in S_k} \frac{1}{|H_i|^2}} . \quad (5.27)$$

The proposed allocation treats one block at a time and processes all the blocks in a given LP-OFDM system iteratively. In each iteration the algorithm treats only one precoding sequence of the given block since the bits are uniformly distributed in a given block as discussed earlier. Due to this uniform distribution, all the precoding sequences in a block are assigned equal transmit power and therefore experience the same transmission behaviour. At the end of each iteration, the resulted numbers of bits are generalized for each precoding sequence of the given block. The algorithm starts by allocating maximum number of bits (i.e. 7) to the precoding sequence of the given block. The SNR of the precoding sequence is calculated using (5.27) and then the SER is calculated from (5.26). If this value of SER is less than 10^{-3} , all precoding sequences of the given block are allocated 7 bits and the algorithm enters into the next iteration (i.e. the next block). Otherwise the number of bits allocated is reduced by 1 and the corresponding expression is used to calculate the SER. This process continues

until we achieve either an SER of less than 10^{-3} or the number of bits allocated equals to 0. The proposed algorithm for an LP-OFDM system can be summarized as follows:

RM FOR LP-OFDM WITH IMPERFECT CSI CONSIDERATION USING IERE()

```

1  for  $k \leftarrow 1$  to  $K$ 
2      do Calculate SNR form (5.27)
3          Calculate SER from (5.26)
4          while  $SER > 10^{-3}$ 
5              do  $b \leftarrow b - 1$ 
6                  switch  $b$ 
7                      case  $b < 2$  :
8                          break
9                      case  $b = 6$  :
10                         Calculate SER from (5.25)
11                     case  $b = 5$  :
12                         Calculate SER from (5.24)
13                     case  $b = 4$  :
14                         Calculate SER from (5.23)
15                     case  $b = 3$  :
16                         Calculate SER from (5.22)
17                     case  $b = 2$  :
18                         Calculate SER from (5.21)
19                 end switch
20             end while
21             Allocate  $b$  to all the precoding sequences of  $k$ 
22              $E_c^k \leftarrow E_k/L$ 
23 end for
```

This algorithm uses different SER expressions for different constellation sizes and allocates bits and powers to the precoding sequences of an LP-OFDM system while taking into account the effects of noisy channel estimation. It underloads the system for high MSEs to sustain a mean BER of the system and fairly increases the system robustness against imperfect CSI without significantly compromising on the system throughput.

5.6.1 Results

In this section, we present the results of simulations carried out for the performance evaluation of the proposed algorithm, which uses IERE approach, in comparison of the iterative RM allocation that does not take into account the effects of imperfect CSI. A complete communication system chain is developed, based on the error model described in Section 5.2. Fig. 5.6 shows the mean BER performance of both allocations for different values of MSE. It can be observed that the proposed allocation is robust against the estimation noise and provides sustainable BER performance as compared

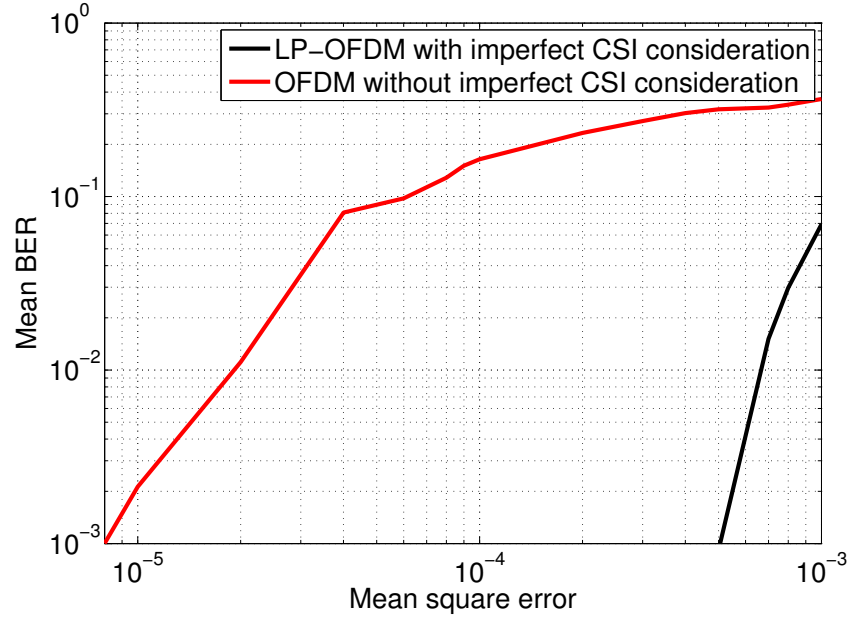


Figure 5.6: Mean BER comparison for different values of mean square error.

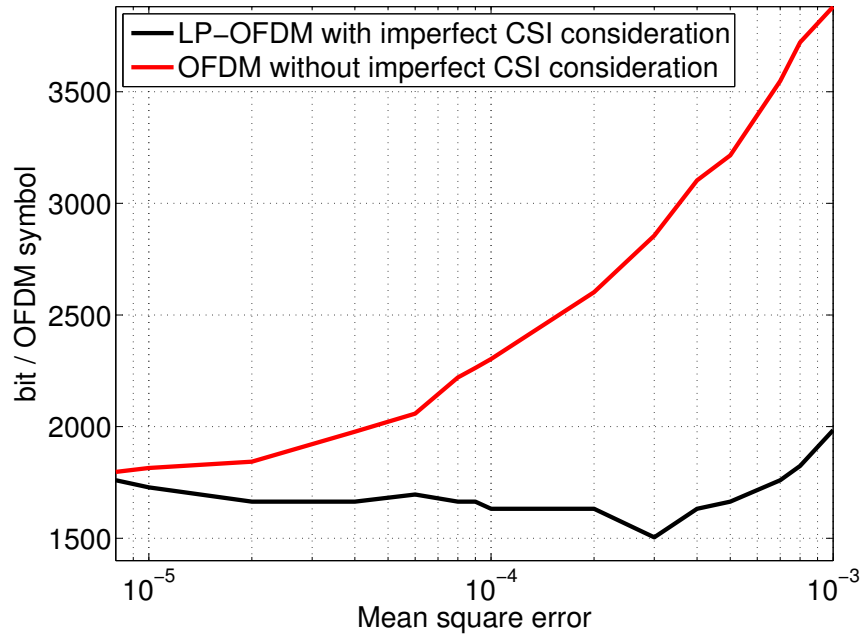


Figure 5.7: Bit rate comparison for different values of mean square error.

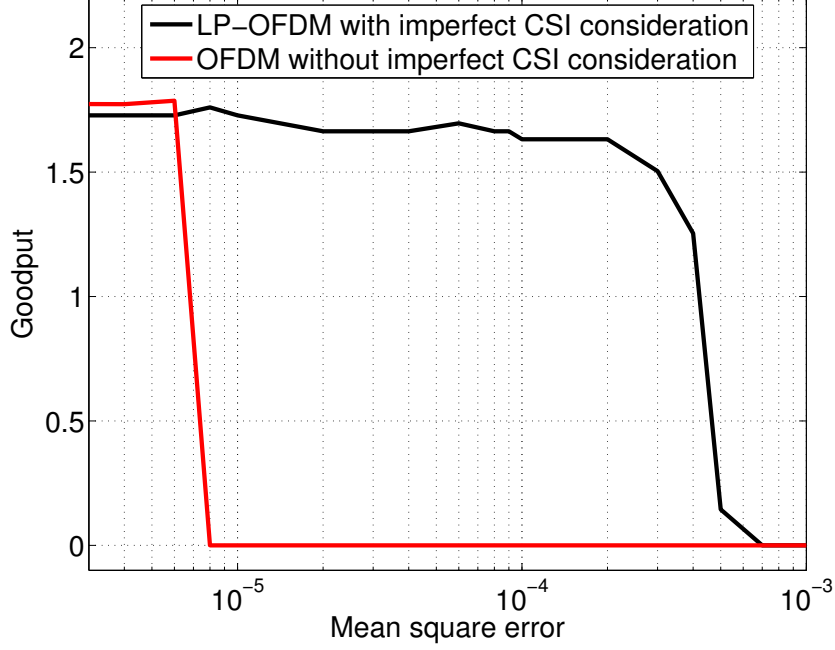


Figure 5.8: Goodput comparison for different values of mean square error.

to iterative OFDM allocation, which does not take into account the effects of imperfect CSI. The proposed allocation is providing better mean BER performance even at much higher values of MSE. For instance, iterative OFDM allocation without imperfect CSI consideration, for MSEs higher than 8×10^{-6} results in mean BERs higher than 10^{-3} , while the proposed allocation gives a mean BER less than 10^{-3} until the MSE reaches at a value of 5×10^{-4} . For an $\text{MSE} = 6 \times 10^{-5}$ the classical OFDM allocation results in a mean BER of 10^{-1} while the proposed LP-OFDM allocation provides a mean BER of 10^{-2} even at an MSE of 6.6×10^{-4} .

Fig. 5.7 compares the throughput performance of both allocations for different values of MSE. The proposed allocation performs almost equal to the classical iterative OFDM allocation for $\text{MSE} = 0$ but underloads the system once the MSE increases, as expected. The classical iterative OFDM is achieving higher bit rate for higher MSEs, but as discussed earlier the mean BER performance of this allocation is collapsing for these MSEs. Thus these higher throughputs are of no use. Instead it is more useful to underload the system at this stage to maintain the mean BER performance and it is exactly what our proposed allocation is doing. For very strong estimation noise (i.e. $\text{MSE} > 3 \cdot 10^{-4}$) the proposed allocation is also increasing the bit rate because at this level the estimation noise is so huge that it is dominating over the channel response. The proposed LP-OFDM allocation that takes into account the estimation noise is still performing better than the iterative OFDM allocation. In

order to clearly demonstrate the better performance of the proposed allocation, we compare the achieved system goodput for both allocations, as defined in (5.12).

Fig. 5.8 compares the goodput performance of both allocations for different values of MSE. It can be observed that the proposed LP-OFDM allocation performs significantly better than the conventional OFDM allocation. The proposed allocation underloads the system for high values of MSE but it maintains the mean BER performance of the system as shown in Fig. 5.6. It is due to this enhanced mean BER performance that the proposed system achieves better system goodput even for high values of MSE. The proposed algorithm is also less complex than the iterative OFDM allocation as the number of iterations has been reduced by grouping together different subcarriers.

5.7 Conclusion

In this chapter, we considered the bit rate maximization strategies under PSD constraint for both OFDM and LP-OFDM systems in PLC context, which take into account the effects of noisy estimations. Most of the existing work in resource allocation and optimization consider perfect CSI at the transmitter. However, a number of papers have discussed the effects of imperfect CSI over system performance [117]-[124]. All these papers, to the best of author's knowledge, consider the effects of imperfect CSI only for conventional OFDM systems. We implemented two different approaches in order to counter the effects of imperfect CSI for both OFDM and LP-OFDM resource allocation. In GERE approach, we found the generalized error rate expression for all considered modulation orders that take into account the effects of imperfect CSI. In IERE approach, individual error rate expressions were devised for each QAM modulation in order to counter the effects of erroneous estimations.

For GERE approach, two loading algorithms were proposed. One for classical OFDM systems and the other for LP-OFDM systems. It was observed that the proposed allocations provide significant robustness against noisy channel estimation. The proposed LP-OFDM system provides even better mean BER performance without significantly compromising on bit rate. It was also shown that LP-OFDM allocation utilizes the available power more efficiently and thus provides much higher bit rates for lower values of MSE. We concluded that the GERE based allocations provide sustainable mean BER performance with reasonable bit rate at higher estimation noise variance and improved bit rate at lower MSEs. This contribution has been published in the proceedings of an international conference [129].

In IERE approach, modified SER expressions were derived for various QAM modulation orders, which incorporate the noisy channel estimation in resource allocation process. A bit and power loading algorithm was proposed to maximize the bit rate of the system taking into account the imperfect CSI. It was observed that the proposed allocation provides significant robustness against noisy channel estimation. The proposed algorithm is also less complex than the classical OFDM allocation, as bits are allocated to groups of subcarriers and to subcarriers. We concluded that the

proposed allocation provides a good trade-off between the maximized bit rate and the mean BER performance of the system and attains sustainable mean BER performance with reasonable bit rate at high estimation noise variance and comparable bit rate at low values of MSE. This work has been published in the proceedings of an international conference [130].

The bit rate performance of GERE approach is better than IERE approach. But in terms of the mean BER, IERE approach outperforms GERE approach since it deals individually with different types of constellation schemes. Furthermore, the complexity of IERE approach is less than the GERE approach in terms of the number of iterations since uniform numbers of bits are allocated to all precoding sequences of a given block. In terms of the memory size, GERE allocations enjoy lesser complexity than IERE allocations because of the generalized error rate expressions for all constellation schemes.

General conclusion and prospects

This thesis primarily investigated various resource allocation and optimization strategies in order to enhance the bit rate and the robustness of multicarrier PLC systems, so that they can be efficiently used in home networking and automation. Theoretical studies were performed to develop a consolidated framework for adaptive bit and power allocation in the context of both conventional OFDM and LP-OFDM systems. Several new ideas were presented such as the integration of channel coding scheme into the resource allocation process, bit rate maximization under mean BER constraint, robustness maximization in terms of mean BER minimization and LP-OFDM resource allocation taking into account the effects of imperfect CSI.

In Chapter 1, we presented a general overview of PLC technology. Because of its already available infrastructure, PLC technology attracts the attention of both business and research communities. We also presented a brief history of the PLC technology in this chapter. Several PLC applications were then presented, with the emphasis on the importance of this wonderful technology. Recent developments in the PLC technology were also highlighted with a description of various consortiums and associations working for the enhancement and standardization of communications over power lines. Important research projects were also listed including the OMEGA project, to which this thesis also contributes. Future trends in the PLC technology were then taken into consideration. This project examines both challenges and advantages offered by the PLC technology.

Chapter 2 was divided into two large parts. The first part discussed OFDM systems in general starting from the principle of MCM to the more advanced form of multicarrier systems. The strong and weak points of the OFDM technique were also elaborated. The discussion of OFDM was followed by an overview of spread spectrum. Various multiple access schemes were also explained and different combinations of OFDM and spread spectrum were illustrated. In the end, the selected LP-OFDM scheme was detailed and the prime advantages of this flexible scheme were discussed that primarily include the presence of linear precoding component. This linear precoding component is quite interesting in the resource allocation and optimization process since it provides an additional degree of freedom in the analytical studies of both bit rate and robustness maximization. In the second part of this chapter, we presented a general overview of the resource allocation and optimization for conventional OFDM systems. Due to quasi static nature of the power line channel, the resource allocation can be efficiently performed for the PLC systems without significantly compromising

on the system complexity since the channel can be known at the transmitter through a simple feedback from the channel estimator. Detailed analyses of RM and RoM problems were performed for both finite and infinite granularity of modulation under PSD constraint. Simulation results were also presented for considered bit and power allocation algorithms.

Chapter 3 primarily focused on the bit rate maximization problem. This chapter was also divided into two large parts. The first part considered the RM problem for LP-OFDM systems under peak BER constraint. In this part, a new resource allocation strategy was devised where the channel coding gains are incorporated in bit and power loading algorithms. An adequate channel coding scheme was selected consisting of an inner Wei's 4D 16-states trellis code and an outer RS code. To the best of our knowledge, the idea of integrating channel coding schemes into the resource allocation process for bit rate maximization has never been used before. The only algorithm that integrates channel coding into power minimization was proposed in [97] only for conventional OFDM systems. The proposed bit and power loading algorithm can handle variable values of the SNR gap Γ for different modulation orders. Although, an efficient channel coding scheme was selected for presenting the performance of the proposed system, the devised bit and power loading algorithm can be used in combination of any channel coding scheme provided, the value of the SNR gap is known for the target error rate. The performance of the proposed system was compared with the existing systems while using the same channel coding scheme for all considered systems. A complete communication system chain was also developed in order to compare the performance of these systems and it was shown that the proposed system outperformed the existing ones especially for lower channel gains. Therefore, the proposed system is quite useful in increasing the range of modern PLC systems. We raised a number of questions in the introduction of this thesis. This part of Chapter 3 particularly answered questions **I** and **II** of the listed questions.

Furthermore, in the second part of Chapter 3, the bit rate maximization problem was considered under mean BER constraint. Instead of fixing the same error rate on all subcarriers/precoding sequences, we allowed different subcarriers/precoding sequences to be affected by different error rate values and we imposed the error rate constraint on an entire OFDM/LP-OFDM symbol. In this way, the same BER performance was achieved (as it is achieved in the case of peak BER constraint) but it resulted in an improved bit rate performance. The transmitted power on each subcarrier must be less than the imposed limit, under PSD constraint. In practical systems, where discrete modulation orders are used, different constellation sizes require different levels of transmitted power in order to respect a given error rate. That is why, we observe a significant difference between bit rates obtained for infinite granularity of modulation and those obtained for finite granularity of modulation. This problem may be solved, to some extent, by using different BER values on each subcarrier/precoding sequence and by imposing a mean BER constraint on an entire OFDM/LP-OFDM symbol. In this way, we get an additional degree of freedom for resource allocation strategies. Discrete bit and power loading algorithms were proposed for OFDM and LP-OFDM

systems in the context of multicarrier PLC communication. These resource allocation algorithms maximize the total bit rate of the system while respecting an imposed PSD constraint and a given mean BER. Performances of these allocations were compared with those of Wyglinski [99] and peak BER constraint allocations. It was shown that proposed algorithms not only perform better than existing allocations but they also have lower computational complexity in comparison with existing ones. It was also shown that proposed algorithms use the available power more efficiently and it resulted in better throughput performance. In this part of Chapter 3, we replied to question **III** of the raised questions in the introduction of the thesis.

Chapter 4 introduced an entirely new way for robustness maximization, where mean BER of the system is minimized to enhance the system robustness against various noise sources. The mean BER approach has been considered only for algorithmic treatment of bit rate maximization in [99, 109], we introduced a theoretical analysis for resource allocation and optimization based on this approach. Furthermore, mean BER approach has never been used for robustness maximization, to the best of author's knowledge. This chapter was divided in three parts. In the first part, analytical study for MBM was performed for conventional OFDM systems where the mean BER of the OFDM system was minimized for a target bit rate and an imposed PSD constraint. The additional degree of freedom, provided by the mean BER approach, was judiciously exploited to attain robust multicarrier PLC systems for modern applications. On the contrary, in conventional MM allocations, all subcarriers have to respect the same error rate constraint and this peak error rate constraint has cumulative adverse effects on the performance of the system in presence of the PSD constraint. Discrete bit loading algorithm was also proposed for practical systems having lower computational complexity because it uses the theoretical analysis to rapidly reach the optimal solution.

The second part of Chapter 4 extended the MBM study to LP-OFDM systems. A theoretical study was performed for LP-OFDM systems to optimize the bit and power distribution among various precoding sequences. Furthermore, the analytical study was extended in order to optimize the number of useful precoding sequences in a given block of LP-OFDM systems for a target bit rate and under PSD constraint. Integer valued bit and power loading algorithms were also proposed for real-life systems. Complete communication chains were developed, with integrated bit and power loading algorithms, to compare the performance of proposed algorithms with existing systems. It was shown that proposed algorithms perform better than existing systems especially for low SNR values. Through all this effort, we answered question **IV** of the listed questions in the introduction of the thesis. Furthermore, an initial study was performed to integrate the effects of channel coding in the resource allocation process of MBM using graphical optimization techniques. Starting from a textbook case, this study was extended to mono block LP-OFDM systems. Bit and power loading algorithms were also discussed in combination of simple convolutional codes and simulation results were presented. This part discussed the issue raised in question **V** of the listed questions in the start of the thesis.

In Chapter 5, we extended the study of resource allocation and optimization for OFDM and LP-OFDM systems to imperfect CSI consideration. Here, for the first time, we introduced RM LP-OFDM allocations taking into account the effects of imperfect CSI. All existing papers, to the best of author's knowledge, considered these effects only for conventional OFDM. Two different approaches were considered to counter adverse effects of noisy estimations in bit and power loading. These allocations underload the system in the presences of high MSEs. The first approach, GERE, consists of generalized error rate expressions for all considered modulation orders. Two bit and power loading algorithms were proposed, one for conventional OFDM and the other for LP-OFDM systems in the context of PLC communications. It was shown that proposed allocations provide significant robustness against noisy channel estimations. They give sustainable mean BER performance with reasonable bit rate at high estimation noise and better bit rate performance for low values of MSE. The second approach, IERE, consists of individual error rate expressions for all modulation orders. A bit and power loading algorithm was proposed for LP-OFDM systems based on the theoretical study performed for modified SER expressions. This loading algorithm takes into account the noisy estimations. It was shown that the proposed algorithm attains even better mean BER and goodput performance than GERE approach. The proposed algorithm is also less complex than the classical OFDM allocation, as bits are allocated to groups of subcarriers and not to subcarriers. We also concluded that both proposed allocations (i.e. GERE and IERE) provide a good trade-off between the maximized bit rate and the mean BER performance in order to attain better goodput performance than conventional systems. Chapter 5 mainly answered questions **VI** and **VII** of the highlighted questions in the general introduction of the thesis.

Various contributions of this thesis have been published in the proceedings of one national and six international conferences. One paper is submitted to an international journal. Additionally, the work on the robustness maximization is to be submitted in IEEE Transactions on Communications. During this thesis, we also collaborated very actively with renowned industrial partners. Particularly the thesis contributed to two different projects, an external research project with Orange Labs and the OMEGA project, an integrated project funded by the European commission. A number of communication chains were also developed for industrial partners and therefore this thesis is a unique combination of theoretical studies and practical implementations.

Many prospects can be listed for future works based on this thesis:

- The work carried out in this thesis has demonstrated the efficiency of systems, which take into account the channel coding gains in the resource allocation process. It has been shown that LP-OFDM systems outperform conventional OFDM systems while taking into account the channel coding gains in bit and power loading algorithms. However, this work may be extended to a comparative study of two different strategies for OFDM/LP-OFDM systems taking into account the channel coding schemes inside and outside the resource allocation process, respectively.

- The performance of proposed bit and power loading algorithms, for rate maximization taking into account the channel coding gains, might be evaluated for other channel coding schemes. The same approach may be applied to multicarrier systems using any channel coding schemes, and specifically turbo or LDPC codes, provided the values of the SNR gap are known in advance for all combinations of modulation orders and coding rates.
- The theoretical study carried out for the MBM allocation, taking into account the channel coding gains in the resource allocation process, can be extended for multi block scenarios and other channel coding schemes may be considered. Performance comparison may be done with other robustness maximization schemes that take into account the channel coding in the resource allocation process.
- The MBM allocation schemes may be extended to the case of imperfect CSI consideration.
- In imperfect CSI consideration strategies for the RM problem, other parameters may also be considered such as feedback errors, the use of channel quality indicators and the presence of different estimated channels at transmitter and receiver.

Through various contributions of this thesis, it has been shown that the application of suitable resource allocation and optimization strategies may significantly increase the bit rate or the robustness of multicarrier PLC systems. Furthermore, they may be helpful in bringing PLC capabilities at par with other high bit rate alternatives in the near future.

Appendix

Appendix A

Modified error rate expressions

Here, we present the detailed analysis carried out to calculate modified error rate expressions in the presence of estimation noise. In the absence of noise, the decoding errors occur when

$$\left| \frac{H_i - \hat{H}_i}{\hat{H}_i} \right| \cdot |X_i| > \frac{d}{2}, \quad (\text{A.1})$$

where H_i is the frequency channel response of subcarrier i , \hat{H}_i is the estimated frequency response of subcarrier i , X_i is the transmitted QAM symbol and d is the minimum distance between constellation points. It can be observed that for a known estimation error, larger constellation points are more vulnerable to decoding errors than smaller constellation points. This is shown in Fig. A.1 for the case of a 32-QAM constellation.

In order to avoid decoding errors due to imperfect CSI, we need

$$\max \left| \frac{H_i - \hat{H}_i}{\hat{H}_i} \right| \cdot |X_i| < \frac{d}{2}. \quad (\text{A.2})$$

The maximum value occurs at the largest constellation point $X_{i,max}$. For odd QAM constellation $X_{i,max}$ can be calculated using Fig. A.1 (where points 00, 02, 04, 06, 16, 18, 20 and 22 are the largest constellation points) and can be given as,

$$X_{i,max} = \left[\left(\sqrt{\frac{9M}{8}} - 1 \right) \cdot \frac{d}{2}, \left(\sqrt{\frac{M}{2}} - 1 \right) \cdot \frac{d}{2} \right], \quad (\text{A.3})$$

where $M = 2^{R_i}$ is the constellation size and R_i is the number of bits per QAM symbol. The largest value $|X_{i,max}|$ for odd QAM constellations can be given as

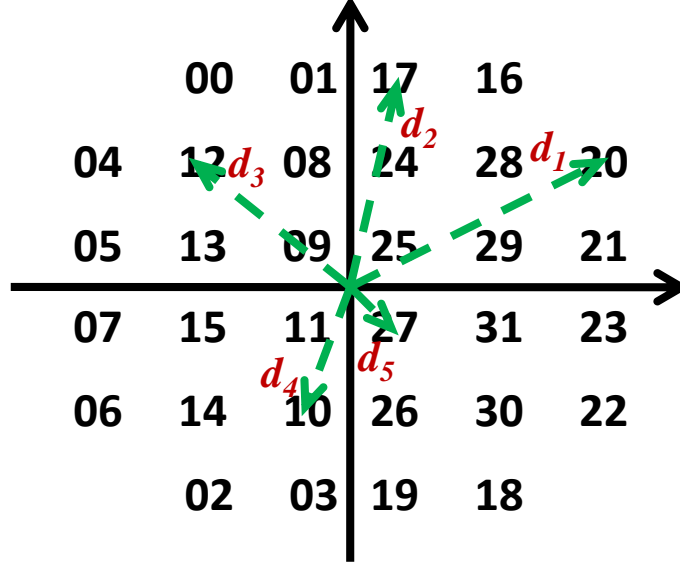


Figure A.1: Effects of imperfect CSI on 32-QAM constellation with Gray coding.

$$|X_{i,\max}| = \frac{d}{2} \sqrt{\frac{13M}{8} - 5\sqrt{\frac{M}{2}}} + 2. \quad (\text{A.4})$$

Thus, there is no decoding error as long as

$$\left| \frac{H_i - \acute{H}_i}{\acute{H}_i} \right| < \frac{d}{2|X_{i,\max}|}, \quad (\text{A.5})$$

and using the value of $|X_{i,\max}|$ defined in (A.4), we obtain

$$\left| \frac{H_i - \acute{H}_i}{\acute{H}_i} \right| < \frac{2\sqrt{2}}{\sqrt{13M - 20\sqrt{2M} + 16}}. \quad (\text{A.6})$$

Imperfect CSI reduces the amount of noise, n_i , that the system can tolerate. For perfect CSI assumption, errors occur when $n_i > \frac{d}{2}$; but in the case of imperfect CSI consideration, decoding errors occur on the i^{th} subcarrier if

$$\begin{aligned}
n_i &> \frac{d}{2} - \left| X_i - \frac{H_i}{\hat{H}_i} \cdot X_i \right| \\
&> \frac{d}{2} - \left| \frac{\hat{H}_i - H_i}{\hat{H}_i} \right| \cdot |X_i| \\
&> \frac{d}{2} - \frac{\alpha \times 2\sqrt{2}}{\sqrt{13M - 20\sqrt{2M} + 16}} \cdot |X_i|,
\end{aligned} \tag{A.7}$$

where $0 < \alpha < 1$ is a measure of the accuracy in channel estimation. The probability of error P^m for each constellation point m on i^{th} subcarrier can be given as

$$\begin{aligned}
P^m &= \text{Prob} \left\{ n_i > \frac{d}{2} - \frac{\alpha \times 2\sqrt{2}}{\sqrt{13M - 20\sqrt{2M} + 16}} \cdot |X_{i,m}| \right\} \\
&= N^m Q \left[\frac{d}{2\sigma} - \frac{d}{2\sigma} \frac{\alpha 4\sqrt{2}}{\sqrt{13M - 20\sqrt{2M} + 16}} \cdot |X_{i,m}| \right],
\end{aligned} \tag{A.8}$$

where N^m is the number of nearest neighbours to the constellation point $X_{i,m}$ and σ^2 is the variance of the noise. Furthermore, for QAM constellations [41]

$$\frac{d}{2\sigma} = \sqrt{\frac{3}{M-1} \cdot \text{SNR}}. \tag{A.9}$$

Thus,

$$P^m = N^m Q \left[\sqrt{\frac{3\text{SNR}}{M-1}} \left(1 - \frac{4\sqrt{2}\alpha |X_i|}{d\sqrt{13M - 20\sqrt{2M} + 16}} \right) \right]. \tag{A.10}$$

The overall probability of error on subcarrier i can be given as

$$P = \sum_m \text{Prob}(X_i = X_{i,m}) \cdot P^m. \tag{A.11}$$

We consider 32-QAM constellation (shown in Fig. A.1) as an example to demonstrate the calculation of overall probability of error under imperfect CSI consideration. The overall probability of error for other constellations can be calculated in the same way. There are 5 different types of constellation points for 32-QAM as shown in Fig. A.1. Each type of point has a different value of $|X_{i,m}|$ represented by a variable d_x in the figure. In the following, each category of points is considered separately to calculate P^m for all constellation points and finally the overall probability of error is found using (A.11). Note that $d = 2$ and $M = 32$ for all constellation points.

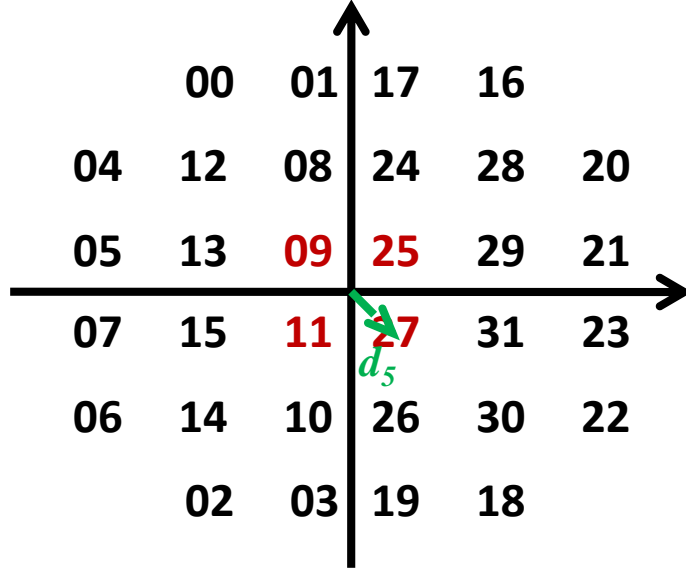


Figure A.2: 4 internal points of 32-QAM.

A.1 4 internal points

The 4 internal points are shown in Fig. A.2. $X_{i,m} = \sqrt{2}$ and $N^m = 4$ for these points. Therefore, P^m for these points can be given as

$$P_1^m = 4Q \left[\sqrt{\frac{3\text{SNR}}{31}} \left(1 - \frac{\alpha}{\sqrt{17}} \right) \right]. \quad (\text{A.12})$$

A.2 4 corner points of internal square

The 4 corner points of internal square are shown in Fig. A.3. $X_{i,m} = \sqrt{18}$ and $N^m = 4$ for these points. Therefore, P^m for these points can be given as

$$P_2^m = 4Q \left[\sqrt{\frac{3\text{SNR}}{31}} \left(1 - \frac{3\alpha}{\sqrt{17}} \right) \right]. \quad (\text{A.13})$$

A.3 8 middle points of internal square

The 8 middle points of internal square are shown in Fig. A.4. $X_{i,m} = \sqrt{10}$ and $N^m = 4$ for these points. Therefore, P^m for these points can be given as

$$P_3^m = 4Q \left[\sqrt{\frac{3\text{SNR}}{31}} \left(1 - \frac{\sqrt{5}\alpha}{\sqrt{17}} \right) \right]. \quad (\text{A.14})$$

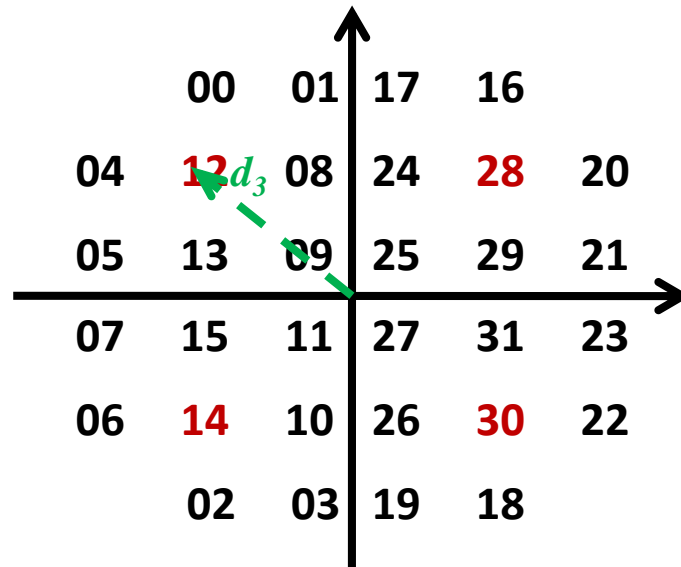


Figure A.3: 4 corner points of internal square.

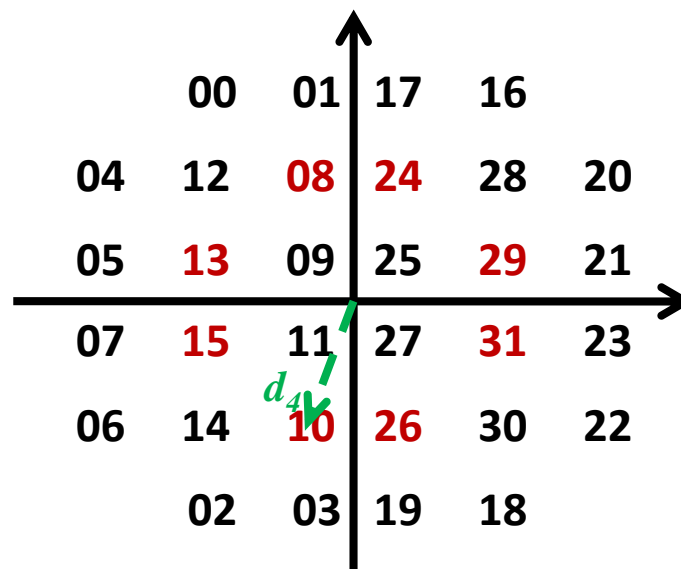


Figure A.4: 8 middle points of internal square.

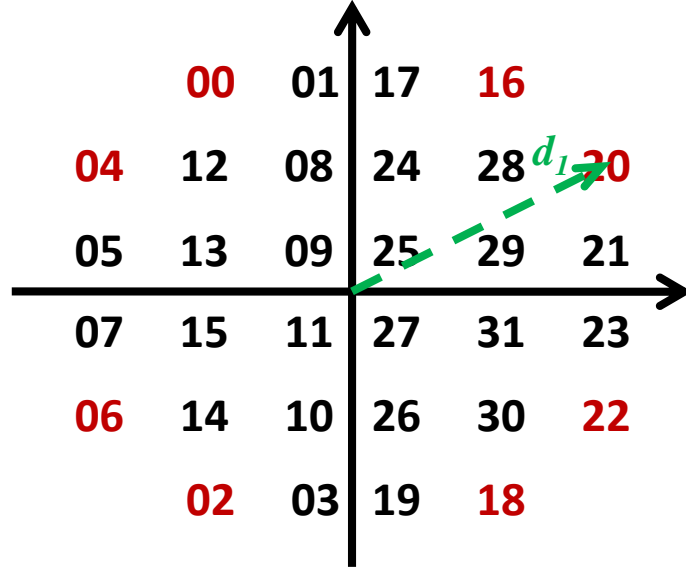


Figure A.5: 8 corner points of circumference.

A.4 8 corner points of circumference

The 8 corner points of circumference are shown in Fig. A.5. $X_{i,m} = \sqrt{34}$ and $N^m = 2$ for these points. Therefore, P^m for these points can be given as

$$P_4^m = 2Q \left[\sqrt{\frac{3\text{SNR}}{31}} (1 - \alpha) \right]. \quad (\text{A.15})$$

A.5 8 middle points of circumference

The 8 middle points of circumference are shown in Fig. A.6. $X_{i,m} = \sqrt{26}$ and $N^m = 3$ for these points. Therefore, P^m for these points can be given as

$$P_5^m = 3Q \left[\sqrt{\frac{3\text{SNR}}{31}} \left(1 - \frac{\sqrt{13}\alpha}{\sqrt{17}} \right) \right]. \quad (\text{A.16})$$

Now, the overall probability of error for 32-QAM with $\beta = \sqrt{\frac{3\text{SNR}}{31}}$, taking into account the estimation error, can be given as

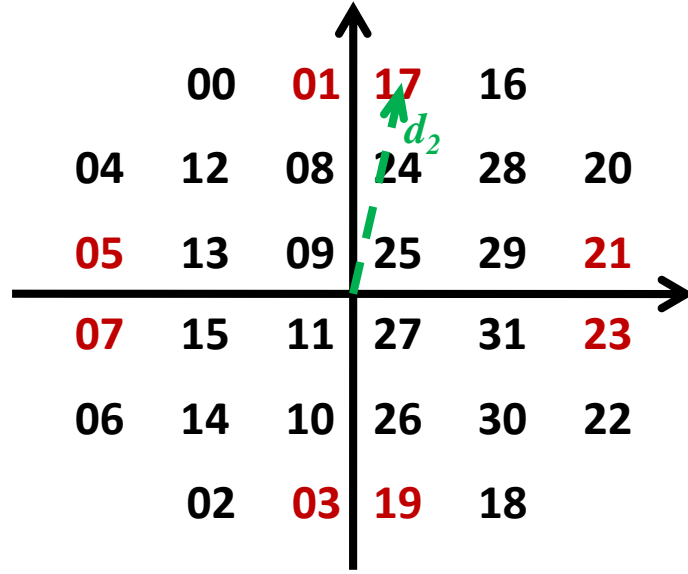


Figure A.6: 8 middle points of circumference.

$$\begin{aligned}
P &= \frac{1}{32} (4P_1^m + 4P_2^m + 8P_3^m + 8P_4^m + 8P_5^m) \\
&= \frac{1}{2}Q [(1-\alpha)\beta] + Q \left[\left(1 - \frac{\sqrt{5}\alpha}{\sqrt{17}}\right)\beta \right] + \frac{1}{2}Q \left[\left(1 - \frac{\alpha}{\sqrt{17}}\right)\beta \right] \\
&\quad + \frac{3}{4}Q \left[\left(1 - \frac{\sqrt{13}\alpha}{\sqrt{17}}\right)\beta \right] + \frac{1}{4}Q \left[\left(1 - \frac{3\alpha}{\sqrt{17}}\right)\beta \right]. \tag{A.17}
\end{aligned}$$

Bibliography

- [1] “OMEGA ICT FP7 Project.” [Online]. Available: <http://europa.eu/rapid/pressReleasesAction.do?reference=MEMO/09/35>
- [2] P. Brown, “Power line communications - past present and future,” in *Power Line Communications and Its Applications, 1999 International Symposium on*, March/April 1999, pp. 97–100.
- [3] J. J. Fahie, “Edward Davy”, *The Electrician*, 1883.
- [4] J. Routin and C. E. L. Brown, “Power line signalling electricity meters,” British Patent 24 833, 1897.
- [5] C. Thoradson, “Meters,” US Patent 784 712 and 784 713,, 1905.
- [6] “International HomePlug alliance.” [Online]. Available: <http://www.homeplug.org/>
- [7] “The PLCforum.” [Online]. Available: <http://www.plcforum.com/>
- [8] “INSTEON.” [Online]. Available: <http://www.insteon.net/>
- [9] M. K. Lee, R. E. Newman, H. A. Latchman, S. Katar, and L. Yonge, “Home-plug 1.0 powerline communication lans - protocol description and performance results,” *International Journal of Communication Systems*, vol. 16, no. 5, pp. 447–473, 2003.
- [10] H. Hrasnica, A. Haidine, and R. Lehnert, *Broadband powerline communications: network design*. John Wiley & Sons Ltd, 2004.
- [11] K. Dostert, *Power Line Communications*. Prentice Hall, 2001.
- [12] E. Biglieri, “Coding and modulation for a horrible channel,” *IEEE Communication Magazine.*, vol. 41, no. 5, pp. 92–98, 2003.
- [13] M. Crussière, J.-Y. Baudais, and J.-F. Héland, “Adaptive spread-spectrum multicarrier multiple-access over wirelines,” *IEEE Journal on Selected Areas in Communications*, vol. 24, no. 7, pp. 1377–1388, July 2006.

- [14] M. Koch, H. Hirsch, and M. Ianoz, "State of art of the emc standardization for power line communication," in *Proc Electromagnetic Compatibility, 2007. EMC 2007. International Symposium on*, Oct. 2007, pp. 59–62.
- [15] A. Vukicevic, "Electromagnetic compatibility of power line communication systems," Ph.D. dissertation, École polytechnique fédérale de Lausanne, Switzerland, 2008.
- [16] S. Bolognani, L. Peretti, L. SSGarbossa, and M. Zigliotto, "Improvements in power line communication reliability for electric drives by random PWM techniques," in *Proc IEEE Industrial Electronics, IECON 2006 - 32nd Annual Conference on*, Nov. 2006, pp. 2307–2312.
- [17] S. Galli and T. Banwell, "Modeling the indoor power line channel: new results and modem design considerations," in *Proc IEEE Consumer Communications and Networking Conference.*, 2004.
- [18] T. Papadopoulos, C. Kaloudas, and G. Papagiannis, "A multipath channel model for PLC systems based on nodal method and modal analysis," in *Power Line Communications and Its Applications, 2007. ISPLC '07. IEEE International Symposium on*, March 2007, pp. 278–283.
- [19] G. Laguna and R. Barron, "Survey on indoor power line communication channel modeling," in *Proc Electronics, Robotics and Automotive Mechanics Conference.*, 2008, pp. 163–168.
- [20] A. Tonello, "An impulse modulation based PLC system with frequency domain receiver processing," in *Proc Power Line Communications and Its Applications, 2005 International Symposium on*, April 2005, pp. 241–245.
- [21] L. Liu, P. So, and E. Gunawan, "Performance analysis of a combined adaptive OFDM transmission scheme for broadband power line communications," in *Proc Information, Communications and Signal Processing, ICICS 2005 - Fifth International Conference on*, 2005, pp. 926–930.
- [22] T. Sartenauer, "Multiuser communications over frequency selective wired channels and applications to the powerline access network," Ph.D. dissertation, Université catholique de Louvain, Belgium, 2004.
- [23] A. Kosonen, "Power line communication in motor cables of variable-speed electric drives - analysis and implementation," Ph.D. dissertation, Lappeenranta University of Technology, Finland, 2008.
- [24] A. Purroy, A. Sanz, and J. Garcia, "Impulsive noise cancellation system based on fuzzy logic for a PLC receiver," in *Proc Power Line Communications and Its Applications, 2005 International Symposium on*, April 2005, pp. 346–350.

- [25] L. P. Do, H. Hrasnica, and G. Bumiller, "Investigation of MAC protocols for single frequency network technique applied in powerline communications," in *Proc Power Line Communications and Its Applications, 2005 International Symposium on*, April 2005, pp. 22–26.
- [26] W. Liu, H. Widmer, and P. Raffin, "Broadband PLC access systems and field deployment in european power line networks," *Communications Magazine, IEEE*, vol. 41, no. 5, pp. 114–118, May 2003.
- [27] Y.-J. Lin, H. Latchman, J. Liu, and R. Newman, "Periodic contention-free multiple access for broadband multimedia powerline communication networks," in *Proc Power Line Communications and Its Applications, 2005 International Symposium on*, April 2005, pp. 121–125.
- [28] N. Papandreou and T. Antonakopoulos, "Resource allocation management for indoor power-line communications systems," *Power Delivery, IEEE Transactions on*, vol. 22, no. 2, pp. 893–903, April 2007.
- [29] M. Crussière, J.-Y. Baudais, and J.-F. Héland, "Loading algorithms for adaptive SS-MC-MA systems over wireline channels: comparison with DMT," *European Transactions on Telecommunications, Special Issue on the 5th Multi-Carrier Spread-Spectrum*, vol. 17, no. 6, pp. 659–669, 2006.
- [30] H. Zou, S. Jagannathan, and J. Cioffi, "Multiuser OFDMA resource allocation algorithms for in-home power-line communications," in *Proc Global Telecommunications Conference, 2008. IEEE GLOBECOM 2008. IEEE*, 30 2008-Dec. 4 2008, pp. 1–5.
- [31] L. Hao and J. Guo, "A MIMO-OFDM scheme over coupled multi-conductor power-line communication channel," in *Power Line Communications and Its Applications, 2007. ISPLC '07. IEEE International Symposium on*, March 2007, pp. 198–203.
- [32] G. Held, *Understanding Broadband over Power Line*. AUERBACH, 2006.
- [33] M. Busser, T. Waldeck, and K. Dostert, "Telecommunication applications over the low voltage power distribution grid," in *Proc. IEEE 5th Int. Symp. Spread Spectrum Techniques & Applications*, vol. 1/3, 1998, pp. 73–77.
- [34] H. Philipps, "Development of a statistical modem for powerline communications channels," in *Proc. IEEE International Symposium on Power-Line Communications and Its Applications (ISPLC)*, vol. 5, 2000, pp. 2049–2053.
- [35] M. Zimmermann and K. Dostert, "A multipath model for the powerline channel," *IEEE Trans. Commun.*, vol. 50, no. 4, pp. 553–559, Apr 2002.

- [36] “OMEGA Deliverable D3.2, *PLC Channel Characterization and Modelling*.” [Online]. Available: http://www.ict-omega.eu/fileadmin/documents/deliverables/Omega_D3.2_v1.1.pdf
- [37] M. Doelz, E. Heald, and D. Martin, “Binary data transmission techniques for linear systems,” *Proceedings of the IRE*, vol. 45, no. 5, pp. 656–661, May 1957.
- [38] R. van Nee, G. Awater, M. Morikura, H. Takanashi, M. Webster, and K. Halford, “New high-rate wireless LAN standards,” *Communications Magazine, IEEE*, vol. 37, no. 12, pp. 82–88, Dec 1999.
- [39] R. v. Nee and R. Prasad, *OFDM for Wireless Multimedia Communications*. Norwood, MA, USA: Artech House, Inc., 2000.
- [40] R. van Nee, “A new OFDM standard for high rate wireless LAN in the 5 GHz band,” in *Vehicular Technology Conference, 1999. VTC 1999 - Fall. IEEE VTS 50th*, vol. 1, 1999, pp. 258–262 vol.1.
- [41] J. G. Proakis, *Digital Communications*. McGraw-Hill, 2000.
- [42] E. Biglieri, J. Proakis, and S. Shamai, “Fading channels: information-theoretic and communications aspects,” *Information Theory, IEEE Transactions on*, vol. 44, no. 6, pp. 2619–2692, 1998. [Online]. Available: <http://dx.doi.org/10.1109/18.720551>
- [43] M. Debbah, *Short introduction to OFDM*. <http://www.supelec.fr/d2ri/flexibleradio/cours/ofdmtutorial.pdf>, 2004.
- [44] A. V. Oppenheim, R. W. Schaffer, and J. R. Buck, *Discrete-time signal processing (2nd ed.)*. Upper Saddle River, NJ, USA: Prentice-Hall, Inc., 1999.
- [45] R. Chang and R. Gibby, “A theoretical study of performance of an orthogonal multiplexing data transmission scheme,” *Communication Technology, IEEE Transactions on*, vol. 16, no. 4, pp. 529–540, August 1968.
- [46] B. Le Floch, M. Alard, and C. Berrou, “Coded orthogonal frequency division multiplex [TV broadcasting],” *Proceedings of the IEEE*, vol. 83, no. 6, pp. 982–996, Jun 1995.
- [47] X. Cai and G. Giannakis, “Bounding performance and suppressing intercarrier interference in wireless mobile OFDM,” *Communications, IEEE Transactions on*, vol. 51, no. 12, pp. 2047–2056, Dec. 2003.
- [48] I. Ivan and B. Muquet, “Reduced complexity decision feedback equalizer for supporting high mobility in wimax,” in *Vehicular Technology Conference, 2009. VTC Spring 2009. IEEE 69th*, April 2009, pp. 1–5.

- [49] M. Bossert, A. Donder, and V. Zyablov, "Improved channel estimation with decision feedback for OFDM systems," *Electronics Letters*, vol. 34, no. 11, pp. 1064–1065, May 1998.
- [50] R. Negi and J. Cioffi, "Pilot tone selection for channel estimation in a mobile OFDM system," *Consumer Electronics, IEEE Transactions on*, vol. 44, no. 3, pp. 1122–1128, Aug 1998.
- [51] J.-J. van de Beek, O. Edfors, M. Sandell, S. Wilson, and P. Borjesson, "On channel estimation in OFDM systems," in *Vehicular Technology Conference, 1995 IEEE 45th*, vol. 2, Jul 1995, pp. 815–819 vol.2.
- [52] U. Tureli and H. Liu, "Blind carrier synchronization and channel identification for OFDM communications," in *Acoustics, Speech and Signal Processing, 1998. Proceedings of the 1998 IEEE International Conference on*, vol. 6, May 1998, pp. 3509–3512 vol.6.
- [53] E. Jaffrot and M. Siala, "Turbo channel estimation for OFDM systems on highly time and frequency selective channels," in *Acoustics, Speech, and Signal Processing, 2000. ICASSP '00. Proceedings. 2000 IEEE International Conference on*, vol. 5, 2000, pp. 2977–2980 vol.5.
- [54] R. van Nee and A. de Wild, "Reducing the peak-to-average power ratio of OFDM," in *Vehicular Technology Conference, 1998. VTC 98. 48th IEEE*, vol. 3, May 1998, pp. 2072–2076 vol.3.
- [55] S. Slimane, "Reducing the peak-to-average power ratio of OFDM signals through precoding," *Vehicular Technology, IEEE Transactions on*, vol. 56, no. 2, pp. 686–695, March 2007.
- [56] I. ho Hwang, H. soo Lee, and K. woo Kang, "Frequency and timing period offset estimation technique for OFDM systems," *Electronics Letters*, vol. 34, no. 6, pp. 520–521, Mar 1998.
- [57] T. Pollet, M. Van Bladel, and M. Moeneclaey, "BER sensitivity of OFDM systems to carrier frequency offset and wiener phase noise," *Communications, IEEE Transactions on*, vol. 43, no. 234, pp. 191–193, Feb/Mar/Apr 1995.
- [58] P. Moose, "A technique for orthogonal frequency division multiplexing frequency offset correction," *Communications, IEEE Transactions on*, vol. 42, no. 10, pp. 2908–2914, Oct 1994.
- [59] P. Melsa, R. Younce, and C. Rohrs, "Impulse response shortening for discrete multitone transceivers," *Communications, IEEE Transactions on*, vol. 44, no. 12, pp. 1662–1672, Dec 1996.
- [60] H. K. Markey and G. Antheil, "Secret communication system," US Patent 2 292 387,, 1942,.

- [61] *Mobile station-base station compatibility standard for dual-mode wideband spread spectrum cellular system*, TIA/EIA/IS-95 Std., July 1993.
- [62] *Universal mobile telecommunications system (UMTS)*, ETSI UMTS (TR 101 112) Std., 1998.
- [63] R. Pickholtz, D. Schilling, and L. Milstein, "Theory of spread-spectrum communications—a tutorial," *Communications, IEEE Transactions on*, vol. 30, no. 5, pp. 855–884, May 1982.
- [64] R. Stankovic, "Some remarks on terminology in spectral techniques for logic design: Walsh transform and hadamard matrices," *Computer-Aided Design of Integrated Circuits and Systems, IEEE Transactions on*, vol. 17, no. 11, pp. 1211–1214, Nov 1998.
- [65] M. Golay, "Complementary series," *Information Theory, IRE Transactions on*, vol. 7, no. 2, pp. 82–87, April 1961.
- [66] R. Prasad, *Universal Wireless Personal Communications*. Norwood, MA, USA: Artech House, Inc., 1998.
- [67] R. Gold, "Optimal binary sequences for spread spectrum multiplexing (corresp.)," *Information Theory, IEEE Transactions on*, vol. 13, no. 4, pp. 619–621, Oct 1967.
- [68] K. Fazel and L. Papke, "On the performance of convolutionally-coded CDMA/OFDM for mobile communication system," in *Proc. IEEE international symposium on personal, indoor and mobile radio communications (PIMRC'93)*, 1993, pp. 468–472.
- [69] N. Yee, J. P. Linnartz, and G. Fettweis, "Multi-carrier CDMA in indoor wireless radio networks," in *Proc. IEEE international symposium on personal, indoor and mobile radio communications (PIMRC'93)*, 1993, pp. 109–113.
- [70] L. Vandendorpe, "Multitone direct sequence CDMA system in an indoor wireless environment," in *Proc. IEEE First Symposium of Communications and Vehicular Technology*, 1993, pp. 4.1.1–4.1.8.
- [71] A. Chouly, A. Brajal, and S. Jourdan, "Orthogonal multicarrier techniques applied to direct sequence spread spectrum CDMA systems," in *Global Telecommunications Conference, 1993, including a Communications Theory Mini-Conference. Technical Program Conference Record, IEEE in Houston. GLOBE-COM '93., IEEE*, Nov-2 Dec 1993, pp. 1723–1728 vol.3.
- [72] V. DaSilva and E. Sousa, "Performance of orthogonal CDMA codes for quasi-synchronous communication systems," in *Universal Personal Communications, 1993. Personal Communications: Gateway to the 21st Century. Conference Record., 2nd International Conference on*, vol. 2, Oct 1993, pp. 995–999 vol.2.

- [73] S. Kaiser, "Multi-carrier CDMA mobile radio systems - analysis and optimization of detection, decoding, and channel estimation," Ph.D. dissertation, Dusseldorf: VDI-Verlag, Fortschritt-Berichte VDI, 1998.
- [74] Z. Wang and G. Giannakis, "Linearly precoded or coded OFDM against wireless channel fades?" in *Wireless Communications, 2001. (SPAWC '01). 2001 IEEE Third Workshop on Signal Processing Advances in*, 2001, pp. 267–270.
- [75] S. Ohno and G. Giannakis, "Optimal training and redundant precoding for block transmissions with application to wireless OFDM," *Communications, IEEE Transactions on*, vol. 50, no. 12, pp. 2113–2123, Dec 2002.
- [76] S. Kaiser and K. Fazel, "A flexible spread-spectrum multi-carrier multiple-access system for multi-media applications," in *Personal, Indoor and Mobile Radio Communications, 1997. 'Waves of the Year 2000'. PIMRC '97., The 8th IEEE International Symposium on*, vol. 1, Sep 1997, pp. 100–104 vol.1.
- [77] S. Nobilet, J.-F. Héland, and D. Mottier, "Spreading sequences for uplink and downlink MC-CDMA systems: PAPR and MAI minimization," *European Transactions on Telecommunications*, vol. 13, no. 5, pp. 465–474, 2002.
- [78] A. Stephan, E. Guéguen, M. Crussière, J.-Y. Baudais, and J.-F. Héland, "Optimization of linear precoded OFDM for high-data-rate UWB systems," *EURASIP Journal on Wireless Communications and Networking*, vol. 2008, 2008.
- [79] D. Mottier and D. Castelain, "A spreading sequence allocation procedure for MC-CDMA transmission systems," in *Vehicular Technology Conference, 2000. IEEE VTS-Fall VTC 2000. 52nd*, vol. 3, 2000, pp. 1270–1275 vol.3.
- [80] D. P. Palomar, A. Pascual-Iserte, J. M. Cioffi, and M. A. Lagunas, "Convex optimization theory applied to joint transmitter-receiver design in MIMO channels," in *Space-Time Processing for MIMO Communications, Chapter 8*. John Wiley & Sons, 2005, pp. 269–318.
- [81] A. Leke and J. Cioffi, "A maximum rate loading algorithm for discrete multitone modulation systems," in *Proc IEEE Global Telecommunications Conf.*, vol. 3, Nov 1997, pp. 1514–1518 vol.3.
- [82] T. Starr, J. M. Cioffi, and P. J. Silverman, *Understanding digital subscriber line technology*. Upper Saddle River, NJ, USA: Prentice Hall PTR, 1999.
- [83] P. Chow, J. Cioffi, and J. Bingham, "A practical discrete multitone transceiver loading algorithm for data transmission over spectrally shaped channels," *IEEE Trans. Commun.*, vol. 43, no. 234, pp. 773–775, Feb 1995.

- [84] M. Crussière, J.-Y. Baudais, and J.-F. Héland, "Robust and high-bit rate communications over PLC channels: a bit-loading multi-carrier spread-spectrum solution," in *Power Line Communications and Its Applications, 2005 International Symposium on*, April 2005, pp. 37–41.
- [85] E. Baccarelli, A. Fasano, and M. Biagi, "Novel efficient bit-loading algorithms for peak-energy-limited ADSL-type multicarrier systems," *Signal Processing, IEEE Transactions on*, vol. 50, no. 5, pp. 1237–1247, May 2002.
- [86] B. Krongold, K. Ramchandran, and D. Jones, "Computationally efficient optimal power allocation algorithms for multicarrier communication systems," *IEEE Trans. Commun.*, vol. 48, no. 1, pp. 23–27, Jan 2000.
- [87] A. Maiga, J.-Y. Baudais, and J.-F. Héland, "An efficient bit-loading algorithm with peak BER constraint for the band-extended PLC," in *Telecommunications, 2009. ICT '09. International Conference on*, May 2009, pp. 292–297.
- [88] C. Shannon, "A mathematical theory of communication," *Bell System Technical Journal*, vol. 27, pp. 623–656, July 1948.
- [89] J. Cioffi, "A multicarrier primer," ANSI T1E1.4/91-157, Tech. Rep., 1991.
- [90] J. Cioffi, G. Dudevoir, M. Eyuboglu, and J. Forney, G.D., "MMSE decision-feedback equalizers and coding. ii. coding results," *Communications, IEEE Transactions on*, vol. 43, no. 10, pp. 2595–2604, Oct 1995.
- [91] Y. Yasuda, K. Kashiki, and Y. Hirata, "High-rate punctured convolutional codes for soft decision viterbi decoding," *Communications, IEEE Transactions on*, vol. 32, no. 3, pp. 315–319, Mar 1984.
- [92] D. Hughes-Hartogs, "Ensemble modem structure for imperfect transmission media," US Patent 4 679 227, 4 731 816, and 4 833 796,, 1987, 1988, and 1989,.
- [93] J. Campello and J. Cioffi, "Optimal discrete loading," ANSI Contribution T1E1.4/98-341, Plano, TX, Tech. Rep., November 1998.
- [94] A. Czylik, "Adaptive OFDM for wideband radio channels," in *Global Telecommunications Conference, 1996. GLOBECOM '96. 'Communications: The Key to Global Prosperity*, vol. 1, Nov 1996, pp. 713–718 vol.1.
- [95] J. Campello, "Practical bit loading for DMT," in *Communications, 1999. ICC '99. 1999 IEEE International Conference on*, vol. 2, 1999, pp. 801–805 vol.2.
- [96] A. Maiga, J.-Y. Baudais, and J.-F. Héland, "An efficient channel condition aware proportional fairness resource allocation for powerline communications," in *Telecommunications, 2009. ICT '09. International Conference on*, May 2009, pp. 286 –291.

- [97] H. Moon, "Efficient power allocation for coded OFDM systems," Ph.D. dissertation, Stanford University, USA, 2004.
- [98] T. Zogakis, J. Aslanis, J.T., and J. Cioffi, "A coded and shaped discrete multitone system," *Communications, IEEE Transactions on*, vol. 43, no. 12, pp. 2941–2949, Dec 1995.
- [99] A. Wyglinski, F. Labeau, and P. Kabal, "Bit loading with BER-constraint for multicarrier systems," *IEEE Trans. Wireless Commun.*, vol. 4, no. 4, pp. 1383–1387, July 2005.
- [100] M. Crussière, "Etude et optimisation de communications à haut-débit sur lignes d'énergie : exploitation de la combinaison OFDM/CDMA," Ph.D. dissertation, Institut National des Sciences Appliquées de Rennes, France, 2005.
- [101] A. Papoulis, *Probability, Random Variables, and Stochastic Processes*. McGraw Hill, 1984.
- [102] L.-F. Wei, "Trellis-coded modulation with multidimensional constellations," *Information Theory, IEEE Transactions on*, vol. 33, no. 4, pp. 483–501, Jul 1987.
- [103] *Very High Speed Digital Subscriber Line Transceivers 2 (VDSL2)*, International Telecommunication Union (ITU) Std., 2006.
- [104] "Universal power line association." [Online]. Available: <http://www.upaplc.org/>
- [105] T. Zogakis, J. Aslanis, J.T., and J. Cioffi, "A coded and shaped discrete multitone system," *Communications, IEEE Transactions on*, vol. 43, no. 12, pp. 2941–2949, Dec 1995.
- [106] —, "Analysis of a concatenated coding scheme for a discrete multitone modulation system," in *Military Communications Conference, 1994. MILCOM '94. Conference Record, 1994 IEEE*, Oct 1994, pp. 433–437 vol.2.
- [107] *Very High Speed Digital Subscriber Line (VDSL)*, European Telecommunications Standards Institute (ETSI) Std., 2003.
- [108] I. Kalet, "The multitone channel," *IEEE Trans. Commun.*, vol. 37, no. 2, pp. 119–124, Feb 1989.
- [109] Y. George and O. Amrani, "Bit loading algorithms for OFDM," in *Proc IEEE Inter. Symp. on Info. Theory*, 2004, pp. 391–391.
- [110] F. Muhammad, J.-Y. Baudais, J.-F. Héland, and M. Crussière, "Coded adaptive linear precoded discrete multitone over PLC channel," in *Power Line Communications and Its Applications, 2008. ISPLC 2008. IEEE International Symposium on*, April 2008, pp. 123–128.

- [111] F. Muhammad, J.-Y. Baudais, J.-F. Hélard, and M. Crussière, "A coded bit-loading linear precoded discrete multitone solution for power line communication," in *Signal Processing Advances in Wireless Communications, 2008. SPAWC 2008. IEEE 9th Workshop on*, July 2008, pp. 555–559.
- [112] F. Muhammad, A. Stephan, J.-Y. Baudais, and J.-F. Hélard, "Bit rate maximization loading algorithm with mean BER-constraint for linear precoded OFDM," in *Telecommunications, 2009. ICT '09. International Conference on*, May 2009, pp. 281–285.
- [113] J. Lambert, "Observations variae in mathesis puram," *Acta Helvetica, physico-mathematico-anatomico-botanico-medica* 3, pp. 128–168, 1758.
- [114] F. Muhammad, A. Stephan, J.-Y. Baudais, and J.-F. Hélard, "Analysis of mean bit error rate minimization for orthogonal frequency division multiplexing," *submitted to Hindawi Journal of Electrical and Computer Engineering*, vol. 2010, no. 5, 2010.
- [115] F. Muhammad, J.-Y. Baudais, and J.-F. Hélard, "Minimisation du TEB moyen d'un système OFDM precodé," in *Colloque Groupe de recherche et d'étude de traitement du signal '09. GRETSI*, Sep 2009, pp. 1–4.
- [116] F. Muhammad, A. Stephan, J.-Y. Baudais, and J.-F. Hélard, "Mean BER minimization loading algorithm for linear precoded OFDM," in *Sarnoff Symposium, 2009. SARNOFF '09. IEEE*, 30 2009–April 1 2009, pp. 1–5.
- [117] D. Dardari, "Ordered subcarrier selection algorithm for OFDM-based high-speed WLANs," *Wireless Communications, IEEE Transactions on*, vol. 3, no. 5, pp. 1452–1458, Sept. 2004.
- [118] A. Leke and J. Cioffi, "Multicarrier systems with imperfect channel knowledge," in *Personal, Indoor and Mobile Radio Communications, 1998. The Ninth IEEE International Symposium on*, vol. 2, Sep 1998, pp. 549–553 vol.2.
- [119] M. Souryal and R. Pickholtz, "Adaptive modulation with imperfect channel information in OFDM," in *Communications, 2001. ICC 2001. IEEE International Conference on*, vol. 6, 2001, pp. 1861–1865 vol.6.
- [120] Q. Su and S. Schwartz, "Effects of imperfect channel information on adaptive loading gain of OFDM," in *Vehicular Technology Conference, 2001. VTC 2001 Fall. IEEE VTS 54th*, vol. 1, 2001, pp. 475–478 vol.1.
- [121] Q. Su, J. Cimini, L.J., and R. Blum, "On the problem of channel mismatch in constant-bit-rate adaptive modulation for OFDM," in *Vehicular Technology Conference, 2002. VTC Spring 2002. IEEE 55th*, vol. 2, 2002, pp. 585–589 vol.2.

- [122] S. Ye, R. Blum, and L. Cimini, "Adaptive OFDM systems with imperfect channel state information," *Wireless Communications, IEEE Transactions on*, vol. 5, no. 11, pp. 3255–3265, November 2006.
- [123] Z. Song, K. Zhang, and Y. L. Guan, "Statistical adaptive modulation for QAM-OFDM systems," in *Global Telecommunications Conference, 2002. GLOBE-COM '02. IEEE*, vol. 1, Nov. 2002, pp. 706–710 vol.1.
- [124] Y. Yao and G. Giannakis, "Rate-maximizing power allocation in OFDM based on partial channel knowledge," *Wireless Communications, IEEE Transactions on*, vol. 4, no. 3, pp. 1073–1083, May 2005.
- [125] P. Xia, S. Zhou, and G. Giannakis, "Adaptive MIMO-OFDM based on partial channel state information," *Signal Processing, IEEE Transactions on*, vol. 52, no. 1, pp. 202–213, Jan. 2004.
- [126] G. Barriac and U. Madhow, "Space-time communication for OFDM with implicit channel feedback," *Information Theory, IEEE Transactions on*, vol. 50, no. 12, pp. 3111–3129, Dec. 2004.
- [127] Z. Hu, G. Zhu, Y. Xia, and G. Liu, "Multiuser subcarrier and bit allocation for MIMO-OFDM systems with perfect and partial channel information," in *Wireless Communications and Networking Conference, 2004. WCNC. 2004 IEEE*, vol. 2, March 2004, pp. 1188–1193 Vol.2.
- [128] Y.-H. Pan, K. Leraief, and Z. Cao, "Space-time coded adaptive transmit antenna arrays for OFDM wireless systems utilizing channel side information," in *Vehicular Technology Conference, 2003. VTC 2003-Spring. The 57th IEEE Semiannual*, vol. 2, April 2003, pp. 1127–1131 vol.2.
- [129] F. Muhammad, J.-Y. Baudais, and J.-F. Héland, "Rate maximization loading algorithm for LP-OFDM systems with imperfect CSI," in *Personal, Indoor and Mobile Radio Communications, 2009. PIMRC 2009. 20th International Symposium on*, Sept. 2009.
- [130] —, "Bit rate maximization for LP-OFDM with noisy channel estimation," in *Signal Processing and Communication Systems, 2009. ICSPCS 2009. 3rd International Conference on*, Sept. 2009, pp. 1–6.

AVIS DU JURY SUR LA REPRODUCTION DE LA THESE SOUTENUE

Titre de la thèse : Various resource allocation and optimization strategies for high bit rate communications on power lines

Nom Prénom de l'auteur : SYED MUHAMMAD Fahad

Membres du jury : Monsieur ROVIRAS
Monsieur SARI
Monsieur HELARD
Monsieur BAUDAIS
Monsieur BELFIORE
Monsieur GORCE
Monsieur LE GOUABLE

Président du jury : *Jean-Charles BELFIORE*

Date de la soutenance : 17/03/2010

Reproduction de la thèse soutenue :



Thèse pouvant être reproduite en l'état



Thèse ne pouvant être reproduite



Thèse pouvant être reproduite après corrections suggérées

Le Directeur,



A. JIGOREL

Rennes, le 17/03/2010

Signature du Président du jury


J.C. BELFIORE

Résumé

Ces dernières années, le développement des réseaux de communication indoor et outdoor et l'augmentation du nombre d'applications conduisent à un besoin toujours croissant de transmission de données à haut débit. Parmi les nombreuses technologies concurrentes, les communications par courant porteur en ligne (CPL) ont leur place en raison des infrastructures déjà disponibles. La motivation principale de cette thèse est d'augmenter le débit et la robustesse des systèmes CPL à porteuses multiples afin qu'ils puissent être utilisés efficacement dans les réseaux domestiques et pour la domotique. Le thème de ce travail de recherche est d'explorer différentes approches de modulation et de codage de canal en liaison avec plusieurs schémas d'allocation et d'optimisation des ressources. L'objectif est ici d'améliorer les capacités des CPL et d'être concurrent face aux autres solutions de communication à haut débit et de faire face efficacement aux inconvénients inhérents au réseau d'alimentation.

Un certain nombre de stratégies d'allocation des ressources et d'optimisation sont étudiées pour améliorer les performances globales des systèmes CPL. La performance d'un système de communication est généralement mesurée en termes de débit, de marge de bruit et de taux d'erreur binaire (TEB) de la liaison. La maximisation de débit (RM) est étudiée pour les systèmes OFDM (en anglais orthogonal frequency division multiplexing) et LP-OFDM (en anglais linear precoded OFDM) sous la contrainte de densité spectrale de puissance (DSP). Deux contraintes différentes de taux d'erreur ont été appliquées au problème RM. La première contrainte est la contrainte de TEB crête où toutes les sous-porteuses ou séquences de précodage doivent respecter le TEB cible. Avec la deuxième contrainte, contrainte de TEB moyen, différentes sous-porteuses ou séquences de précodage sont affectées par des valeurs différentes de TEB et une contrainte de TEB moyen est imposée sur le symbole complet OFDM ou LP-OFDM. Les algorithmes d'allocation sont également proposés en prenant en compte les gains de codage de canal dans le processus d'allocation des ressources. En outre, un nouveau schéma de minimisation de TEB moyen est introduit qui minimise le TEB moyen de systèmes pour un débit donné et un masque imposé de DSP.

Pour l'allocation des ressources dans un système à porteuses multiples, il est généralement supposé que l'état du canal (CSI) est parfaitement connu par l'émetteur. En réalité, les informations de CSI disponibles au point d'émission sont imparfaites. Aussi, nous avons également étudié des schémas d'allocation des ressources dans le cas de systèmes OFDM et LP-OFDM en prenant compte, et de manière efficace, les impacts des estimations bruitées. Plusieurs chaînes de communication sont aussi développées pour les systèmes OFDM et LP-OFDM.

Abstract

In recent years, the thriving growth of indoor and outdoor communication networks and the increase in number of data heavy applications are driving an ever increasing need for high speed data transmission. Among many competing technologies, power line communication (PLC) has its unique place due to already available power supply grids in both indoor and outdoor environments. The primary motivation of this thesis is to increase the bit rate and the robustness of multicarrier PLC systems so that it can be efficiently used in home networking and automation. The theme of this research work is to explore different modulation and coding approaches in conjunction with various resource allocation and optimization schemes to bring PLC capabilities at par with other high bit rate alternatives and to cope efficiently with inherent disadvantages of power supply grid.

A number of resource allocation and optimization strategies are investigated to improve the overall performance of PLC systems. The performance of a communication system is generally measured in terms of bit rate, noise margin and bit error rate (BER) of the system. The bit rate maximization scheme is studied for both orthogonal frequency division multiplexing (OFDM) systems and linear precoded OFDM (LP-OFDM) systems under power spectral density constraint. Two different error rate constraints have been applied to the bit rate maximization problem. The first constraint is the peak BER constraint where all subcarrier or precoding sequences must respect the target BER. With the second constraint, known as mean BER constraint, different subcarriers or precoding sequences are allowed to be affected by different values of BER and a mean BER constraint is imposed on an entire OFDM or LP-OFDM symbol. Discrete bit and power loading algorithms are also proposed taking into account the channel coding gains in the resource allocation process. Furthermore, a new robustness maximization scheme, known as mean BER minimization, is introduced that minimizes the mean BER of multicarrier systems for a given bit rate and an imposed power spectral density mask.

For optimal allocation of bit and power to different subcarriers or precoding sequences in a multicarrier system, it is generally supposed that perfect channel state information (CSI) is available at the transmitting side (i.e. estimation noise is absent). In reality, the CSI available at the transmitter is imperfect. We also suggested resource allocation schemes for OFDM and LP-OFDM systems taking into account the effects of noisy estimations in an efficient manner. A number of communication chains are also developed for OFDM and LP-OFDM.